DEVELOPMENT OF DEFENSIBLE REGIONAL CLIMATE CHANGE PROJECTIONS FOR ADAPTATION AND POLICY

Report to the
Water Research Commission

by

Bruce Hewitson, Chris Jack, Lisa Coop, Piotr Wolski, Ross Blamey & Anna Steynor

Climate System Analysis Group
Department of Environmental and Geographical Science
University of Cape Town

WRC Report No. 2061/1/14
ISBN 978-1-4312-0632-2

February 2015

Obtainable from:

Water Research Commission
Private Bag X03
Gezina, 0031

orders@wrc.org.za or download from www.wrc.org.za

The publication of this report emanates from a project entitled *Developing predictive tools and adaptive measures to global climate change and hydro-climatic variability*
(WRC Project No. K5/2061)

DISCLAIMER

This report has been reviewed by the Water Research Commission (WRC) and approved for publication. Approval does not signify that the contents necessarily reflect the views and policies of the WRC nor does mention of trade names or commercial products constitute endorsement or recommendation for use.

© Water Research Commission

EXECUTIVE SUMMARY

This report addresses issues underlying the critical question "*How do I assess the regional climate change information for my sector / location / decision / policy?"* This is a nuanced issue, and within this context this report explores the multiplicity of approaches for developing robust regional understanding of climate change. In many respects this is a problem of ethics; the challenges only exist because of the choices humankind has made, and our future depends on the choices we will make – choices that are now, in part, predicated on projected climate change.

At the regional scale our choices are complicated by the large uncertainties in the degree and rate of change and our incomplete knowledge of how human and physical systems will respond (Hewitson et al., 2013). The central problem is the pressure to operationalize what is effectively incomplete and ongoing research by the global scientific community.

The approach adopted considers the historical changes from observed data, changes in the driving circulation patterns, the projected changes at the regional scale from the Global Circulation Models (GCMs), and from the information downscaled from the GCMs. This approach was the conceptualized intent of the IPCC 4th Assessment Report's chapter on Regional Climate Projections (Christensen et al., 2007). At the core is a need to provide information that is credible (as in, it is realistic), defensible (meaning it is rooted in an understanding of physical processes), and ultimately actionable (with high enough confidence to support implementation in policy and adaptation measures).

The report covers each avenue of potential sources of information on regional change, and concludes with a framework for integrating these in a sector-specific context to inform decision makers and policy. This is developed as a transferable and scalable approach to support decision makers and policy development.

1. The four foundations

a) Observed historical changes. The exploration of historical observations of weather and climate serves a dual role in the context of developing defensible regional projections for a particular region. Firstly, observations and the analysis of these observations enhance our understanding of the nature of a variable climate as expressed in a particular region. Secondly, it is often very useful for decision makers to know if the climate has exhibited a consistent long term change over the past decades as this can provide some insight into historical trends of impacts such as water scarcity, crop yields, dam levels, etc.

Station selection for this analysis draws from a suite of 4034 rainfall observing stations across South Africa extending from as early as 1850 through to the end of 2012. Stations for the analysis were selected by finding all stations that had less than 10% of values missing during the period 1960 through to the end of 2012. This resulted in 784 stations in the subset.

There can be very complex patterns of trends through the year for a particular location, and to evaluate the seasonal nature of change, the analysis aggregates daily statistics up to monthly statistics and all trend analysis is done on individual calendar months through time. The focus is on monthly total rainfall, rain days, rain days > 10 mm, rain days > 20 mm, and maximum daily rainfall in a month. The results are presented as monthly maps of station trends. For each month, only those stations that exhibit a statistically significant trend at the 90^{th} percent level are displayed.

A large number of results present a nuanced picture of historical change, and a close examination is required in the context of the user's vulnerability. A number of important features stand out. Most notably is the strong drying trend across the central and northeast of the country in April which appears to relate to an earlier cessation to the summer rainfall regime. Also of interest is the indication of increasing rainfall across the centre of the country (slightly to the west) in the summer months December to February. December, in particular, shows an increase in rainfall across the Free State suggesting a stronger start to the rainfall season.

Many of the trends are statistically significant suggesting a response to an underlying process, presumably global climate change, though other drivers should also be considered. The observed trends are complex, varying from positive to negative and significant or not significant at the same location through different months of the year. Nationally there are trends of both wetting and drying with a fairly strong suggestion of a shortening of the summer rainfall season and a shortening and/or later shift in the winter rainfall season. Trends in derived statistics such as monthly rain days appear to be more statistically significant than first order total monthly rainfall statistics.

b) Modes of variability in climate models. The regional messages derived from models are contingent on the model's skill in simulating the driving circulation processes. The objective of this step is to explore the relevant attributes of the General Circulation Models[1] (GCMs) from the perspective of circulation – the skilful scale of GCMs. Two approaches are explored; the model's ability to reproduce the large scale processes of relevance to the southern Africa, and an examination of model performance of the regional scale circulation patterns.

Results show that the CMIP5 models have some skill in simulating the leading mode of global variability: ENSO. Most of the models tend to show dry conditions (although weaker in magnitude) over southern Africa during strong El Niños, and the newer versions of the GCMs are starting to produce marginally more realistic results.

The regional circulation patterns are credible across models, although the biases between models and the diversity of frequency of regional circulation models **highlight the critical importance of not using any single one model**. The information from circulation changes lies in assessing the results across models, and taking one model in isolation is as likely to lead to an erroneous conclusion as it is to provide some partial value.

[1] Some refer to GCMs as "Global Climate Models".

c) Assessing uncertainty in the climate projections. The uncertainty associated with climate modeling is one of the leading problems in climate change studies. Uncertainty arises from the inherent stochastic and chaotic behavior of the climate system, from structural errors of models, from simplifications in the modeling system, from lack of scientific knowledge, and a host of other secondary factors. The 2013 IPCC WG1 AR5 report states: *"...there does not exist at present a single agreed on and robust formal methodology to deliver uncertainty quantification estimates of future changes in all climate variables"*.

A number of experimental and traditional methods are explored. Analyses are motivated by the need to provide quantitative estimates of projection uncertainty for South Africa consistent with state-of-the-art of relevant methods and concepts. In particular, we address a comprehensive description of uncertainties, explore two relatively new avenues of assessing GCM performance, analyze uncertainties involved in statistical downscaling of GCM output to higher resolution, local scale level, and evaluate climate projection uncertainty using traditional methods.

We introduce approaches to analyze multi-method ensembles and the consistency in time and space between the spread of the method-specific ensembles to explore its implication to the interpretation of climate change signal derived from individual methods. Three dominant "spaces" are identified where uncertainty in projections of future climate arise; the socio-economic space, climate system space, and model space. Each of these is discussed.

Quantitative assessment is explored through a new experimental procedure to examine the climate system high-dimensional space to characterize the local-scale variance in context of the larger determining state of the atmosphere. This indicates a strong value potential for this approach, but will need significant further work to develop to the point of robustness.

Following this the role of small scale (sub-grid) processes in contributing to uncertainty of rainfall projections is examined. The uncertainty arising from this probabilistic nature of local response to large-scale synoptic forcing is relatively large and this uncertainty is only partly sampled by the ensembles. Because of its magnitude, it may be important for determination of significance of the change signal, and the interpretation of ensemble results in terms of change signal consistency and significance against the natural variability.

Finally, the uncertainty of projections is assessed through more traditional approaches by analysing ensemble spread from multi-model, multi-method data sets. The degree of agreement between methods (ensembles) varies between variables and seasons. For summer rainfall there is a broad consistency and for summer temperatures there is relatively little difference in tendency and magnitude in each of the ensembles. For winter temperatures the ensemble differences are more pronounced.

At the sub-continental scale, the multi-model, multi-method data (GCMs and statistical downscaling) allows for a straightforward derivation of climate change messages with varying degrees of confidence dependent on location, season and variable. There is more confidence in temperature projections in the coastal regions than in the continental interior. For rainfall, there are indications of higher confidence in low rainfall regions.

In summary, the analysis of agreement/differences in ensemble spread and tendency from three methods has potential to contribute to confidence statements about local and regional climate change messages.

d) Downscaled projections. This section focuses on downscaled data, which is the next source of climate data to be included in the conceptual framework for integrating regional information. Downscaling seeks to add finer resolution information to GCM output and is seen as the only viable approach to achieve regional scale information consistent with the global and hemispheric forcing. Two sources of downscaling are considered. First is that of the Coordinated Regional Downscaling Experiment (CORDEX) operating under the Working Group on Regional Climate (WGRC) of the World Climate Research Programme (WCRP). The main goal of CORDEX is to develop an improved generation of regional climate change projection information for input into impact and adaptation studies. Second is statistical downscaling, which is based on the established method from CSAG.

A clear message of warming over South Africa is seen in the raw GCM output as well as both downscaling methods. Warming is projected to be most intense over the drier parts of the interior, while less intense along the coast. Some measure of disagreement in the exact spatial distribution and magnitude of warming is evident between GCMs and between different downscaling products, but does not undermine the basic message.

Projected changes in precipitation into the future are less confident than for temperature. GCMs disagree on the sign of change over the region with some projecting strong wetting while others projecting strong drying. The range projected by the two downscaling methods is narrower than that of the driving GCMs. However, there is still strong disagreement in the sign of change and placement of areas of wetting or drying. The ensemble mean change also disagrees between the two downscaling methods which widens the spread of projected changes.

This section once again highlights the dangers of using a single GCM or a GCM downscaled by a single downscaling method. The next step is to explore ways of better distilling relevant and robust messages from the different sources and interpreting them in the light of historic trends and variability and understanding the large-scale dynamics and processes responsible for these changes.

2. Framework of integration

In any climate data source there is both implied and real information, and the final robustness of any message is subject to the interpretation of the scientists and users. Context is highly relevant, and a product can be robust at larger scales but questionable at small scales. The information required by users is highly dependent on the application, the relevant scales in time and space, and the user's risk exposure. The final section of the report thus demonstrates how the climate information may be a) distilled to key messages, and b) integrated with the sector and/or place-based context of any application.

The approach is based on the idea of progressive layering of information to find the intersection of individual elements of robust information, and so to lead to a conclusion that is defensible and informative to the user. One begins by ignoring the climate information to first identify the points of vulnerability in a system, and then consider whether and how these points of system vulnerability are sensitive to climate factors. With an initial assessment of systems vulnerabilities, independent of the climate factors, one is in a position to layer on additional climate information drawing from the understanding of each of the foundation sources of information. At this point one has an emerging picture of the system vulnerabilities alongside what one can say with reasonable robustness about the past changes in the climate system.

In the final stage, one looks for the intersection of sensitivities in the sector / place with the identified strong messages of change. This approach allows for quick identification of how critical points of vulnerability that are sensitive to climate forcing relate to the defensible climate change understanding. In some respects the process is relatively intuitive. However, articulating vulnerabilities in terms of thresholds is difficult, and often not attempted. Further, the propensity of users to treat data as information means the distillation of the multiple lines of evidence is commonly not undertaken, which leads to subsequent confusion when climate data introduces contradictions.

3. Examples of application

The developed framework was applied in two contexts. First through a series of workshops, which engaged stakeholders in the Berg River municipality of the Western Cape. Second, the evolving ideas were tested in a separate project action with 5 African cities.

In each case the activities began with examining the non-climate stressors and key sector/place sensitivities and vulnerabilities independent of climate change. Following this the four avenues of climate information were examined, and the robust messages that could be drawn were then identified. Last, the climate messages, as a function of scale and time, were assessed against the sector / place sensitivities and vulnerabilities to evaluate what can be said about the impact of climate change with some confidence, in order to inform the adaptation and decision options.

It is apparent from the experiences that the conceptual approach presents a powerful co-exploration paradigm that productively departs from the linear supply chain mentality. Of particular note is how the climate scientists learned from, and were greatly sensitized by engaging the sector participants, and vice versa; this mutual exchange of understanding was a significant factor to finding defensible and rational messages for action.

The activities clearly indicate that it is possible to identify robust points of intersection between the multiple and disparate data sources – arguably the leading contribution to maladaptation in the decision maker's sphere of activities.

ACKNOWLEDGEMENTS

The project team gratefully acknowledges the support from the WRC, and particularly the valuable input from the reference committee, who comprised:

Mr C Moseki (Chair, WRC)
Dr E Archer, CSIR
Mr S Tefera, WRC
Mr A Moatshe, ESKOM
Dr M Shongwe, SAWS
Dr W Landman, CSIR
Prof GGS Pegram, Pegram and Associates

The following Postdoctoral Research Fellow was engaged in some or all of the project work:

Joseph Daron (United Kingdom)

The following PhD students have incorporated the project activities in their thesis:

Arlindo Meque (Mozambique)
Michael Kent (South Africa)
Hussen Seid (Ethiopian)
Izidine Pinto (Mozambique)
Kamoru Abiodun Lawal (Nigeria)

The following research assistants were engaged in some or all of the project work:

Lisa Coop (South Africa)
Kate Sutherland (South Africa)
Anna Steynor (South Africa)

The following interns were directly engaged in project activities (interns are appointed to CSAG for one year following their undergraduate degree):

Claire van Wyk (South Africa)

Finally, the authors would also like to thank Sabina Abba Omar and Sheveenah Taukoor who were involved in compiling the final report.

Table of Contents

EXECUTIVE SUMMARY iii
ACKNOWLEDGEMENTS viii
TABLE AND FIGURE LIST xii
LIST OF ABBREVIATIONS xvii
1. PROJECT OBJECTIVES AND MOTIVATION 1
1.1. Context 1
1.2. Summary of approach 2
1.3. Ethical considerations 4
1.4. Objectives 4
1.5. Structure of the Report 5
2. OBSERVED CLIMATE CHANGE OVER SOUTH AFRICA 6
2.1. Introduction 6
2.2. Monthly historical station trends over South Africa 6
2.2.1. *Station Selection* 7
2.2.2. *Monthly statistics* 7
2.2.3. *Statistical Significance* 8
2.2.4. *Visualisation* 8
2.3. Results 9
2.3.1. *South Africa* 9
2.3.2. *Western Cape* 13
2.4. Conclusions 17
3. MODES OF VARIABILITY REPRESENTED IN CLIMATE MODELS WITHIN THE CMIP5 FRAMEWORK 18
3.1. Introduction 18
3.2. Background to Model Evaluation 18
3.3. Modes of Variability 20
3.3.1. El Niño – Southern Oscillation (ENSO) 20
3.3.2. The representation of ENSO in GCMs 23
3.3.3. The Indian Ocean Dipole (IOD) 25
3.3.4. The IOD in GCMs 26
3.4. Datasets and methods 27
3.5. Preliminary results 28
3.5.1 ENSO in CMIP5 28
3.6. CMIP5 Model Circulation Patterns 32

3.7. Summary 35
4. APPROACHES TO QUANTIFY UNCERTAINTY OF CLIMATE PROJECTIONS 38
4.1. Introduction 38
4.2. Sources of uncertainty of climate change projections 39
4.2.1. *Uncertainties in the socio-economic space* 40
4.2.2. *Uncertainties in the climate system space* 42
4.2.3. *Uncertainties in the model space* 43
4.2.4. *Climate simulation ensembles and projection uncertainty* 44
4.2.5. *Multi-model ensembles* 45
4.3. Exploring model representation in high-dimensional space 46
4.4. Evaluating the role of small scale (sub-grid) processes in contributing to uncertainty of rainfall projections 48
4.4.1. *Methods* 49
4.4.2. *Results* 50
4.5. Assessing uncertainty of projections in the model space – analysing ensemble spread from multi-model, multi-method data set 56
4.5.1. *Methods* 56
4.5.2. *Results* 57
5. PROJECT SPECIFIC DOWNSCALED PRODUCTS FOR SOUTH AFRICA 74
5.1. Overview 74
5.2. Downscaling Structure 75
5.3. CMIP5 GCMs 76
5.4. CORDEX 77
5.4.1. *SMHI-RCA4* 78
5.4.2 *CLMcom CCLM4* 79
5.5. Self-Organising Map based Downscaling 82
5.6. Climate Change Results 85
5.6.1 *CMIP5 GCM Results* 85
5.6.2 *Dynamically Downscaled Results* 91
5.6.3. *Statistically Downscaled Results* 95
5.7. CONCLUSION 103
6. FRAMEWORK FOR INTEGRATING LINES OF EVIDENCE 104
6.1. Objectives 104
6.2. What climate data ideally seeks to achieve 105
6.3. Frameworks for using regional downscaling information 106
6.3.1. *Physical climate information* 107

6.3.2. *Integration in a context of non-climate stressors* 108
6.4. Summary 113
7. EXAMPLES OF INTEGRATING LINES OF EVIDENCE 115
7.1. Background 115
7.2. A stressor-driven approach in the Berg River Municipality 116
7.2.1. *Investigating vulnerabilities and historical climate* 116
7.2.2. *Investigating climate impact on current activities* 118
7.2.3. *Examining the impact of future projections of change and adaptation options* 120
7.3. African Cities case study 122
7.3.1. *CSAG/START workshop summary* 123
7.4. Conclusions and Outcomes 123
8. REFERENCES 125
APPENDIX A 134
APPENDIX B 136

TABLE AND FIGURE LIST

Table 4.1 | *Schematic of sources of uncertainty in climate projections, and their quantification in typical model experiments. Column widths represent entire uncertainty range for given source, shading represents part quantified within given experiment. Widths of shaded sections are arbitrary, and are intended to convey information only of "bigger than" or "less than" nature, which is valid only within each column.* 41
Table 7.1 | *Example of a stressor vs livelihood matrix from the Berg River Municipality* *119*
Table 7.2 | *Including future projections in stressors vs livelihoods matrix* *121*

Figure 1.1 | *An overview of the project activity components building toward deliverable robust messages of regional change.* 3
Figure 2.1 | *Statistically significant (90-99% levels) monthly total rainfall trends for stations across South Africa expressed as percentage change per decade.* 10
Figure 2.2 | *Monthly rainfall anomalies at 'Dombietersfontein' (see map insert, top right hand corner, for station location) from 1960-2012. The month and average rainfall (in brackets) is given at the top of each panel. The dashed (solid) black line shows the trend (statistically significant - 90th percentile) as the decadal change in monthly rainfall. If the trend is significant the decadal change is given in the top left hand corner (mm/decade).* 11
Figure 2.3 | *Statistically significant (90-99%) monthly wet day trends for stations across South Africa expressed as percentage change per decade.* 12
Figure 2.4 | *Average monthly rainfall (mm, blue bars), maximum temperature (°C, red line) and minimum temperature (°C, green line) for stations located in a) Cape Town, b) George, c) Durban and d) Johannesburg. Note that the y-axis values vary per graph.* 13
Figure 2.5 | *Monthly rainfall anomalies at Owen Dam (see map insert, top right hand corner, for station location) from 1960-2012. The month and average rainfall (in brackets) is given at the top of each panel. The dashed (solid) black line shows the trend (statistically significant - 90th percentile) as the decadal change in monthly rainfall. If the trend is significant the decadal change is given in the top left hand corner (mm/decade).* 14
Figure 2.6 | *Statistically significant (90-99% levels) monthly total rainfall trends for stations across the Western Cape expressed as percentage change per decade.* 15
Figure 2.7 | *Statistically significant (90-99%) monthly wet day trends for stations across the Western Cape expressed as percentage change per decade.* 15
Figure 2.8 | *Monthly rainfall anomalies at 'Herold-Pol' station (see map insert, top right hand corner, for station location) from 1960-2012. The month and average rainfall (in brackets) is given at the top of each panel. The dashed (solid) black line shows the trend (statistically significant - 90th percentile) as the decadal change in monthly rainfall. If the trend is significant the decadal change is given in the top left hand corner (mm/decade).* 16
Figure 3.1 | *Normalised SST anomalies for the month of December 1997 (El Niño event; left) and December 1987 (La Niña event; right) in the Pacific Ocean. The black box refers to the Niño 3.4 region (5°N - 5°S; 170°W - 120°W) which is used to create the Niño-3.4 index illustrated in Fig. 3. 2. The data used to create the figures is from HadISSTv1.1 and the mean is based on the 1950-2010 period.* 21

Figure 3.2 | *Standardized anomalies for the Niño-3.4 index (see Fig. 3.1 for location) for the 1950-2009 period using HadISST1.1 data. This monthly data is at a 1° x 1° spatial resolution and available from 1870 to present. Time series is smoothed using a 5-month running mean.* 22
Figure 3.3 | *Global rainfall anomalies (mm/day) during the austral summer months (DJF) associated with five of the strongest El Niño events since 1980 (determined from the Niño-3.4 index in Fig. 3.2). GPCP data is used to create the figure, which is available at 2.5° resolution from 1979-2011.* 23
Figure 3.4 | *The figure, showing SST anomalies in the Indian Ocean during September 1997, depicts the location of the western and eastern regions used to calculate the IOD (top black squares) and SIOD (bottom black squares). In this example, the anomalies illustrate a positive IOD and negative SIOD.* 26
Figure 3.5 | *ENSO seasonality determined from the std. dev. of SST anomalies (for 100 years and detrended) in the Niño-3 region (5°N - 5°S; 150°W - 90°W). Results from the eight models, which are discussed in the text, and for the observation dataset (HadISST1.1; 1900-1999) are shown. Note that the 12 months have been doubled so that the austral summer (DJF) is the centre of the figure.* 29
Figure 3.6 | *Mean SST std. dev. (°C) for 100 year of monthly data from eight models discussed in the text. The observations (top left corner) are taken from HadISST1.1 data for the 1900-1999 period.* 30
Figure 3.7 | *Mean DJF rainfall (mm/day) for the period 1980-2009 in GPCP data.* 31
Figure 3.8 | *Mean DJF rainfall (mm/day) for the period 1976-2005 in various CMIP5 models. Note that the models used here may not necessarily be the same as those used previously.* 31
Figure 3.9 | *DJF anomalies (mm/day) for the five strongest ENSO events in the last 30 years of the models (1976-2005). Note that SST data was not available for two of the models (both are versions of MIROC) and hence, no data is displayed.* 32
Figure 3.10 | *December-February circulation archetypes of daily geopotential height at 700 hPa from the ERA-Interim dataset1979-2012. Decreasing geopotential heights from red – blue.* 34
Figure 3.11 | *Percentage frequency on December-February circulation archetypes of daily geopotential height at 700 hPa for observed ERA-Interim 1979-2012 (grey) and for 11 GCMs (1976-2005). Numbers represent the percentage frequency while the blue to red shows the model bias in frequency of each archetype.* 35
Figure 3.12 | *Projected change in circulation archetypes into the future for each of the 11 GCMs. The change in percentage frequency between 1976-2005 and 2040-2069 period. Both numbers and shading represents the absolute change in percentage frequency.* 36
Figure 4.1 | *Point clouds of daily data plotted in two of the EOF dimensions, with a sample short time trajectory of the data.* 47
Figure 4.2 | *Point cloud of daily data plotted in three EOF dimensions strongly related to the local scale precipitation response. Points are coloured by the magnitude of precipitation observed on each day.* 47
Figure 4.3 | *Point cloud of daily data plotted in three EOF dimensions weakly related to the local scale precipitation response. Points are coloured by the magnitude of precipitation observed on each day.* 48
Figure 4.4 | *Relationship between probabilistic component IQR of Monte-Carlo ensemble) and overall wetness (expressed as mean annual rainfall) as well as rainfall variability (expressed as standard deviation of daily rainfall) for three rainfall indices* 52
Figure 4.5 | *Relative importance of the probabilistic component (IQR expressed as a % of median of the Monte-Carlo ensemble) as a function of overall wetness (expressed as mean annual rainfall) for three rainfall indices* 53

Figure 4.6 | *Spatial distribution of median values and probabilistic component (IQR of Monte-Carlo ensemble) for three rainfall indices.* 54
Figure 4.7 | *Spatial distribution of relative importance of probabilistic component, expressed by IQR as a percentage of median value of the Monte Carlo ensemble, for three rainfall indices.* 55
Figure 4.8 | *"Cascade of uncertainty" for change in mean monthly rainfall for DJF (left) and JJA (right) for two RCP scenarios and three ensembles: 16 GCMs (gcm16), 10 statistical downscaling realizations (somds10) and 8 regional climate model realizations (rcm8) averaged over the domain covering the land body of southern Africa (35^o-20^{o}S, 10^o-40^{o}E). Bars on the right-hand side of the graphs mark IQR for each ensemble/RCP combination.* 59
Figure 4.9 |*"Cascade of uncertainty" for change in mean monthly minimum temperature for DJF (left) and JJA (right) for two RCP scenarios: 16 GCMs (gcm16), 10 statistical downscaling realizations (somds10) and 8 regional climate model realizations (rcm8) averaged over the domain covering the land body of southern Africa (35°-20°S, 10°-40°E). Bars on the right-hand side of the graphs mark IQR for each ensemble/RCP combination.* 60
Figure 4.10 | *"Cascade of uncertainty" for change in mean monthly maximum temperature for DJF (left) and JJA (right) for two RCP scenarios: 16 GCMs (gcm16), 10 statistical downscaling realizations (somds10) and 8 regional climate model realizations(rcm8) averaged over the domain covering the land body of southern Africa (35°-20°S, 10°-40°E). Bars on the right-hand side of the graphs mark IQR for each ensemble/RCP combination.* 61
Figure 4.11 | *Maps of IQR of future-past change in rainfall (upper row) and ensemble median of the future-past change in rainfall, in somsd10, gcm16 and rcm8 ensembles, for DJF, under RCP 4.5.* 65
Figure 4.12 | *Maps of IQR of future-past change in rainfall (upper row) and ensemble median of the future-past change in rainfall, in somsd10, gcm16 and rcm8 ensembles, for JJA, under RCP 4.5.* 66
Figure 4.13 | *Maps of IQR of future-past change in minimum temperature (upper row) and ensemble median of the future-past change in minimum temperature, in somsd10, gcm16 and rcm8 ensembles, for DJF, under RCP 45.* 67
Figure 4.14 | *Maps of IQR of future-past change in minimum temperature (upper row) and ensemble median of the future-past change in minimum temperature, in somsd10, gcm16 and rcm8 ensembles, for JJA, under RCP 45.* 68
Figure 4.15 | *Maps of IQR of future-past change in maximum temperature (upper row) and ensemble median of the future-past change in maximum temperature, in somsd10, gcm16 and rcm8 ensembles, for DJF, under RCP 45.* 69
Figure 4.16 | *Maps of IQR of future-past change in maximum temperature (upper row) and ensemble median of the future-past change in maximum temperature, in somsd10, gcm16 and rcm8 ensembles, for JJA, under RCP 45.* 70
Figure 4.17 | *Comparison of IQR of future-past change in rainfall somsd10 (left column) and gcm10 (middle column) and difference between them – significant at 0.05 confidence level hatched (right column), for DJF (upper row) and JJA (lower row), RCP 45.* 71
Figure 4.18 | *Comparison of IQR of future-past change in minimum temperature in somsd10 (left column) and gcm10 (middle column) and difference between them – significant at 0.05 confidence level hatched (right column), for DJF (upper row) and JJA (lower row), RCP 45.* 72
Figure 4.19 | *Comparison of IQR of future-past change in maximum temperature in somsd10 (left column) and gcm10 (middle column) and difference between them – significant at 0.05 confidence level hatched (right column), for DJF (upper row) and JJA (lower row), RCP* 73
Figure 5.1 | *The conceptual framework for developing regional climate change information.* 74
Figure 5.2 | *Typology of downscaling approaches.* 76

Figure 5.3 | *The framework of the dynamic downscaling experiment design in CORDEX. The boxes in brown represent on going work by the community of modellers.* 78
Figure 5.4 | *The top left panel shows the mean June-August-September precipitation of the GPCP observational data set. The remainder of the top row are the bias of other observational data sets with respect to the GPCP. Below this are the anomalies of 12 RCM simulations relative to the GPCP. While the RCM biases are marginally larger than the biases between the observational data sets, the results indicate the RCMs can capture credibly the regional climate of Africa (Nikulin et al. 2012).* 80
Figure 5.5 | *This figure explores the issue of model bias further by examining the bias of the RCMs relative to a single observational data set (GPCC) over the southern Africa region during austral summer. The results show that all models have a wet bias over South Africa during the austral summer season especially over the eastern interior with some also showing a slight dry bias over the far north of the country (Kalognomou et al., 2013).* 81
Figure 5.6 | *Seasonal mean daily precipitation for WFDEI observed climatology (top row), for ERA-Interim statistically downscaling climatology (middle row) and bias (bottom row).* 84
Figure 5.7 | *Seasonal mean daily maximum for WFDEI observed climatology (top row), for ERA-Interim downscaling climatology (middle row) and downscaling bias (bottom row).* 85
Figure 5.8 | *Future anomalies for summer (DJF) daily minimum temperature (°C) for the mid-21st century (2041-2070 – 1976-2005) under the RCP8.5 emission scenario for 11 raw CMIP5 GCMs.* 87
Figure 5.9 | *Future anomalies for summer (DJF) daily maximum temperature (°C) for the mid-21st century (2041-2070 – 1976-2005) under the RCP8.5 emission scenario for 11 raw CMIP5 GCMs.* 88
Figure 5.10 | *Future anomalies for summer (DJF) daily mean precipitation (mm/day) for the mid-21st century (2041-2070 – 1976-2005) under the RCP8.5 emission scenario for 11 raw CMIP5 GCMs.* 89
Figure 5.11 | *Future anomalies for spring (SON) daily mean precipitation (mm/day) for the mid-21st century (2041-2070 – 1976-2005) under the RCP8.5 emission scenario for 11 raw CMIP5 GCMs.* 90
Figure 5.12 | *Future anomalies for summer (DJF) daily precipitation (mm/days) for the mid-21st century (2041-2070 – 1976-2005) for 8 GCMs dynamically downscaled using the SHMI-RCA4. Top panel is ensemble mean anomaly while all other plots are for individual models.* 92
Figure 5.13 | *Future anomalies for spring (SON) daily precipitation (mm/day) for the mid-21st Century (2041-2070 – 1976-2005) under the RCP8.5 emission scenario for 8 CMIP5 GCMs dynamically downscaled using the SHMI-RCA4 RCM. Top panel is the ensemble mean anomaly while all other plots are for individual models.* 93
Figure 5.14 | *Future anomalies for annual mean daily precipitation for the future period (2036-2065). Results are shown for four GCMS under both the RCP4.5 and RCP8.5 scenario (a1 – h1); dynamically downscaled results from the SMHI RCA4 model (m-t) and the CCLM model (e-l) along with the GCM ensemble mean (c & d) and RCM ensemble mean (a & b) under the two emission scenarios.* 94
Figure 5.15 | *Future anomalies for summer(DJF) daily minimum temperature (°C) for the mid-21st century (2041-2070 – 1976-2005) under the RCP8.5 emission scenario for 11 statistically downscaled CMIP5 GCMs. Top left panel is the ensemble mean anomaly while all other plots are for individual models.* 96
Figure 5.16 | *Future anomalies for summer(DJF) daily minimum temperature (°C) for the mid-21st century (2041-2070 – 1976-2005) under the RCP8.5 emission scenario for 11 statistically*

downscaled CMIP5 GCMs. Top left panel is the ensemble mean anomaly while all other plots are for individual models. 97
Figure 5.17 | *Future anomalies for summer(DJF) daily mean precipitation (mm/day) for the mid-21st century (2041-2070 – 1976-2005) under the RCP8.5 emission scenario for 11 statistically downscaled CMIP5 GCMs. Top left panel is the ensemble mean anomaly while all other plots are for individual models.* 98
Figure 5.18 | *Future anomalies for spring (SON) daily mean precipitation (mm/day) for the mid-21st century (2041-2070 – 1976-2005) under the RCP8.5 emission scenario for 11 statistically downscaled CMIP5 GCMs. Top left panel is the ensemble mean anomaly while all other plots are for individual models.* 99
Figure 5.19 | *Statistical downscaled average maximum temperature (top) and monthly total precipitation (bottom) results for Warmbad Towoomba station using 11 GCM under the RCP8.5 emission scenario for the period 2040-2060 minus 1980-2000. The future anomaly for each GCM is represented by a black line, while the ensemble 10^{th} and 90^{th} percentile is shown in red or blue depending on which statistic is being investigated. The observed climatology is presented as grey bars for the precipitation statistics.* 101
Figure 5.20 | *Statistical downscaled average maximum temperature (top) and monthly total precipitation (bottom) results for Cape Town Weather Office station using 11 GCM under the RCP8.5 emission scenario for the period 2040-2060 minus 1980-2000. The future anomaly for each GCM is represented by a black line, while the ensemble 10^{th} and 90^{th} percentile is shown in red or blue depending on which statistic is being investigated. The observed climatology is presented as grey bars for the precipitation statistics.* 102
Figure 6.1 | *Idealized representation of conceptual information issues in relation to using climate information for a given scale, variable, metric, and application. The curves are hypothetical, and in practice each line is a zone of gradation, but is represented here as a simple line for clarity (after Landman et al., 2010).* 105
Figure 6.2 | *Idealized and hypothetical matrix of a place-based approach to identify sensitivities and vulnerabilities to changes in drivers and stressors.* 109
Figure 6.3 | *Idealized and hypothetical example of a matrix for identifying robust understanding of past climate change.* 110
Figure 6.4 | *Idealized example of a matrix for identifying robust understanding of projected future climate change.* 111
Figure 6.5 | *Considering the sensitivities in terms of the disaggregated climate information to examine the overlay of strong messages with the system vulnerabilities.* 112
Figure 6.6 | *Example matrix from the City of Maputo. Note: Each cell within the matrix is divided in half. The left half corresponds to the impact of the non-climate stressor on the element (Low, Medium or High), and the right half corresponds to the change in impact when bringing in the climate stressor.* 114
Figure 7.1 | *A group discussion around current stressors* 117
Figure 7.2 | *Example of identified stressors from the Berg River Municipality* 117

For brevity, tables and figures in the appendix are not listed here

LIST OF ABBREVIATIONS

AAO	Antarctic Oscillation
AOGCMs	Atmosphere-Ocean General Circulation Models
AR4	Fourth Assessment Report
AR5	Fifth Assessment Report
CCLM	Climate Limited-Area Modelling Community
CMIP	Coupled Model Intercomparision Project
CMIP3	Coupled Model Inter-comparison Project Phase 3
CMIP5	Coupled Model Inter-comparisons Project Phase 5
CORDEX	Coordinated Regional Climate Downscaling Experiment
CSAG	Climate System Analysis Group
DJF	December, January and February
DMI	Dipole Mode Index
ENSO	El Niño-Southern Oscillation
GCM	General Circulation Model
GHG	Greenhouse Gas
GPCC	Global Precipitation Climatology Centre
GPCP	Global Precipitation Climatology Project
ICE	Initial Condition Ensemble
IOD	Indian Ocean Dipole
IPCC	Intergovernmental Panel for Climate Change
IQR	Inter-Quantile Range
ITCZ	Intertropical Convergence Zone
JJA	June, July and August
LTAS	Long Term Adaptation Strategy
MAM	March, April and May
MME	Multi-Model Ensemble
NCAR	National Centre for Atmospheric Research
NCEP	National Centre for Environmental Prediction
PDA	Plausible, Defensible and Actionable
PPE	Perturbed Physics Ensembles
RCA3	Rossby Centre Regional Climate Model
RCMD	Dynamical Regional Climate Model
RCP	Representative Concentration Pathway
SAM	Southern Annual Mode
SAWS	South African Weather Service
SIOD	Subtropical Indian Ocean Dipole
SMHI	Swedish Meteorological and Hydrological Institute
SOI	Southern Oscillation Index
SOM	Self Organising Map
SOMD	Self Organising Map based Downscaling
SON	September, October and November

SRES	Special Report Emission Scenarios
SST	Sea Surface Temperatures
TTT	Tropical-Temperate Trough
UCT	University of Cape Town
WFDEI	WATCH Forcing Data 20th Century Dataset ERA
WG1	Working Group 1
WGCM	Working Group on Coupled Modelling
WRCP	World Climate Research Program

Chapter 1

PROJECT OBJECTIVES AND MOTIVATION

1.1. Context

This report addresses issues underlying the critical question "*How do I assess the regional climate change information for my sector / location / decision / policy?"*

The challenges of understanding the regional manifestations of climate change are nuanced and embedded in significant conceptual awareness that is delicate and complex. Within this context this project addresses a particular subset of avenues (see section 1.4 on overarching objectives). The reader is strongly advised to especially take Chapter 21 of the AR5, "*Regional Context*", for which the principle investigator of this project was also the AR5 coordinating lead author. The project has anticipated the outcomes of, and evolved in parallel to the activities of the IPCC's 5th Assessment Report (AR5), as well as drawn upon the project investigators participation in the AR5.

Chapter 21 of the AR5 frames the discussion of both global and regional issues in a decision-making context including both the physical and socio-economic aspects that surrounds changes in the physical climate system, the associated impacts and vulnerabilities, and the degree of confidence that we have in understanding these on a regional basis.

Anthropogenic climate change is, in many respects, a problem of ethics. The challenges only exist because of the choices humankind has made, and our future depends on the choices we will make – choices that are now, in part, predicated on projected climate change. At the regional scale our choices are complicated by the large uncertainties in the degree and rate of change and our incomplete knowledge of how human and physical systems will respond (Hewitson et al., 2014). The recognition that change is already happening has accelerated investment in adaptation, yet this is compounded by the disparate and conflictual information resources available to the user.

The report does not present definitive answers for South Africa, but instead recognizes that the information and data sources (the two are not equivalent) are constantly evolving. The central problem is that the broader scientific community is seeking to operationalize what is effectively incomplete and ongoing research, and doing so under the imperative of user needs.

There is a time imperative that is real (we need to understand the local expression of the global change), that is perceived (not everyone is actually in need of this knowledge), and that is due to the danger of maladaptation from miscomprehension of the available information. As noted by Sarewitz (2011), "*"Progress waits not on better science, nor on better science communication, but on new approaches that focus first on articulating an*

inclusive and compelling politics built on a rich array of possibilities for the future. Only then can the meaning of science production become clear."

To this end the project seeks to explore avenues that can productively contribute to the development of an integrative framework that can facilitate the defensible development of relevant regional climate change messages.

Current knowledge about climate change has led to some high-level key messages (the world is warming, the system is changing) in which we have high confidence as regards to the large scale. However, at regional scales of critical relevance to resource management, decision makers, and policy there remains a lack of clarity on some essential aspects. This results in reduced confidence on regional details of projected climate change.

1.2. Summary of approach

To advance our understanding of regional change requires a number of issues to be addressed, such that the integration of multiple lines of evidence may be drawn upon to best explore the data and so construct defensible messages of relevance. The approach should ideally maximize the use of the multiple lines of evidence available to the user in order to derive as robust a conclusion as possible. Figure 1.1 outlines a conceptual framework for accomplishing this. In this approach one considers the historical changes from observed data, changes in the driving circulation patterns, the projected changes at the regional scale from the Global Circulation Models (GCMs), and from the information downscaled from the GCMs. This approach was the conceptualized intent of the IPCC 4th Assessment Report's chapter on Regional Climate Projections (Christensen et al., 2007).

The report adopts this approach, working through the core elements and concluding with a worked example for the Western Cape, South Africa.

Of central importance in undertaking this approach is identifying sources of uncertainty and attributing probability / confidence levels to these projections. Addressing this requires a unique mix of analysis covering historical baseline data, an understanding and application of climate models, skill in multi-method downscaling, and expertise in developing envelope approaches to projecting the future response of the quasi-stochastic climate system. At the core is a need is to provide information that is credible (as in, it is realistic), defensible (meaning it is rooted in an understanding of physical processes), and ultimately actionable (with high enough confidence to support implementation in policy and adaptation measures). When examining the chain of information from scenarios of greenhouse gas emissions, through modeling and downscaling, to adaptation and policy response, and coming full circle to mitigation, there are key elements limiting society's response.

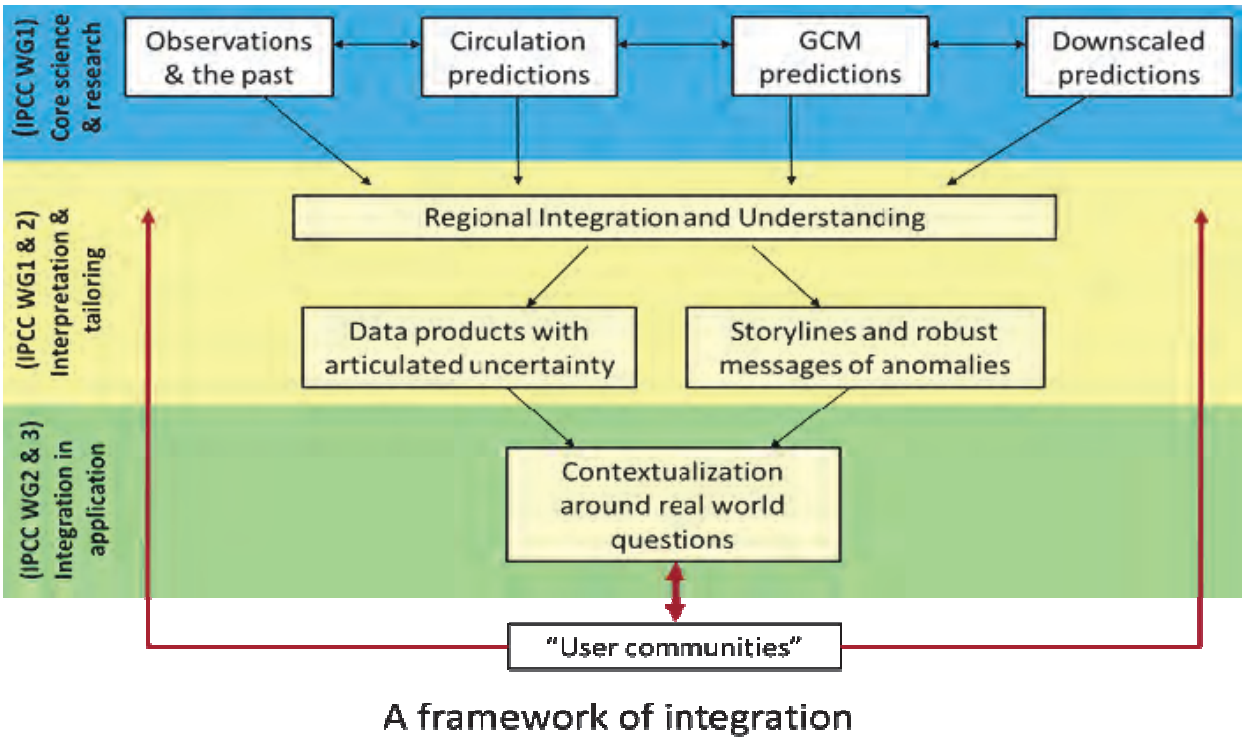

Figure 1.1 | *An overview of the project activity components building toward deliverable robust messages of regional change.*

These sources of uncertainty can be usefully categorized, such as in the IPCC guidance document on uncertainty (IPCC, 2005), but in the context of South Africa water resources, they center on uncertainty from structural issues (from the models and tools employed), climate system dynamics (such as feedbacks, teleconnections, natural variability, etc.), and inappropriately tailored products (as when temporal and spatial resolution are mismatched to the user need). The greatest opportunity for advancing knowledge for water resource management lies in addressing the weak links within this framework. The priority areas for this are:

- Developing approaches to selecting and integrating data from models (e.g. Pierce et al., 2009)
- Using multi-model ensemble data sets in order to assess the envelope and probability basis of projected change
- Assessing the natural variability of the system in order to appropriately contextualize the climate change projection
- Employing defensible downscaling and tailoring of climate change information to stakeholder needs, with associated confidence measures

If solid advances can be made in these areas, South Africa will have an excellent foundation for framing future long term developments, and at the same time improve the robustness of current climate information for impact and adaptation work. Conversely, if these issues are not dealt with in a rigorous manner, climate change information will continue to be fragmented and difficult for users to assess and apply.

1.3. Ethical considerations

While this is beyond the scope of the project, it is raised here as an intrinsic issue related to the production, communication and uptake of information. Thus, is critical for the user and producer of climate change information to be cognizant of these issues, and to take them into consideration when acting on information provided.

Decision makers are, and will continue to establish decision pathways into the future. These in turn set in place outcomes with real societal consequence, and with real costs of reversal if required. This is undertaken on the basis of the (perceived and accessible) knowledge authorities about relevant climate change. The questions are thus raised as to who holds the knowledge, how is this constructed, what is chosen for dissemination, how is this communicated, by what authority is this done so, what responsibility do purveyors of information carry, and what accountability is in place (if any)?

Consequently, this project is predicated on the ideals that:

a) When engaged in face-to-face interaction between scientist and "user", the need for co-exploration of climate information by scientist and user is explicitly recognized, and through this is tolerant of sub-optimal and/or conflicting and/or confusing data resources.
b) In Africa, where we have an enormous capacity deficit for face-to-face interaction, there is necessarily a large element of communication through written and online resources which is inherently incomplete in terms of time and space scales of relevance.

Thus, the ethical and responsible approach is to enable a robust framework for assessing information, as is the focus of this report.

1.4. Objectives

The project proposal identified eight overarching objectives for exploration. Some of these have dependencies beyond the projects control, such as availability of emerging data sets, while others were anticipated to be of a nature that may lead to dead-ends, but nonetheless needed to be explored. The initial proposed objectives were:

1. Explore the changes in regional rainfall in relation to climate processes on multiple scales, and so develop a more confident understanding of the regional expression of anthropogenic climate change in relation to natural variability.
2. Assess techniques in probability / uncertainty analysis for application to South Africa climate change projections, drawing on existing literature, perturbed physics simulation techniques, and contextualized by understanding of natural variability.
3. Integrate emerging data sources, and especially from multiple models of CMIP5, CORDEX, along with local institutional climate modeling activities to support the

development of regional climate change projections with associated measures of the envelope of possibilities and uncertainty.

4. Develop region-relevant skill assessment of model and downscaled climate change projections, and apply appropriate measures for evaluating the quality and value of the different data sources so as to maximize the development of robust interpretations and probability measures.
5. Develop and test a framework for incorporating the advances of the above aims into a robust approach to developing regional climate change projections, with appropriate support information on probability and confidence.
6. Leverage the value of existing perturbed physics model simulations for South Africa (from the UCT/Hadley centre collaboration) to strengthen the assessment of possible attribution of regional climate change.
7. Incorporate new knowledge in relation to the above aims in existing climate services activities for the dissemination and communication of regional climate change.
8. Subject to resources, incorporate the regional projections into a hydrological model and/or collaborate with external partners to assess the consequences in relation to the existing literature.

As is the nature of research, the exploration of these objectives led to evolving directions as results emerged, and with the oversight of the reference committee's input, the project developed to the final product of this report.

1.5. Structure of the Report

Central to the development of robust regional messages is the concept of co-exploration; that is, a partnership between user and producer in the examination of the information. The user brings an application specific understanding of the information needs, while the producer contributes the scientific insight on limits and strengths of the data for the given application.

Within this context, Chapter 1 lays out the motivation, while Chapter 6 continues to unpack the approach of integrating multiple lines of evidence, and Chapter 7 presents an implementation of the conceptual approach. Complementing these, the intervening chapters provide a more technical exploration of the possible analytical approaches that can inform our understanding of the historical, circulation, GCM and downscaled data sources. These chapters examine the assumptions inherent in these data sources, and demonstrate what can be interpreted through different analyses.

Chapter 2

OBSERVED CLIMATE CHANGE OVER SOUTH AFRICA

2.1. Introduction

The exploration of historical observations of weather and climate serves a dual role in the context of developing defensible regional projections for a particular region. Firstly, observations and the analysis of these observations enhance our understanding of the nature of a variable climate as expressed in a particular region. Typically, fine scale observations reveal that the regional expressions of large scale climate shifts are far more complex and nuanced than might be expected. Indeed, one of the real challenges emerging out of regional climate modelling is the difficulty even relatively high resolution climate models have in reproducing historically observed patterns of change in many regions. It is therefore essential that we continue to explore and better describe historical change and variability in our region of interest.

Secondly, it is often very useful for decision makers to know if the climate has exhibited a consistent long term change over the past decades as this can provide some insight into historical trends of impacts such as water scarcity, crop yields, dam levels, disease spread, etc. Linking historical climate change with observed impacts of this change provides very useful insights into the potential impacts of climate change in the future. It is also very useful if a statistically significant fit can be found for some underlying driver, such as global warming, as this may provide some insight into the future impacts of global warming, at least on shorter time frames such as the next decade. Beyond the decadal time frame, the robustness of an extrapolation is very suspect as non-linear feedbacks and other complexities could rapidly begin to alter the regional response in ways that have not been observed.

This chapter therefore describes some methods for exploring observed trends in a regional climate system using South Africa as the exemplar region of interest. The broader spatial patterns of observed rainfall changes will be described, including some discussion on statistical significance and the seasonality of trends.

2.2. Monthly historical station trends over South Africa

Determining historical trends of rainfall over southern Africa, including South Africa, has been an ongoing challenge for many years. The challenge is largely a result of two factors; high natural rainfall variability that results in low occurrence of statistically significant trends, and low data continuity and coverage over a significant time period. The recent work done by MacKellar et al. (2014), emerging from work contributing to the Long Term Adaptation Strategy (LTAS) historical change report, re-iterated these particular challenges

and reports on only a small number of stations that show statistically significant rainfall trends.

The work done for this report relaxes some of the data constraints applied in MacKellar et al. (2014) in an attempt to gain some broader insights into historical changes. It is important to note up front that statistical significance tests for trends are merely used as an indicator of the likelihood that the trend observed is the result of some underlying monotonic process such as global warming. Lack of significance therefore does not imply that a change in rainfall has not occurred but rather that we cannot ascribe it to linearly varying underlying drivers. In terms of impacts, even non-significant trends can still be experienced as an impact and this is often corroborated by the experiences of farmers and other members of society who experience real change.

The analysis below draws on the most comprehensive set of daily observational data for South Africa that CSAG is currently able to provide. The only important data that has not been included due to the time frames and finalisations of usage agreements is a suite of stations from Lesotho. Due to the high importance of the Lesotho highlands as water catchment areas for South Africa this added suite of stations would provide useful insights into possible rainfall trends in this area. This data will be included in due course and the analysis repeated.

2.2.1. Station Selection

Station selection for this analysis draws from a suite of 4034 rainfall observing stations across South Africa extending from as early as 1850 through to the end of 2012 which is the most recent update of data obtained from the South African Weather Service (SAWS).

Stations for the analysis were selected by finding all stations that had less than 10% of values missing during the period 1960 through to the end of 2012. This resulted in 784 stations in the subset. Rather than attempt to find a subset of stations that provide 90% coverage for all three primary variables (minimum temperature, maximum temperature and precipitation), we focus on each variable independently and so greatly expand the set of rainfall reporting stations included. Indeed the same constraints applied to temperature results in a much smaller subset of 17 stations.

2.2.2. *Monthly statistics*

Prior analysis (see progress reports) has shown that there can be very complex patterns of trends through the year for a particular location. Some analyses focus on trends in annual statistics. This ignores the fact that many trends manifest as changes in seasonality (onset, duration, intensity and cessation) which may or may not also impact trends in annual aggregate statistics. For this reason other analyses such as MacKellar et al. (2014) have aggregated statistics on seasonal time scales (DJF, MAM, JJA, SON). However, as the

results below will show, even such seasonal analyses have the potential to blur and hide potentially important trends in particular months.

Therefore, this analysis aggregates daily statistics up to monthly statistics and all trend analysis is done on individual calendar months through time. The result is a greater number of figures but through effective visualisation the potential complexity can be facilitated. While the focus initially is on monthly total rainfall, similar analysis have been done for rain days, rain days > 10 mm, rain days > 20 mm, and maximum daily rainfall in a month.

2.2.3. *Statistical Significance*

Statistical significance of trends is derived from the p-value stemming from a t-test. The p-value indicates the probability that the trend observed could have been the result of random variability rather than some underlying process such as global warming. The p-value threshold selected is arbitrary and generally pragmatic. In some cases thresholds of 0.01 (99%) are used. In other cases this is relaxed significantly to 0.1 (90%). In this analysis a low significance level is used as an absolute threshold (90%) but the p-value itself is carried through to the visualisation in order to provide more information about trends and their varying significance levels. This is a middle position or compromise between ignoring significance completely and imposing very tight significance thresholds.

The Kendall-tau method is used to determine the p-value of the various trends and ordinary least squares regression is used to calculate the slope of the trends.

2.2.4. *Visualisation*

The results are presented as monthly maps of station trends. For each month, only those stations that exhibit a statistically significant trend at the 90^{th} percent level are displayed. Because trends are calculated for individual months through time this means that different months will produce a different set of stations with statistically significant trends. Therefore the station maps for each month will differ from other months.

Furthermore, the stations are represented as filled circles where the size of the circle indicates the degree to which the p-value is less than 0.1. Therefore, if a trend produces a p-value of 0.1 it will appear only as a very small circle. If the p-value is 0.05 then the circle will appear of medium size. For very small p-values approaching zero the circle will appear large. The colour of the circle indicates a positive (blue) or negative (red) rainfall trend with a colour range centred on white for zero trends. Trends are currently presented as percentage change over 10 years (i.e. per decade). Percentage change is problematic because it can identify very strong trends in very dry months (e.g. summer months in Cape Town) which are seldom really important. Absolute trends likewise are problematic as they will almost always show strong trends in very wet months but the magnitudes of the trends may not be significant in

comparison to the underlying climatology. It is therefore important to examine the trends with due consideration of the underlying climatology.

It is acknowledged that larger station circles will overlap on the map and will intensify the colour of a region. This is partly by design as a visual cue to identify regions with high density of statistically significant trends. The disadvantage is that sometimes single stations with opposite direction of trend can be "lost". This is a small caveat regarding the visualisation.

2.3. Results

2.3.1. *South Africa*

Figure 2.1 below shows the monthly trends for monthly total rainfall for stations across South Africa. A number of important features stand out. Most notably is the strong drying trend across the central and northeast of the country in April. MacKellar et al. (2014) identifies a similar trend in the MAM trend statistics. These results isolate the trend largely to the month of April indicating an early cessation to the summer rainfall regime. The strong drying trend in the centre of the country in July is an example of where percentage change can distort the interpretation. Mean monthly rainfall for many of the identified stations in July is around 5 mm and absolute trends over 10 years show a reduction of about 2.5 mm. These are very small changes and society is already resilient to low rainfall in these months.

Also of interest is the indication of trends in increasing rainfall across the centre of the country (slightly to the west) in the summer months December to February (e.g. Fig. 2.1 and Fig. 2.2). December, in particular, shows an increase in rainfall across the Free State suggesting a stronger start to the rainfall season. The positive trend seen in the monthly totals could be linked to the increase in frequency of wet days per month. Figure 2.3 shows the national map of trends of monthly wet days (in percentage change per decade). The patterns are roughly similar to the monthly total rainfall trend patterns which are to be expected but the dominant message emerging is that there are far more stations showing strong trends and statistically significant trends in rain days than for monthly total rainfall.

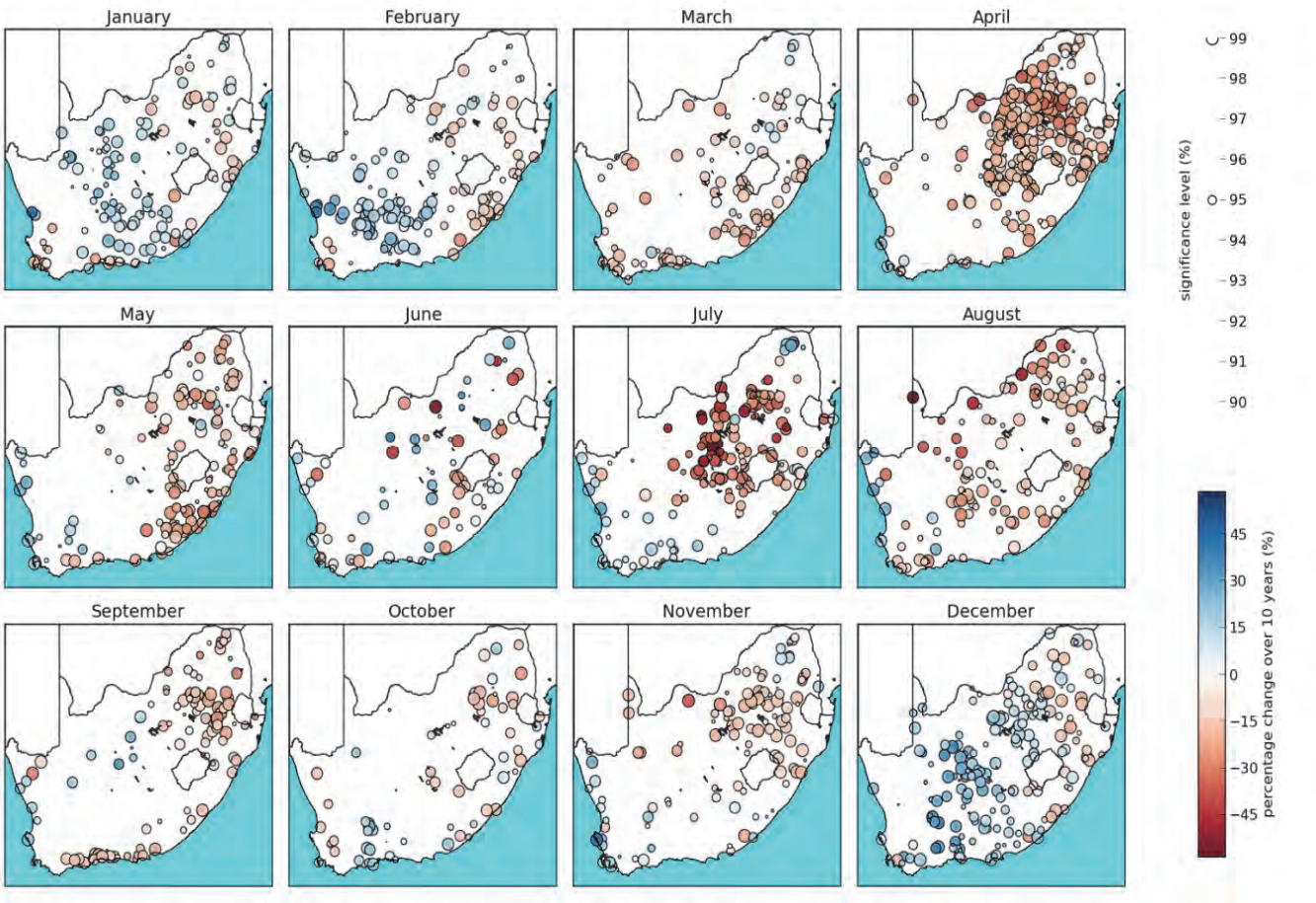

Figure 2.1 | *Statistically significant (90-99% levels) monthly total rainfall trends for stations across South Africa expressed as percentage change per decade.*

A common large-scale feature over southern Africa during the summer months are cloud bands evolving from tropical-extratropical interactions. These cloud bands, locally known as tropical-temperate troughs (TTT), typically extend diagonally from the northwest to the southeast over both the continent as well as the adjacent southwest Indian Ocean (Harrison, 1984). Not only are these cloud bands responsible for a large portion of the southern African summer rainfall, they are also known to produce heavy rainfall events (Hart et al., 2012). The mean positioning of these systems during summer can vary depending on large-scale drivers, such as sea surface temperatures in the Pacific Ocean (e.g. Cook, 2001; Fauchereau et al., 2009). Thus, any future analysis should include looking at trends in circulation patterns or large-scale climate drivers that may be behind the increase in summer rainfall over the interior.

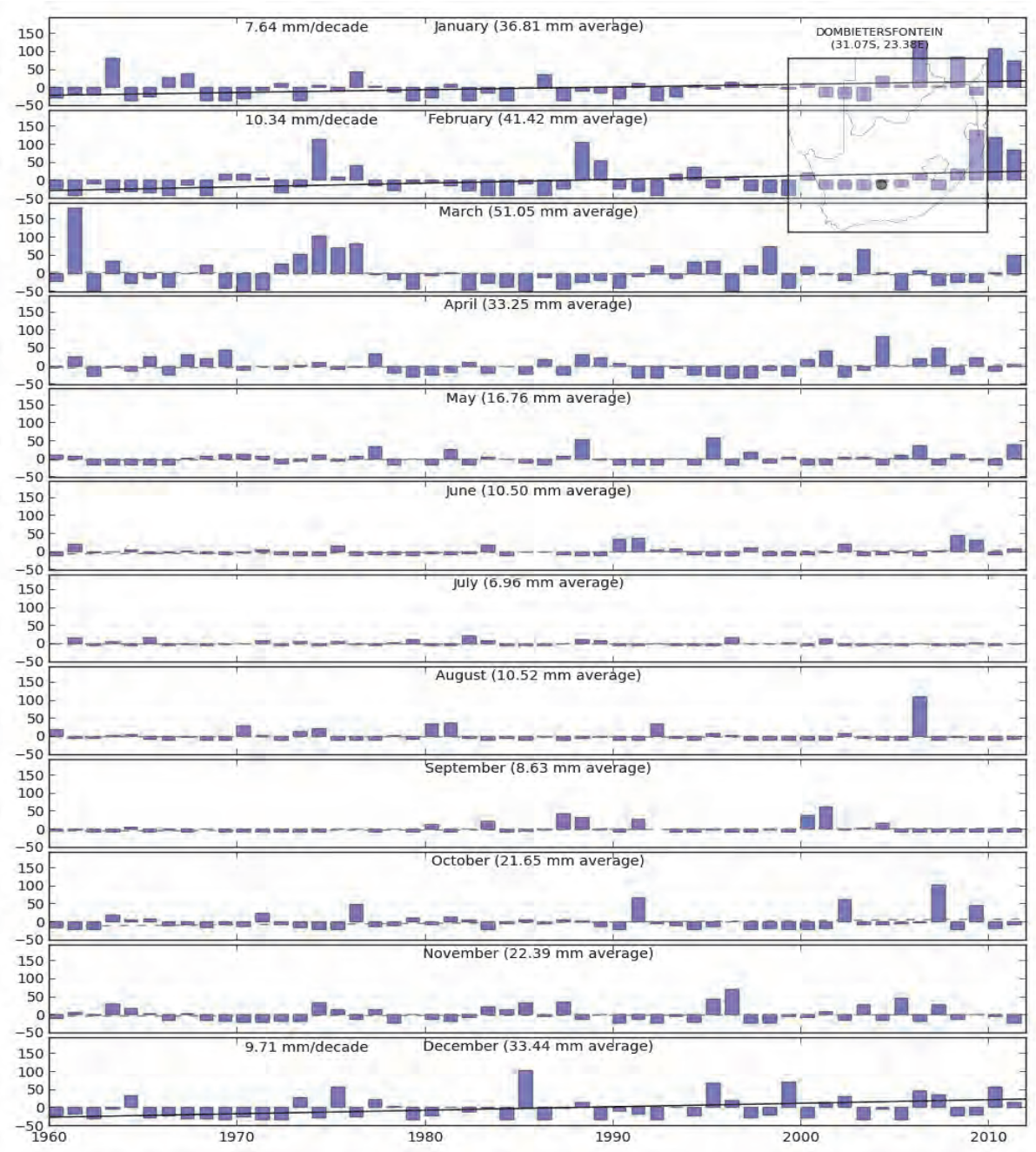

Figure 2.2 | *Monthly rainfall anomalies at 'Dombietersfontein' (see map insert, top right hand corner, for station location) from 1960-2012. The month and average rainfall (in brackets) is given at the top of each panel. The dashed (solid) black line shows the trend (statistically significant - 90th percentile) as the decadal change in monthly rainfall. If the trend is significant the decadal change is given in the top left hand corner (mm/decade).*

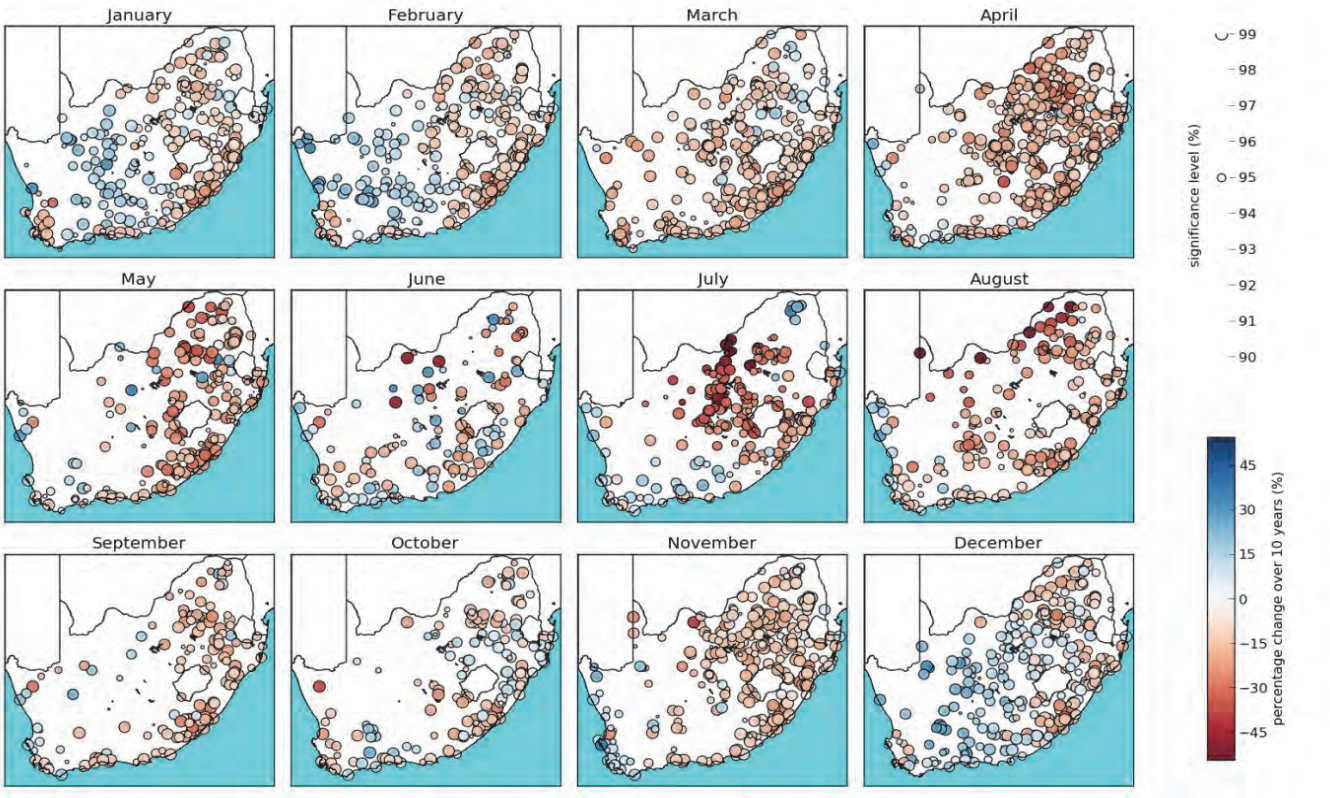

Figure 2.3 | *Statistically significant (90-99%) monthly wet day trends for stations across South Africa expressed as percentage change per decade.*

Another clear pattern is the decrease in rainfall during April over much of the summer rainfall regions, which includes the provinces of Gauteng, Free State, KwaZulu-Natal and Mpumalanga (top right hand corner in Fig. 2.1). A full analysis on the atmosphere dynamics is required in order to understand the causes behind this change. In terms of interpretation, it suggests that over the past few decades there has been a steady decrease in autumn rainfall in these regions. This potentially could have an impact on agricultural activities, depending on the importance of the little rainfall that generally falls during this time of the year (example shown in Fig 2.4d).

Parts of the southern KwaZulu-Natal and the Eastern Cape coastal region seem to show a drying trend for both the late summer months and autumn months (Fig. 2.1 and Fig.2.5). Although, the latter months (e.g. May) are generally moderately dry in the region (e.g. Fig. 2.5) so this may not be of great concern. However, the drying of the late summer months requires further exploration. Again, the drying trend during these months is found to coincide with a decrease in the number of monthly rainfall events (Fig. 2.3).

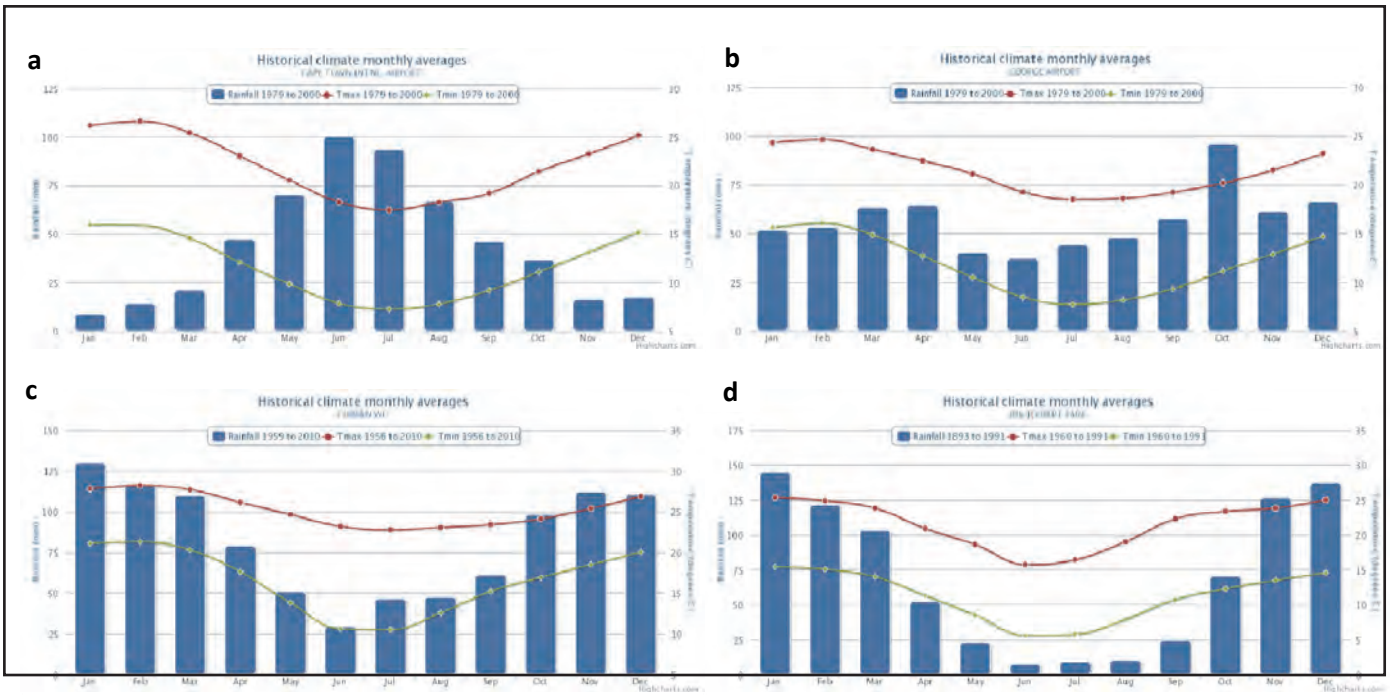

Figure 2.4 | *Average monthly rainfall (mm, blue bars), maximum temperature (°C, red line) and minimum temperature (°C, green line) for stations located in a) Cape Town, b) George, c) Durban and d) Johannesburg. Note that the y-axis values vary per graph.*

2.3.2. *Western Cape*

The Western Cape climate is classed as Mediterranean and as such, is largely a winter (June-August) rainfall region (e.g. Fig. 2.4a). Most of the winter rainfall is produced by cold fronts and associated extra-tropical cyclones, but other westerly disturbances, such as cut-off lows, may on occasion also produce significant rainfall over the region (Singleton and Reason 2006; 2007). The southern coastal areas of the province contain a slightly different rainfall pattern in that they experience rainfall almost all year round (e.g. Fig. 2.4b). This is a result of the onshore flow of moisture from the south (over the warm Agulhas Current), rising up the coastal mountains and producing summer rainfall. Additionally, moisture originating from the tropics is transported southwards towards the southern cape during the summer months, which leads to occasional favourable conditions for rainfall. However, Western Cape rainfall as a whole contains considerable spatial variability as well as interannual variability. This is likely due to the geographic location of the region, surrounding oceans and the complex regional topography.

In the previous section, highlighting rainfall trends across South Africa, it was evident that the stations along the southern cape coast have experienced a drying trend at the start of spring (i.e. September) over the past few decades. Figures 2.6 and 2.7 provide a zoomed in view of the Western Cape with regards to monthly rainfall trends and monthly rain days,

respectively. An example of the decrease in September rainfall at a station positioned along the south coast is provided in figure 2.8.

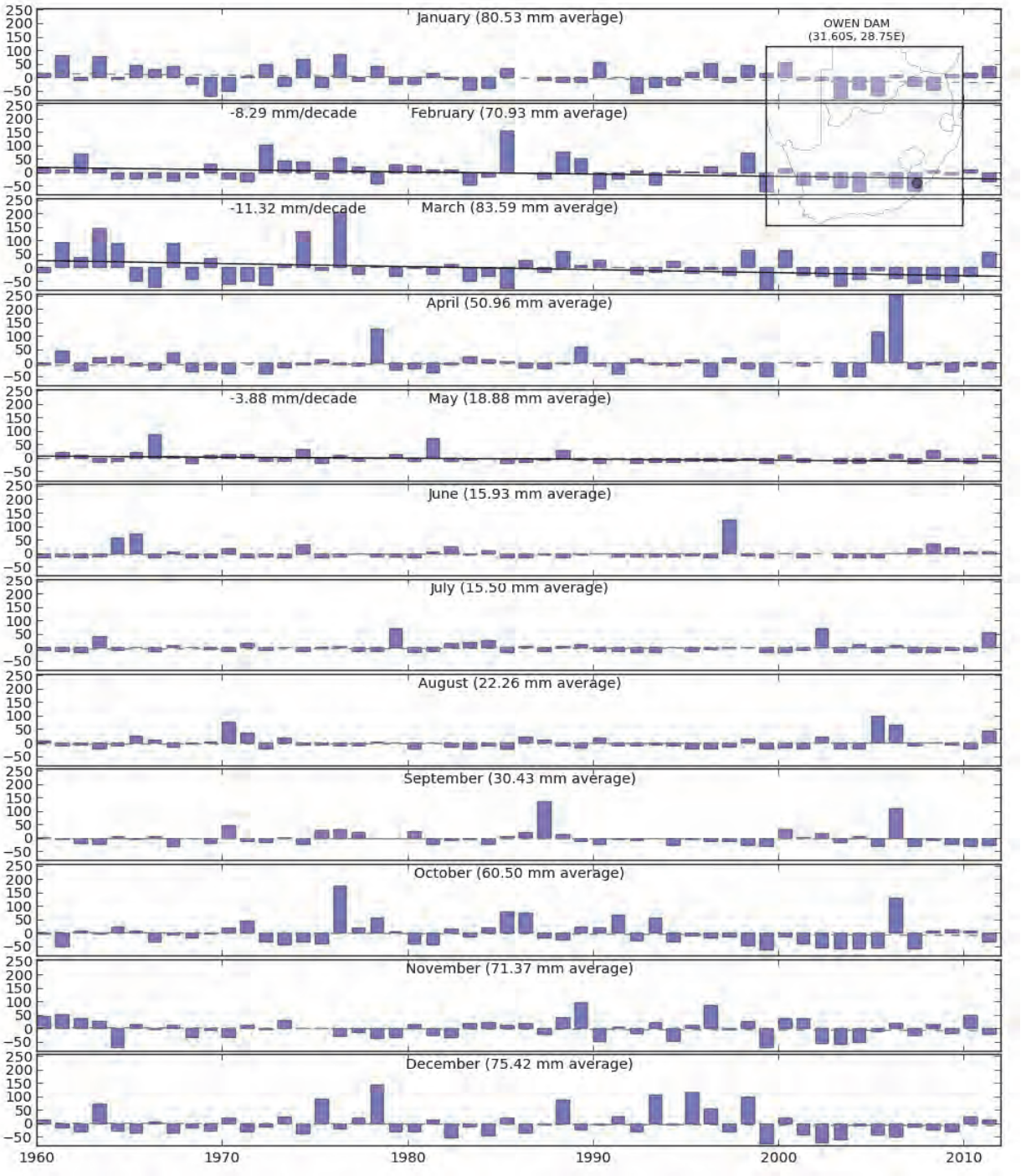

Figure 2.5 | *Monthly rainfall anomalies at Owen Dam (see map insert, top right hand corner, for station location) from 1960-2012. The month and average rainfall (in brackets) is given at the top of each panel. The dashed (solid) black line shows the trend (statistically significant - 90th percentile) as the decadal change in monthly rainfall. If the trend is significant the decadal change is given in the top left hand corner (mm/decade).*

Figure 2.6 | *Statistically significant (90-99% levels) monthly total rainfall trends for stations across the Western Cape expressed as percentage change per decade.*

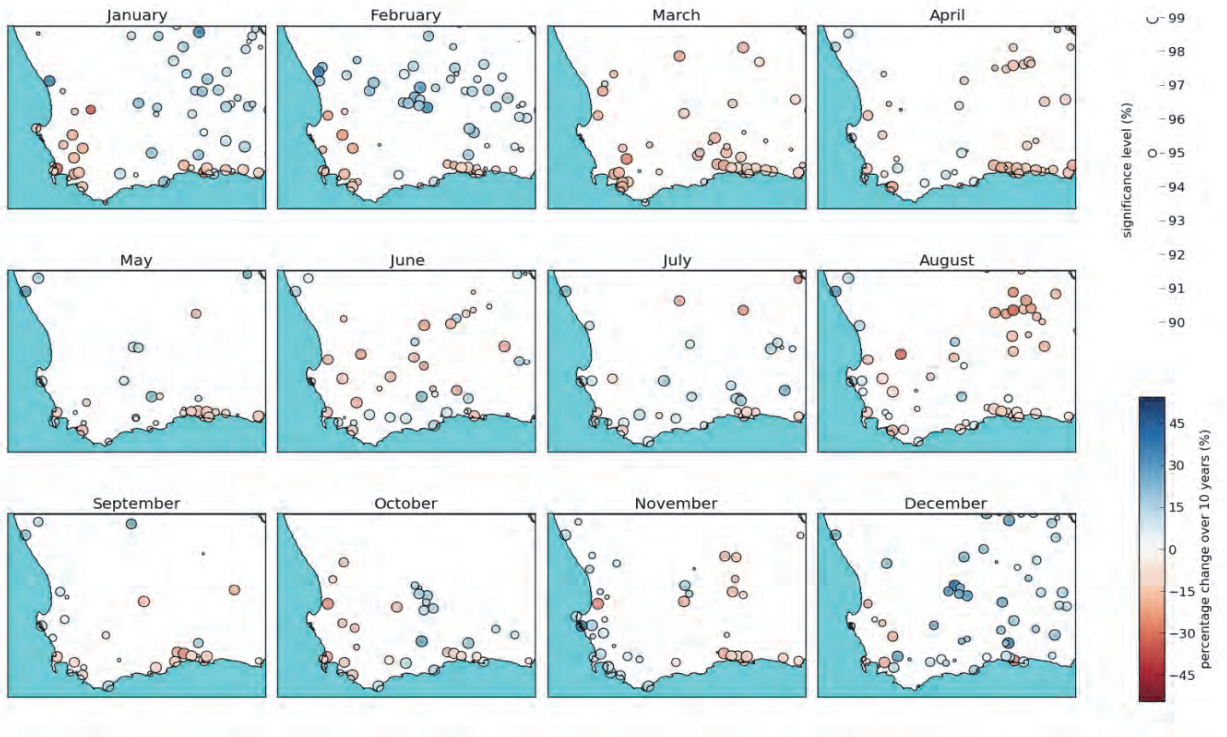

Figure 2.7 | *Statistically significant (90-99%) monthly wet day trends for stations across the Western Cape expressed as percentage change per decade.*

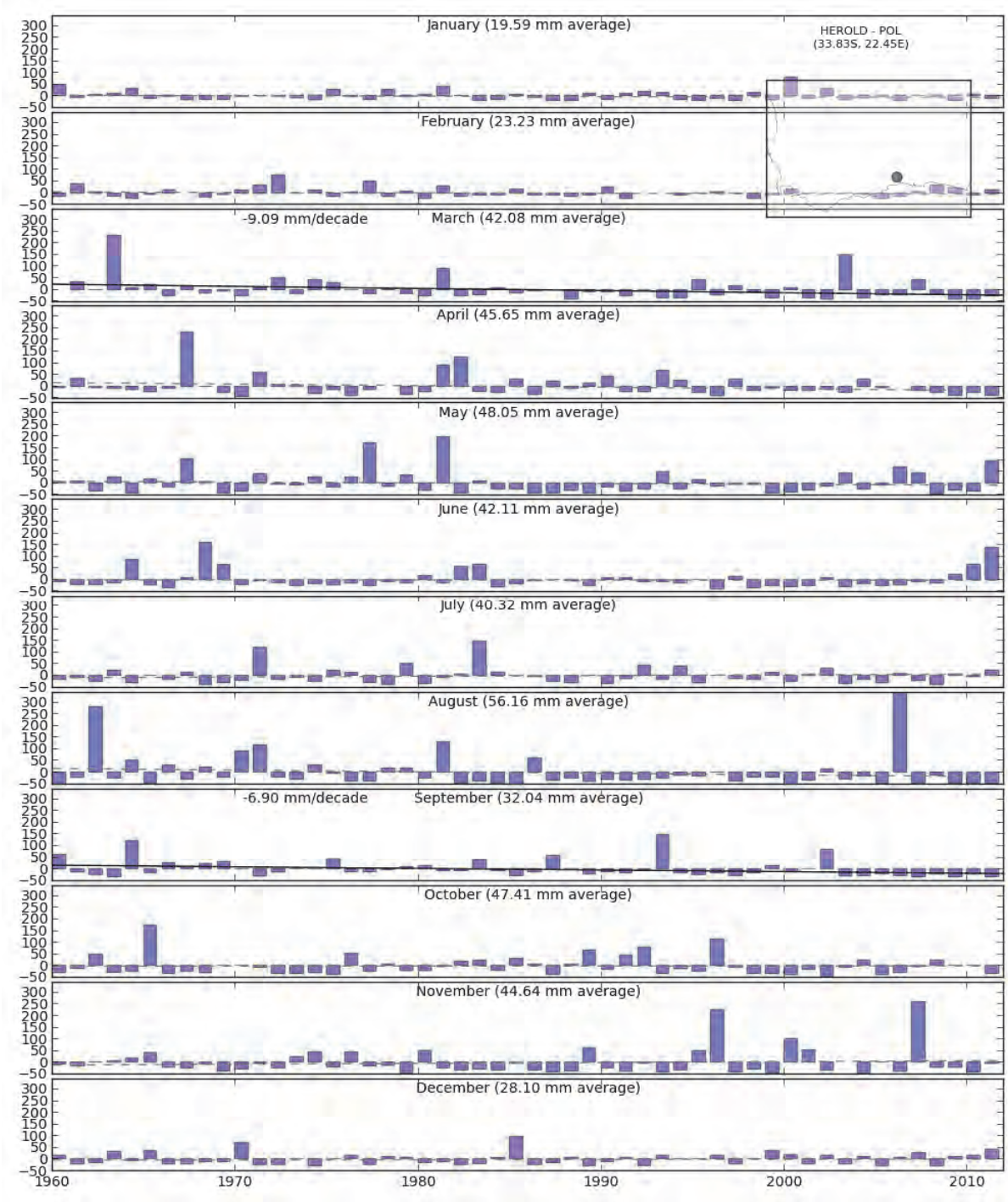

Figure 2.8 | *Monthly rainfall anomalies at 'Herold-Pol' station (see map insert, top right hand corner, for station location) from 1960-2012. The month and average rainfall (in brackets) is given at the top of each panel. The dashed (solid) black line shows the trend (statistically significant - 90th percentile) as the decadal change in monthly rainfall. If the trend is significant the decadal change is given in the top left hand corner (mm/decade).*

It is also interesting that for the Western Cape (Fig. 2.7) there is a much clearer and more consistent message of a reduction in the number of rain days throughout the winter rainfall season. Similar findings are also present form the late summer/early autumn months for stations positioned along the southern cape coast. In contrast, stations inland in the Western Cape tend to suggest that there has been an increase in rainfall and rain days during the summer months.

While the lack of observations and statistical significance limits the interpretation, there does seem to also be some difference in trends between locations in the mountains and those on the coast or on coastal planes, particularly in April, May, and June. The potentially opposite response of mountain locations and low lying locations to changes in synoptic weather systems, as a result of climate change, is one of the large sources of uncertainty in climate projections for the Western Cape. However, it is a critical question to explore and answer as the mountains are the catchment areas for all the dams in the region and the province as a whole, particularly the City of Cape Town, is already close to being water stressed.

2.4. Conclusions

This chapter concludes by stating that there are indeed observed changes in monthly rainfall and temperature (not shown) patterns across South Africa. Many of these trends are statistically significant suggesting a response to an underlying process, presumably global climate change, though other drivers should also be considered. The observed trends are complex, varying from positive to negative and significant or not significant at the same location through different months of the year. In some areas locations within 50km of each other can exhibit opposite trends in the same month of the year presumably as a result of local topography and the resultant differing response to large scale circulation shifts.

Nationally there are trends of both wetting and drying with a fairly strong suggestion of a shortening of the summer rainfall season and a shortening and/or later shift in the winter rainfall season with many complex and nuanced variations involved. Trends in derived statistics such as monthly rain days appear to be more statistically significant than first order total monthly rainfall statistics. Analysis of trends in extremes (e.g. heavy rainfall events) is not directly addressed in this work due to the different methodology required. However previous work has suggested that on long time scale there is evidence of increases in intensity of rainfall events across South Africa.

Some early results indicate there appear to be several important trends in regional scale circulation patterns (not shown) which in some cases can be associated with the station scale observed trends in rainfall. These associations provide important information and insight which can be applied when exploring other sources of climate change information such General Circulation Model (GCM) and Regional Climate Model (RCM) projections of circulation patterns.

Chapter 3

MODES OF VARIABILITY REPRESENTED IN CLIMATE MODELS WITHIN THE CMIP5 FRAMEWORK

3.1. Introduction

The objective of this chapter is to explore the relevant attributes of the general circulation models[2] (GCMs) from the perspective of circulation – the skilful scale of GCMs. While many jump straight to the diagnostic fields of surface rainfall and precipitation, these are functions of the forcing dynamics represented in the circulation fields.

Two approaches are explored here. The first considers the models in terms of their ability to reproduce the large scale processes that are of relevance to the southern Africa regional climate responses. Second is an approach that examines the models performance of the regional scale circulation patterns over the sub-continent.

3.2. Background to Model Evaluation

Climate models have progressed significantly since their first inception in the 1950s, developing from one-dimensional energy balance models to fully coupled atmosphere-ocean general circulation models (AOGCMs) that represent the major climate system components (atmosphere, ocean, land surfaces, and cryosphere). These models are the most advanced tools used for investigating the response of the climate system to various forcings, either natural or human induced. Simply put, a climate model is an executable computer code that solves a set of mathematical equations, which are designed to approximate the dynamics of the climate system. These equations (i.e. equations of motion, and conservation of energy, mass, and momentum) are discretized on a grid and solved numerically with the use of powerful computers. Values assigned to each grid box represent the average atmospheric state (temperature, humidity, wind speed, etc.) within the box. Numerical methods are used to represent transfers of mass, moisture, and energy between boxes according to physical principles.

The process is not as straight forward as it appears, because an infinite number of boxes are required to accurately represent the atmospheric state at any moment in time. Processes that occur on scales smaller than the grid size of the model (e.g. convective processes that form rain clouds) have to be approximated, in a process known as parameterization. Modelers try to avoid parameterization problems by increasing the spatial resolution (size of the boxes). This increase in resolution results in the complex parameterized processes being resolved in

[2] Some refer to GCMs as “Global Climate Models”.

the model. However, there are two limitations here; firstly, there are computational constraints (i.e. computers are not powerful enough to simulate very large numbers of boxes), and secondly, our understanding of some of the physical processes that take place in the atmosphere is not complete.

While climate models have enabled significant advances in our understanding of the climate system, our ability to predict future weather and the impact of changing greenhouse gas emissions, there remain significant challenges and limitations. In the context of climate change, model disagreement stands out as one of the greatest challenges. There now exist more than 30 different coupled climate models scenarios (see Appendix A) that have been used to produce projections of future climate change given different emission scenarios. However, for the same emission scenario, these different models produce wide-ranging projections of the future climate, particularly regarding rainfall. This poses a serious challenge to the use of the climate projections derived from climate models.

Model disagreement is a result of a number of factors. While most models are based on the same physical principles and even use largely similar numerical methods, there are many choices available to model developers during model development. Different numerical methods can be used to solve the fundamental physical equations, while different approximations (i.e. parameterizations) can be used to represent processes such as convective rainfall, cloud, and radiation balances. The result is that each model, while following the same basic principles, can produce different simulations of the current climate and different projections of the future climate state.

Questions remain on how does one go about evaluating a model or assessing the model performance? The latest IPCC (2013) report incorporates a combination of techniques and measures in the assessment of models. The most straightforward approach is to compare a simulated variable from the model, such as global mean temperature, with an observationally based estimate. Such a method is obviously limited to the variable or phenomena for which observational data exists (spatially and temporally). Other limitations include the quality of the observation data used and the uncertainty within it. Such an approach can be applied to a single model or to an ensemble of models, generally referred to as a multi-model ensemble (MME)[3].

More complicated assessments are based on quantitative statistical measures, often referred to as performance metrics (e.g. Gleckler et al., 2008). There is still much discussion about how best to design a set of metrics that evaluated the performance of a model/s, both individually and collectively. To date there appears to be no individual objective method that evaluates climate model performance any better than other. Although evaluation of model skill has been around for some time, it has mainly been focused on numerical weather prediction (i.e. shorter timescales). One of the difficulties in evaluating climate models is that there is very little opportunity to evaluate the predicative ability of the model. In contrast, numerical

[3] Ensemble methods are used to explore uncertainty in climate model simulations that are brought about through internal variability, boundary conditions, parameterizations and model structure.

weather prediction is continuously evaluated against observed conditions and on fewer variables.

Climate model evaluation is also not only focused around the mean climate, but also involves investigating how well they simulate historical climate change, climate variability on various time scales and the influence of the main modes of variability on regional climate. As alluded to earlier, one of the objectives in this chapter is to evaluate and summarise how well current climate models simulate the main modes of variability (discussed in the next section) that are thought to influence the climate of southern Africa. For the purposes of this report, focus is placed on one particular mode of variability, the El Niño – Southern Oscillation (ENSO). Some discussion highlighting other modes is also provided.

3.3. Modes of Variability

It is well documented that the climate varies on all time scales, ranging from one year to the next, in between decades and even over centuries and millennia. The factors behind this variability are considerably complex and as yet, are not all completely understood, particularly those that involve non-linear feedbacks. Some of the drivers behind the variability may be external, such as changes in sun activity, while others may be internal, such as sea surface temperature anomalies. The focus in this report is on internal modes of variability that feature on shorter time scales. While these modes may not necessarily be periodic, they are oscillatory in nature and can be monitored by an index.

3.3.1. El Niño – Southern Oscillation (ENSO)

Arguably the most dominant mode of global interannual climate variability is the *El Niño-Southern Oscillation* (ENSO). This phenomenon is characterized by anomalous sea surface temperatures (SSTs) in the equatorial Pacific Ocean (see Figure 3.1 for location). Periods where the equatorial Pacific Ocean are dominated by warmer than usual SSTs are referred to as El Niño conditions (warm ENSO phase), while periods that are cooler than the average are known as La Niña (cold ENSO phase). ENSO events tend to follow the mean seasonal cycle, with SST anomalies usually first appearing in the eastern Pacific during the austral spring, where they then peak (normally in the months of November to January) and then terminate in the central Pacific in the austral autumn (March-May). ENSO is a strongly coupled ocean-atmosphere phenomenon, with SST anomalies in the equatorial Pacific having a direct effect on Pacific sea level pressure (i.e. the southern oscillation). It is associated with a modulation of the trade winds and a shift of tropical Pacific precipitation. Not only do the SST anomalies induce changes in the local tropical circulation, but the effects are propagated globally through atmosphere teleconnections, affecting weather patterns worldwide (McPhaden et al., 2006).

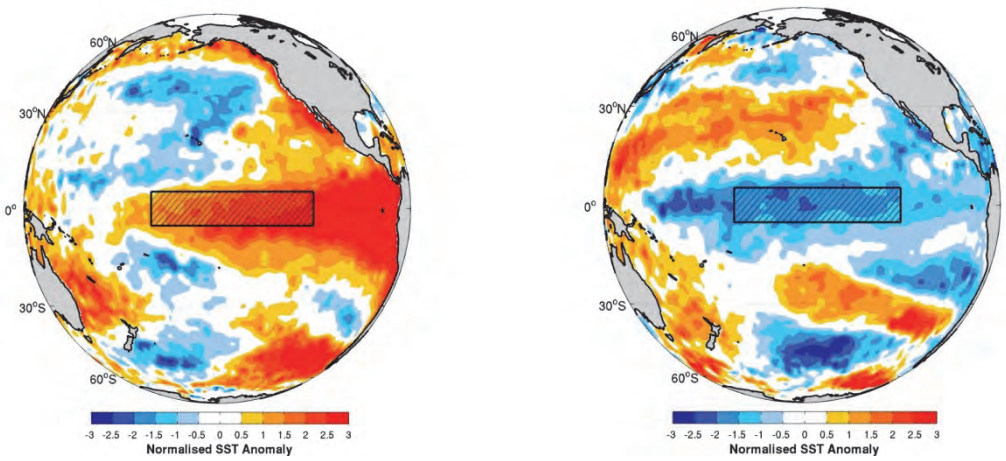

Figure 3.1 | *Normalised SST anomalies for the month of December 1997 (El Niño event; left) and December 1987 (La Niña event; right) in the Pacific Ocean. The black box refers to the Niño 3.4 region (5°N - 5°S; 170°W - 120°W) which is used to create the Niño-3.4 index illustrated in Fig. 3. 2. The data used to create the figures is from HadISSTv1.1 and the mean is based on the 1950-2010 period.*

The frequency and amplitude of ENSO is somewhat irregular, with events occurring approximately every 2 to 7 years, and El Niños tending to be more frequent and stronger than La Niña events (particularly between the mid-1970s to late 1990s; Figure 3.2). This skewed distribution towards positive values in ENSO SST anomalies may partly be explained by nonlinear processes favouring stronger El Niños than La Niñas (An and Jin, 2004) or possibly be some evidence of decadal modulation of ENSO (e.g. Fedorov and Philander, 2000). There is still much debate about the processes resulting in the development of ENSO, with the theoretical explanations roughly clustered into two groups (see Wang and Picaut 2004 for a review). Some of the evidence tends to suggest that ENSO is a self-sustained and naturally oscillating mode of the coupled ocean-atmosphere system (i.e. freely oscillates between cold and warm events), while other studies indicate that ENSO occurs when the ocean-atmosphere system in the tropical Pacific, which resides in a preferred state of cold water in the east and warm in the west, is energized by high-frequency stochastic forcing. It is also possible that the system may actually alternate between these two explanations on multi-decadal epochs (Fedorov and Philander, 2000).

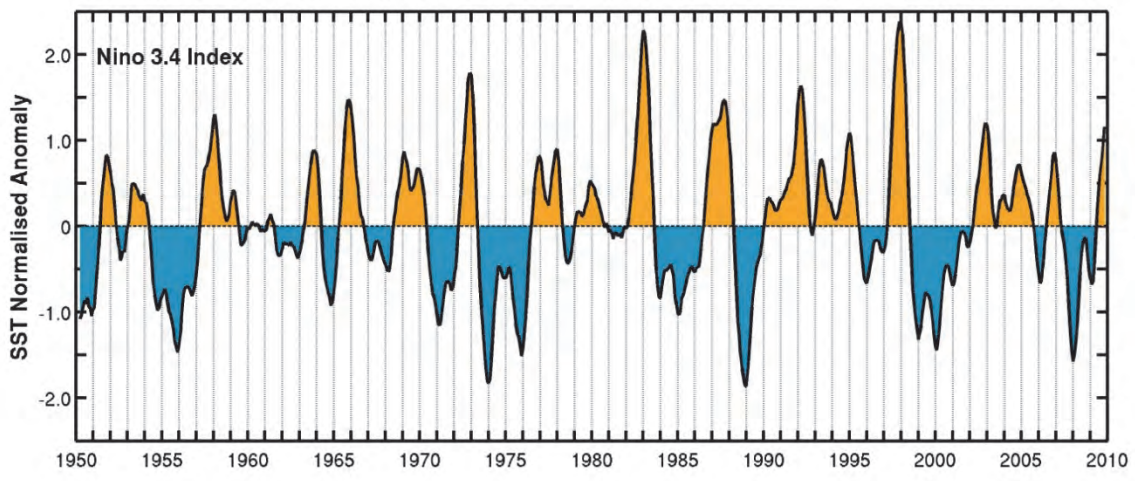

Figure 3.2 | *Standardized anomalies for the Niño-3.4 index (see Fig. 3.1 for location) for the 1950-2009 period using HadISST1.1 data. This monthly data is at a 1° x 1° spatial resolution and available from 1870 to present. Time series is smoothed using a 5-month running mean.*

Perhaps the most obvious signature of climate impacts during ENSO is found in precipitation patterns in the Pacific region. Drought conditions in countries along the western Pacific (e.g. Australia, Indonesia, etc.) and flood events along the eastern Pacific (e.g. west coast of South America) are attributed to El Niño conditions in the eastern and central Pacific (e.g. Fig. 3.3). La Niña often results in climate anomalies that are generally opposite to that of El Niño (i.e. places that receive less rainfall during El Niño, typically receive more during La Niña). These impacts are not confined to the Pacific region, with the remote effects of ENSO found in all ocean basins and on all continents (Trenberth et al., 1998; McPhaden et al., 2006).

Considering that ENSO is primarily a tropical Indo-Pacific phenomenon, the influence it has on equatorial east Africa and southern Africa is perceived to be through modulation of the local Walker Circulation and SSTs in the neighbouring Indian and Atlantic Oceans (e.g. Lindesay 1988; Rocha and Simmonds, 1997; Reason et al., 2000; Cook, 2001). It has been well established that during El Niño conditions, large portions of southern Africa experience dry conditions (e.g. Figure 3.3), while the opposite occurs during La Niña conditions. Effectively, during El Niño, unfavourable precipitation conditions occur over the continent through a reduction in moisture convergence, uplift and instability. In equatorial east Africa the opposite generally applies, with the region experiencing above (below) average rainfall during El Niño (La Niña) conditions (e.g. Ropelewski and Halpert, 1987; Farmer, 1988; Hutchinson, 1992; Hastenrath et al., 1993). It was also originally perceived that ENSO only influenced the summer rainfall regions of southern Africa (i.e. the summer rainfall coincides with the peak in SST anomalies during ENSO), but new evidence by Phillipon et al. (2011) suggests that ENSO may also affect the winter rainfall region (Western Cape).

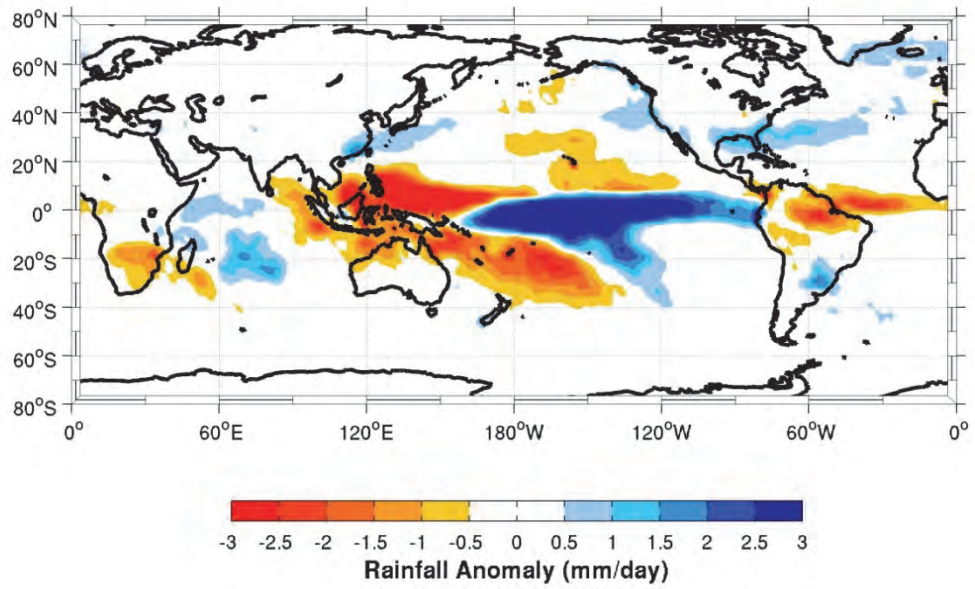

Figure 3.3 | *Global rainfall anomalies (mm/day) during the austral summer months (DJF) associated with five of the strongest El Niño events since 1980 (determined from the Niño-3.4 index in Fig. 3.2). GPCP data is used to create the figure, which is available at 2.5° resolution from 1979-2011.*

Unlike the tropical Pacific or neighbouring landmasses, the impacts from ENSO are not as consistent in regions remote from the Pacific, which is partly due to other regional modes of climate variability or interference from "weather noise" (McPhaden et al., 2006). El Niño conditions in the Pacific are not a prerequisite for reduced rainfall over southern Africa (e.g. the strong 1997/1998 El Niño coincided with normal to above average rainfall conditions). Thus, it needs to be reminded that this ENSO-South Africa rainfall relationship is non-linear (Fauchereau et al., 2009; Boulard et al., 2012). Overall, this highlights the complex relationship and suggests that SST conditions in the Pacific are not a simple determinant of rainfall conditions over parts of southern Africa. It is for this reason that other factors need to be taken into consideration, such as SST patterns with the Indian and Atlantic Ocean or other modes of variability, such as the Antarctic Oscillation (AAO).

3.3.2. The representation of ENSO in GCMs

Given the importance of ENSO on global climate, knowing whether any of its characteristics (i.e. frequency, intensity and amplitude) will change in a warmer world remains a vital question the scientific community still needs to address. Previous investigations into how ENSO may respond in a warmer climate using GCMs have produced inconclusive results (e.g. Latif and Keenlyside, 2009; Collins et al., 2010; Stevenson, 2012). It should be remembered that a large part of the uncertainty as to whether ENSO will change under global warming is linked to the lack of understanding of how well current climate models simulate

this phenomenon. Not just in terms of SSTs in the Pacific Ocean, but how well the changes induced by the warming/cooling are propagated throughout the tropics and into higher latitudes. An ensuing question would be whether the new generation of models (Coupled Model Inter-comparisons Project Phase 5 - CMIP5[4]) have improved the simulation of such a phenomenon compared to earlier model projects (i.e. CMIP2 and CMIP3)? As noted by Roberts et al. (2009), an increase in model resolution can lead to a better simulation of the ocean and atmosphere in a coupled model. Guilyardi et al. (2004) suggest that the maximum atmospheric grid spacing of about 1° is necessary for an accurate simulation of ENSO. Considering that some of the new CMIP5 models have a grid resolution closer to this than their predecessors, it is worth investigating any progress in this field.

However, an increased grid resolution will not likely solve all problems. It needs to be emphasised that an accurate simulation of ENSO in GCMs depends heavily on the interaction of a number of feedbacks, which either amplify or dampen the associated interannual anomalies (see Wang and Picaut, 2004; Jin et al., 2006). Understanding how these feedbacks are represented in the GCM could assist in the understanding of why a model may or may not represent ENSO particularly well (Guilyardi et al., 2009a).

Although an accurate simulation of ENSO, in terms of frequency, amplitude and seasonality, in coupled general circulation models remains a challenge there have been quite considerable improvements over the last decade or so (see Guilyardi et al. (2009a) for a review). Models from the third Coupled Models Intercomparison Project (CMIP3) were found to struggle with the overall simulation of ENSO. In particular, the models were shown to capture a large diversity of ENSO amplitude (e.g. van Oldenborgh et al., 2005), they did not capture the broad spectral peak in the 2-7 year band (e.g. AchutaRao and Sperber, 2006) and poorly represented the seasonal phase locking (e.g. AchutaRao and Sperber, 2006; Bellenger et al., 2013). They also contained variability that extended too far into the western Pacific / warmest SSTs are shifted to far to the west (e.g. Meehl and Teng, 2007; Yu and Kim, 2010). Not only did CMIP3 models struggle with ENSO, but they also had difficulty simulating the long-term mean and annual cycle in the Pacific Ocean. This has been suggested as a possible source of biases in the modelled ENSO (van Oldenborgh et al., 2005).

Preliminary results from CMIP5 indicate that some of the key characteristics of ENSO, such as the ENSO life cycle, are better resolved in the models than their predecessors in CMIP3 (Bellenger et al., 2013). However, there still remain considerable challenges, such as accurately resolving feedbacks, such as the wind-SST feedback or shortwave radiation – SST feedback, which are both underestimated (Bellenger et al., 2013). It should be taken into consideration that many CMIP5 models are a lot more complex and simulate more processes than that found in models used in earlier projects. Overall this currently makes simulating the Earth's climate a lot more difficult due to there being more processes that can produce errors or biases. It should be encouraging that preliminary results so far from CMIP5 do show improvements compared to CMIP3.

[4] CMIP5 is discussed in more detail later on.

3.3.3. The Indian Ocean Dipole (IOD)

Closer to the east African coastline, coupled ocean-atmosphere phenomenon within the Indian Ocean are perceived to play a key role on the regional climate of southern Africa. Anomalous SST conditions within this ocean basin are thought to influence atmospheric circulation patterns, which play a crucial role in enhancing or weakening the atmospheric moisture transported into the region. Questions remain about how independent SST conditions in the Indian Ocean are from ENSO. Results by Washington and Preston (2006) suggest that particular SST conditions within the Indian Ocean, which are statistically independent of ENSO, can play a key role in extreme precipitation over southern Africa. Thus, the evidence suggest that Indian Ocean SSTs alone may have a considerable impact on regional circulation patterns, including moisture transport, and rainfall.

In particular, two different dipole type SST patterns within the Indian Ocean have been highlighted as two of the leading modes of regional climate variability. The first refers to a zonal (east-west) equatorial pattern commonly known as the Indian Ocean Dipole (IOD). This dipole pattern is not limited to just the ocean, with similar patterns in atmosphere processes, such as precipitation, outgoing longwave radiation (a proxy for cloud cover) and sea level pressure, occurring during the same period (Yamagata et al., 2003). Typically, warm (cool) SST anomalies in the eastern tropical Indian Ocean coinciding with cool (warm) SSTs in the western tropical Indian Ocean are used to describe a positive (negative) phase in the IOD[5] (Fig. 3.4). It has been shown that during the positive (negative) phase of the IOD, there is often heavier (less) rainfall experienced over eastern equatorial Africa (e.g. Saji et al., 1999; Behera et al., 2005). This relationship is often more apparent over equatorial eastern Africa, compared to subtropical southern Africa.

The IOD index has displayed an upward trend since the 1950s, which has been linked to variations in warming in the Indian Ocean (Cai et al., 2009; Cai et al., 2013). Although globally there has been widespread warming of the world's oceans linked to anthropogenic climate change, surface warming in the Indian Ocean has not been spatially uniform. There has been an evolving trend where the eastern tropical regions are warming slower than the west, leading to an apparent zonal temperature gradient (e.g. Alory et al., 2007). This warming pattern is linked to the increase in frequency in positive IOD events in recent decades (Ihara et al., 2008).

[5] Commonly measured by a *dipole mode index* (DMI) – defined as the difference of SST anomalies in the west (50°E to 70°E and 10°N and 10°S) minus east (90°E to 110°E and 10°S to 0°).

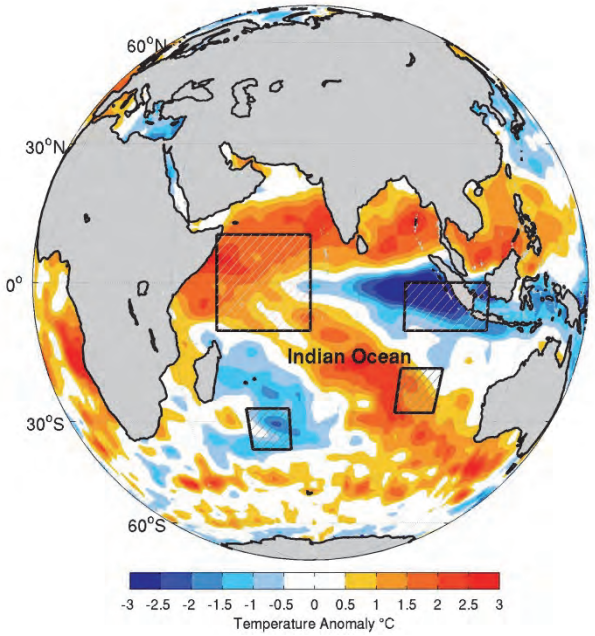

Figure 3.4 | *The figure, showing SST anomalies in the Indian Ocean during September 1997, depicts the location of the western and eastern regions used to calculate the IOD (top black squares) and SIOD (bottom black squares). In this example, the anomalies illustrate a positive IOD and negative SIOD.*

Further poleward in the Indian Ocean, another dipole pattern known as the *Subtropical Indian Ocean Dipole* (SIOD) has been shown to influence the climate of the neighbouring continents. Similar to the IOD, a positive (negative) SIOD is characterized by warm (cool) SST anomalies in the southwest Indian Ocean, cool (warm) SSTs in the southeast and above (below) average rainfall over parts of southern Africa (Behera and Yamagata 2001; Reason 2001). However, a specific dipole pattern in this region is not a prerequisite for rainfall variability over the African continent. Warm (cold) SST anomalies in the southwest Indian Ocean have often been linked to southern Africa experiencing above (below) average summer rainfall (e.g. Jury, 1992; Reason and Mulenga, 1999; Reason, 2001; Reason, 2002).

3.3.4. The IOD in GCMs

To date, little focus has been placed on either the IOD or SIOD in CMIP5 compared to that of ENSO. Recent results from Weller and Cai (2013) indicate that there has been no substantial improvement in the simulation of the IOD, both in pattern and amplitude, in CMIP5 compared to that in CMIP3. Most of the models were found to produce a larger variance of SSTs in the eastern Indian Ocean as well as producing an amplitude that is larger than that observed. This suggests that some of the feedback mechanisms, such as the Bjerknes feedback, within the models are too strong. Models that contain an IOD amplitude that is too large have been shown to produce greater changes in mean rainfall in IOD-influenced regions

(Weller and Cai, 2013). Thus, any realistic simulation of regional climate patterns requires models that can realistically simulate the mean climate of the Indian Ocean and the statistical properties of the IOD (Cai et al., 2013).

3.4. Datasets and methods

The GCMs used in this project came from the latest Coupled Model Inter-comparisons Project Phase 5 (CMIP5; Taylor et al., 2012) archive. This archive contains simulations of the historic and future climate from multiple GCMs run by the world's leading climate modelling institutes. The simulations were run for the historic period using the observed greenhouse gas concentrations and then continued into the future using greenhouse gas concentrations based on two emission scenarios (RCP 4.5 and RCP 8.5[6]). SST data were available from the historical runs for eight of the eleven CMIP5 models used at CSAG for downscaling activities (see Appendix A). Data from these historical runs are at varying spatial resolutions and cover most of the nineteenth century to near present (2005), but for the purposes of this study only data starting from 1900 are used. Other data incorporated here from the CMIP5 models include, precipitation, mean sea level pressure and surface temperature. In order to compare the model data to the reanalysis data, all the output data are mapped to a 2° x 2° latitude/longitude grid.

Due to the complexity of ENSO, a set of metrics have been devised by the CLIVAR[7] Pacific Panel working group which may be applied when analysing model output to some observational reference data (Guilyardi et al., 2009b). Ideally these metrics are designed to assist in assessing ENSO characteristics in terms of theoretical/mechanistic understanding of the phenomena and not just based at local statistics. As discussed by Guilyardi et al. (2009a), local statistics, such as just SST anomalies (e.g. Niño-3 index), may be misleading with a model producing the "right" anomaly, but for the wrong reason. These metrics include the ENSO amplitude (Niño-3 standard deviation), structure (Niño-3 and Niño-4 amplitudes), frequency (root mean square of Niño-3 spectra) and heating source (Nino-4 precipitation standard deviation). For the purposes of this study, the key focus is placed on how well the models represent the temperature variability over the tropical Pacific, with particular focus being on the location and amplitude. The HadISST1.1 data (Rayner et al., 2003) is used as the reference SST dataset to determine ENSO characteristics. This monthly data is available at a 1° x 1° spatial resolution and is available from 1860 until present. It should be noted that only data from the 1900-2010 period is used in this study (smaller subsets are incorporated for various methodologies when needed).

---

[6] In CMIP5, the Special Report on Emission Scenarios (SRES) used in CMIP3 were replaced by Representative Concentration Pathways (RCPs). Four RCPs have been defined – one "low" scenario (RCP 2.6), two intermediate (RCP 4.5 and RCP 6), and one high (RCP 8.5). The number indicates the equivalent top of tropopause change in radiative forcing in the year 2100. These are documented in Moss et al. (2010).

[7] Climate Variability and Predictability (CLIVAR) is one of the core projects of the World Climate Research Programme

El Niño composites of mean sea level pressure and precipitation for the austral summer (DJF) are computed to determine if the ENSO signal is apparent over South Africa. Observed precipitation estimates come from the Global Precipitation Climatology Project (GPCP; Huffman et al., 1995, 1997) and are used to validate the models. The 2.5° horizontal resolution product, which extends from 1979 to 2011, includes both satellite data (microwave and infrared) and rain-gauge observations. The mean sea level pressure is obtained for the National Center for Environmental Prediction/National Center for Atmospheric Research (NCEP/NCAR) Reanalysis 2 data (Kanamitsu et al., 2002). This data is available globally, at a monthly timescale, from 1979 to present. An El Niño event is categorised as months where standardised SST anomalies, with a 5-month running mean, exceeded 0.6 in the Niño-3.4 region. This threshold ensures that only moderate to strong events are included in the analysis (Weare, 2012). However, questions have been raised whether including all ENSO events (i.e. moderate cases) may weaken or distort any ENSO signal over South Africa. For this reason and given the relatively short time frame of observations only the five strongest or intense El Niños (based on the DJF normalised anomaly value) are included in the composites.

Considering that ENSO is a coupled ocean-atmosphere phenomenon, a more stringent method would be to include standardised anomalies (also exceeding 0.6) of surface air temperature over the Niño-3.4 region and the southern oscillation index (SOI) to ensure a consistent atmosphere-ocean response (AchutaRao and Sperber, 2006). Due to limitations in the observations, only events between the years 1980-2009 (30 years) are considered. For consistency, only warm ENSO events identified in the historical model output from 1976-2005 (30 years) are used for the model composite analysis. It should be noted that results from such a composite analysis can be fairly sensitive to the length of record (Weare, 2012).

3.5. Preliminary results

3.5.1 ENSO in CMIP5

It has previously been found that GCMs produce a variety of El Niño variability timescales, with power spectrum plots that range from models producing near-biennial oscillations to spectra that more closely resemble the observed 2-7 year cycle (e.g. Fig.2 in AchutaRao and Sperber, 2006). In their analysis, Bellenger et al. (2013) find that the CMIP5 models show some improvement in this statistic compared to CMIP3. However, the 2-7 year timescale is a key property of ENSO variability that remains a challenge to simulate in climate models.

ENSO variability is also characterised by strong phase locking to the seasonal cycle, with El Niño and La Niña anomalies reaching a peak in austral summer months (DJF) and are weakest in austral autumn (MAM). The phase locking has been shown to be important for ENSO teleconnections, such as the relationship between El Nino and the Indian summer monsoon (e.g. Webster et al., 1998). Five of the eight models used here appear to capture the seasonal phasing locking relatively well, while other models do not show much seasonal

variation (e.g. MRI-CGCM3) or they peak in the wrong season (e.g. GFDL-ESM2M; Figure 3.5).

The combination of the incorrect simulation (or biases) of ENSO 2-7 year timescales and seasonal phase locking are known to result in the errors currently experienced in ENSO amplitude, irregularity, skewness or spatial patterns (Guilyardi et al., 2009a). This problem is still inherent in the current CMIP5 models. Figure 3.6 shows that there is no consistent ENSO pattern amongst the models. Some models, such as the GFDL-ESM2M and MIROC5 models, contain considerable variability that extends too far in the western Pacific. Only the MRI-CGCM3 model shows both a weaker variability and amplitude than that found in the observations. Essentially, the cause of such bias in the models is likely due to feedbacks not being represented accurately.

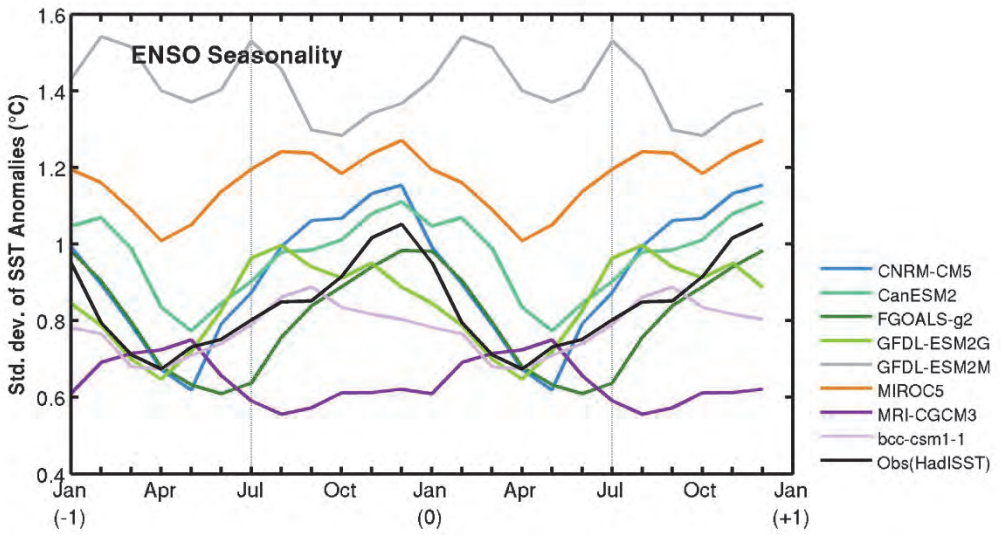

Figure 3.5 | *ENSO seasonality determined from the std. dev. of SST anomalies (for 100 years and detrended) in the Niño-3 region (5°N - 5°S; 150°W - 90°W). Results from the eight models, which are discussed in the text, and for the observation dataset (HadISST1.1; 1900-1999) are shown. Note that the 12 months have been doubled so that the austral summer (DJF) is the centre of the figure.*

The way ENSO is simulated in models can have a considerable influence on rainfall patterns across the world. Figures 3.7 and 3.8 show the mean DJF rainfall in the observations and the models, respectively. It is evident that some of the models show a bias with excessive rainfall either side of the equator, yet not enough rainfall over the equator. This tropical bias within GCMs has been referred to as the double-ITCZ problem (Mechoso et al., 1995). The double-ITCZ is often associated with an anomalously extended cold tongue of water along the equator (Mechoso et al., 1995; Lin, 2007). Ultimately, this could have an effect on accurately simulating the tropical modes of variability, such as ENSO. On a regional scale,

most of the models also simulate too much rainfall over both equatorial Africa and southern Africa.

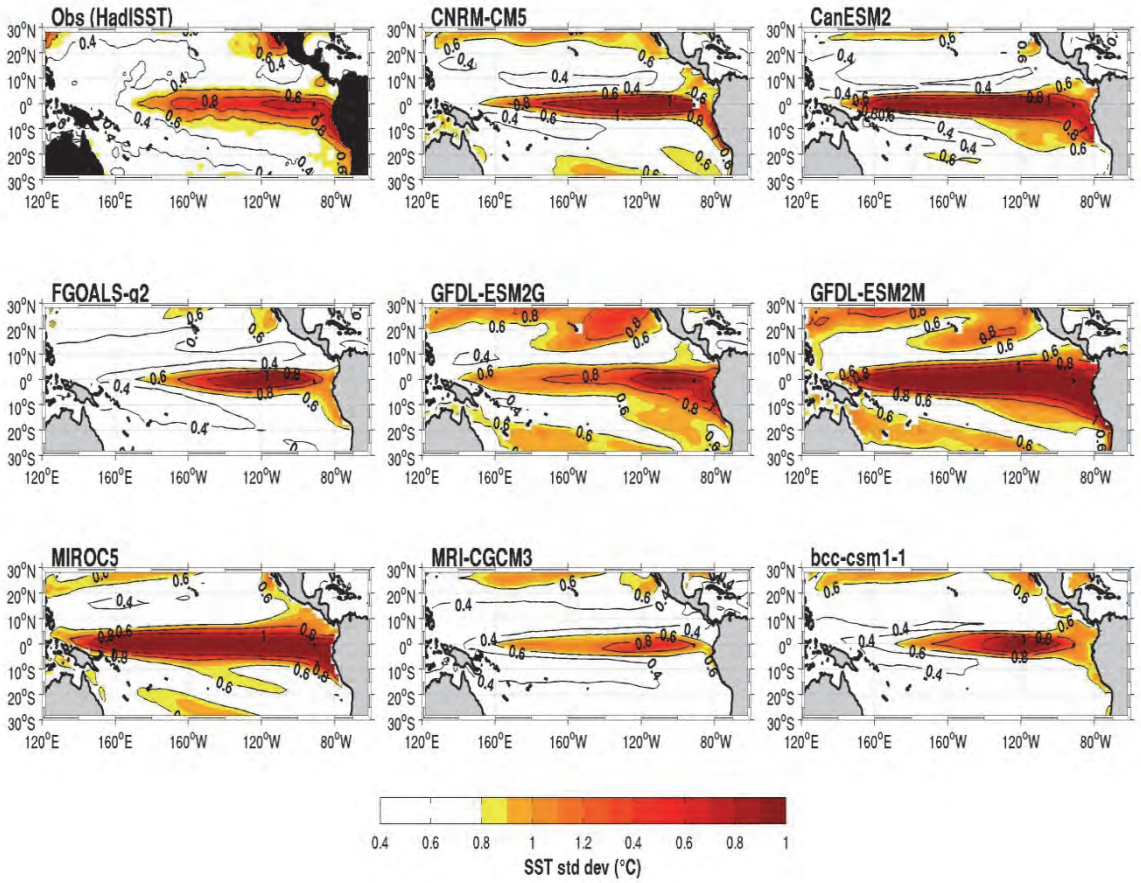

Figure 3.6 | *Mean SST std. dev. (°C) for 100 year of monthly data from eight models discussed in the text. The observations (top left corner) are taken from HadISST1.1 data for the 1900-1999 period.*

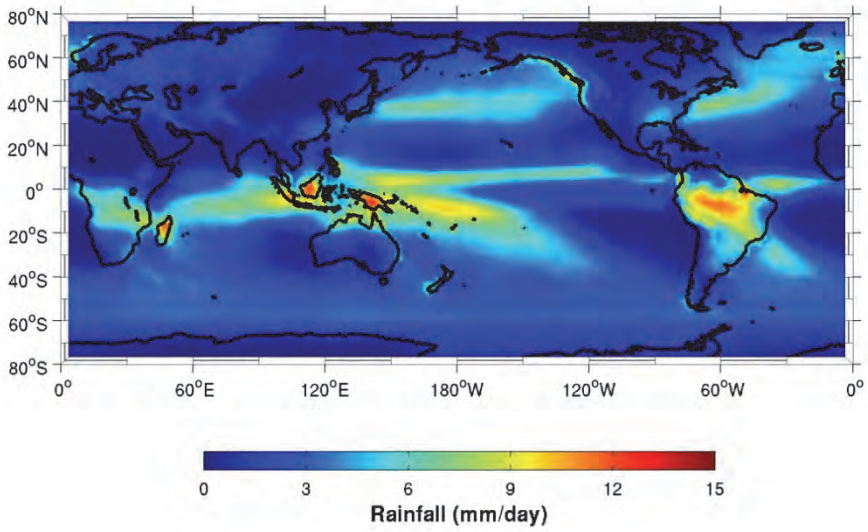

Figure 3.7 | *Mean DJF rainfall (mm/day) for the period 1980-2009 in GPCP data.*

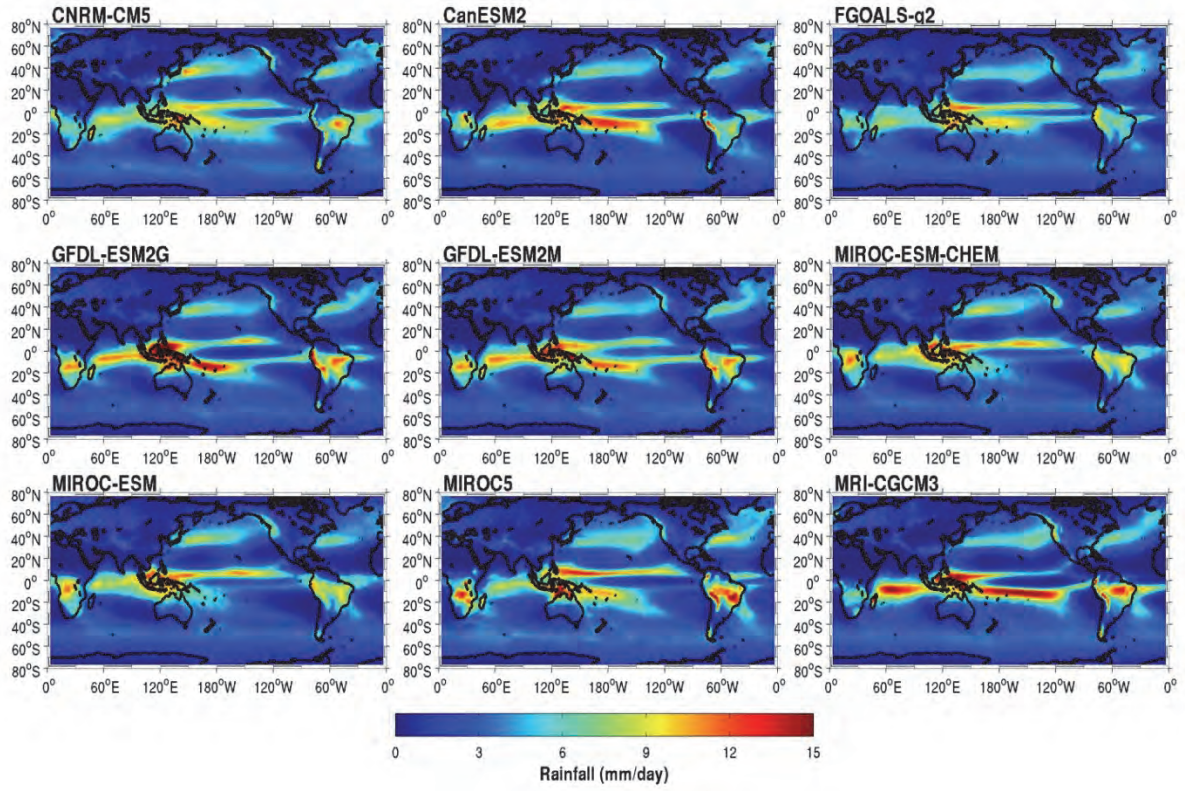

Figure 3.8 | *Mean DJF rainfall (mm/day) for the period 1976-2005 in various CMIP5 models. Note that the models used here may not necessarily be the same as those used previously.*

The DJF rainfall anomalies during the five strongest El Niño events are shown in Figure 3.9. It is evident that one of the more consistent errors compared to the observations is that

positive rainfall anomalies are located too far to the west. Rainfall anomalies in some of the models also appear to be meridionally confined in the tropics compared that in the observations (Fig. 3.3). The poor representation of Pacific rainfall anomalies is a persistent problem in GCMs (AchutaRao and Sperber, 2006; Bellenger et al., 2013). Over southern Africa, most of the models do tend to show a decrease in rainfall during the ENSO events. However, the magnitude of the anomalies are considerably weaker than that found in the observations (Fig. 3.3). In some models, an increase in rainfall is even simulated over the summer rainfall region, such as the MRI-CGCM3 model. An increase in DJF rainfall, varying in magnitude, is also evident over equatorial east Africa, which is also found in the observations.

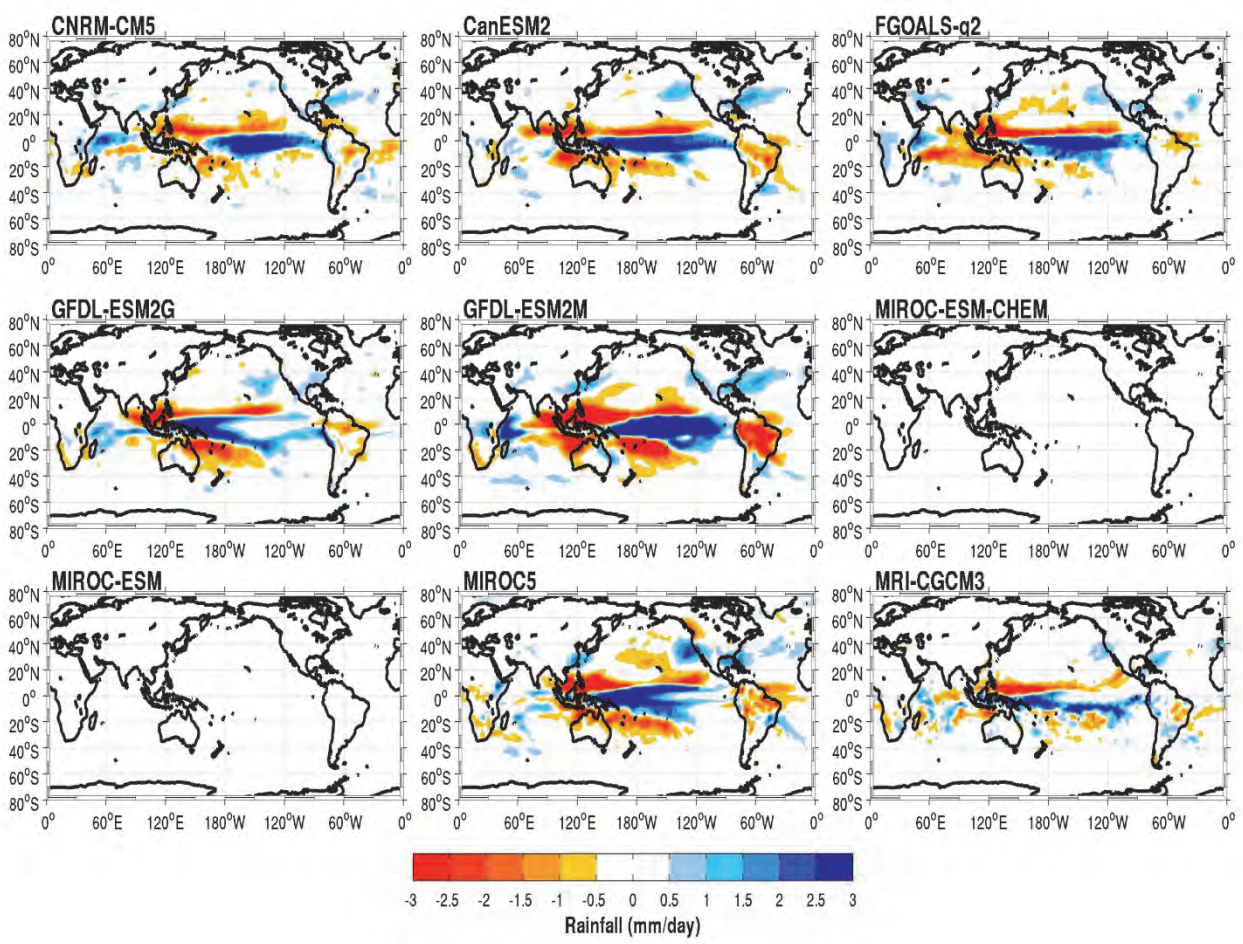

Figure 3.9 | *DJF anomalies (mm/day) for the five strongest ENSO events in the last 30 years of the models (1976-2005). Note that SST data was not available for two of the models (both are versions of MIROC) and hence, no data is displayed.*

3.6. CMIP5 Model Circulation Patterns

As alluded to previously, the model's skill in simulating the climate of the earth can be evaluated in many ways. Thus, the focus of the chapter now turns to the model's ability to

simulate the range and frequency of circulation patterns. The regional circulation patterns or atmospheric states can be explored and characterized using a number of clustering techniques and can incorporate a range of variables at different vertical levels. This analysis makes use of Self-Organizing Maps (SOMs) (Kohonen, 1995) to define and organize the range of circulation patterns found over the southern African domain (see Hewitson and Crane (2002) for further details on methodology).

The approach is illustrated in this report using a single variable, daily geopotential height at 700 hPa from the ERA-Interim reanalysis dataset[8]. It builds upon that shown in Deliverable 4 which investigated the characteristics and distribution of the regional circulation patterns over the last three decades. Once again only the summer months (December-February) results are presented, but the figures for the other three seasons can be found in Appendix B.

Figure 3.10 presents a SOM showing the characteristics and distribution of all summer mid-level pressures (geopotential height at 700 hPa) over the southern African domain obtained from ERA-Interim reanalysis and can be used as a reference distribution of atmospheric states. Figure 3.11 presents the frequency of occurrence of each of the synoptic states. The top left panel shows the real observed frequency over the last 3 decades, while the other panels show the simulated frequency of each of the 11 CMIP5 GCMs over the 30-year period 1976-2005. The values show the actual model frequency, while the shading show the frequency bias (i.e. information on how well the models match the observed frequency with over-estimations shown in red and under-estimations shown in blue).

A few clear messages can be extracted from the analysis; firstly all the models show biases in the frequency distribution of the circulation patterns, but some have stronger biases (for example BNU-ESM) than others (MRI-CGCM3). All models under-estimate the top left nodes (mid-latitude trough to the south west of the continent), which is the most common state in the observed record. Many of the models overestimate the central nodes (very zonal mid-latitude flow) or those along the bottom of the SOM (mid latitude trough to the south or south-east of the country, and associated with states where the South Atlantic High pressure cell is stronger).

While there are detailed differences in biases on individual nodes between models, there is nonetheless a general pattern of bias that is in agreement across the models. The physical basis for this will need to be explored, but some speculative ideas could be related to model resolution and topography, barotrophic phase of the westerly waves locking in relation to the Agulhas. The understanding of these biases can help to assess the model credibility for climate change projections.

[8] ERA Interim Daily Fields data-portal.ecmfwf.int/data/d/interim_daily

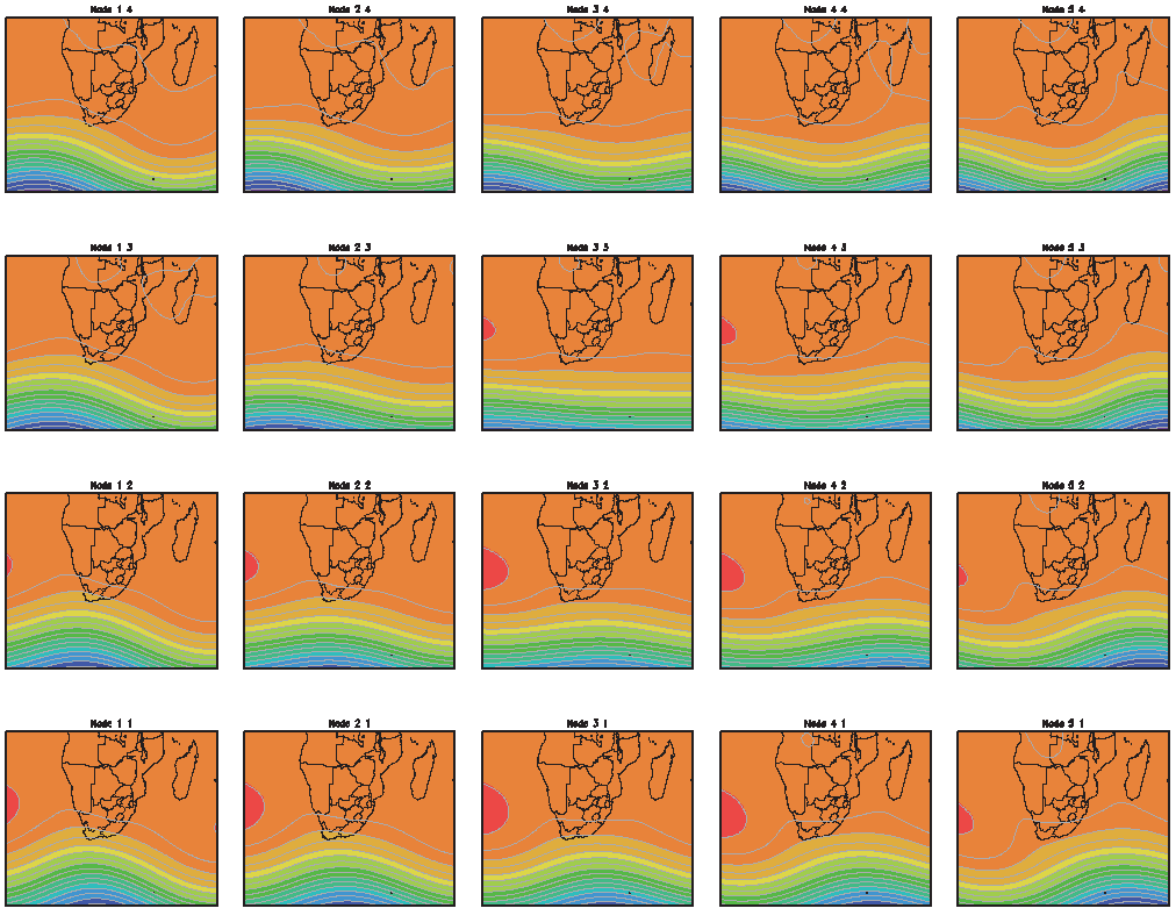

Figure 3.10 | *December-February circulation archetypes of daily geopotential height at 700 hPa from the ERA-Interim dataset1979-2012. Decreasing geopotential heights from red – blue.*

As a brief look at the implications of mode frequency under future climate, a logical extension of this step although going beyond this chapter, we can take a brief look at the projections. The CMIP5 GCMs simulate both the current climate as well as the future climate under a specified greenhouse gas emission pathway (RCP 8.5). It is therefore possible to also investigate how the GCMs project the frequency of synoptic states to change into the future. Figure 3.12 presents the results for the 11 GCMs as the difference between the future period 2040-2069 (using the RCP8.5 emission scenario) and the historical period 1976-2005.

The first clear message is that the model bias (previous figure) is larger than the projected change in frequency into the future. Secondly, there is no clear systematic pattern of change between the models. However, this is for one circulation variable (700hPa) in a preliminary analysis, so this should only be seen as a conceptual test ahead of further work.

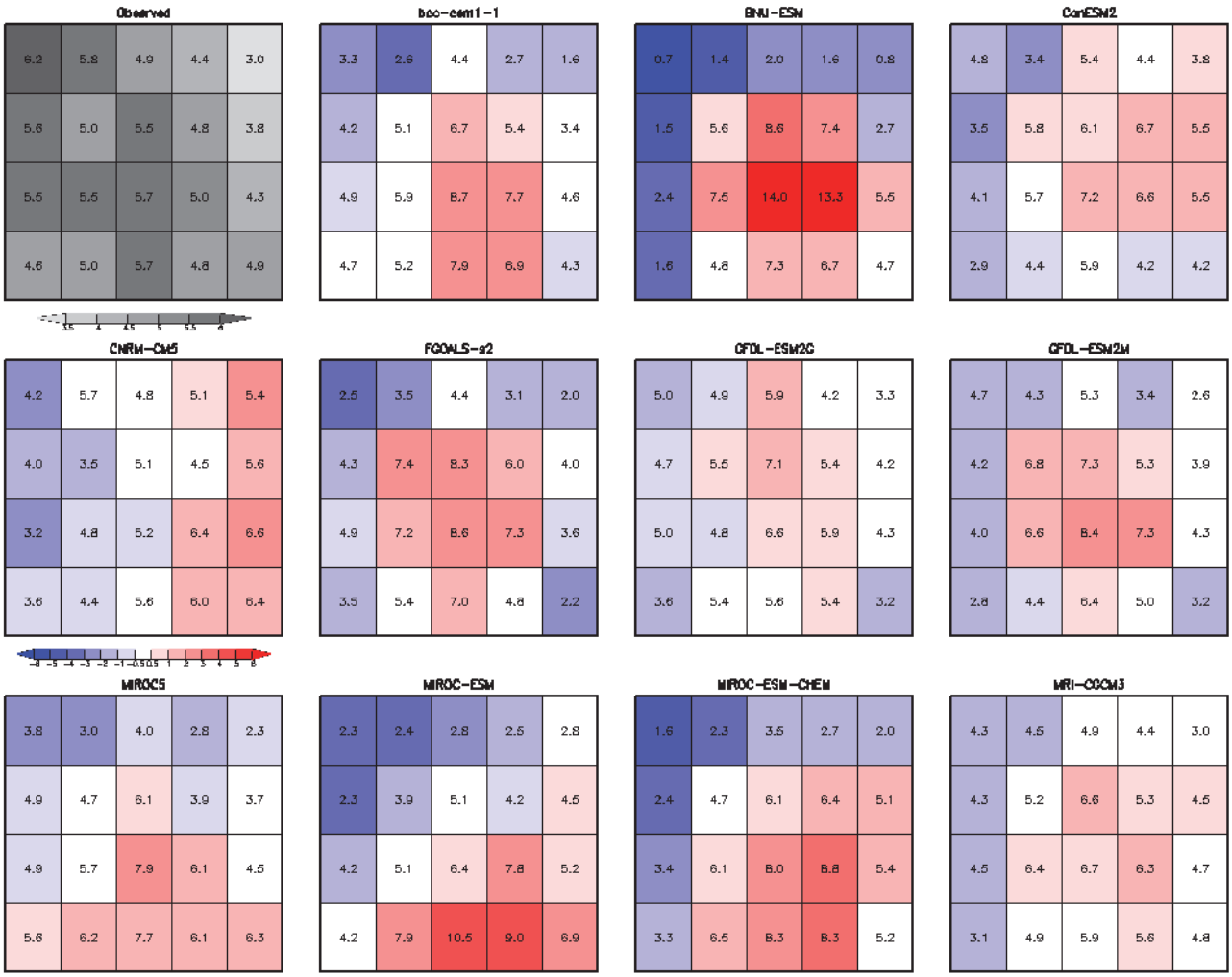

Figure 3.11 | *Percentage frequency on December-February circulation archetypes of daily geopotential height at 700 hPa for observed ERA-Interim 1979-2012 (grey) and for 11 GCMs (1976-2005). Numbers represent the percentage frequency while the blue to red shows the model bias in frequency of each archetype.*

3.7. Summary

Not only is ENSO the dominant mode of climate variability globally but it is widely accepted as the mode that has the greatest impact on subtropical southern Africa during austral summer, the season where large portions of the region receives most of its rainfall. It is for this reason that the skill of GCMs in simulating phenomena like ENSO are vital in order to have confidence in any projected future changes in the regional climate. The focus of this chapter has been looking at relevant ways to explore how GCMs reproduce the large scale processes that are important for South African weather and climate. In this case, two approaches were used, the first looking at how one of the main modes of variability is represented in current climate models and the second looking at regional circulation patterns.

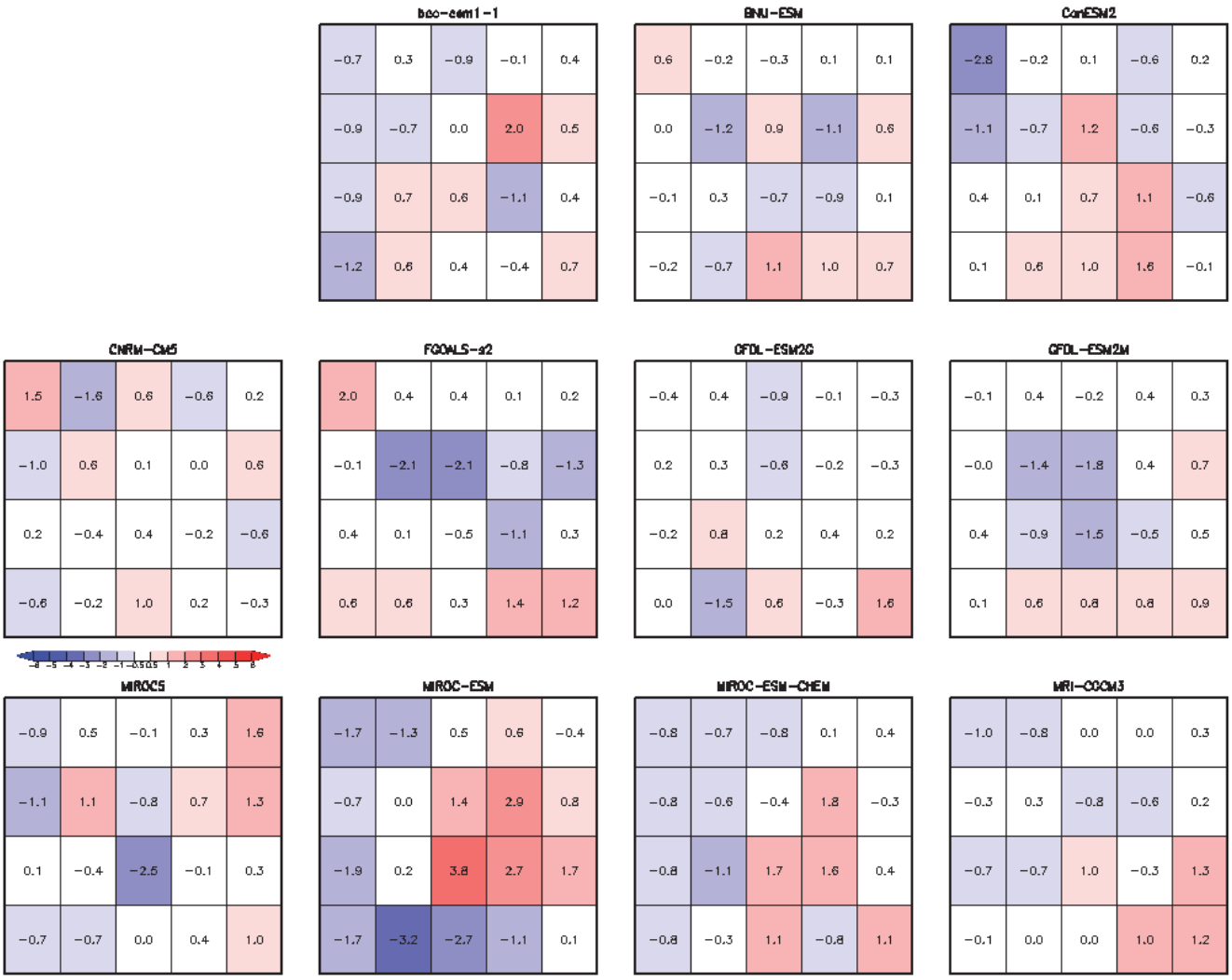

Figure 3.12 | *Projected change in circulation archetypes into the future for each of the 11 GCMs. The change in percentage frequency between 1976-2005 and 2040-2069 period. Both numbers and shading represents the absolute change in percentage frequency.*

The results here alone are not sufficient to deduce any skill in CMIP5 models in how they represent ENSO and its impacts over southern Africa. Further analysis is required to assess whether ENSO teleconnection properties are simulated correctly within CMIP5. Nevertheless, preliminary results do show that the CMIP5 models have some skill in simulating ENSO events. Additionally, most of the models tend to show dry conditions (although weaker in magnitude) over southern Africa during strong El Niños. When compared to CMIP3 results in the literature, it is evident that the newer versions of the models are starting to produce marginally more realistic results. It needs to be remembered that climate models have become considerably more complex, which to some degree has increased the uncertainty and disagreement amongst models.

A few assumptions are made when identifying/analysing modes of variability within climate models, both from a historical and future climate perspective. For example, the relationship

between current modes of variability and teleconnection properties in the future is considered to remain the same as currently observed. Careful consideration needs to be taken when looking at the frequency of such modes of variability in future climate scenarios. As highlighted by Cai et al. (2013), with regards to the IOD, the frequency of positive events is dependent on what is defined as the mean climate. The gradual increase in the west minus east SST gradient seen in the Indian Ocean over the past few decades causes the SST anomalies to cross the current defined positive IOD index more frequently. Thus, when assessing possible changes in such modes of variability, it has become common practice to separate the reference time-evolving mean climate from the anomalies above and below it.

A limitation to this study has been narrow focus on one of the key modes of climate variability in the Southern Hemisphere. Future work should be extended to include some analysis on other phenomena that are possibly just as important for South African climate. However, there is still much debate as to whether other modes of variability, such as the IOD, play an important role in South African rainfall patterns. Part of the discussion is based around whether such modes act independently of ENSO or are trigged by ENSO events (i.e. whether ENSO sis still the underlying mechanism for the rainfall anomaly). To date there are still some gaps in the understanding of the drivers behind South African rainfall variability.

Finally, the discussion within this chapter has been on variability centred in the tropics within the major ocean basins. The Antarctic Oscillation (AAO, Southern Annual Mode (SAM) or high latitude mode (Kidson, 1988), is another mode of variability (atmosphere) that would be extremely useful to understand how it is represented in CMIP5. The AAO is characterised by pressure anomalies of one sign centred over Antarctica and anomalies of the opposite sign centred near 40°-50°S. It is seen as the dominant mode of circulation variability south of 20°S. The AAO is either identified as the leading principal component of the 850 geopotential height anomalies south of 20°S (Wallace and Thompson, 2000) or as the zonal difference in mean sea level pressure between 40°-65°S (Gong and Wang, 1999). Results by Reason and Rouault (2005) suggest that the AAO may have a considerable impact on the winter rainfall region of the Western Cape through changes in the subtropical jet stream and low level moisture flux upstream over the South Atlantic. This result suggests that further analysis could also focus on drivers behind winter rainfall in South Africa and how they are represented in GCMs.

Chapter 4

APPROACHES TO QUANTIFY UNCERTAINTY OF CLIMATE PROJECTIONS

4.1. Introduction

The uncertainty associated with climate modeling is one of the leading problems in climate change studies. Uncertainty arises from the inherent stochastic and chaotic behavior of the climate system, from structural errors of models, from simplifications in the modeling system, from lack of scientific knowledge, and a host of other secondary factors. The problem of quantification of projections uncertainties has received a considerable attention in the last years. In spite of this, however, as the 2013 IPCC WG1 AR5 report states: *"...there does not exist at present a single agreed on and robust formal methodology to deliver uncertainty quantification estimates of future changes in all climate variables"*.

A number of methods, or model experiments, have been developed and implemented in the past, to resolve, or address, certain aspects of projection uncertainty. These methods rely on multiple simulations of future climate – so called ensemble model simulations – and differ by the way the ensembles are formulated. It is important to realize, however, that ensemble model simulations are able to resolve only certain aspect of total projection uncertainty. This results from the fact that firstly there is uncertainty that cannot be resolved within the model domain, and secondly, model ensembles may lack capacity to properly capture entire "possibility" space, thus underestimating, or overestimating uncertainty. For example, the common way of representing uncertainty in climate model projections is through the spread of the multi-model ensemble, such as CMIP3 or CMIP5 GCM ensembles. The approach of considering model spread as an expression of projection uncertainty assumes model democracy – that is, each model is equally weighted as if each model was equally skillful, which of course cannot be true. The problem is that we do not know which models are more skillful in terms of responding to anthropogenic forcing, and such skill will be time, location, variable, and circulation mode dependent. To work with a multi-model ensemble for purposes of developing robust regional understanding or signal and its uncertainty, we need to better understand the combined influences of different sources of uncertainty.

Analyses and results presented in this section are motivated by the need to provide quantitative estimates of projection uncertainty for South Africa consistent with state-of-the-art of relevant methods and concepts. Recognizing the on-going methodological and conceptual evolution of underlying science and the lack of established, uncontested methods, we illustrate here the current and evolving methodologies, and highlight their important aspects, rather than provide comprehensive and exhaustive results ready for "off-the-shelf" use in any application.

In particular, we address the following:

- We formulate the projection uncertainty model – a comprehensive description of uncertainties involved in the process of projecting future climate using the current, state-of-the-art models and methods, and illustrate how the various elements of the uncertainty are captured by various model experiments, focusing on model ensembles and on integration of GCM and downscaled projections.

- We explore two relatively new avenues of assessing GCM performance with the ultimate outlook to reduce model uncertainty by firstly, rejecting unrealistic models, and secondly, contributing to the body of knowledge leading towards sound quantitative assessment of the adequacy of multi-model ensemble. These two avenues are:
    - Studying model representation of the frequency of synoptic modes (described in Chapter 3)
    - Analysing model results in high-dimensional space

  These avenues provide early results that have strong potential to improve our understanding of "model space" uncertainties, and point towards approaches for improving the quantification of projection uncertainty. We feel, however, that they require further scrutiny and more work in order to be robustly and confidently applied in the process of routine assessment of climate change signals in the context of impact and adaptation studies.

- We analyse uncertainties involved in statistical downscaling of GCM output to higher resolution, local scale level. These uncertainties arise due to stochastic character of local scale response to the (deterministic in the model space) large scale forcing.

- Finally, we explore climate projection uncertainty using traditional methods – analysing spread of multi-model multi-method ensemble. We focus here on methods of determination and analysis of ensemble spread that are consistent with the understanding of the multi-model ensemble formulation, i.e. distribution-free approaches. Also, we introduce approaches to analyse multi-method ensembles, presenting internally-consistent ensembles of GCM, statistical downscaling and dynamical downscaling. We analyse consistency in time and space between the spread of the method-specific ensembles, and explore its implication to the interpretation of climate change signal derived from individual methods.

4.2. Sources of uncertainty of climate change projections

There exist three dominant "spaces" where uncertainty in projections of future climate arise (Table 4.1):

- Socio-economic space – uncertainty in emissions of greenhouse gases (GHGs) resulting from the uncertainty in future societal energy pathways, the pace of technology development and implementation and nature of policies regulating socio-economic activity.
- Climate system space – uncertainty related to natural internal variability in the climate system.
- Model space – uncertainty related to model simplifications and imperfections in the representations of the climate system.

These are schematized in Table 4.1 which also presents extent to which various types of model experiments allow for capturing or quantification of the various components of the projection uncertainty.

4.2.1. *Uncertainties in the socio-economic space*

The specification of future anthropogenic emissions (or concentrations) of greenhouse gases, aerosols and other atmospheric gases which contribute to radiative forcing in the Earth's climate is uncertain. These emissions depend on the level of population, land use and economic growth as well as technological developments, which are affected by environmental, economic and institutional changes. Also, future emissions depend on the implementation of mitigation policies and actions. Due to unpredictability in how society will evolve in the future, in the context of the analyses of climate change these variables are dealt with by concentration scenarios (representative concentration pathways – RCPs) – plausible trajectories of greenhouse gas concentrations, chemically active gases and land use/land cover – each of which can be associated with plausible socio-economic and technological development scenarios (Moss et al., 2010).

It is impossible to reliably estimate probabilities associated with each of the scenarios and therefore a reasonable strategy is to treat each as equiprobable (Collins et al., 2013). It can be argued, however, that there is no need to quantify or reduce the emission uncertainty so long as reliable information can be given for the outcome of any particular plausible future (Stainforth et al., 2007). In such a situation a particular pathway can be encouraged, as the pathway society follows depends largely on policy decisions taken now and in the future. Such encouragement may be guided by interpretation of impacts and consequences projected for a range of scenarios.

Table 4.1 | *Schematic of sources of uncertainty in climate projections, and their quantification in typical model experiments. Column widths represent entire uncertainty range for given source, shading represents part quantified within given experiment. Widths of shaded sections are arbitrary, and are intended to convey information only of "bigger than" or "less than" nature, which is valid only within each column.*

Uncertainty space or domain	Socio-economic space	Climate system space		Model space	
Uncertainty source	GHG and aerosol emissions, mitigation options etc.	Temporal climate variability		Model imperfections	
		large scale processes (atmospheric circulation)	local scale processes	structural, process and parameter uncertainty	model inadequacy
Quantification of uncertainty in model experiments:	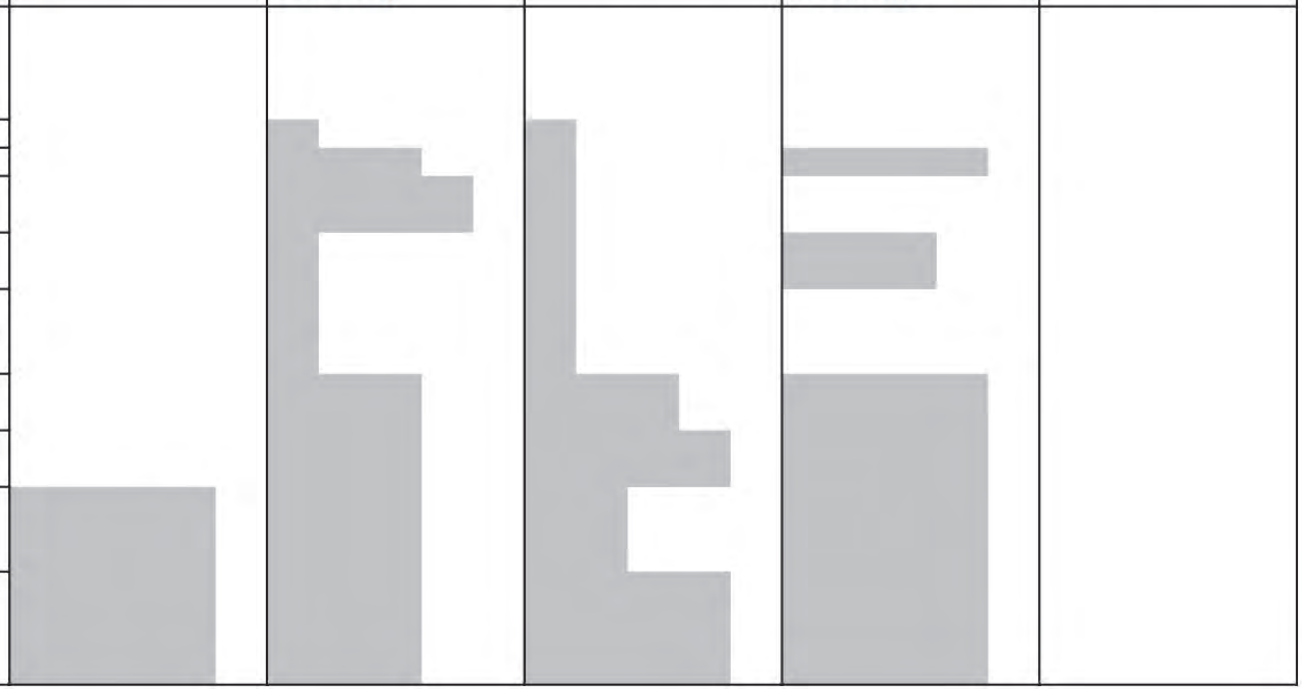				
single GCM run					
MME GCM					
Initial condition ensemble, single GCM					
Perturbed physics ensemble, single GCM					
Downscaling, single method or RCM, single GCM					
MME GCM, downscaled with single method					
MME GCM, downscaled with multiple methods					
CMIP5 GCM ensemble (multi-model, multi-RCP)					
CORDEX-like ensemble (multi-model, multi-downscaling, multi-RCP)					

Importantly, scenarios, or RCPs, although comprehensive, may not be exhaustive, i.e. there is a possibility of a future evolution of the concentration greenhouse gases that is not covered by the set of RCPs. Such a future may occur, for example, due to processes not yet fully understood, or not anticipated within the current state of knowledge of the global socio-economic system. In other words, although all emission scenarios are considered to be plausible, there is always a chance that an "implausible" future will occur. As such, uncertainty of climate projections associated with the socio-economic space (or greenhouse gas emissions) cannot be fully explored within the model space using the concept of emission or concentration scenarios.

4.2.2. *Uncertainties in the climate system space*

Climate, defined as the statistical distribution of atmosphere-ocean states for a given spatial scale, varies on annual, decadal, multi-decadal, centennial and longer timescales. Even in the absence of externally forced changes to the system, such as those associated with long-term orbital variations, the climate system exhibits internal variability as a result of nonlinear behaviour and feedbacks, which complicates our interpretation of climate change (Rial et al., 2004). Appreciation of these natural, internally-induced fluctuations in short-term climates is important from societal point of view as they have the potential to counter the longer-term trends that are associated with anthropogenic climate change, or alternatively, magnify these trends considerably.

When observing the system over years or decades, and in attempting to project the distribution of atmosphere-ocean states for some period in the future, we must therefore acknowledge internal variability in the climate system and quantify the uncertainty arising from variability on multiple time scales. Quantifying this uncertainty is straightforward in a stationary climate, i.e. when there is no external forcing such as GHG-induced radiative forcing, and when records/simulations are available for time periods longer than the characteristic time scales of internal variability. Under such conditions, uncertainty arising from natural variability can be equated to sampling uncertainty. The latter is an expression of error in the determination of the "true" mean value of the process underlying the variability of a particular property from a single "realization" of that process, and is simply captured by standard error of long-term mean of observed or simulated climatic variable. This form of uncertainty can be reduced by extending the time series.

However, in practice, we deal with relatively short time series (instrumental observations rarely exceed 100 years), in a non-stationary system (anthropogenic emissions and land use change may be influencing climate in the last 150 years or longer), and thus we are not able to comprehensively sample natural variability at a range of relevant time scales.

The climate system is inherently chaotic (Lorenz, 1970); the trajectory the system takes is sensitively dependent on the initial state of the system. Even with a perfect model, in the absence of perfect observations, we must acknowledge this sensitivity. However, we can use this to our advantage to help quantify the uncertainty arising of internal variability. This

uncertainty can be partly quantified in the model space – acknowledging that the available models are not synonymous with the climate system, and that there are uncertainties arising within the model space. This is normally done by running models many times from different initial conditions (using an initial condition ensemble [ICE]). By using an ICE, under the assumption of ergodicity, we can provide a description of possible trajectories that the climate system may take (Daron and Stainforth, 2013). The reliability of the ICE is dependent, however, on whether the simulated variability is consistent with observations. When assessed within the model space, the natural variability uncertainty is sometimes termed the initial condition uncertainty (e.g. Stainforth et al., 2007).

4.2.3. *Uncertainties in the model space*

Uncertainty arises in the model space due to the obvious need to simplify climatic processes in order to construct, and run simulations on, a mathematical representation of the climate system. In addition, both because of the need to simplify the system and imperfect knowledge of specific process, models do not incorporate all of the processes and factors influencing climate system. In other words, the model space uncertainty is a reflection of imperfect nature of climate models. That uncertainty can be divided into two parts: uncertainty resulting from model inadequacy, and uncertainty resulting from model resolution and associated parameterizations. The former reflects the fundamental uncertainty in the representation of the real system that models can achieve. The latter captures the fact that we are uncertain as to what parameter values, or indeed parameterization schemes, are likely to provide the most informative results.

The uncertainty from imperfect and imprecise knowledge of Earth system processes can be partially quantified by constructing ensembles of models that use different formulations or parameterizations of these processes. The multi-model methods are predicated on the fundamental reality that no model is the true model, and there is value in synthesizing projections from an ensemble, even when the individual models seem to disagree with one another. This assumption has been frequently shown to yield improvement in weather forecasting.

However, models are “related” to each other, i.e. they share computational algorithms, parameterization schemes and parameter sets (Masson and Knutti, 2011). Also, some processes may be missing from the set of available models, and alternative parameterizations of processes may share common systematic biases. Such limitations imply that available model ensembles are not a systematic, exhaustive representation of possible range of distributions of “process parameterization space”, and thus multi-model ensembles are often termed “ensembles of opportunity”. As a consequence, there is an unquantifiable uncertainty even in the envelope of multi-model ensemble results. An additional consequence of the “ensemble of opportunity” is the lack of basis for a statistically sound error or uncertainty model underlying the ensemble.

Regional downscaling methods, both statistical and dynamical, have been developed in part to address the uncertainties involved in the process parameterization problem (Hewitson and Crane, 2006). By resolving and/or translating large-scale processes to finer spatial scales, it is possible to better understand, and ultimately quantify, the model uncertainty at sub-GCM grid scales.

The relative role of the different sources of uncertainty—model, scenario and internal variability—as one moves from short- to mid- to long-term projections and considers different variables at different spatial scales has to be recognized (Hawkins and Sutton, 2009). The three sources exchange relevance as the time horizon, the spatial scale and the variable change

4.2.4. *Climate simulation ensembles and projection uncertainty*

As outlined above, climate model simulations may be used to quantify some aspects of projection uncertainty, however, how much of the total uncertainty is addressed depends on the type and number of models performing similar simulations (Table 4.1).

Individual model runs, as they reflect some aspects of climate variability, allow for capturing a fraction of the climate space uncertainty, but are not informative about model space uncertainty.

Initial condition ensembles (ICE) of a single GCM enable a more comprehensive capturing of natural variability, particularly if initial states are generated within a well-formulated statistical framework.

Perturbed physics ensembles (PPE) and multi-model ensembles (MME) capture a part of the model space uncertainty, and also natural variability-related uncertainty (because in practice, different models are initialized from different initial conditions). The PPE are systematically constructed through structured sampling of model parameter values from predetermined distributions. As a consequence, PPE output lends itself to statistical interpretability and modeling, and PPE ensemble spread is a straightforward expression of uncertainty related to the sampled parameter space.

Linking GCMs with downscaling (either dynamical or statistical) allows for separation of climate space uncertainty into two components: large, or synoptic scale uncertainty, and local scale uncertainty. The former encompasses processes of large-scale atmospheric circulation and teleconnections, the former reflects the role of meso-scale atmospheric processes, stochastic nature of local responses to deterministic synoptic forcing, and local scale land-atmosphere feedbacks.

4.2.5. *Multi-model ensembles*

Multi-model ensembles, MME, as available through CMIP3 and CMIP5, are not created in coordinated manner and they form a statistical sample that is neither random nor systematic, with possible dependencies among the members (Tebaldi and Knutti, 2007). As a consequence, there is a general consensus that such ensembles lack the underlying intrinsic characteristics that would allow quantitative interpretation of ensemble properties (Knutti et al., 2010). Such interpretations are made, however, within two frameworks. One possible concept is the so-called 'truth plus error' view, i.e. that each ensemble member represents a sample from a distribution centered around the truth (e.g. Smith et al., 2009). In this case, models in an ensemble are considered to be random draws from a distribution centered on observations. Another concept considers that each of the members is 'exchangeable' with the other members and with the real system (Annan and Hargreaves, 2010). In this case, observations are viewed as a single random draw from a distribution of the space of all possible but equally credible climate models and all possible outcomes of Earth's processes. A 'perfect' independent model in this case is also a random draw from the same distribution, and so is 'indistinguishable' from the observations in the statistical model. The results obtained within these frameworks are not, however, robust, and depend heavily on further assumptions made, such as weights assigned to individual members, or prior distributions of parameters. There is as yet, no consensus as to which of these assumptions are universally correct (Collins et al., 2013).

Analysis of multi-model ensemble results may embrace the concept that all models are treated equally or, alternatively, that they are weighted based on their performance (Knutti, 2010). Recent studies have begun to explore the value of weighting the model projections based on their performance measured by process evaluation, agreement with present-day observations, past climate or observed trends, with the goal of improving the multi-model mean projection and more accurately quantifying uncertainties. However, a robust approach to assigning weights to individual model projections of climate change is yet to be identified (Knutti, 2010).

In summary, there are important caveats to the interpretation of ensemble spread as a measure of climate change projections uncertainty:

- Uncertainty around the future climate state is not fully captured by the spread of a multi-model ensemble.
- Multi-model ensembles, such as CMIP3/CMIP5 or CORDEX, lack intrinsic characteristics (i.e. a well-defined error model) allowing for deriving quantitative estimates of uncertainty from ensemble spread.
- A robust approach to assigning weights to individual model projections of climate change has yet to be identified
- Degree of agreement between multiple models can, however, be a source of information in an uncertainty assessment to strengthen confidence statements.
- Confidence cannot be inferred from model agreement alone.

4.3. Exploring model representation in high-dimensional space

Climate system data is three dimensional in space, and autocorrelated in space and time. The consequence is that in terms of the raw data it is very difficult to understand what aspects are driving the regional climate, how the model skill is dependent on place and time, or the robustness of a regional signal from anthropogenic forcing. The approach adopted here is to orthogonalize the high-dimensional autocorrelated raw data and explore the system in a lower dimensional space.

The objective is to characterize the local-scale variance in context of the larger determining state of the atmosphere. In this approach one takes as a given that for any place the local co-located regional atmospheric cube defines the conditioning dynamic state of the regional climate response. This local atmospheric cube is of course conditioned by the larger scales up to and including the global modes of variability, but these larger scales are necessarily translated by and reflected in the local atmospheric cube.

For the model, this cube is a reduced-complexity and simplified representation of the real world, and forms the boundary conditions for the local climate response – inherently these attributes introduce uncertainty.

The concept to analyze this is to use the sample set of data to examine the volume and variability of the volume occupied by the model in the continuum of the data space. Comparison of this representation for a model with that of the real world (or as best can be represented by a reanalysis data set) allows one to understand where the uncertainty in the model simulation arises from.

For the method, we use the atmospheric cube represented by the u, v, q, t, and RH variables. For the initial examples presented here, we use reanalysis data that forms a point-cloud of samples in the n-dimensional space, defining the known span of the atmospheric states

As the atmospheric data are highly autocorrelated, the dimensions of the raw data are non-orthogonal. We initially transform the data onto a geodesic grid (for latitude independence), and then orthogonalize the daily data of the 3-dimensional cube of data atmospheric state over a location using EOFs (with a Monte-Carlo test to determine EOF significance). The significant EOFs typically reduce the original data to between 7-12 dimensions. We can then examine aspects such as the local variance of response around each sample in the n-dimensional. An example, showing two of the dimensions and an arbitrary time trajectory through the point cloud of samples is given in Figure 4.1. The trajectory defines the evolution of the atmospheric state.

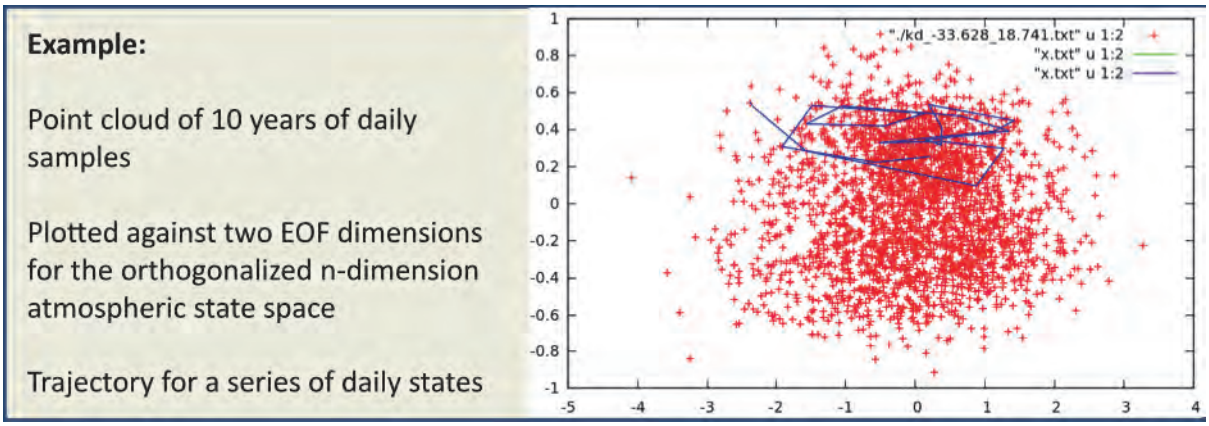

Figure 4.1 | *Point clouds of daily data plotted in two of the EOF dimensions, with a sample short time trajectory of the data.*

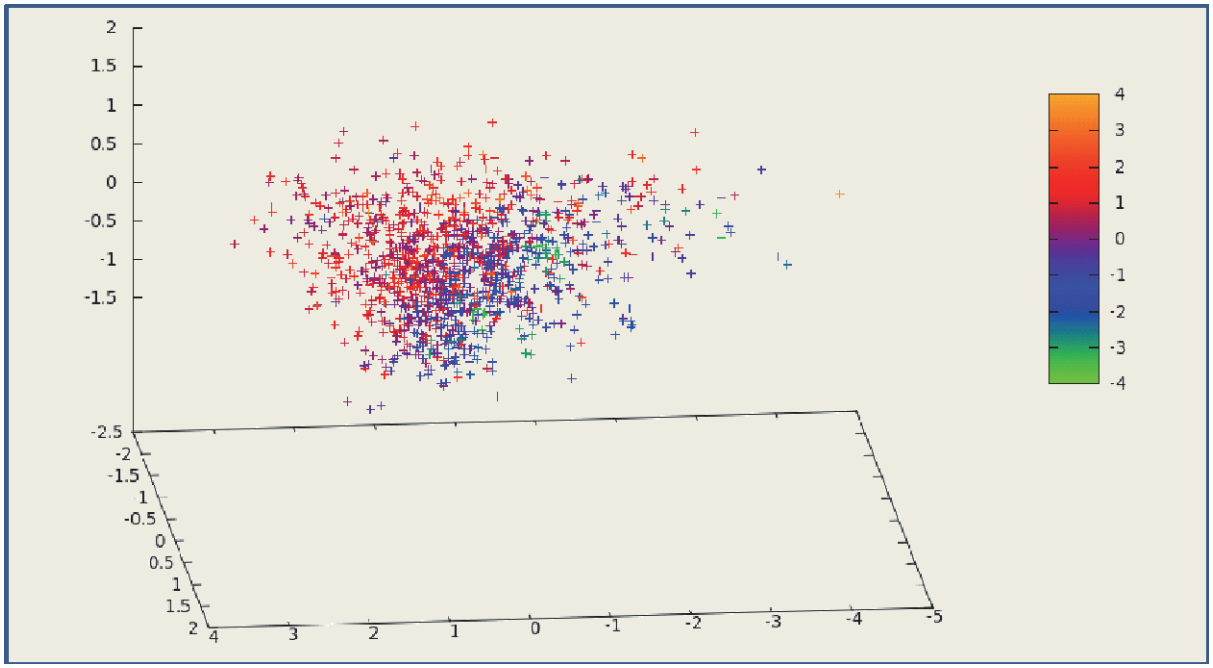

Figure 4.2 | *Point cloud of daily data plotted in three EOF dimensions strongly related to the local scale precipitation response. Points are coloured by the magnitude of precipitation observed on each day.*

The data can further be evaluated in terms of the what aspects of the data dimensions are strongly determining the local climate response, and which are not. Through this one can examine how a model is responding on a regional scale in terms of the critical data dimensions.

For example, Figure 4.2 shows the point cloud of data where each point is colored by the magnitude of the precipitation response at the local scale. In Figure 4.2 the three dominant

data dimensions in relation to the precipitation response are used. The figure shows how the precipitation response is well disaggregated in relation to the three EOF dimensions. .

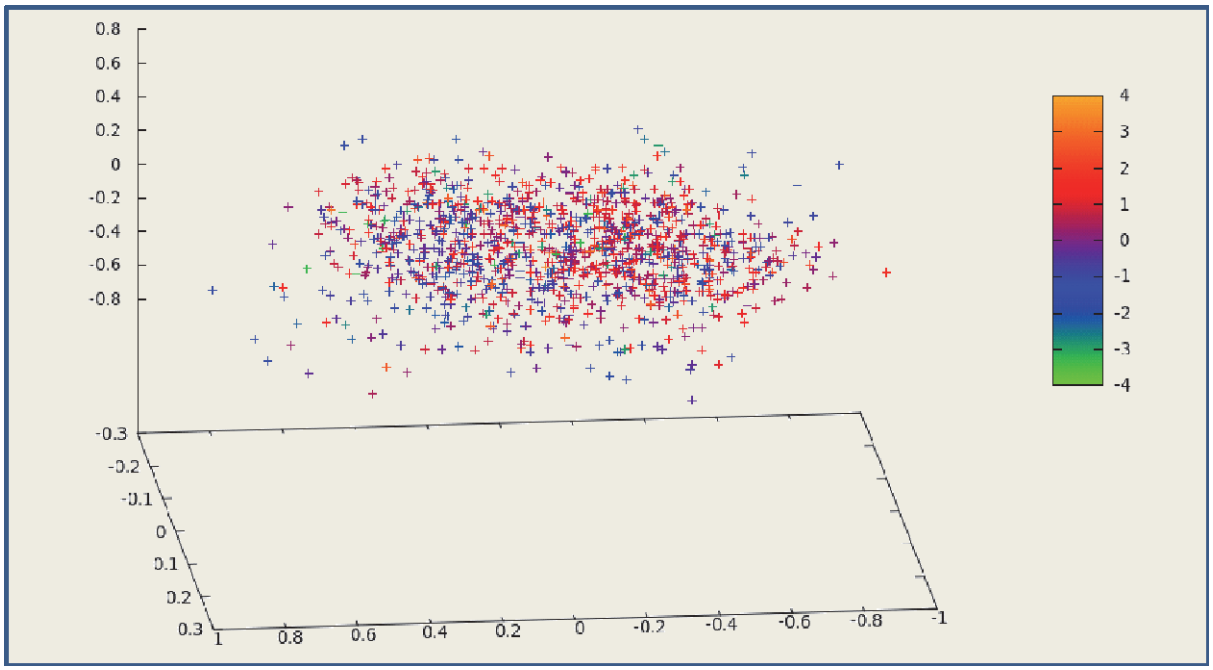

Figure 4.3 | *Point cloud of daily data plotted in three EOF dimensions weakly related to the local scale precipitation response. Points are coloured by the magnitude of precipitation observed on each day.*

For contrast, Figure 4.3 shows the same data, but plotted in terms of three data dimensions that are weakly determining the precipitation response. In this case it is apparent that there is no clear disaggregation of the precipitation response. By comparing the point clouds between models and between models and observational data, once can assess the source of a models introduced uncertainty.

At this stage the project has coded the algorithms to undertake this analysis, and application to the CMIP5 models is now underway. From this the intention is to inform about the relative contribution to uncertainty from each model, as a function of season and location.

The approach shows strong potential to address a broad range of questions. However, developing the code from proof of concept into a robust tool requires resources beyond that of this project. This development will take place under the auspices of other ongoing project work, for some of which it will now form a core methodology following the results obtained here

4.4. Evaluating the role of small scale (sub-grid) processes in contributing to uncertainty of rainfall projections

One of elements contributing to uncertainty from GCM simulations is the fact that the models discretize the climate system into large spatial grids (typically 100-300 km horizontal

resolution). Processes occurring at spatial scales larger than the model grid (such as large-scale synoptic circulation) are resolved, or explicitly accounted for in the GCM. Processes occurring at the spatial scale lower that the model grid (such as mesoscale convective systems) are parameterized, or simply expressed by a set of functions, often empirical in nature. The resulting outputs are deterministic and spatially uniform within the grid.

In reality, climate and weather responses at sub-grid scales are a combination of large scale synoptic forcings, and local scale forcings. The latter are variable in space, depending on within-grid characteristics of, for example, topography and land cover, and secondly variable in time due to time-varying conditions such as soil moisture related energy fluxes. Due to the unresolved nature of small-scale processes and the nonlinear relationships between the large- and small-scale, local weather and climate responses are also characterized by a probabilistic component; it may or may not rain at a given location under given synoptic and mesocale conditions. Such spatial scale dependencies and relationships have rarely been considered in the literature and practice, and is the subject of this section of our project.

Dynamical and statistical downscaling methods seek to alleviate the grid-size related deficiency of GCM output, the former by reducing the computational grid size, the latter by introducing empirical relationship between local scale responses and large scale forcing, which is conditioned on the past observations. Each of these has advantages and disadvantages and introduces additional method-related uncertainty. However, statistical downscaling has the ability to explicitly address the probabilistic component of the local climate responses, as this component is central to the formulation of method's principles, i.e.:

Local scale response=f(large scale forcing) + unexplained (probabilistic) variance

Here, we assess the magnitude of the probabilistic component of local rainfall using the SOM-based downscaling method applied to NCEP reanalysis data with a set of 1100 rainfall stations located in the southern Africa.

4.4.1. *Methods*

Self-organizing maps-based downscaling (SOMD) is a statistical downscaling method based on a probabilistic description of the relationship between large-scale synoptic variables and local (point) responses. During the training phase, for each analysed point (rain gauge), a number of relatively distinct large-scale synoptic conditions are identified through clustering of observed mean daily fields of variables such as wind, pressure and temperature from the region around this point, using the SOM method. The clusters, or SOM nodes, reflect conditions present during different (not necessary adjacent) days, but each day maps onto a unique SOM node. A PDF of the response variable is then formulated for each node by selecting values of that variable for days mapping onto that node from the time series of measurements. When the method is applied to downscaling of GCM output, GCM daily fields are mapped onto the SOM, and for each day of GCM simulation, a value of the response variable is randomly drawn from the PDF for the corresponding SOM node.

In our analysis, SOMs were developed (trained) from the 1979-2010 NCEP 2.0 re-analysis product, for 1100 rain gauge locations in continental southern Africa (south of 20°S). These locations were selected from a rainfall database by the condition that daily rainfall data with at least 10 years overlap with the NCEP data period were available.

During the application phase, NCEP synoptic fields were re-mapped onto the SOMs and used as a basis for generating output time series of the response variable, i.e. rainfall. The latter was done in the Monte-Carlo mode, i.e. we have generated 1000 daily time series (the Monte-Carlo ensemble) covering the NCEP data period (i.e. 1979-2010) for each analysed location.

The resulting time series of daily rainfall were characterized by their statistics – we have selected three indices reflecting rainfall frequency, intensity and overall wetness, namely: number of rain days per year, median daily rainfall and mean annual rainfall. Subsequently, we have calculated two statistics of the Monte-Carlo ensemble of each of these indices for each of the stations, namely mode and 20^{th}-80^{th} inter-quantile range (IQR). The latter one expresses the magnitude of the probabilistic component of local rainfall, and is subject to further analyses.

Maps expressing spatial distribution of the ensemble median, IQR and various derivatives were prepared using ordinary kriging with isotropic and spatially uniform linear variogram fitted to the data. Kriging was done only for areas with at least 5 data points within the nearest 200 km.

4.4.2. *Results*

In general, the magnitude of IQR for number of rain days and mean annual rainfall increases with increase in location wetness (mean annual rainfall) and overall variability (standard deviation of daily rainfall) (Figure 4.4). That relationship is weaker and opposite for median daily rainfall, i.e. IQR of median daily rainfall seems to decrease with increasing wetness and overall variability. Importantly, the correspondence between overall variability of rainfall (as expressed by standard deviation of daily rainfall) and IQR in mean annual rainfall is linear and very well defined (Figure 4.4), which seems to indicate that both express the same underlying probabilistic processes – i.e. driving forces of rainfall variability.

The strength of the probabilistic component relative to the median value of a given index is stronger for drier locations, where IQR (which in our formulation: p80-p20 covers 60% of variability range) may reach 30-40% of the median (Figure 4.5). Spatial distribution of IQR is very similarly to that of the median for rainfall frequency and mean annual rainfall, and roughly reflects the pattern of mean annual rainfall with decrease from east to west, and higher values in the southern coast of the Western Cape (Figure 4.6). The spatial pattern for IQR of median daily rainfall is approximately opposite to the above, however, with more erratic and patchy character (Figure 4.6, middle figure in the lower row).

The relative magnitude of IQR relative to the median displays a similar pattern for all three indices, with low values throughout eastern and central South Africa, elevated values in the Karoo, reaching high values in southern Namibia (Figure 4.7).

In summary, the uncertainty in rainfall arising from the probabilistic nature of local response to large-scale synoptic forcing is relatively large – for 30-year mean annual rainfall the 20^{th}-80^{th} IQR that falls within the range of 5-40% of that mean, with larger values associated with lower mean rainfall. For other rainfall indices, this uncertainty falls within 5-30% of their mean values, with higher values associated with lower mean values of these indices.

This uncertainty is only partly sampled by the GCM and SOMD ensembles, and because of its magnitude, it may be important for determination of significance of the change signal, and interpretation of ensemble results in terms of change signal consistency and significance against the natural variability.

In the context of analyses of uncertainty of climate change projections from an ensemble of model simulations, the probabilistic component of rainfall expressed here by IQR can be interpreted as a range of responses that would arise during downscaling procedure even if the source GCMs simulated identical large-scale circulation. Under such interpretation the IQR represents an un-reducible part of the spread of the downscaled multi-GCM ensemble, and thus indirectly, also a limit to detectability of climate change signal.

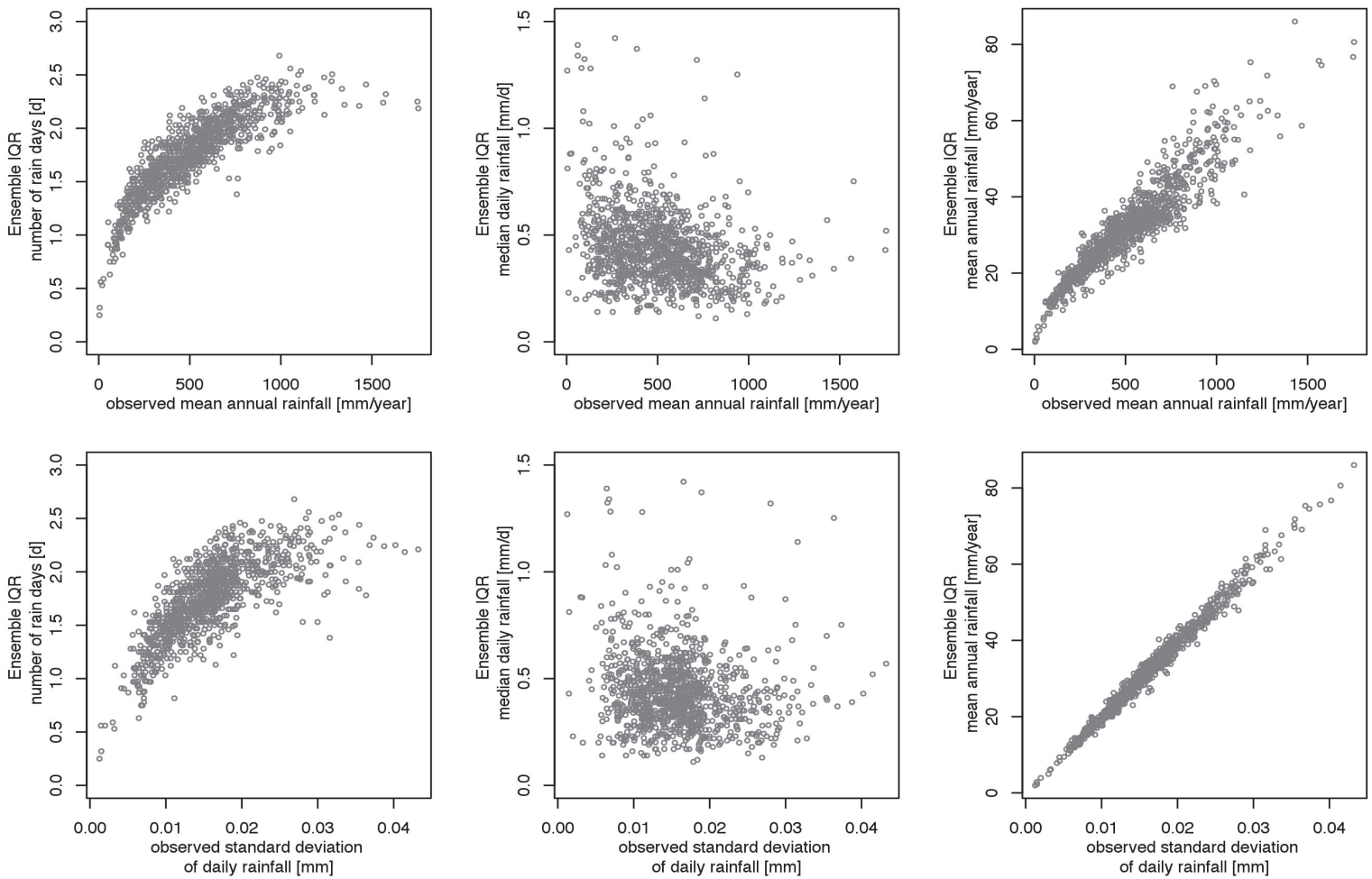

Figure 4.4 | *Relationship between probabilistic component IQR of Monte-Carlo ensemble) and overall wetness (expressed as mean annual rainfall) as well as rainfall variability (expressed as standard deviation of daily rainfall) for three rainfall indices*

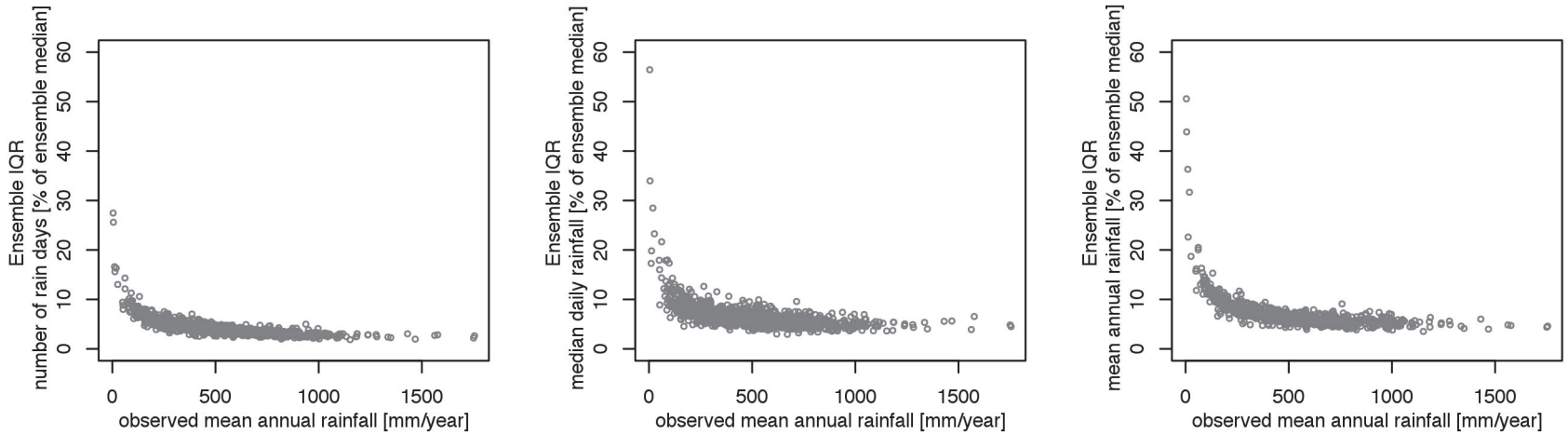

Figure 4.5 | *Relative importance of the probabilistic component (IQR expressed as a % of median of the Monte-Carlo ensemble) as a function of overall wetness (expressed as mean annual rainfall) for three rainfall indices*

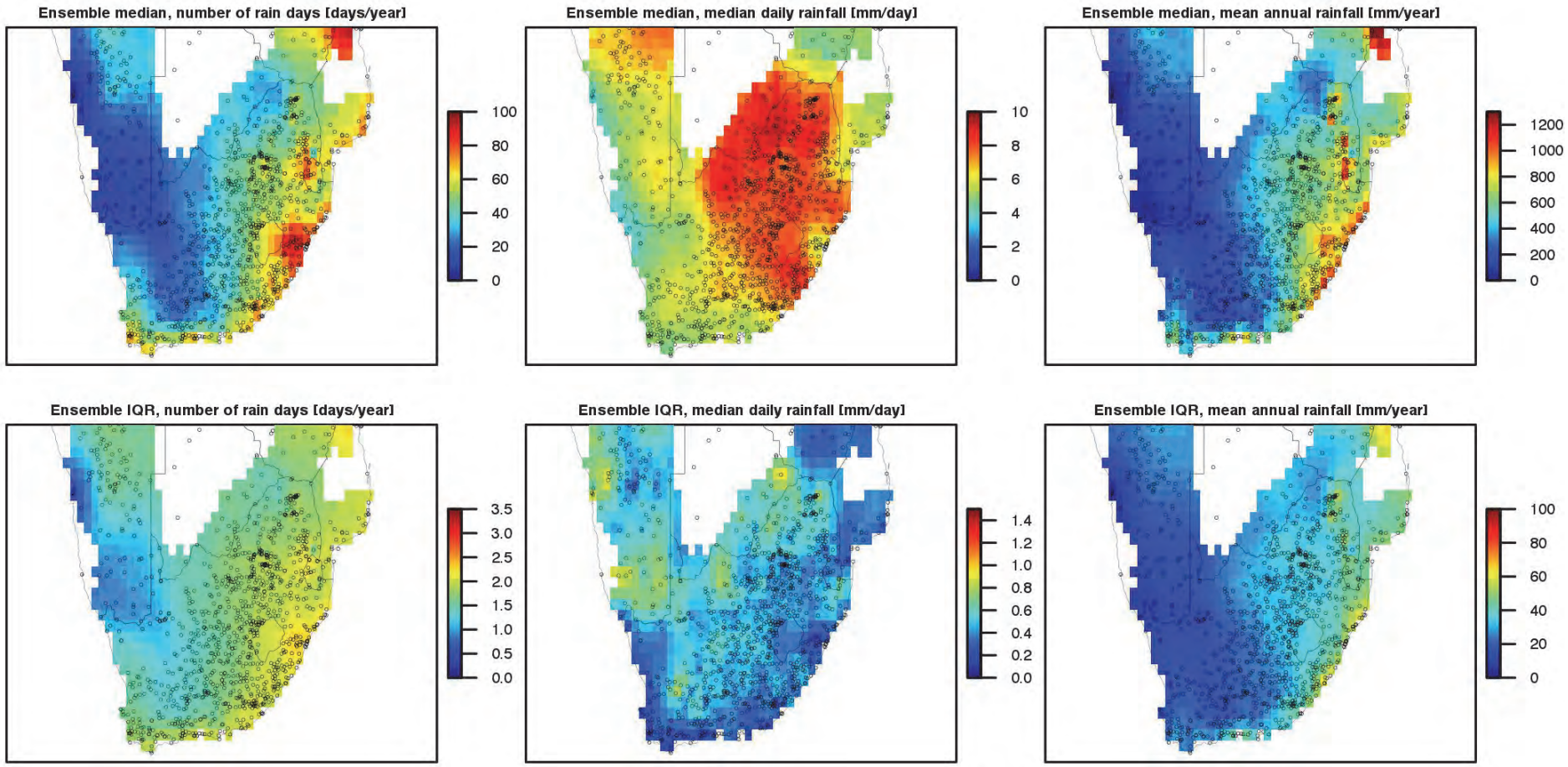

Figure 4.6 | *Spatial distribution of median values and probabilistic component (IQR of Monte-Carlo ensemble) for three rainfall indices.*

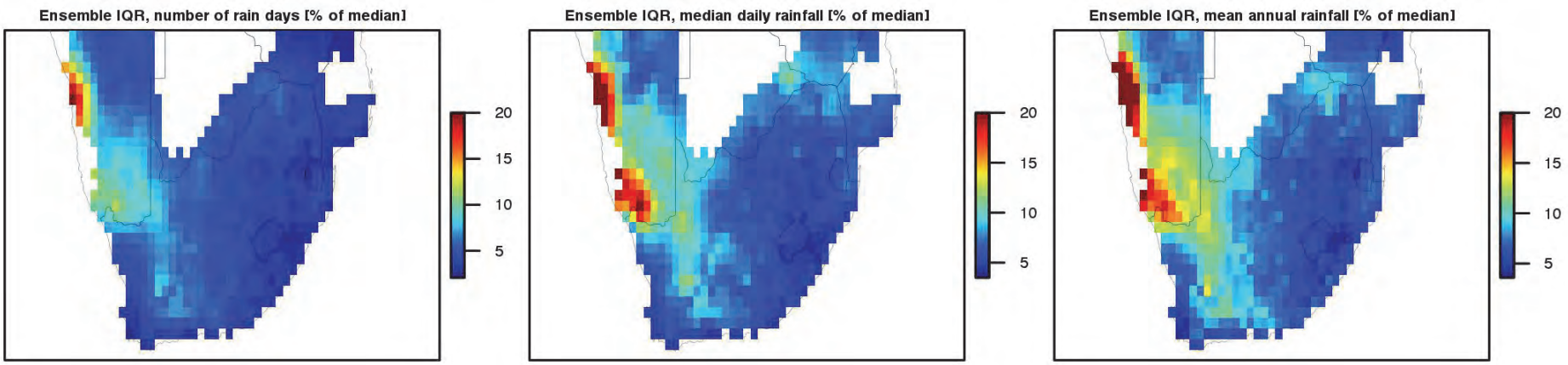

Figure 4.7 | *Spatial distribution of relative importance of probabilistic component, expressed by IQR as a percentage of median value of the Monte Carlo ensemble, for three rainfall indices.*

4.5. Assessing uncertainty of projections in the model space – analysing ensemble spread from multi-model, multi-method data set

This section aims at assessment of uncertainty of climate change projections in the multi-model, multi-method ensemble, considering that both magnitude of the ensemble spread and method-to-method agreement carry some information about the uncertainty/probability of projections. This assumption is not unreasonable taking into consideration that the "experiment" analysed here, i.e. multi-model ensemble of GCMs (GMC ensemble), downscaled with a single statistical downscaling method, SOM-based downscaling (SOMD ensemble) and with a single dynamical regional climate model (RCMD ensemble), covers a considerable part of the uncertainty range arising within model and climate system spaces, as presented in Table 4.1.

However, since we deal here with the "ensemble of opportunity" of GCM projections and limited selection of statistical downscaling and dynamical downscaling methods (a situation rather likely in practical situations), we therefore have no basis for statements on how large fraction of the uncertainty range we do cover. Also we have no basis for assuming a particular distribution of model anomalies about the true value of climate change signal. As a consequence of these, we do not analyse the GCM, SOMD and RCMD ensembles within one coherent statistical framework. Rather, we treat them as three subsets of a broader "super-ensemble", and seek for information about signal and uncertainty in the consistency of ensemble ranges and ensemble tendencies across methods, in the spatial and temporal context. In this methodological paradigm, we are not precisely quantifying uncertainty ranges associated with particular projected values, but we are assessing where and when projections seem to be more or less reliable, contributing to enforcing or supporting messages arising within the broader multi-source robust climate change messages framework.

To analyse ensemble spread, we use inter quantile range, which is a distribution-free, and bias-resistant measure, used in similar context (e.g. within IPCC AR4/AR5 reports). Additionally, we do not consider ensemble average (mean or median, equiprobable or weighted) as a reliable measure of climate change emerging from the analysis of the ensembles. We use the ensemble median, however, as an expression of overall tendency of the ensemble, and always in corroboration with the measure of ensemble spread.

We illustrate approach here, rather than provide exhaustive results applicable at a range of spatial and temporal scales. The chosen context is that of difference in mean rainfall and temperature between the future and past 30-year periods (2041-2070 and 1976-2005 respectively).

4.5.1. *Methods*

Ensemble of sixteen GCM runs obtained from CMIP5 archive, thereafter called gcm16 ensemble. Ten of the GCMs have been downscaled using Self Organizing Maps based statistical downscaling procedure (SOMSD), forming somsd10 ensemble. Downscaling has

been done with the WFDEI daily rainfall, minimum and maximum temperature and ERA-interim synoptic variables for 1979-2009 as training datasets. Downscaling output is a daily gridded dataset with horizontal resolution of 0.5 deg, covering entire Africa for the period of 1950-2100. Additionally, eight of the GCMs were downscaled using SMHI-RCA4 regional climate model, generating rcm8 ensemble. Furthermore, an ensemble (or sub-ensemble) gcm10 was created, comprising the same ten GCMs that were downscaled with SOMSD method. Creation of similar sub-ensemble for RCM simulations was not feasible, as there was overlap of only 4 models between the gcm16 and rcm8 ensemble.

Analyses were performed using the traditional future-past change index:

$$\Delta X_i = X_{future,\ i} - X_{past,\ i}$$

where *X* is variable of interest, i.e. rainfall P, minimum daily temperature T_{min}, or maximum daily temperature T_{max}, averaged over a period of time, calculated for each member *i* of the *n*-member ensemble. In the analyses, future period of 2041-2070, and past, reference period of 1976-2005, and 3 months integration time were used. Values of the change index were calculated for each of the three analysed variables on the 0.5 deg grid-to-grid basis. For the GCM and RCM ensembles, data at this resolution were obtained from bilinear resampling from the original resolution of each individual dataset.

Ensemble spread was measured by inter quantile range (IQR), expressing the distance between 80th and 20th percentile of the ensemble distribution, i.e.:

$$IQR = p80(\Delta X_{i=1..n}) - p20(\Delta X_{i=1..n})$$

IQR was calculated separately for the gcm16, somsd10, rcm8 and gcm10 ensembles. Spatially articulated differences and similarities between the IQR of the various method-specific ensembles were juxtaposed against the spatial patterns of magnitude and ensemble tendency, and interpreted in terms of possible underlying local and regional scale climate processes.

For the purpose of quantitative comparison of differences between IQR of the gcm10 and somsd10 ensemble that difference was quantified as:

$$IQR_{diff} = (IQR_{somsd10} - IQR_{gcm10}) / IQR_{gcm10}$$

In order to test for significance of IQR_{diff}, a non-parametric permutation-based test was used. In this test, p-value was obtained by comparing observed IQR_{diff} with distribution of IQR_{diff} obtained from 1000-fold random draw of pooled values ΔX_i of gcm10 and somsd10 ensembles.

4.5.2. *Results*

Figure 4.8-4.5 present “cascades of uncertainty” for the three analysed ensembles (somsd10, gcm16, and rcm8), for change in seasonal (austral summer DJF, and winter JJA) means of

three variables (rainfall, minimum and maximum temperatures), averaged over southern African domain, for two concentration scenarios – RCP4.5 and RCP8.5. In the figures, ensemble results are presented as individual model results, as the ensemble median, and as the average of results for two concentration scenarios. Ensemble median is used here to illustrate the overall ensemble tendency, and the scenario average is presented purely for the sake of illustration of scenario-independent tendency in the ensemble.

The degree of agreement between methods (ensembles) varies between variables and seasons. For summer rainfall (Figure 4.8), there is a broad consistency in tendency (as expressed by "location" of IQR) between gcm16 and somsd10 ensembles – i.e. they both span between a decrease and a small increase in rainfall. IQR of somsd10 is, however, smaller than that of gcm16. The IQR of rcm8 is in general of the same order of magnitude as that of the other ensembles, but its location is shifted towards the negative change.

For winter rainfall (Figure 4.8), IQR of gcm16 ensemble is shifted towards negative change, while somsd10 and rcm8 "straddle" the no-change condition, and are located predominantly on the negative change side. IQR of somsd10 is much smaller than that of the two other ensembles.

In both seasons, differences between concentration scenarios are minimal.

For summer temperatures (Figure 4.9 and Figure 4.10), there is relatively little difference in tendency and magnitude of IQR in each of the ensembles, apart, perhaps, from IQR for minimum temperature being narrower in rcm8 than in the other ensembles. Not unexpectedly, there are relatively strong differences in ensemble tendency between the two concentration scenarios.

For winter temperatures (Figure 4.9 and Figure 4.10), the ensemble differences are more pronounced. The most striking are a) the differences in the width of IQR, with rcm8 the largest and somsd10 the lowest, and b) difference in tendency of the ensembles, with rcm8 indicating considerably larger increases in temperatures than the other ensembles.

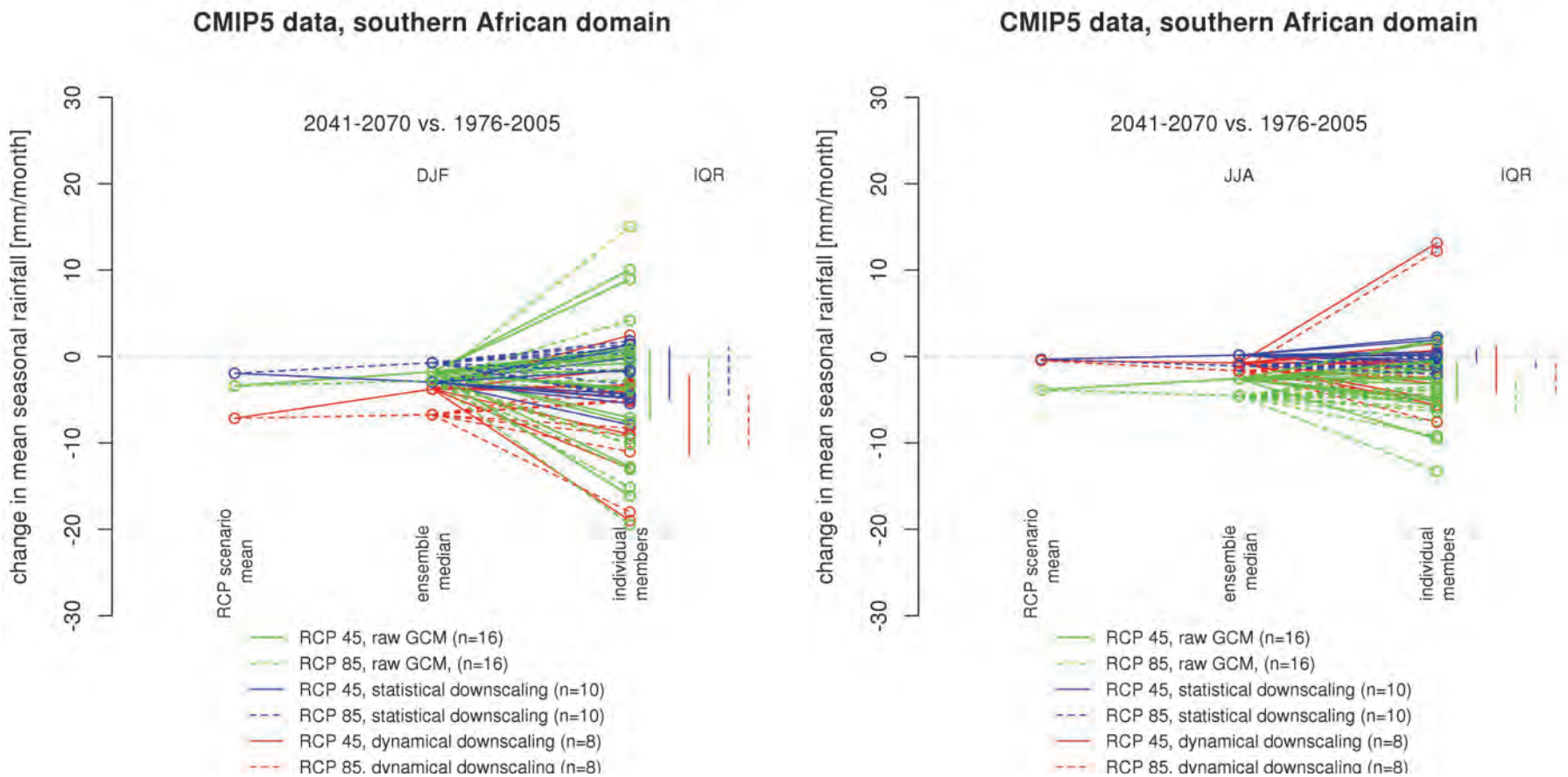

Figure 4.8 | *"Cascade of uncertainty" for change in mean monthly rainfall for DJF (left) and JJA (right) for two RCP scenarios and three ensembles: 16 GCMs (gcm16), 10 statistical downscaling realizations (somds10) and 8 regional climate model realizations (rcm8) averaged over the domain covering the land body of southern Africa (35°-20°S, 10°-40°E). Bars on the right-hand side of the graphs mark IQR for each ensemble/RCP combination.*

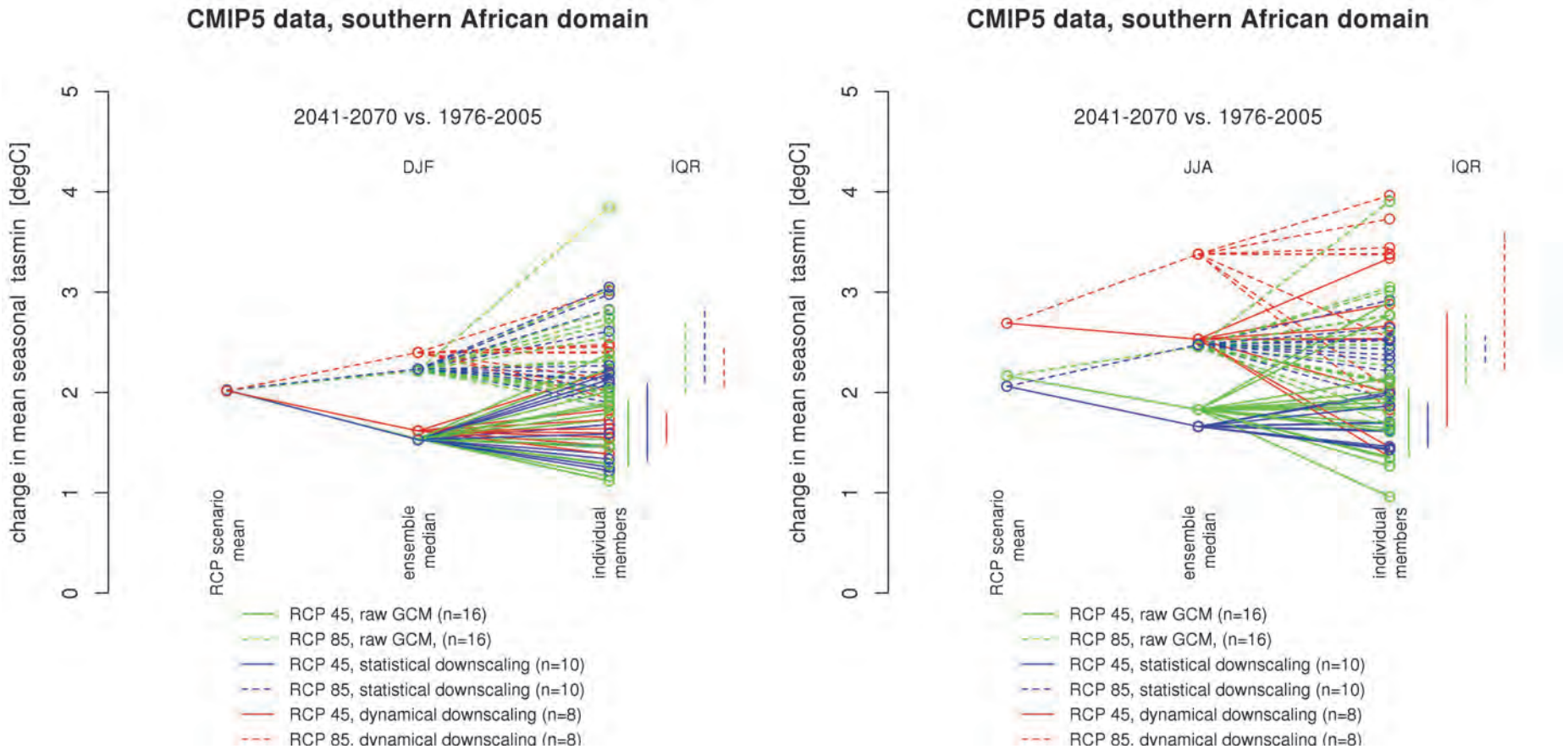

Figure 4.9 |*"Cascade of uncertainty" for change in mean monthly minimum temperature for DJF (left) and JJA (right) for two RCP scenarios: 16 GCMs (gcm16), 10 statistical downscaling realizations (somds10) and 8 regional climate model realizations (rcm8) averaged over the domain covering the land body of southern Africa (35°-20°S, 10°-40°E). Bars on the right-hand side of the graphs mark IQR for each ensemble/RCP combination.*

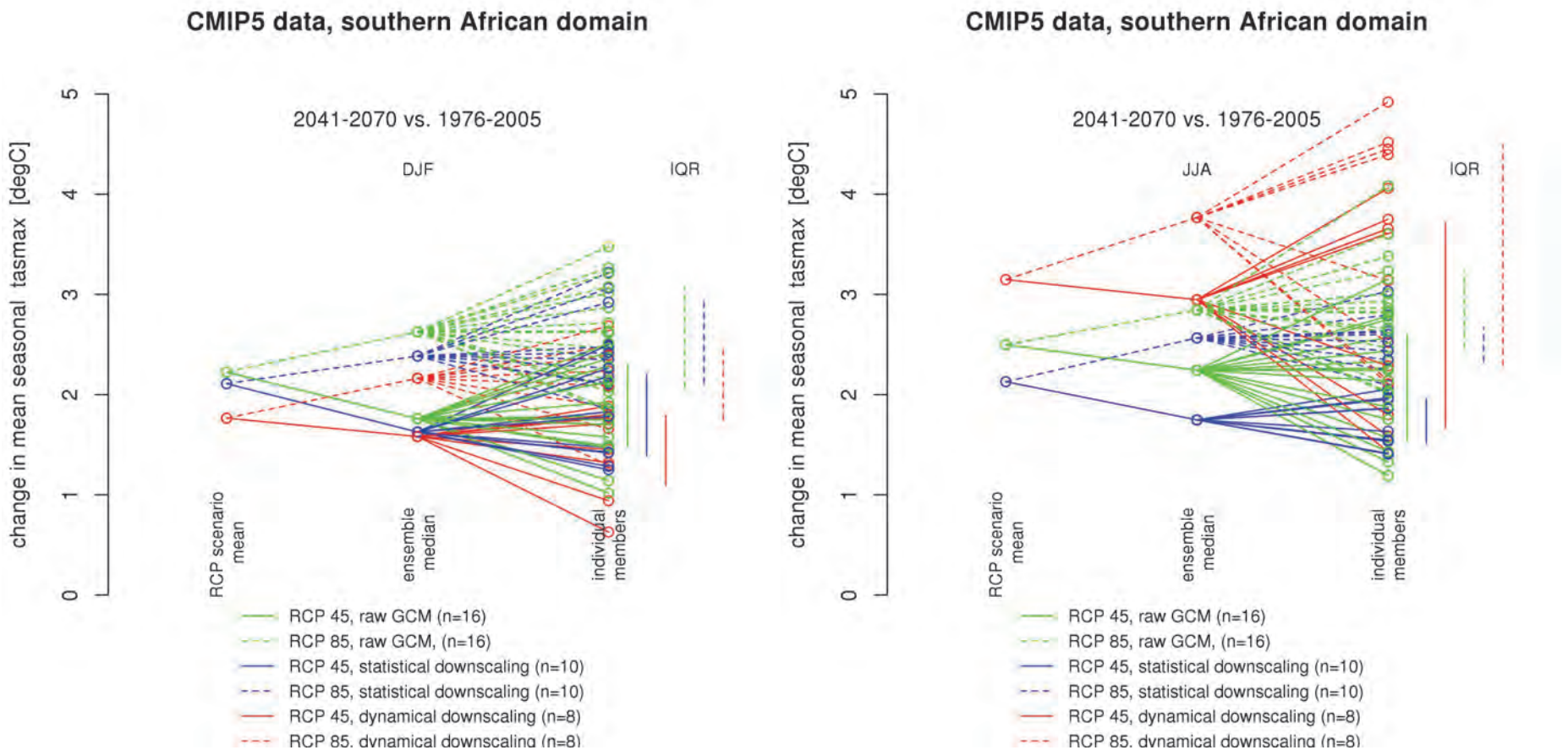

Figure 4.10 | *"Cascade of uncertainty" for change in mean monthly maximum temperature for DJF (left) and JJA (right) for two RCP scenarios: 16 GCMs (gcm16), 10 statistical downscaling realizations (somds10) and 8 regional climate model realizations(rcm8) averaged over the domain covering the land body of southern Africa (35°-20°S, 10°-40°E). Bars on the right-hand side of the graphs mark IQR for each ensemble/RCP combination.*

4.5.2.1. Local scale responses

For rainfall, the broad spatial pattern in ensemble spread appears to follow the spatial pattern in rainfall magnitude (and thus rainfall variability). In summer, ensemble spread is narrower in the south-west, and wider in the north-east (Figure 4.11). In winter, ensemble spread is wider along the east and southeast coast (Figure 4.12).

For temperatures, for gcm16 and somsd10, ensemble IQRs seem to be broader in the interior of the continent, and narrow along the coasts. For rcm8, IQR is also wider along the west coast of southern Africa, particularly during summer (Figure 4.13 to Figure 4.16).

4.5.2.2. Comparison of spread of GCM and statistical downscaling ensemble

The results of analyses presented above were derived for ensembles of GCMs, statistical downscaled models and regional climate models, which were composed of various models, not necessary "related" to each other – there was a number of GCMs in the gcm16 which were not downscaled, and there were only 4 models overlapping between the rcm8 and gcm16 ensembles. In such a situation, parts of differences in ensemble location and spread can potentially be attributed to accidental peculiarities and idiosyncrasies of the individual models contributing to each of the ensembles. In order to illustrate the method-related differences rather than the sample-related differences between the ensembles, comparison of IQR derived for somsd10 and gcm10 derived for identical set of models is presented in Figure 4.17 to Figure 4.19. The purpose is to illustrate factors that influence the spatial differences in the spread of ensembles.

For rainfall and for maximum temperature, the somsd10 ensemble has generally lower IQR than does the gcm10. The widespread statistically significant (at 0.05 significance level) differences occur, however, only for summer rainfall. For other variables and seasons, statistical significance of differences occurs only locally. The narrower IQR for somsd10 is, to a certain extent expected, as the SOM downscaling is constrained by observations, while GCM output is not. Interestingly, the locations where IQR of the somsd10 is larger than that of gcm10 are mostly distributed along the east coast, in the Cape Peninsula and in parts of the Limpopo Province. This perhaps reflects the situation the variation of responses that occurs over land is reflected by SOM downscaling, while it is constrained by the influence of inert ocean within large grid cells of GCMs.

4.5.2.3. Climate change messages derived from the analysis of the three ensembles

At the sub-continental scale, the multi-model, multi-method data allows for a straightforward derivation of climate change messages with a certain degree of confidence only for summer temperatures (Figure 4.9 and Figure 4.10). For this variable, the three methods agree well in terms of location and width of ensemble IQR (although there is somewhat better "location"

agreement for minimum than for maximum temperatures). There is uncertainty around the magnitude of change in summer temperatures, but that uncertainty does not appear to be method-dependent.

For changes in rainfall, and changes in winter temperatures, messages have to be derived taking into consideration method-to-method differences in representing atmospheric processes underlying changes in these variables, and these are, perhaps, better assessed when considering the spatial distribution of IQR for each of the ensembles.

At local scale, for temperatures, the general regional pattern is that of an increase of ensemble spread towards the interior of the sub-continent, and this pattern is present in each of the three analysed ensembles (Figure 4.13 to Figure 4.16). Since there is a generally higher continental warming as opposed to lower oceanic and coastal warming, the effect of larger interior IQR may simply be the consequence of the model-to-model differences in climate sensitivity (and thus in mean global warming) and a proportionally stronger response of continental over coastal regions. Additionally, secondary factors, such as the strength of moisture advection, and land surface-atmosphere feedbacks, may play a role in determining this regional pattern. These may be important factors underlying the much stronger continental anomaly in IQR width and tendency of the winter temperatures in rcm8 ensemble (Figure 4.14 and Figure 4.16). In this anomaly, the maximum IQR and maximum change in temperatures are not co-located – peak IQR occurs in a diagonal belt extending across the Limpopo province and eastern Zimbabwe, while the peak of temperature change is centered over the Karoo. Since the rcm8 ensemble is composed of climate realizations by multiple GCMs downscaled by a single RCM, it is possible that the rcm8 anomalies reflect peculiarities of that RCM, and would be less prominent if the RCM ensemble was composed of realizations with multiple RCMs.

In spite of these effects, it seems that the three ensembles supports a robust, although general message about uncertainties of temperature projections – there is more confidence in temperature projections in the coastal regions than in the continental interior. Other aspects of projected changes in temperatures have to be interpreted in the context of other data sources, such as circulation and trends.

Apart from the general coastal-to-interior regional pattern of IQR, spatial differences in ensemble spreads arise for summer temperatures – there is a much wider IQR of rcm8 ensemble along the west coast of southern Africa. The rcm8 ensemble also projects higher temperatures in that region. These effects may be related to the strong sensitivity of the regional climate model in that area to the sea surface temperatures (SST) of the Benguela current. This sensitivity, not captured by GCMs due to their low resolution, will magnify differences in SST occurring in the parent GCMs to generate a very wide set of responses of the RCM. Importantly, similar effects do not occur in the somsd10 ensemble. Clarification of this issue needs further analysis and exploration using a broader suite of models; data which will only be forthcoming after the completion of this project, but which will form a core component of the evolving CORDEX analysis activities. The identification of this issue here is a significant contribution to the broader communities activities.

For rainfall, the IQR appears to indicate higher confidence in results (narrower IQR) in low rainfall regions – i.e. towards southwest in summer and northwest in winter, with the general regional pattern similar in each of the three ensembles (Figure 4.11 and Figure 4.12). The IQR is, however, expressed here in absolute terms (i.e. in mm of change), and thus partly reflects natural rainfall variability (which is larger in absolute terms for locations with higher mean rainfall). Nonetheless, similarly to that for temperatures, the general agreement between the methods forms the basis for a general message about uncertainty of rainfall projections – from ensemble spread alone, there is more confidence in climate change signal in low rainfall regions.

There is a general agreement between the somsd10 and rcm8 in the regional pattern of ensemble tendency for summer rainfall, although the magnitudes differ (Figure 4.11). Both these ensembles indicate drier conditions towards the north-east, and less drying, or even wetting towards the south-west. The regional pattern in gcm16 ensemble is, however, different, with wetter tendency of the ensemble in the north-east, and drier in the south-west. At this stage the causative factors for this are not clear. However, early analysis of the CORDEX results suggests that inadequacies in the convective parameterization of the RCMs may be a significant factor. Equally, it is possible that potential non-stationarity vulnerability in the statistical downscaling may be a contributing factor, although subjectively that seems less likely with current understanding. These issues have been highlighted with the broader community, and have helped motivate the WGRC to conduct an expert meeting on how to distill these differences, and which will take place later in 2014.

For winter rainfall, there is relatively little consistency ensemble tendencies (Figure 4.12). Importantly, however, the signal-to-noise ratio is very low: ensemble median change, even in areas where there it is relatively high (e.g. in the Cape region, and along the east coast of South Africa in Figure 4.12) is comparable to the IQR (which by definition represents only 60% of the ensemble variability), and thus the eventual emerging changes may be largely indistinguishable from natural variability.

In summary, as shown above, the analysis of agreement/differences in ensemble spread and tendency from three methods has potential to contribute to confidence statements about local and regional climate change messages. However, as it was shown in a few cases, additional information is needed in order to arrive at robust and defensible messages. This information has to originate from sources such as analysis of circulation patterns, understanding of climate physics and other independent sources, in the coherent framework of multiple sources of evidence.

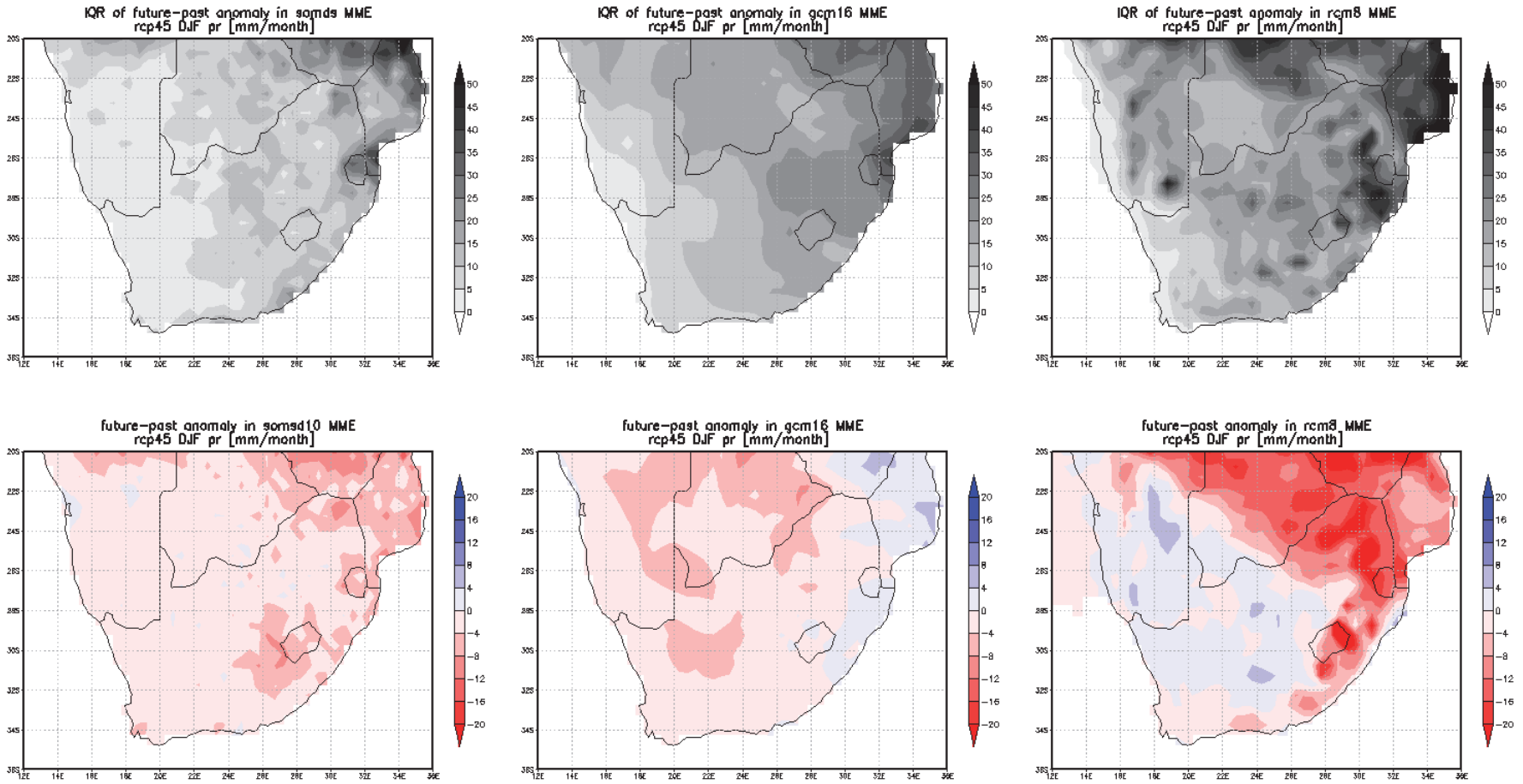

Figure 4.11 | *Maps of IQR of future-past change in rainfall (upper row) and ensemble median of the future-past change in rainfall, in somsd10, gcm16 and rcm8 ensembles, for DJF, under RCP 4.5.*

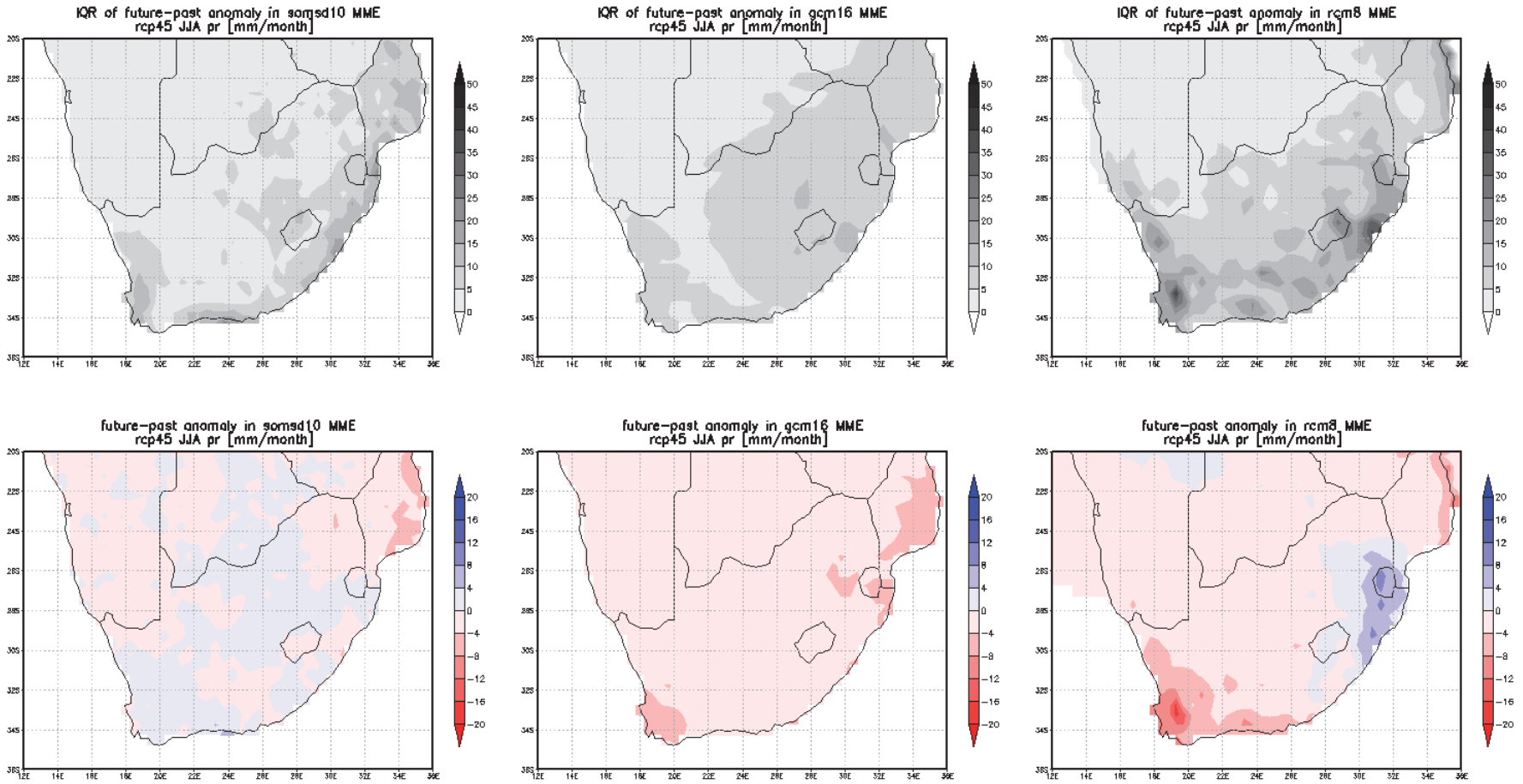

Figure 4.12 | *Maps of IQR of future-past change in rainfall (upper row) and ensemble median of the future-past change in rainfall, in somsd10, gcm16 and rcm8 ensembles, for JJA, under RCP 4.5.*

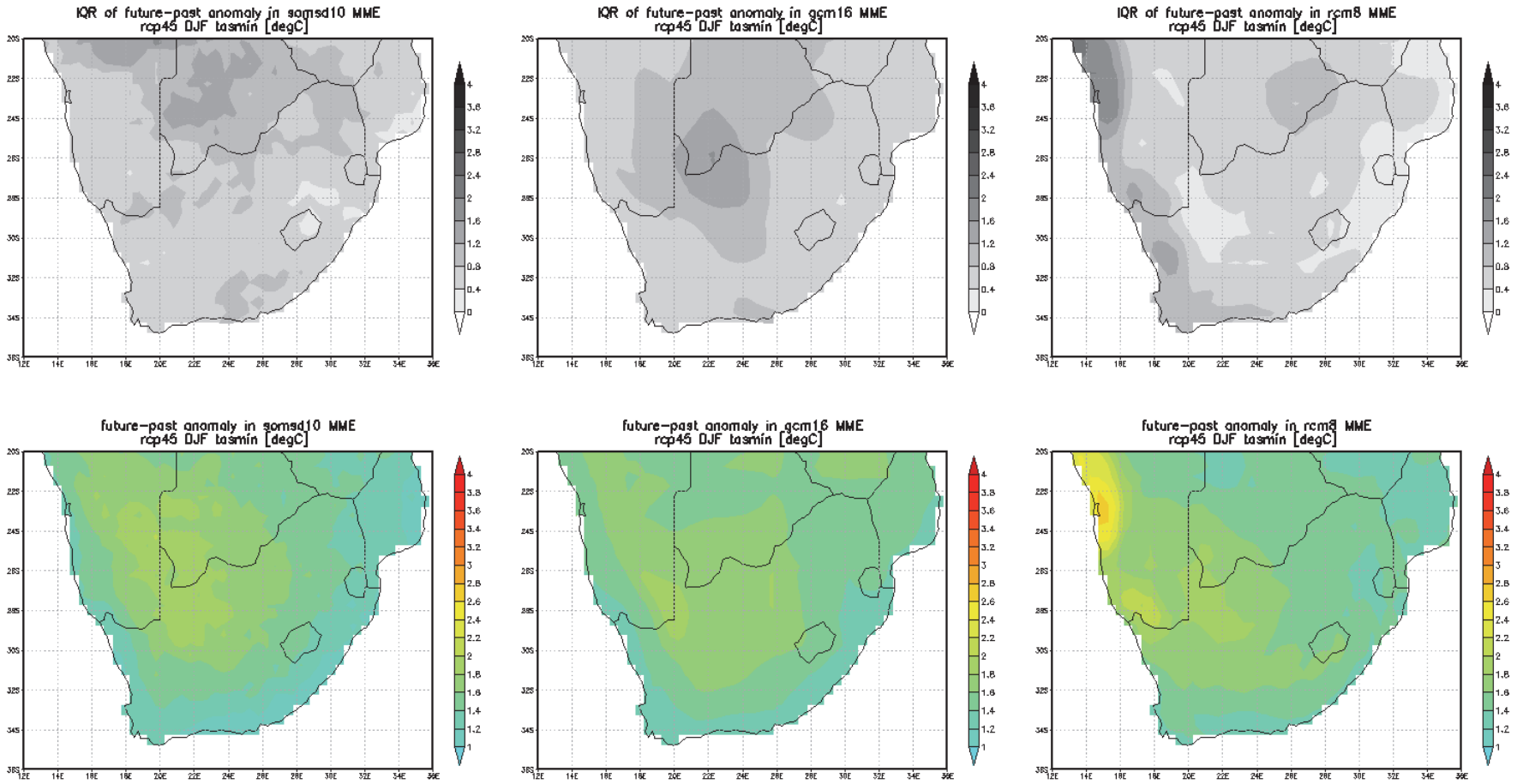

Figure 4.13 | *Maps of IQR of future-past change in minimum temperature (upper row) and ensemble median of the future-past change in minimum temperature, in somsd10, gcm16 and rcm8 ensembles, for DJF, under RCP 45.*

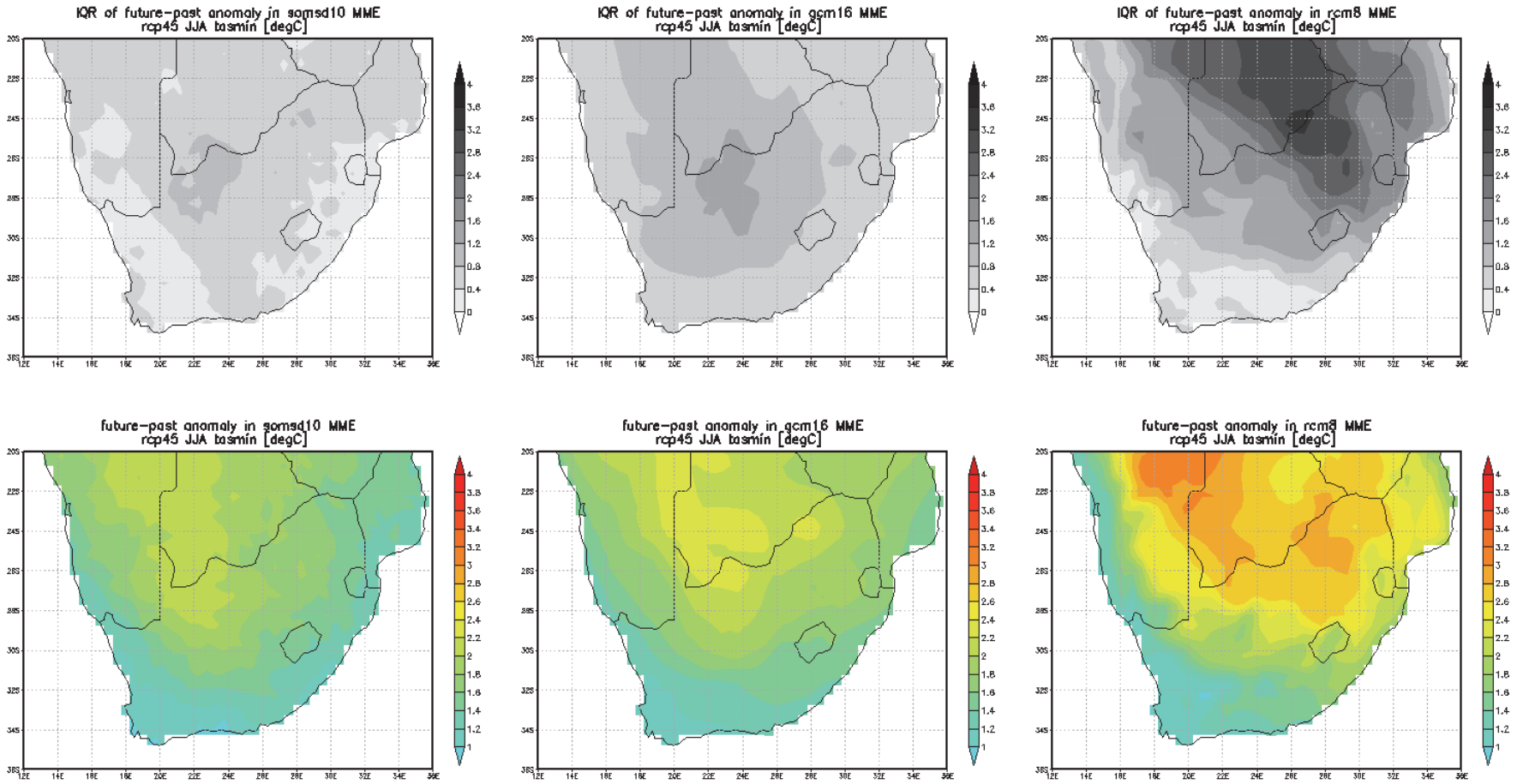

Figure 4.14 | *Maps of IQR of future-past change in minimum temperature (upper row) and ensemble median of the future-past change in minimum temperature, in somsd10, gcm16 and rcm8 ensembles, for JJA, under RCP 45.*

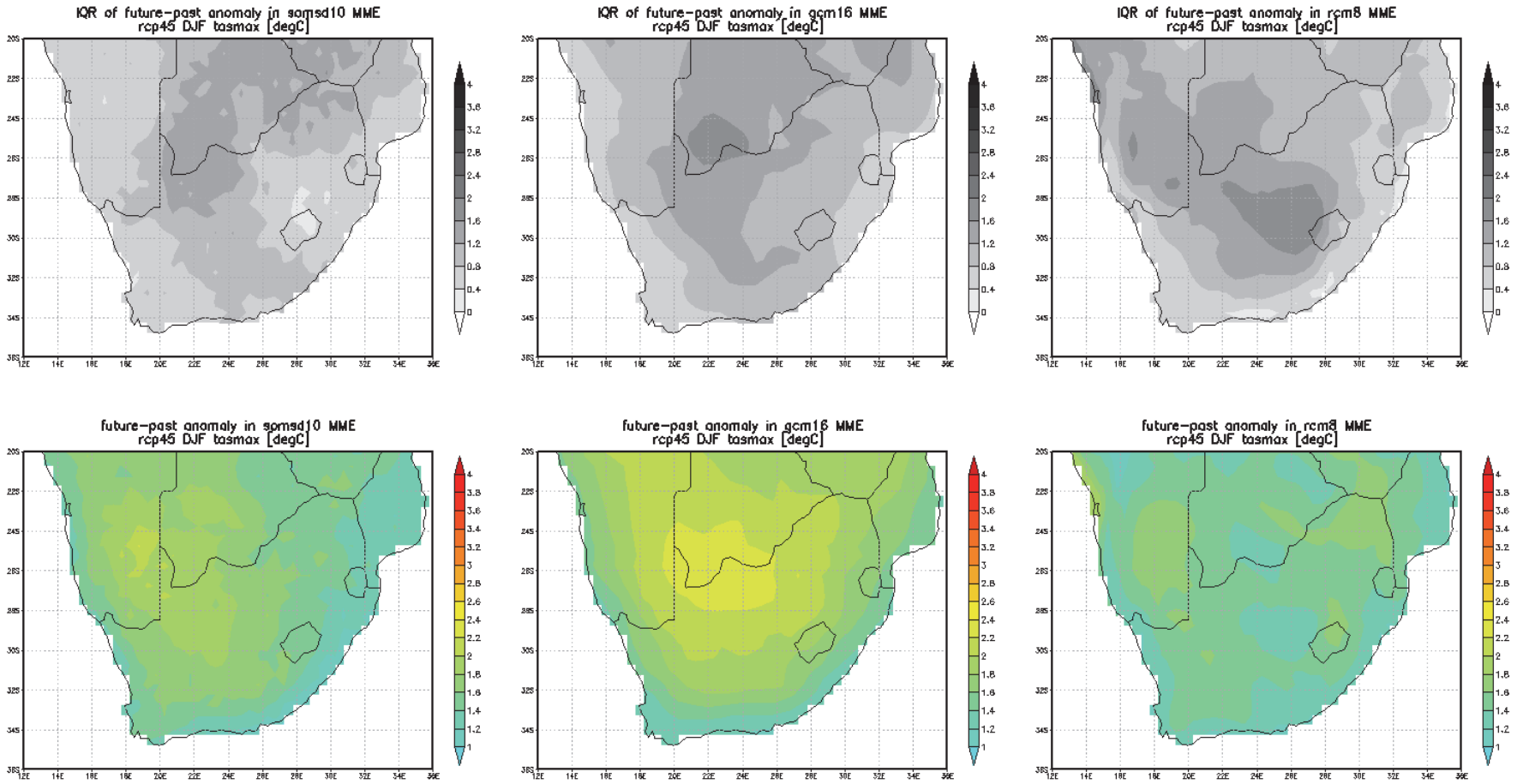

Figure 4.15 | *Maps of IQR of future-past change in maximum temperature (upper row) and ensemble median of the future-past change in maximum temperature, in somsd10, gcm16 and rcm8 ensembles, for DJF, under RCP 45.*

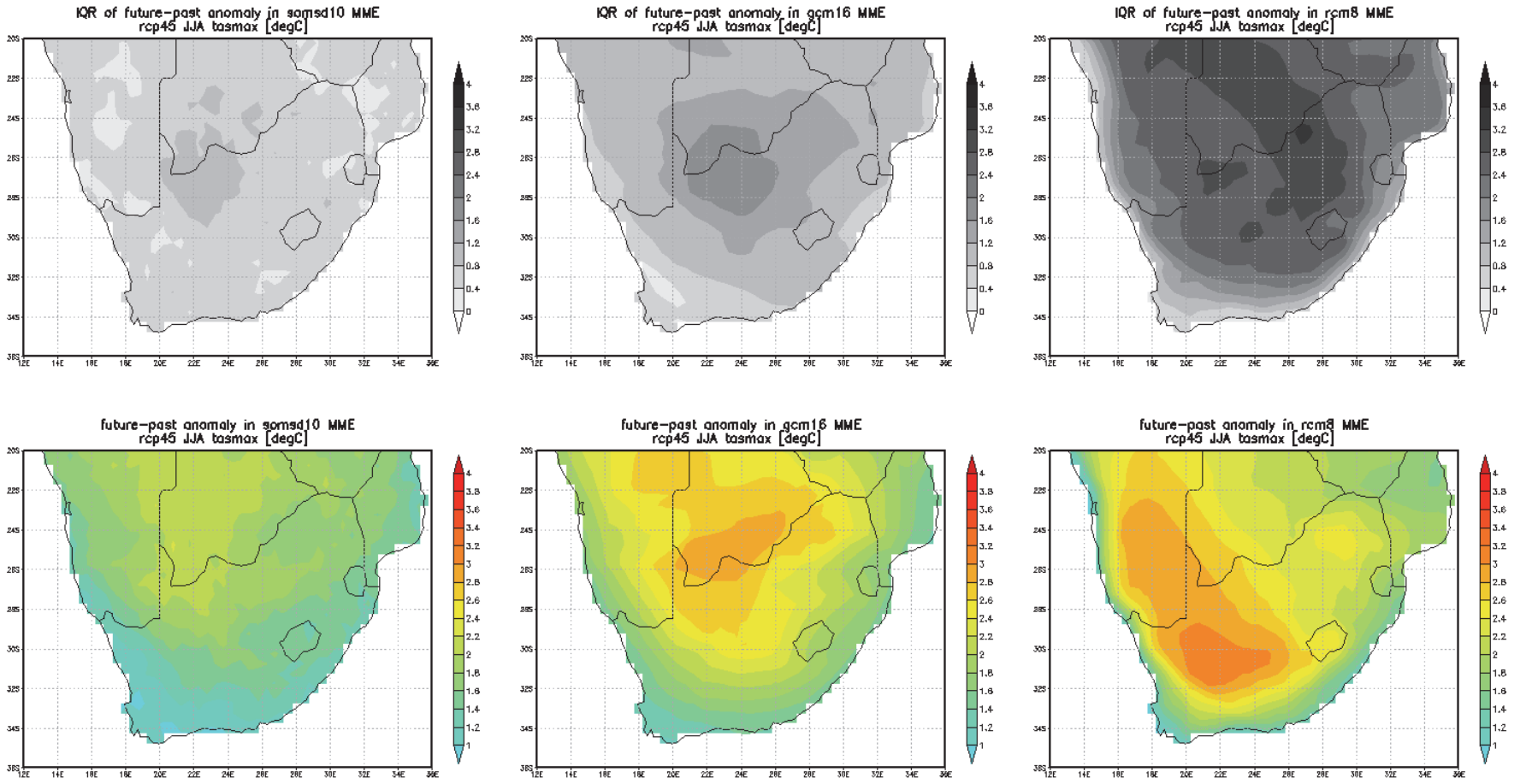

Figure 4.16 | *Maps of IQR of future-past change in maximum temperature (upper row) and ensemble median of the future-past change in maximum temperature, in somsd10, gcm16 and rcm8 ensembles, for JJA, under RCP 45.*

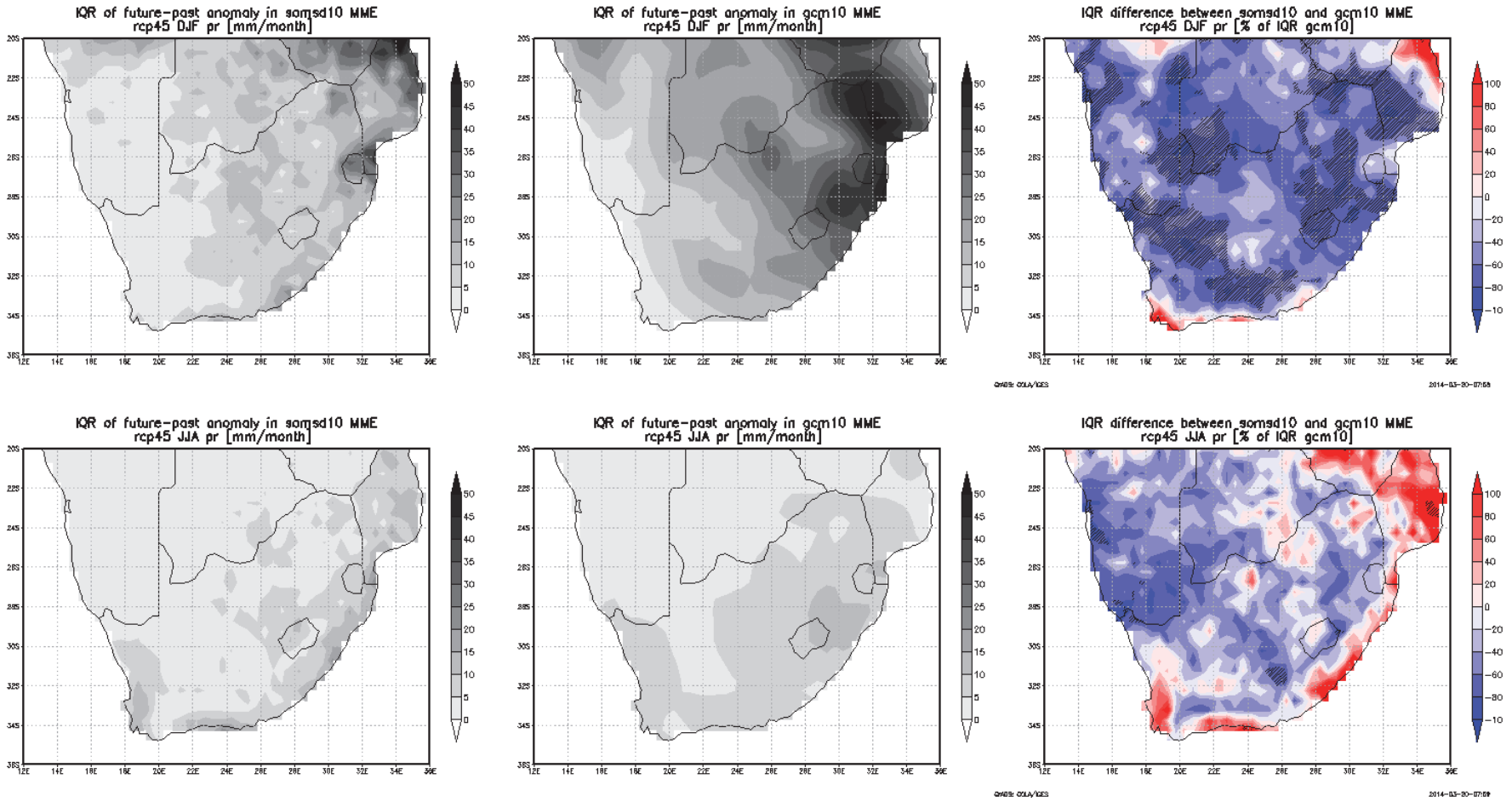

Figure 4.17 | *Comparison of IQR of future-past change in rainfall somsd10 (left column) and gcm10 (middle column) and difference between them – significant at 0.05 confidence level hatched (right column), for DJF (upper row) and JJA (lower row), RCP 45.*

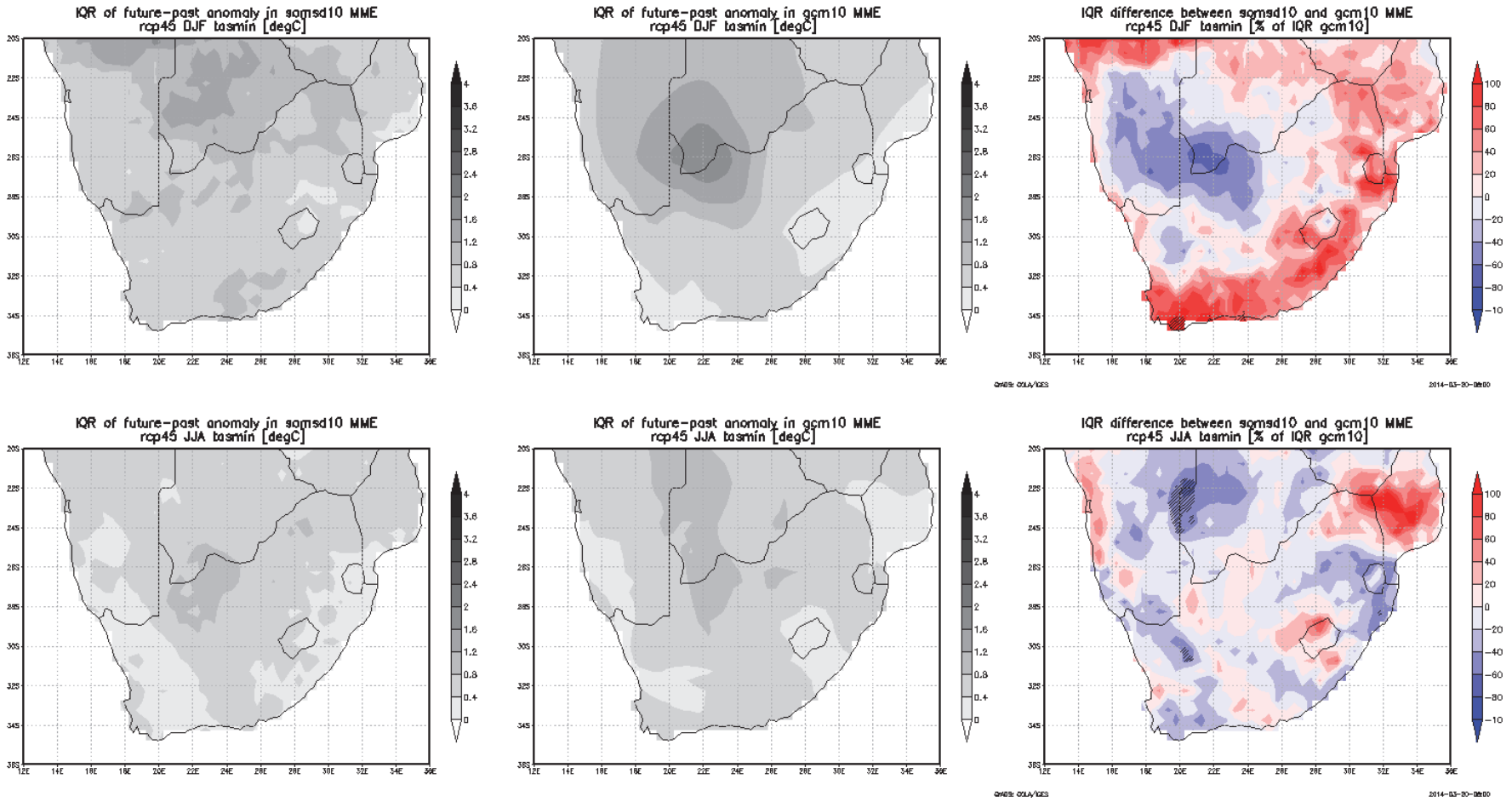

Figure 4.18 | *Comparison of IQR of future-past change in minimum temperature in somsd10 (left column) and gcm10 (middle column) and difference between them – significant at 0.05 confidence level hatched (right column), for DJF (upper row) and JJA (lower row), RCP 45.*

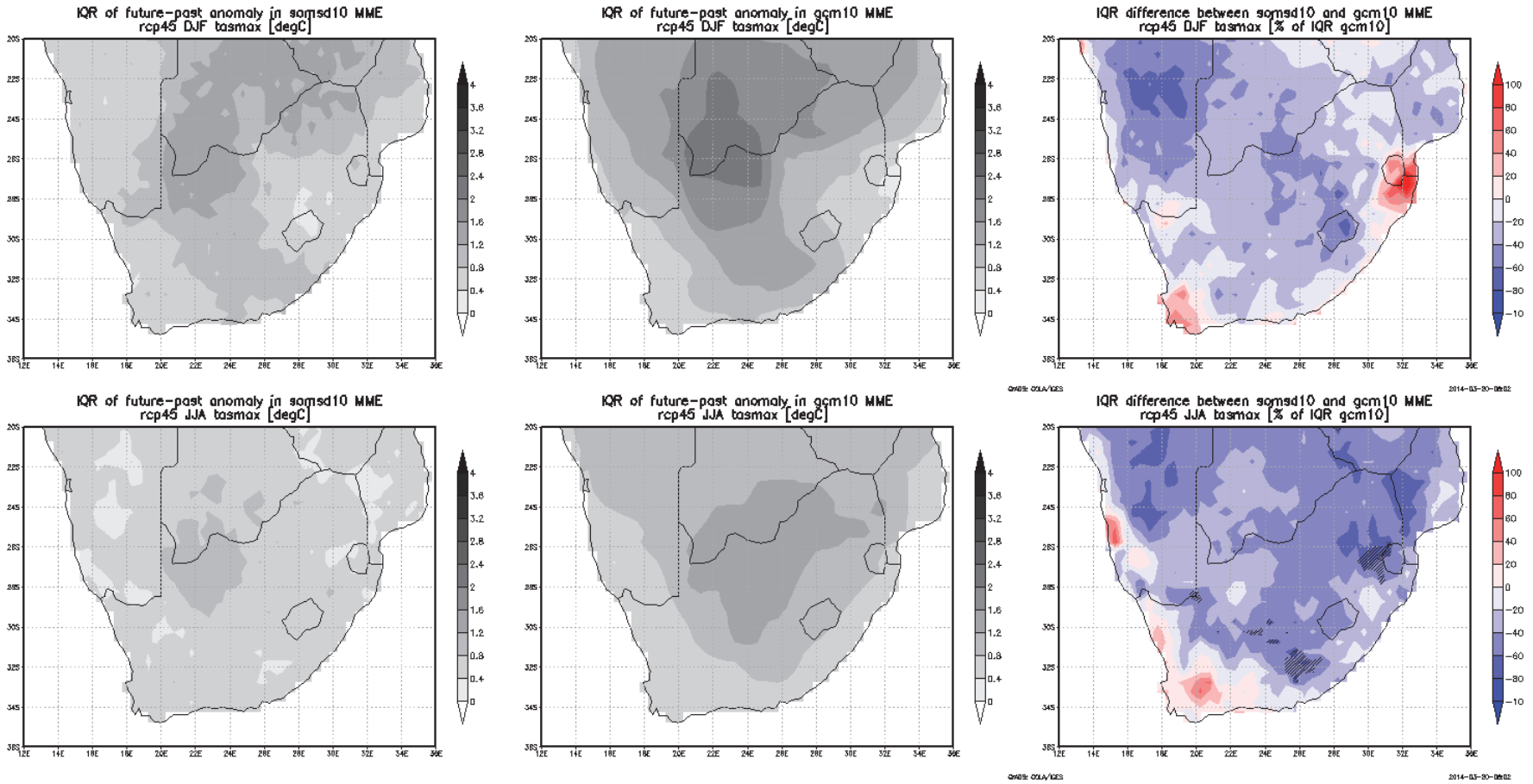

Figure 4.19 | *Comparison of IQR of future-past change in maximum temperature in somsd10 (left column) and gcm10 (middle column) and difference between them – significant at 0.05 confidence level hatched (right column), for DJF (upper row) and JJA (lower row), RCP*

Chapter 5

PROJECT SPECIFIC DOWNSCALED PRODUCTS FOR SOUTH AFRICA

5.1. Overview

The anticipation of high quality and defensible regional climate change information, to inform policy and decision making, has been tempered in recent years. This has emerged as it has become clear that the regional scale limitations of the Global Climate Models (GCMs) preclude deriving directly the information needs of local scales. Downscaling, through dynamical or statistical approaches, likewise are vulnerable to the limits of the chosen method and of the driving data from GCMs. This is compounded by the inherent uncertainty from stochastic and chaotic elements of the atmosphere. The advent of the new CMIP5[9] GCM and CORDEX[10] data significantly opens the door to greater exploration of true skill assessment of the projections. The framework adopted for the project is shown in figure 5.1 below. The project focuses on each of the core building blocks (top row) with a view to integration and the development of robust messages of projected change.

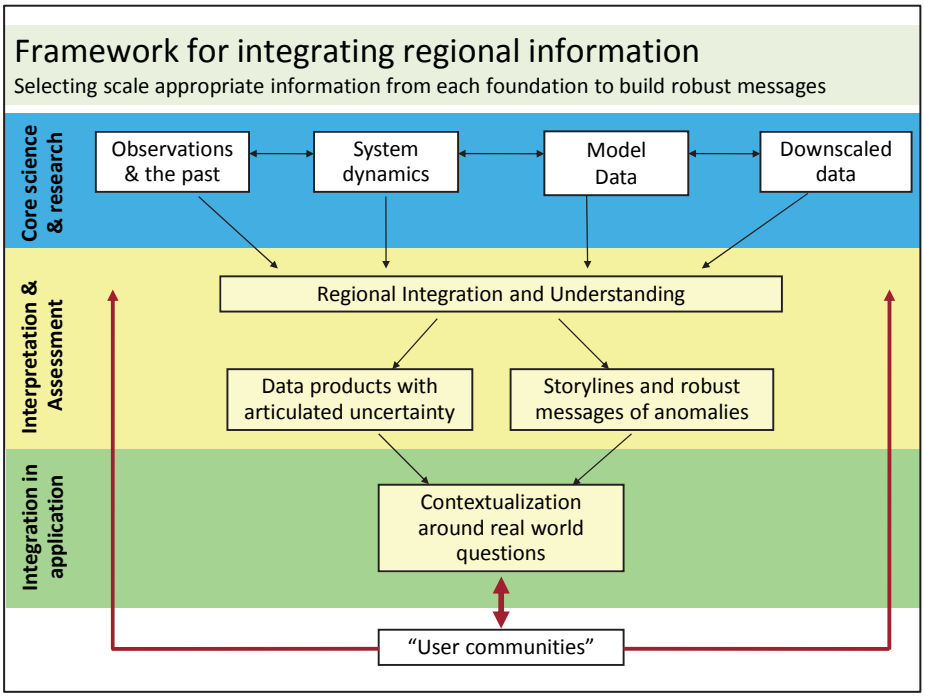

Figure 5.1 | *The conceptual framework for developing regional climate change information.*

This chapter builds on the prior work leading to the integration of the climate information, but focuses on downscaled data which is the fourth source of climate data included in the

[9] http://cmip-pcmdi.llnl.gov/cmip5/
[10] http://wcrp.ipsl.jussieu.fr/SF_RCD_CORDEX.html

conceptual framework for integrating regional information (figure 5.1). The chapter first provides a brief summary of downscaling methodologies and the two most relevant modelling experiments, namely the fifth phase of the Coupled Model Intercomparison Project (CMIP5) and the Coordinated Regional Downscaling Experiment (CORDEX). It then discusses in more detail the Regional Climate Model (SHMI-RCA4) and the statistical downscaling approach (Self-Organising Map based Downscaling) used in this project. The remainder of the chapter focuses on the climate change results obtained from the CMIP5 GCMs and from the dynamical and statistical downscaling approaches. This report ends with some concluding remarks.

5.2. Downscaling Structure

Downscaling seeks to add finer resolution information to GCM output and is seen as the only viable approach to achieve regional scale information consistent with the global and hemispheric forcing. Downscaling can be separated into two distinct classes; dynamical and statistical/empirical downscaling, with the latter being further separated into three subclasses (Hewitson and Crane, 1996; Wilby and Wigley 1997). Figure 5.2 outlines these basic classes of downscaling. All have differing strengths and weaknesses; the dynamical downscaling is theoretically the most viable, but introduces notable structural uncertainty in the results, as well as additional stochastic variance and error from the parameterization schemes. As a result the multi-model spread can be broad. It is also unclear whether the increased complexity of nested models or high/variable resolution models actually adds to the signal. For example Maslin and Austin (2012) pose the question of whether climate models have researched their limit of ability to directly tackle the regional deterministic signals. Statistical downscaling covers a broad range of methodologies (Wilby et al., 1998; Hewitson et al., 2014) and in principle can present a clearer picture of the first-order large scale forced signal at the local scale. Within the variants of statistical downscaling methods, weather generators need long time series to train the method, index/analogues are particularly vulnerable to stationarity issues, and transfer function approaches can miss the tails of the distribution. Most effective is thus a blended statistical approach, as is used here (Hewitson and Crane (2006).

There is also a frequent use of “perturbed-observed” approaches, but while this produces excellent apparent spatial detail, it in fact tracks the raw GCM and does not add additional signal information. Consequently is it not recommended here in the context of this project.

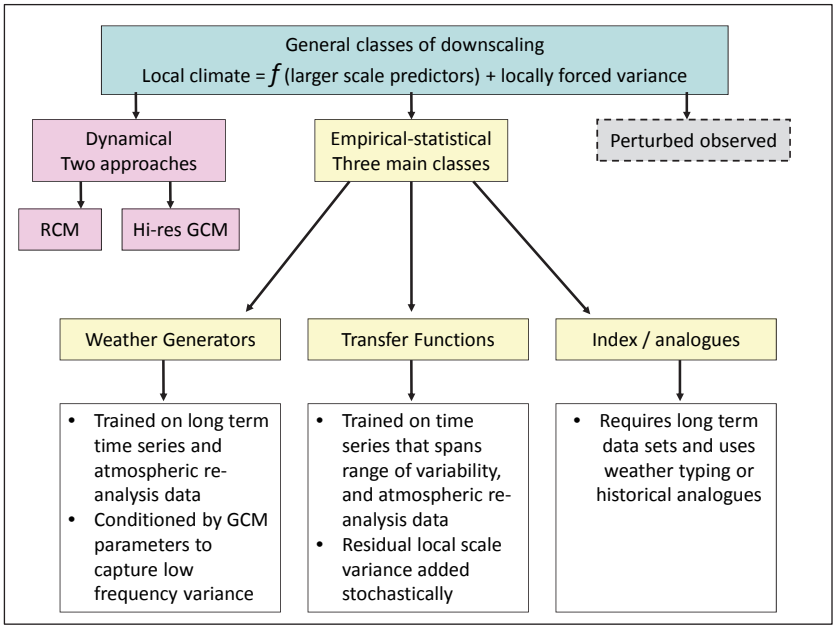

Figure 5.2 | *Typology of downscaling approaches.*

5.3. CMIP5 GCMs

The Coupled Model Intercomparision Project (CMIP) was established under the World Climate Research Program (WRCP) by the Working Group on Coupled Modelling (WGCM). The goal was to provide a standard experimental protocol for studying the output of coupled Atmosphere-Ocean GCMs in order to facilitate model improvement through better model quality control and a better understanding of model behavior (Meehl et al., 2000). The output of phase three of CMIP was used extensively in the Intergovernmental Panel for Climate Change (IPCC) Fourth Assessment Report (AR4). The fifth phase of the Coupled Model Intercomparison Project (CMIP5) is the latest set of coordinated climate model experiments (see Taylor et al., 2012).

CMIP5 is the latest iteration of this project and this current generation of models offer more complexity than those used in earlier joint modelling projects. Both near- and long-term experiments are run with Atmosphere Ocean General Circulation Models (AOGCMs), which were also used for earlier CMIP projects. The CMIP5 models have a spatial range of 0.5° to 4° for the atmosphere and 0.2° to 2° for the ocean. Nearly half of the CMIP5 atmospheric models have an average latitudinal resolution finer than 1.3°, compared to one model in CMIP3 (Taylor et al., 2012). Similar resolution increases are found in the ocean component of the models. Additionally, the long-term experiments are also being coupled to biogeochemical components that account for the important carbon fluxes between the ocean, atmosphere, and land carbon reserves (i.e. the carbon cycle). These more advanced models (Earth System Models) have not been used before in CMIP (Taylor et al., 2012).

The earlier generations of CMIP models used the Special Report Emission Scenarios (SRES). However, these are replaced in CMIP5 by RCPs (Representative Concentration Pathways). These are documented in Moss et al. (2010). The motivation for using RCPs was to avoid the complexity of describing multiple global scale socio-economic scenarios and translating these into greenhouse gas concentrations, as RCPs focus directly on different scenarios of atmospheric radiative forcing. Four RCPs have been defined – one "low" scenario (RCP 2.6), two intermediate (RCP 4.5 and RCP 6), and one high (RCP 8.5). The number indicates the equivalent top of tropopause change in radiative forcing in the year 2100. So RCP 8.5 represents a pessimistic scenario where the radiative forcing produced by continuously increasing greenhouse gases is equivalent to 8.5 $W.m^{-2}$ by 2100. RCP 2.6 represents a scenario where emissions begin to drop well before 2100 and so represents a relatively optimistic scenario incorporating various mitigation actions.

5.4. CORDEX

The increasing need for detailed, high-resolution regional information regarding future climate has been acknowledged by the international climate modelling community. This lead to the establishment of the Coordinated Regional Downscaling Experiment (CORDEX) by the WCRP task force on Regional Climate Downscaling. The main goal of CORDEX is to develop an improved generation of regional climate change projection information for input into impact and adaptation studies. Both dynamical and statistical downscaling approaches are included; however the statistical/empirical community lags behind that of the dynamical downscaling or RCM community and is still building the framework and developing the experiment design for their simulations. The RCM community has laid out a clear framework and set up a uniform experimental design (Figure 5.3) and have embarked on their modelling activities.

The boundary forcing conditions for the CORDEX RCMs are based ERA-Interim for the evaluation phase and on the CMIP5 projections, both the historical simulations (1950 to 2005) and the future projections (2006 to 2100), for the climate projection phase. The priority was placed on the RCP 4.5 and 8.5 projection runs, while RCP 2.6 was considered optional depending on the user group's computational facilities (storage and processing). The spatial domains were selected to cover all continental regions (with the exception of Antarctica) at a spatial resolution of ~50km.

Africa was identified as one of the key domains for CORDEX activities, which is due to the region's perceived high vulnerability to climate change and the sparse availability of regional data on climate change. Currently only the evaluation phase – where CORDEX-Africa simulations are forced by ERA-Interim – have been completed and published (Nikulin et al., 2012; Kalognomou et al., 2013; Panitz et al., 2013). The second phase of CORDEX-Africa makes use of the climate change simulations from CMIP5 to produce regional climate change projections. This phase is still on-going and only one modelling group, the Swedish

Meteorological and Hydrological Institute (SMHI), has completed and officially disseminated their runs. To date, no climate change projections making use of CORDEX-Africa results have been published for the South African region.

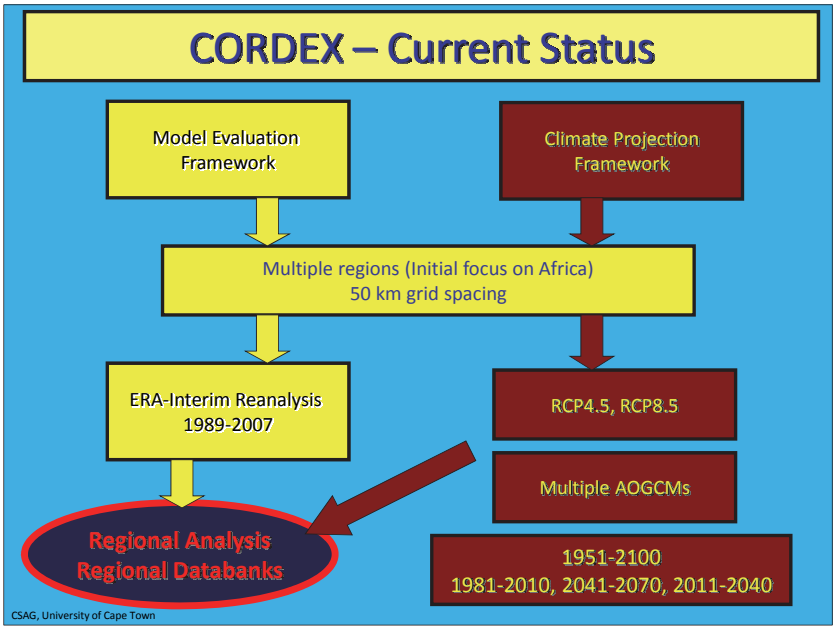

Figure 5.3 | *The framework of the dynamic downscaling experiment design in CORDEX. The boxes in brown represent on going work by the community of modellers.*

5.4.1. *SMHI-RCA4*

The Swedish Meteorological and Hydrological Institute (SMHI) is an active member of the CORDEX-Africa running the Rossby Centre Regional Climate Model (RCA3). The full description of the RCA3 model and its performance can be found in a paper by Samuelsson et al. (2011). The results from the SMHI RCA35 were included in a number of evaluation papers, most notably Nikulin et al. (2012) which compared the ERA-Int runs over Africa, and Kalognomou et al. (2013) which focussed on the southern Africa region. These papers both show that the SMHI RCA35 provides a realistic simulation of the African and southern African historical climate at a number of temporal scales (Figure 5.4 and Figure 5.5) which provides some confidence in the model's ability to simulate the climate under future emission scenarios.

The most recent version of the SMHI RCA model, RCA4 (full model description currently unpublished) has been used to downscaled eight CMIP5 GCMs for both the RCP4.5 and RCP8.5 emission scenarios for the period 1950-2100. These models are: CanESM2, CNRM-CM5, EC-EARTH, GFDL-ESM2M, HadGEM2-ES, MIROC5, MPI-ESM-LR and NorESM1-M. A selection of the precipitation results are presented in a following section.

5.4.2 *CLMcom CCLM4*

The Climate Limited-Area Modelling Community (CLMcom CCLM) (Rockel et al., 2008) has released some of their future projection runs. The performance of the model in simulating the current African climate is discussed in Panits et al. (2013), and the model is also included in the same evaluation papers mentioned above and presented in Figure 5.4 & 5.5. Four CMIP5 GCMs have been downscaled by the CMMcom CCLM for both the RCP4.5 and RCP8.5 emission scenarios.

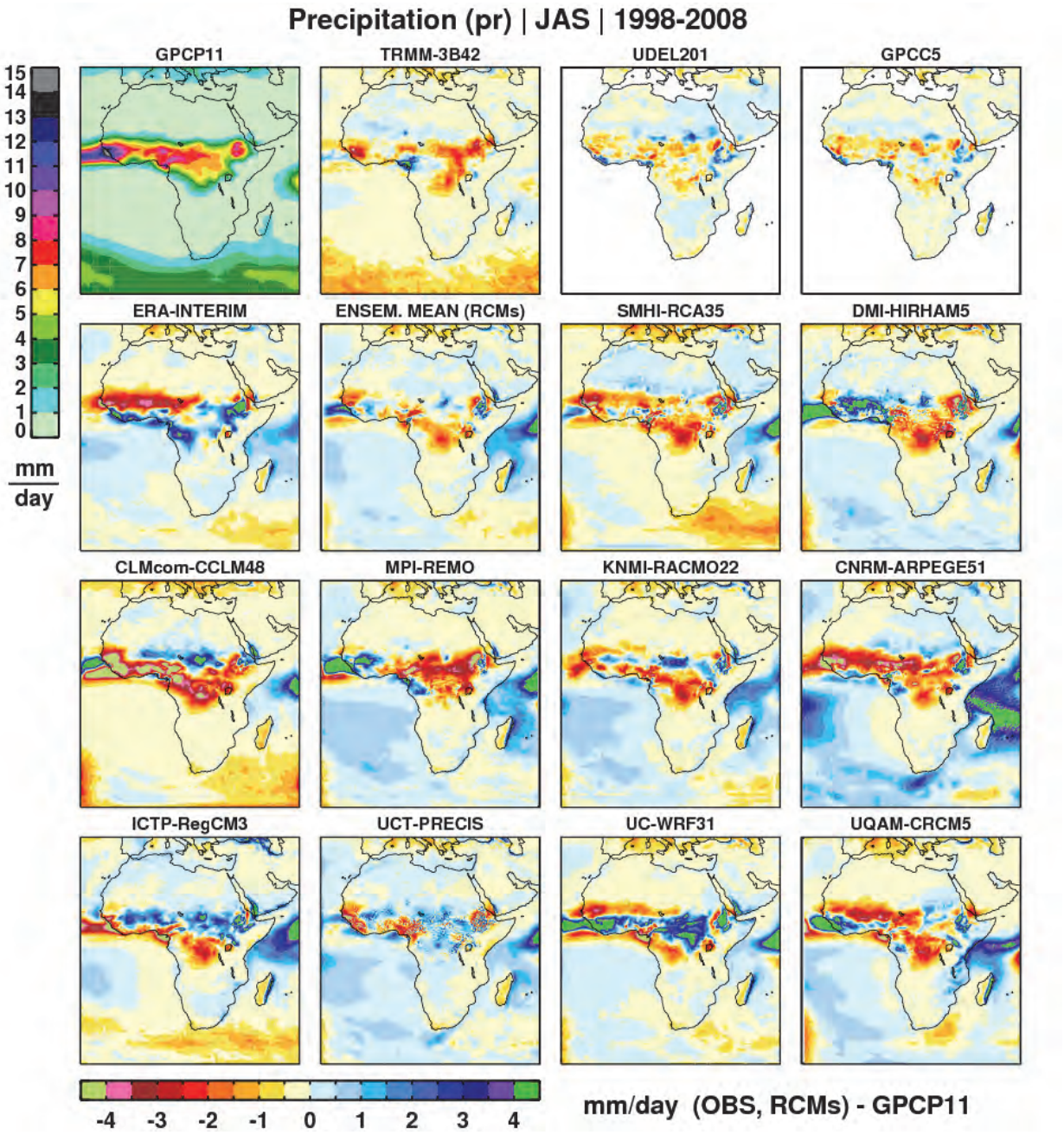

Figure 5.4 | *The top left panel shows the mean June-August-September precipitation of the GPCP observational data set. The remainder of the top row are the bias of other observational data sets with respect to the GPCP. Below this are the anomalies of 12 RCM simulations relative to the GPCP. While the RCM biases are marginally larger than the biases between the observational data sets, the results indicate the RCMs can capture credibly the regional climate of Africa (Nikulin et al., 2012).*

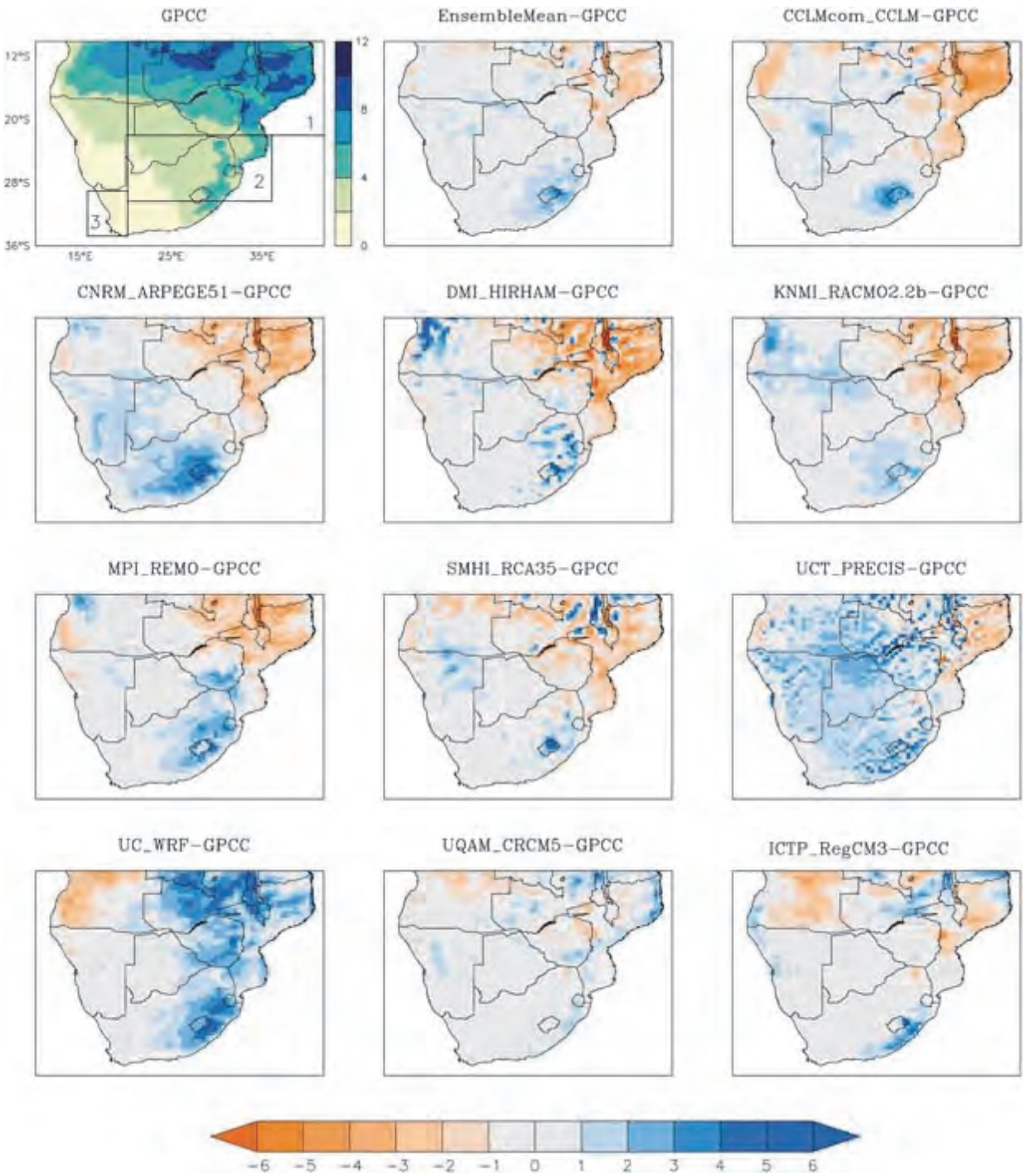

Figure 5.5 | *This figure explores the issue of model bias further by examining the bias of the RCMs relative to a single observational data set (GPCC) over the southern Africa region during austral summer. The results show that all models have a wet bias over South Africa during the austral summer season especially over the eastern interior with some also showing a slight dry bias over the far north of the country (Kalognomou et al., 2013).*

5.5. Self-Organising Map based Downscaling

As mentioned earlier, the statistical-empirical side of CORDEX lags behind that of the dynamical side and is currently clarifying the experimental design. One of the methods that will be included is the Self-Organizing Map based Downscaling (SOMD) which has been developed in-house within the Climate System Analysis Group (Hewitson and Crane 2006). This is a leading statistical/empirical downscaling technique for Africa and provides meteorological station level or gridded response to global climate change forcing.

The downscaling of a GCM is accomplished by deriving the normative local response from the atmospheric state on a given day (predictors) as defined from historical observed data (predictants). The method recognises that the regional response is both stochastic as well as a function of the large scale synoptics. As such it generates a statistical distribution of observed responses to past large scale observed synoptic states. These distributions are then sampled based on the GCM generated synoptics in order to produce a time series of GCM downscaled daily values for the variable in question (in this case temperature and rainfall). Advantages of this method are that it is computationally much less expensive than dynamical downscaling, and that the relatively unskilled grid scale GCM precipitation is not used but rather the relatively high skilled large scale circulation (temperature, wind and humidity) fields are employed.

The SOMD methodology has undergone a number of key modifications over the last few years. These include the modification of the code to allow it to handle the 140 year continuous period provided by the CMIP-5 GCMs (the CMIP-3 archive only provided data for a 40-year historical period and for two 20-year future periods). The representation of the temperature delta function was also improved so that it now varies not just according to synoptic state, but also increases into the future. The last major changes are associated with the stochastic element of how the code samples the local response under a given synoptic state. In the original version, there was strong auto-correlation in the sampling between grid cells. This produced an unrealistic spatial pattern of daily rainfall and resulted in an overestimation of the temporal variance when sampled over an area. The current version has a far more sophisticated method of sampling the local response for each grid cell; a random sampling field is generated so that each grid point has a random time series, but the correlation between each time series and each of the surrounding 8 grid points approximates the spatial correlation of observed precipitation.

In the current version of the SOMD the observed daily atmospheric states, or predictors, are obtained from the ERA-Interim Reanalysis dataset for the period 1979-2010. The variables used include; near surface temperatures and winds, atmospheric temperature lapse rate, relative humidity and winds. The local responses to these states, or predictants, are characterised using daily rainfall and temperatures from the WATCH Forcing Data 20th Century Dataset ERA-Interim (WFDEI) which provides a spatially continuous – though relatively low resolution – historical record. The choice of the training predictors and predictants (ERA-Interim and WFDEI in this case) is non-trivial. This is especially true over Africa where historic observations – on which reanalysis and gridded datasets are largely

evaluated – are often short and incomplete, if they exist at all. Each dataset differs from the others in the spatial organisation and magnitude of precipitation or temperature and represents an area and time aggregate value which may fail to capture the true statistical relationship between the circulation and local response. This has the potential to result in differences in the magnitude or even sign of change in future projections when different observed predictor or predictant datasets are used (See Hewitson et al., 2014 for further details). Observed station records arguably provide the most accurate first order local response to the large-scale synoptics, though for a very specific location. We therefore also include statistical downscaling of station data over South Africa as an alternative predictant dataset. We use the original CCWR observed dataset – updated to 2012 using stations from the South African Weather.

The skill of the SOMD method can be explored by comparing an observed seasonal climatology from an observational dataset, in this case WFDEI, to that obtained by downscaling a reanalysis product, in this case ERA-Interim. Figure 5.6 illustrates the seasonal mean daily precipitation for each of the four seasons (December-February (DJF), March-May (MAM), June-August (JJA) and September-November (SON)) from left to right. The top row presents the observed climatology, the middle row presents the downscaled equivalent and the bottom row shows the bias or difference between the downscaled output and that of the observed climatology.

The SOMD output realistically captures the seasonality and the spatial distribution of the precipitation climatology in each season. It clearly depicting the east west gradient across the country, but also simulates the regional differences due to topography, and proximity to the coast, etc. However, the downscaling output shows a bias in the magnitude of precipitation of up to 1.5 mm/day. Generally this bias is due to the downscaling simulating a reduced seasonal cycle compared to observations; underestimating the precipitation during summer and over estimating the precipitation during March-August in the summer rainfall areas. The underestimation is most clearly evident over the areas of maximum precipitation, which may be due to the methodology not fully capturing the local / convective drivers of the region, and or it not capturing the more extreme daily precipitation events. It may also be as a result of it not fully separating the circulation patterns associated with the core summer and winter seasons from those of the shoulder seasons.

Figure 5.7 presents the same analysis but for mean maximum temperature. The spatial distribution of seasonal maximum temperature produced by the statistical downscaling matches that of observations (WFDEI) in each season. It is able to resolve the fine spatial differences due to complex topography, continentally and ocean effects. There is again a clear underestimation of the seasonal cycle compared to observations, with summer temperatures being too cool and winter temperatures being too warm. This may be because the predictors were not originally selected to characterise the empirical link between surface temperature and circulation patterns, but could also be due to the downscaling mixing circulation patterns across seasons.

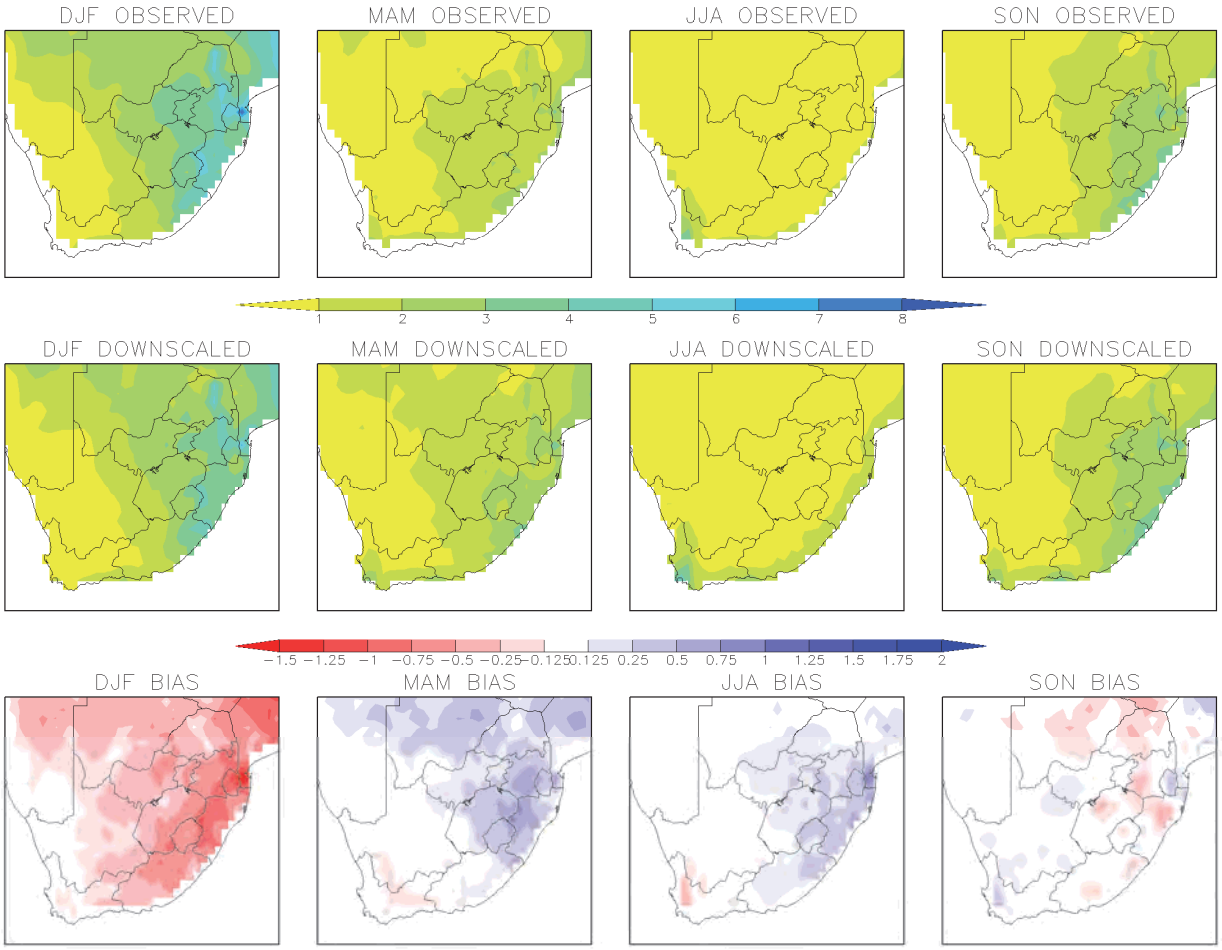

Figure 5.6 | *Seasonal mean daily precipitation for WFDEI observed climatology (top row), for ERA-Interim statistically downscaling climatology (middle row) and bias (bottom row).*

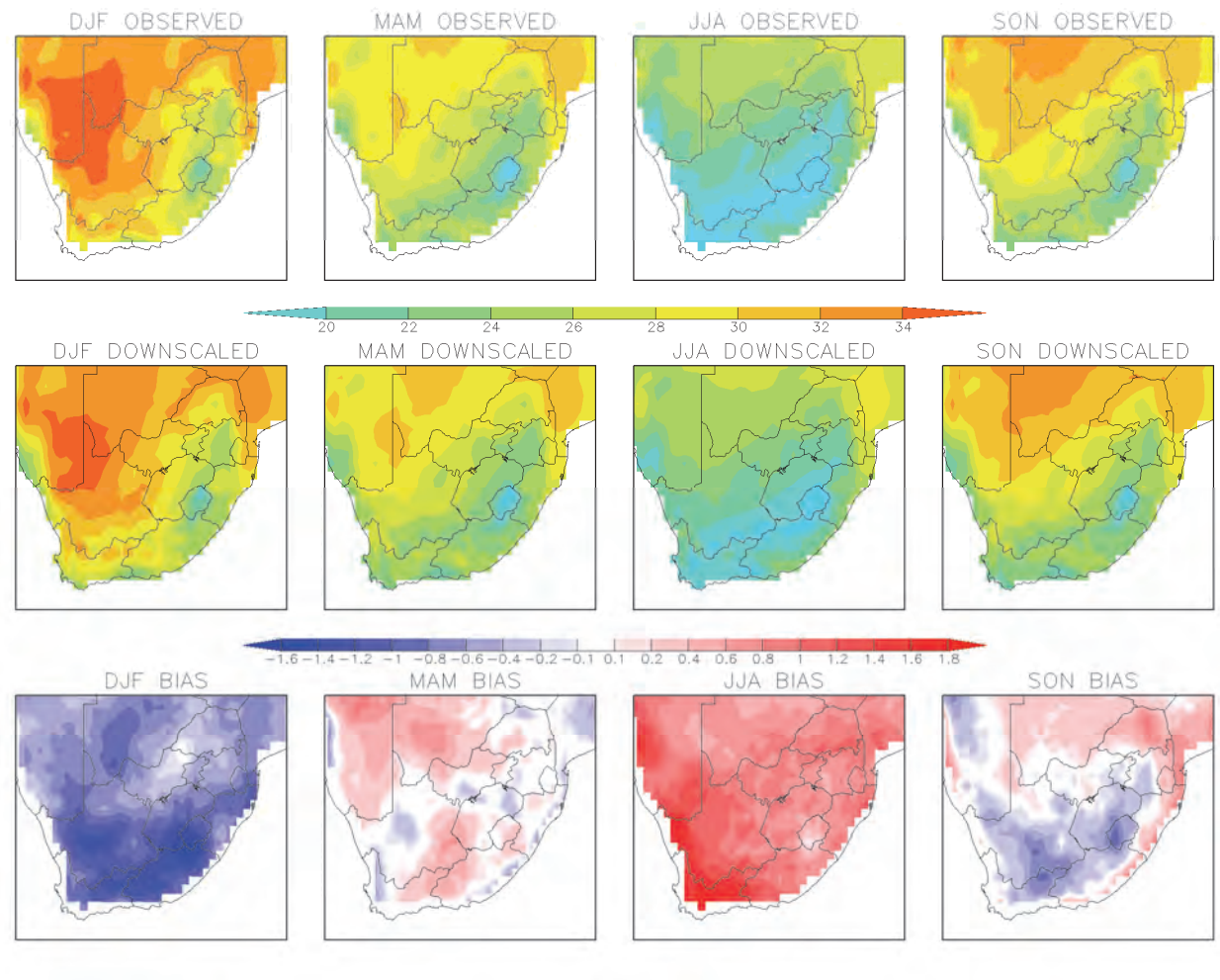

Figure 5.7 | *Seasonal mean daily maximum for WFDEI observed climatology (top row), for ERA-Interim downscaling climatology (middle row) and downscaling bias (bottom row).*

5.6. Climate Change Results

5.6.1 *CMIP5 GCM Results*

This chapter focuses on regional downscaled projections over South Africa. However, it is useful to first explore the results from the driving GCMs. The 11 GCMs used in the statistical downscaling are presented at their native grid cell resolution, which illustrates an important difference in complexity of the models included in the CMIP5 archive (see Appendix A for further details on each models complexity and components). A range of statistics can be explored; however we have chosen to focus on the seasonal average future anomalies for daily mean precipitation and daily maximum and minimum temperature.

South Africa is projected to warm into the future in all seasons and under both the RCP4.5 and RCP8.5 scenario. This is shown in the raw CMIP5 GCM output which focuses on the change or anomalies in the summer (December-January-February) season by the mid-21st

Century (2041-2070 minus 1976-2005) under the RCP8.5 emission scenario. Figure 5.8 and 5.9 presents the projected change in summer mean minimum and maximum temperature respectively (Results for the other seasons can be found in Appendix B). All models show clear warming, especially over the interior of the country. However, strong differences in both the spatial pattern and magnitude of warming are evident between the different models.

The future change in precipitation over South Africa is less certain and differs between GCMs, emission scenarios and through time. Figure 5.10 shows the projected change or anomaly in mean daily precipitation during summer (December-January-February). Strong differences are evident between the models in the spatial organisation, magnitude and even the sign of change. There is some suggestion of drying over the western half and wetting of over the far north east of South Africa, but this not supported by all models. The projected change in precipitation is more consistent between models for the spring season (September-October-November) with most models projecting drying or no change (Figure 5.11). This being said, it is important to remember that precipitation is a diagnostic variable from the GCM and its skill level is far coarser than that of the grid cell resolution and therefore these results should not be over interpreted.

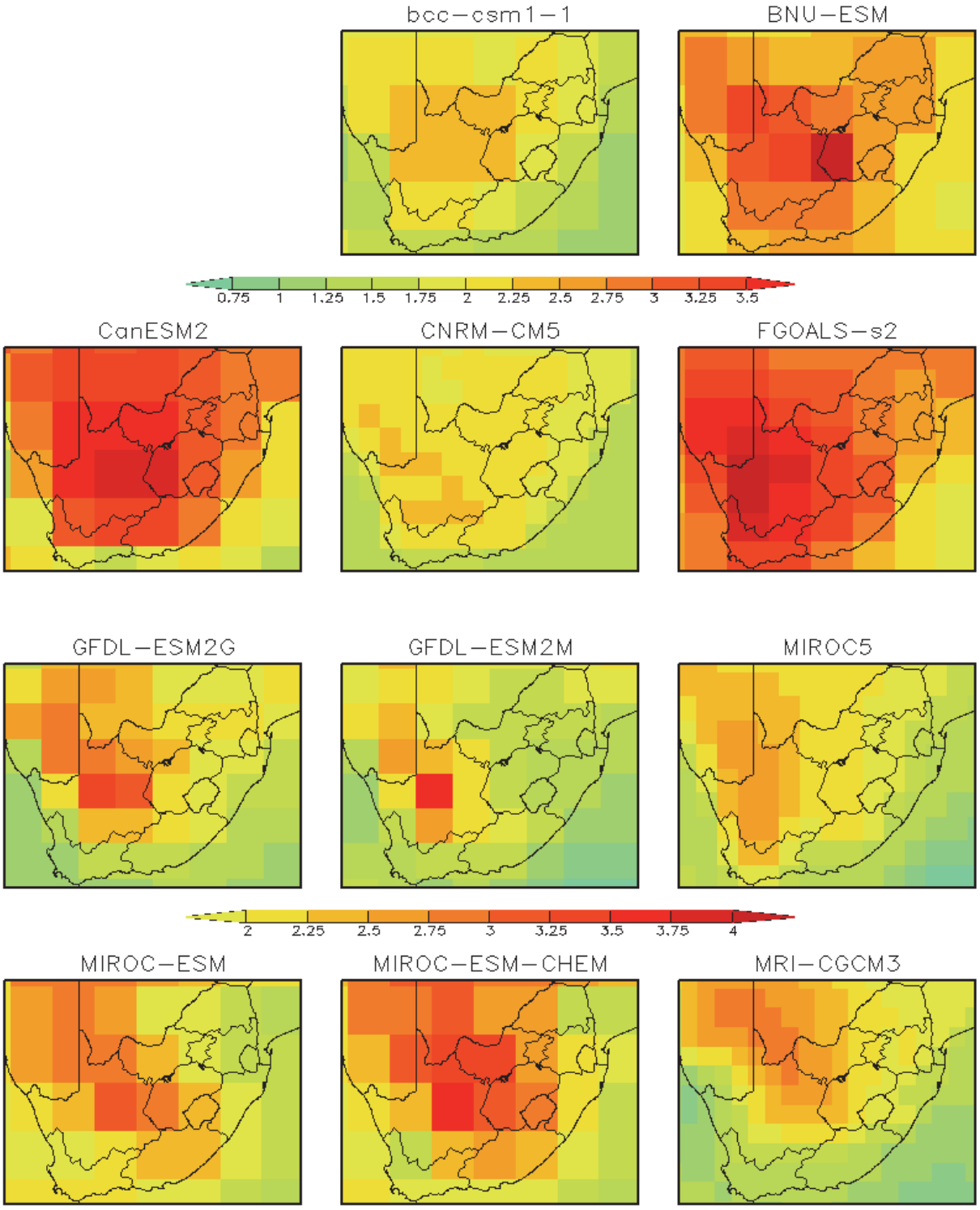

Figure 5.8 | *Future anomalies for summer (DJF) daily minimum temperature (°C) for the mid-21st century (2041-2070 – 1976-2005) under the RCP8.5 emission scenario for 11 raw CMIP5 GCMs.*

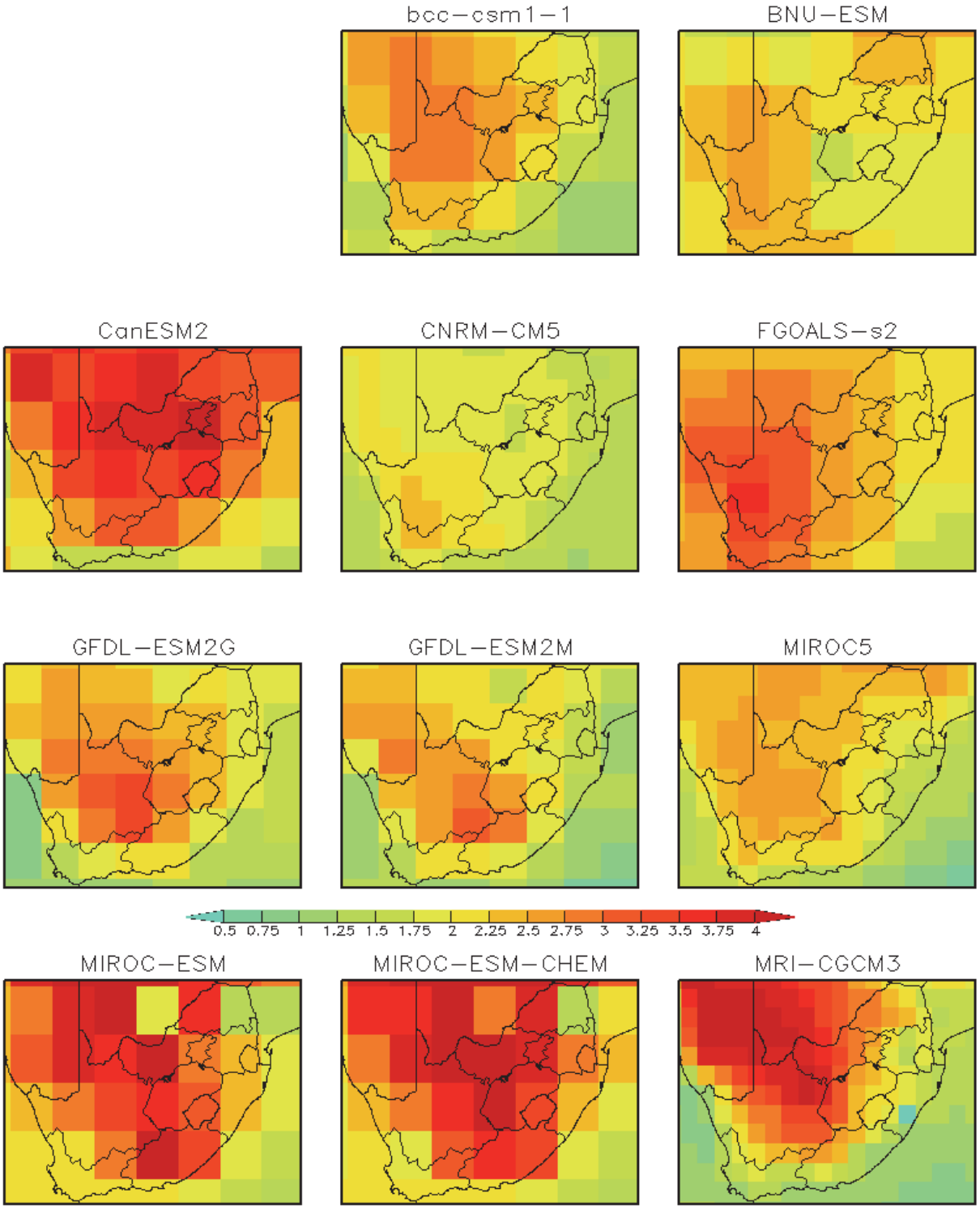

Figure 5.9 | *Future anomalies for summer (DJF) daily maximum temperature (°C) for the mid-21st century (2041-2070 – 1976-2005) under the RCP8.5 emission scenario for 11 raw CMIP5 GCMs.*

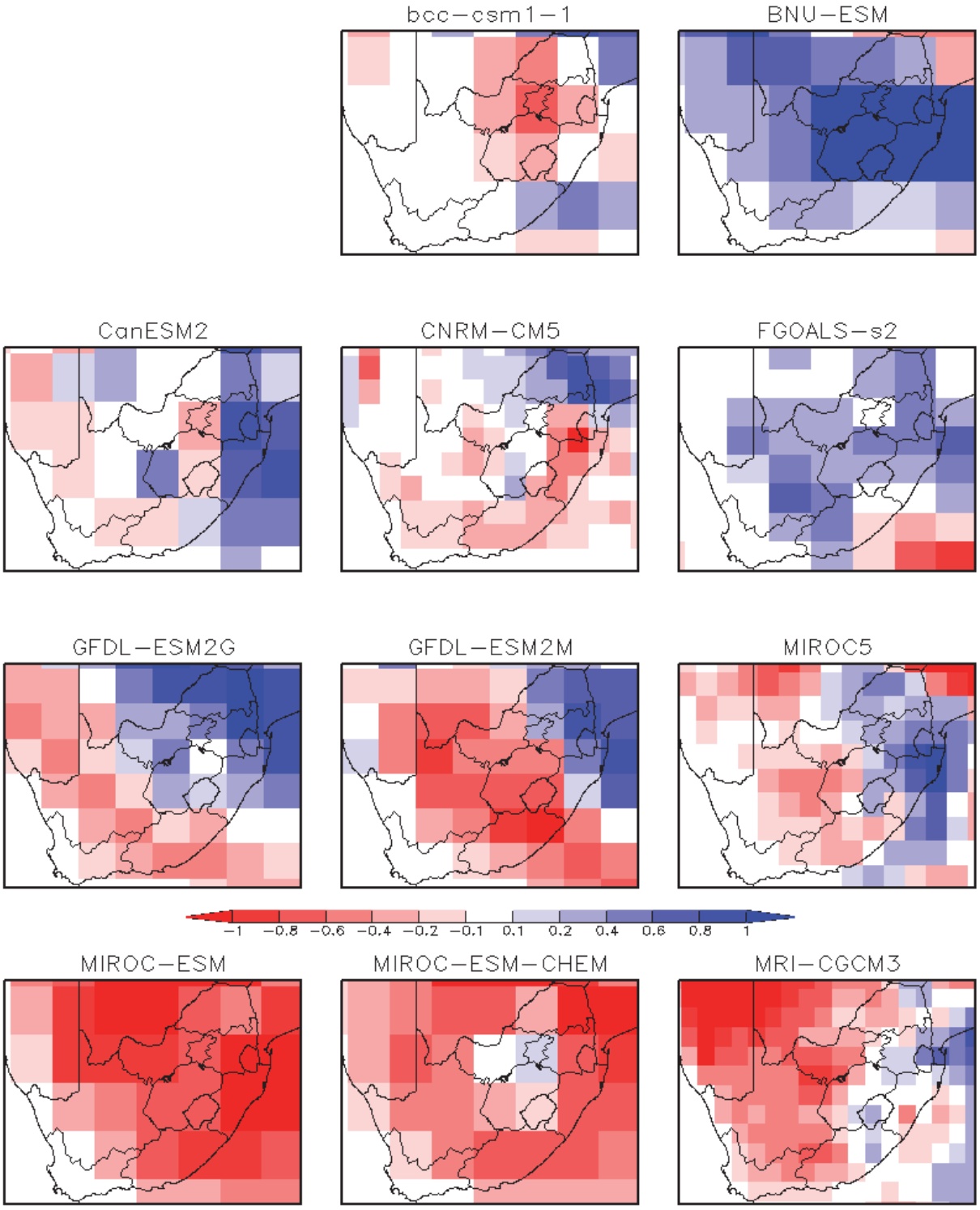

Figure 5.10 | *Future anomalies for summer (DJF) daily mean precipitation (mm/day) for the mid-21st century (2041-2070 – 1976-2005) under the RCP8.5 emission scenario for 11 raw CMIP5 GCMs.*

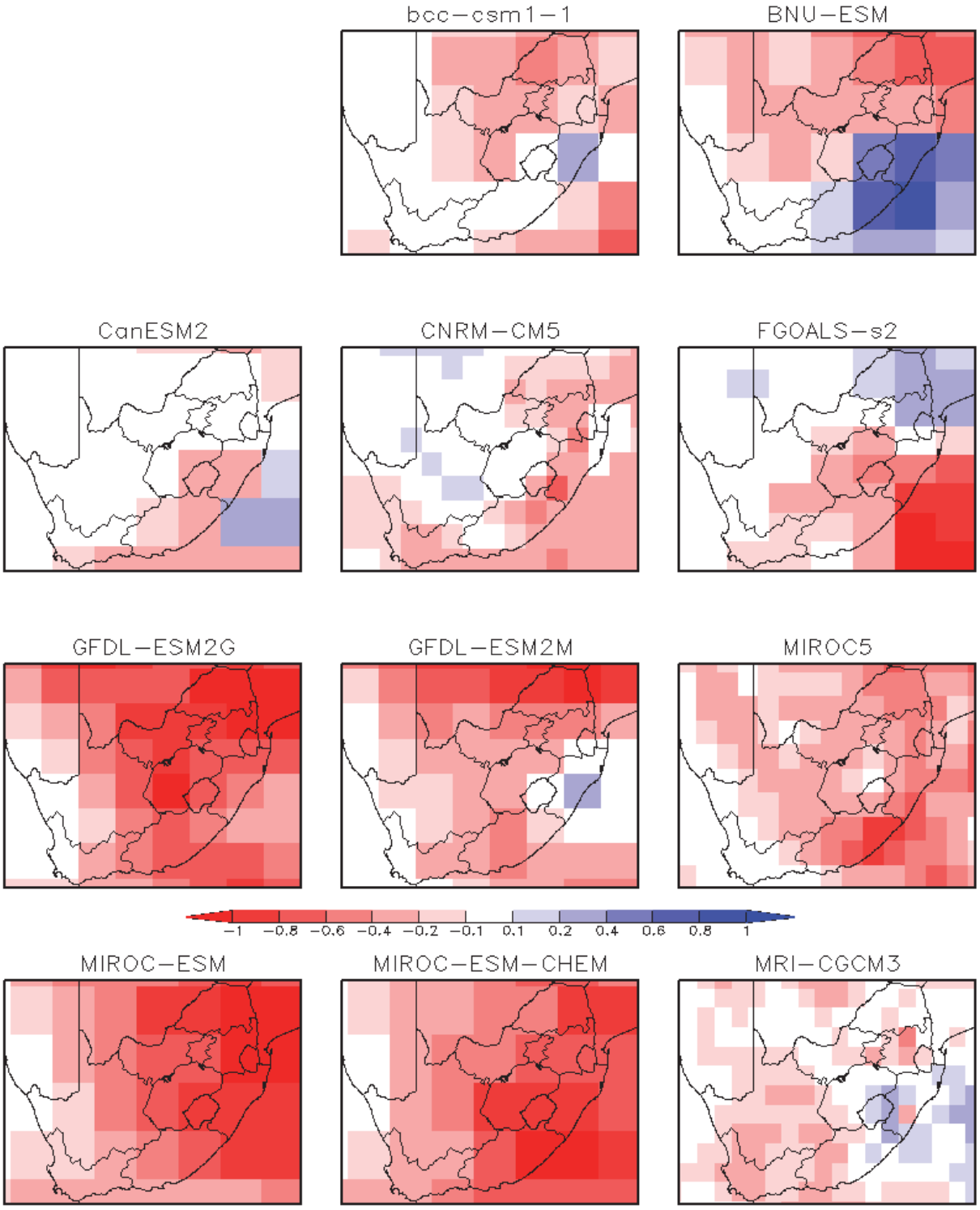

Figure 5.11 | *Future anomalies for spring (SON) daily mean precipitation (mm/day) for the mid-21st century (2041-2070 – 1976-2005) under the RCP8.5 emission scenario for 11 raw CMIP5 GCMs.*

5.6.2 *Dynamically Downscaled Results*

Runs from the Swedish Meteorological and Hydrological Institute Rossby Centre Regional Climate Model (SMHI-RCA4) have been publically release and the results have been included in this chapter. The RCM downscaled eight GCMs: CanESM2, CNRM-CM5, EC-EARTH, MIROC5, HadGEM2-ES, MPI-ESM-LR, NorESM1-M and GFDL_ESM2M (see Appendix A for further details on these models) under both the RCP4.5 and RCP8.5 emission scenarios. A selection of the results is presented here to illustrate the climate change messages coming out of this source of downscaled data. Results are presented in the same way as that for the raw GCMs: Seasonal anomalies of daily precipitation (mm/day) for the mid-21st century (2041-2070 – 1976-2005) under the RCP8.5 emission scenario.

The ensemble mean of daily mean summer precipitation suggests an increasing over the eastern interior, with some mountainous areas along the south and east coast and in Limpopo province showing drying into the future (Figure 5.12). This message is not carried through when looking at an individual GCM where each model varies in the placement, intensity and even direction of change in daily precipitation into the future. The climate change message for the spring season (September-October-November) (Figure 5.13**)** differs from that of the core summer season. During this period the ensemble mean shows a drying over the far north, and along the east and south coast of the county. Wetting is constrained to a smaller area centered on Lesotho. The individual models show more agreement on the general direction of change during this season, with most of the differences being in the exact placement and intensity of wetting or drying into the future. No measure of significance is attached to these results and it is important to recognise that these results are based on only eight GCMs downscaled by a single RCM and the actual envelope of possible change may be far larger than shown by this results.

Four downscaled GCM results from the SMHI RCA4 model are also compared to those downscaled by another RCM participating in the CORDEX-Africa experiment, the Climate Limited-Areas Modelling Community model (CLMcom CCLM4.8). Results are shown for the future anomaly of annual mean daily precipitation by the 2036-2065 period under both the RCP4.5 and RCP8.5 emission scenario. The results are presented in figure 5.14 which is a complicated figure and provides a wealth of information, however only a few key messages are discussed here.

The RCM ensemble mean suggests that at the annual mean scale, the region is projected to dry or remain the same (a & b), this is a slightly stronger message than that found in the raw GCM ensemble mean (c & d). Figure 5.14 also highlights that messages coming from the two RCMs – even those driven by the same GCM – differ quite strongly from each other and from the GCM. For example the MPI-ESM-LR model under the RCP8.5 scenario (f1) shows strong drying over the far north of the country, slight drying over the Western Cape and wetting along the east coast. The RCA4 downscaled projections (r) are for less strong drying over the far north, stronger drying over the Western Cape and wetting extending from the east coast into the interior. In contrast, the CCLM RCM projects a much stronger drying over the full South African domain (j). It is important to note that annual mean statistics may

not be the most informative time-scale to focus upon since it could hide stronger messages occurring at the seasonal or monthly scale.

The RCM results presented here are just a small subset of what will eventually be included in the CORDEX-Africa experiment. There are 10 regional climate modelling groups participating in CORDEX Africa experiment and all these groups have agreed to downscale a number of GCMs under at least two emission scenarios. The clear differences in future projections are evident in the results presented here and this range of possible climate change messages will almost certainly increase with each additional RCM.

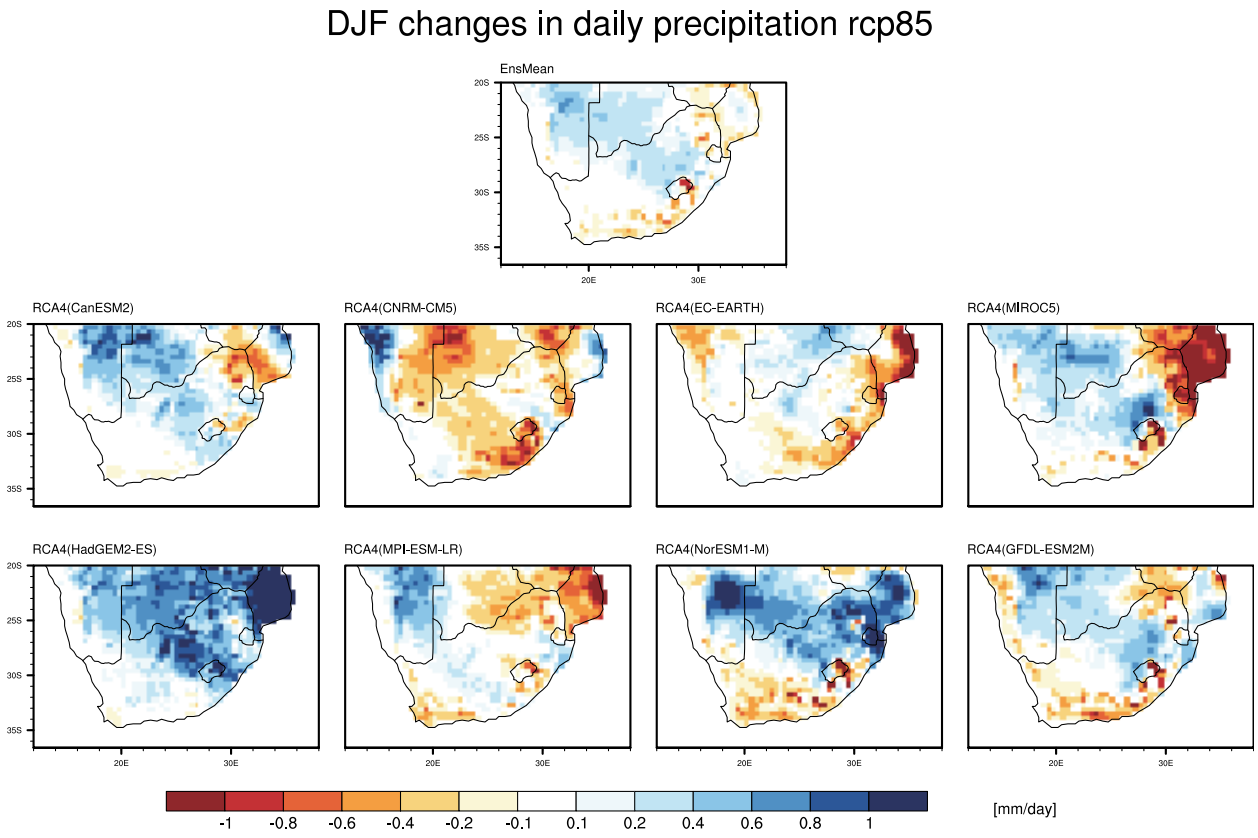

Figure 5.12 | *Future anomalies for summer (DJF) daily precipitation (mm/days) for the mid-21st century (2041-2070 – 1976-2005) for 8 GCMs dynamically downscaled using the SHMI-RCA4. Top panel is ensemble mean anomaly while all other plots are for individual models.*

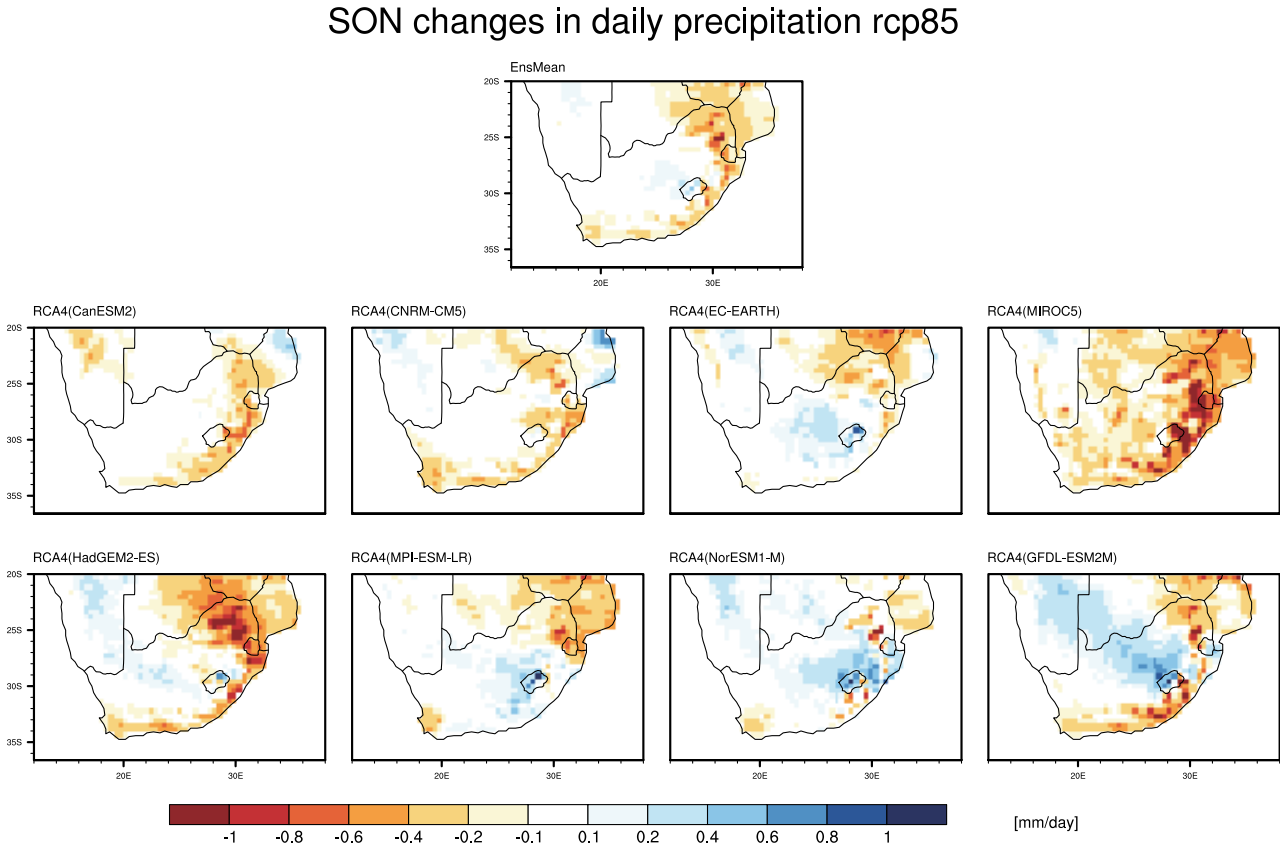

Figure 5.13 | *Future anomalies for spring (SON) daily precipitation (mm/day) for the mid-21st Century (2041-2070 – 1976-2005) under the RCP8.5 emission scenario for 8 CMIP5 GCMs dynamically downscaled using the SHMI-RCA4 RCM. Top panel is the ensemble mean anomaly while all other plots are for individual models.*

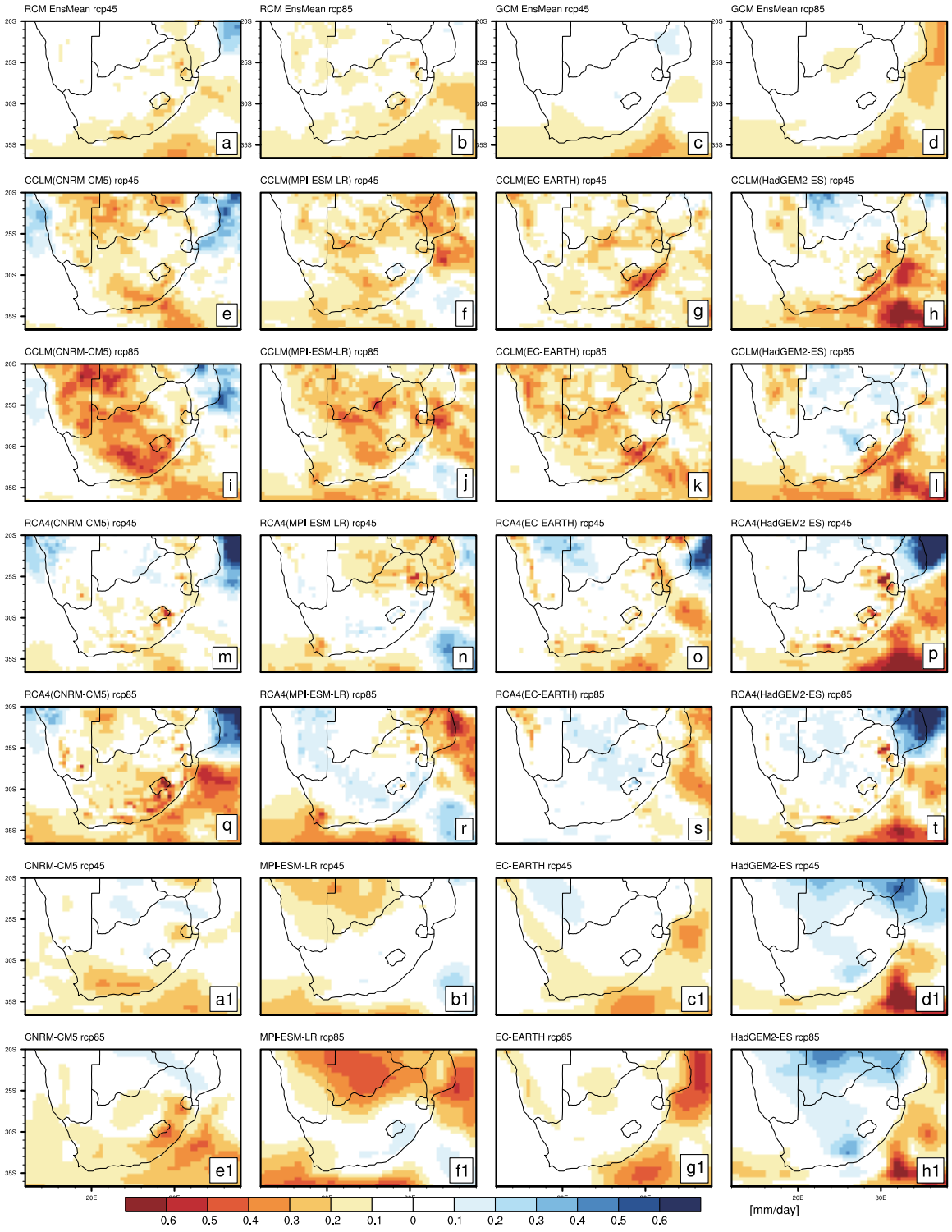

Figure 5.14 | *Future anomalies for annual mean daily precipitation for the future period (2036-2065). Results are shown for four GCMS under both the RCP4.5 and RCP8.5 scenario (a1 – h1); dynamically downscaled results from the SMHI RCA4 model (m-t) and the CCLM model (e-l) along with the GCM ensemble mean (c & d) and RCM ensemble mean (a & b) under the two emission scenarios.*

5.6.3. *Statistically Downscaled Results*

11 CMIP5 GCMs have been statistical downscaled using the Self-Organising Map based Downscaling (SOMD) for both the RCP4.5 and RCP8.5 emission scenario for the period 1960-2100 and a selection of these projections are presented here. Currently, only four of these models (CanESM2, CNRM-CM5, MIROC5 and GFDL-ESM2M) are also included in the dynamical downscaling performed by SMHI which makes a direct comparison between downscaling methods more difficult (See appendix A for further details on the CMIP5 GCMs). Downscaling of a further six GCMs are currently underway and will be added to ensemble once their output has been evaluated. Three of these GCMs are also included in the ensemble by SMHI which will allow for a more robust comparison between downscaling methods.

Figures 5.15 and 5.16 presents the downscaled projected change in summer mean minimum and maximum temperature respectively (results for the other seasons can be found in Appendix B). Each model's output is presented along with the ensemble mean. All models show clear warming by the mid-21st century but with clear disagreement in the magnitude and spatial pattern of the warming. The downscaling provides more realistic spatial detail than the raw GCM with stronger warming over the north west and more moderate warming along the coast.

The statistically downscaled climate change projections for precipitation over South Africa are less certain than those for temperature. Figure 5.17 and Figure 5.18 present the seasonally average change in daily mean precipitation by the mid-21st century under the RCP8.5 emission scenario for the summer and spring seasons respectively. The multi-model mean shows a slight suggestion of drying over the eastern interior and wetting over the south coast during summer, however there is clear disagreement on the magnitude and regional expression of wetting or drying between individual models. The message during spring is equally uncertain, though the ensemble mean suggests some drying over the cape and over Mpumalanga, but individual models strongly disagreeing on the magnitude and sign of change over the rest of the country.

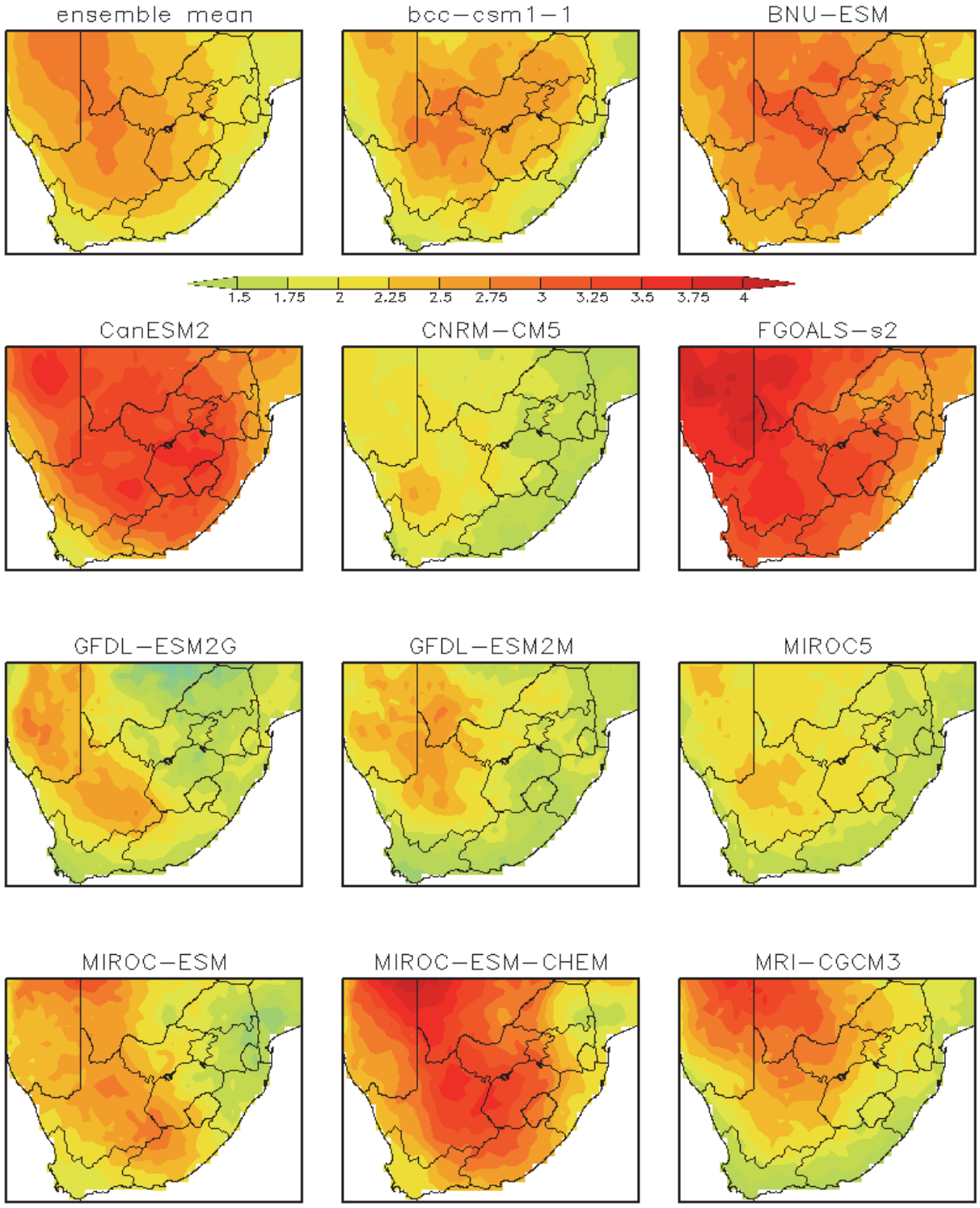

Figure 5.15 | *Future anomalies for summer(DJF) daily minimum temperature (°C) for the mid-21st century (2041-2070 – 1976-2005) under the RCP8.5 emission scenario for 11 statistically downscaled CMIP5 GCMs. Top left panel is the ensemble mean anomaly while all other plots are for individual models.*

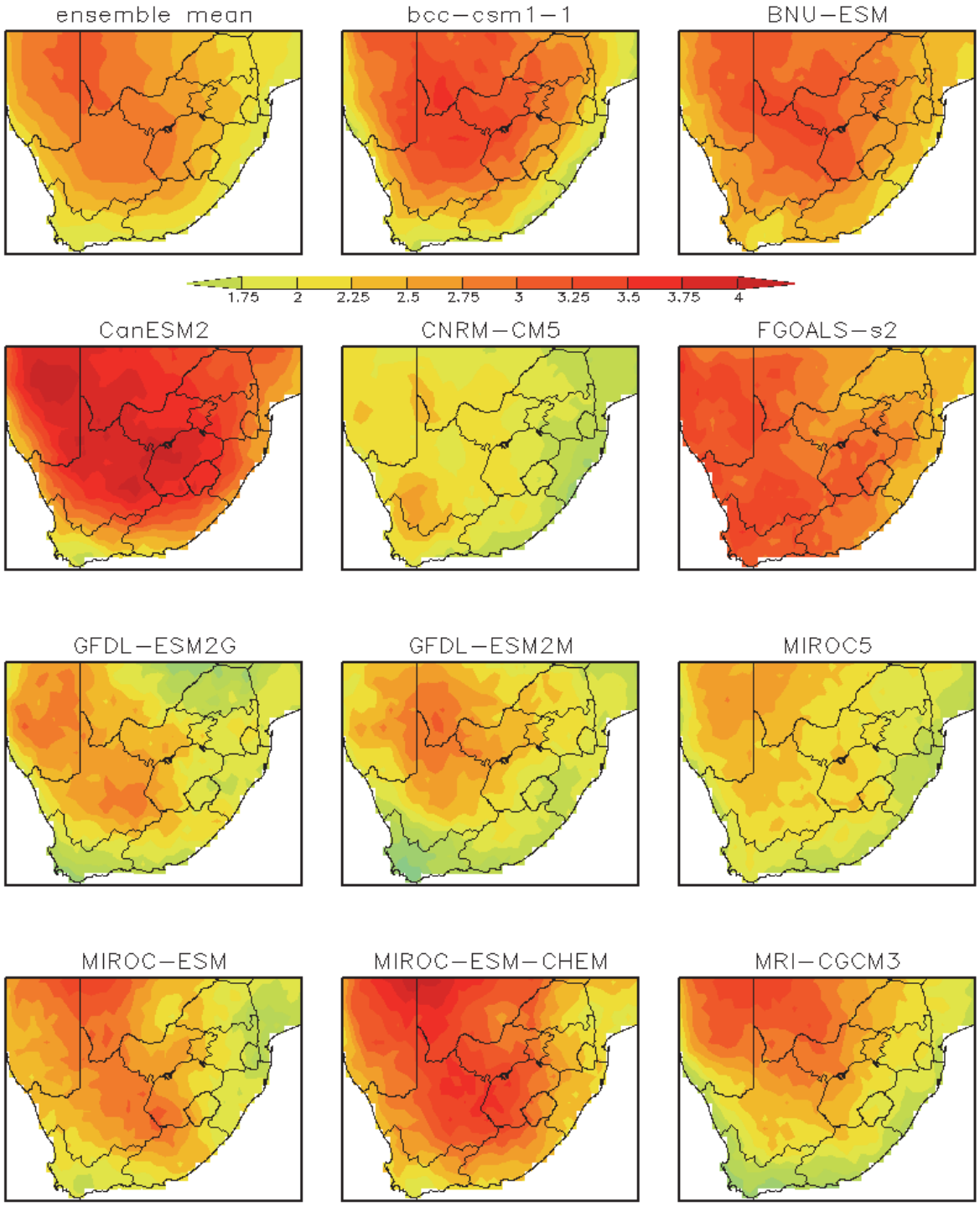

Figure 5.16 | *Future anomalies for summer(DJF) daily minimum temperature (°C) for the mid-21st century (2041-2070 – 1976-2005) under the RCP8.5 emission scenario for 11 statistically downscaled CMIP5 GCMs. Top left panel is the ensemble mean anomaly while all other plots are for individual models.*

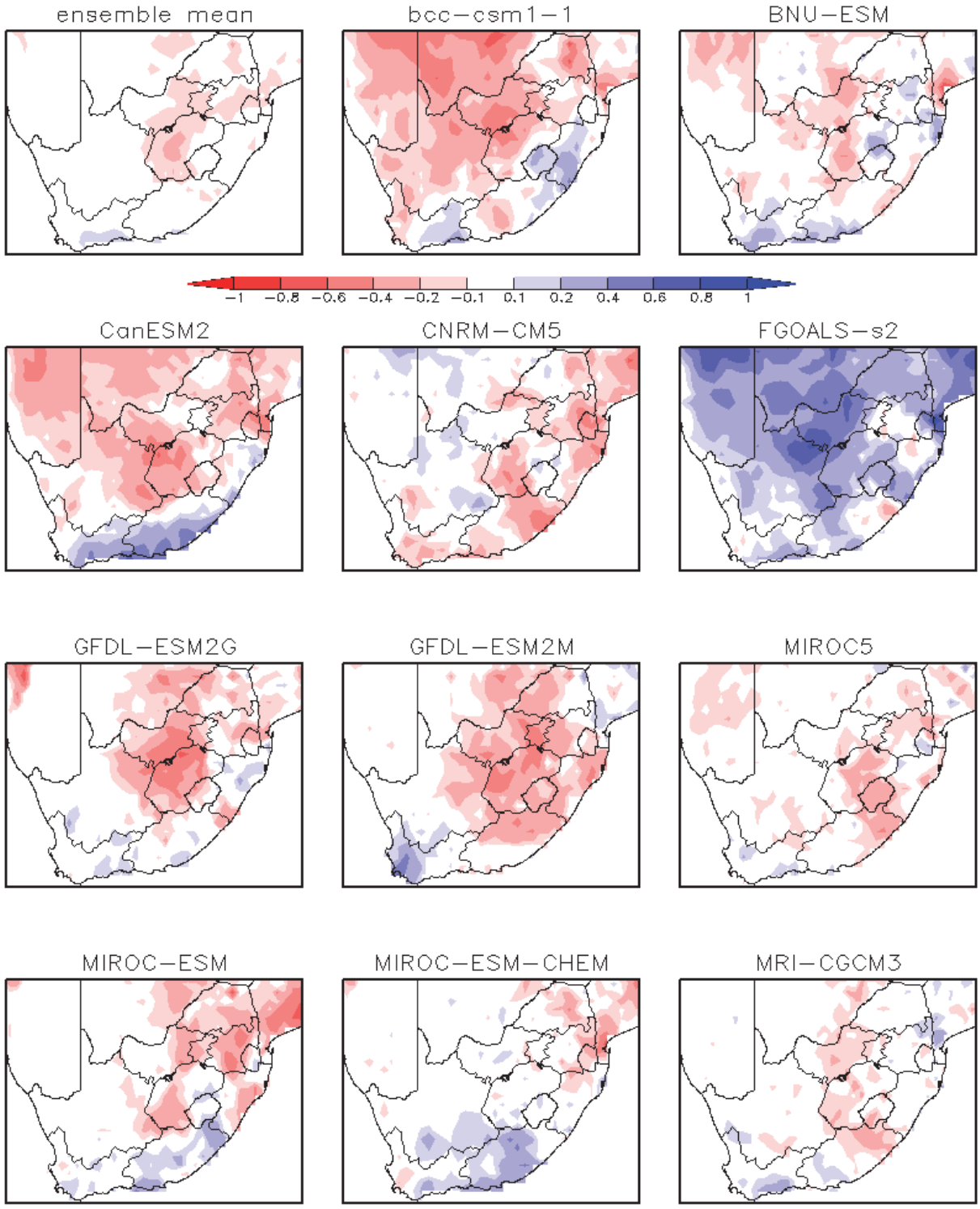

Figure 5.17 | *Future anomalies for summer(DJF) daily mean precipitation (mm/day) for the mid-21st century (2041-2070 – 1976-2005) under the RCP8.5 emission scenario for 11 statistically downscaled CMIP5 GCMs. Top left panel is the ensemble mean anomaly while all other plots are for individual models.*

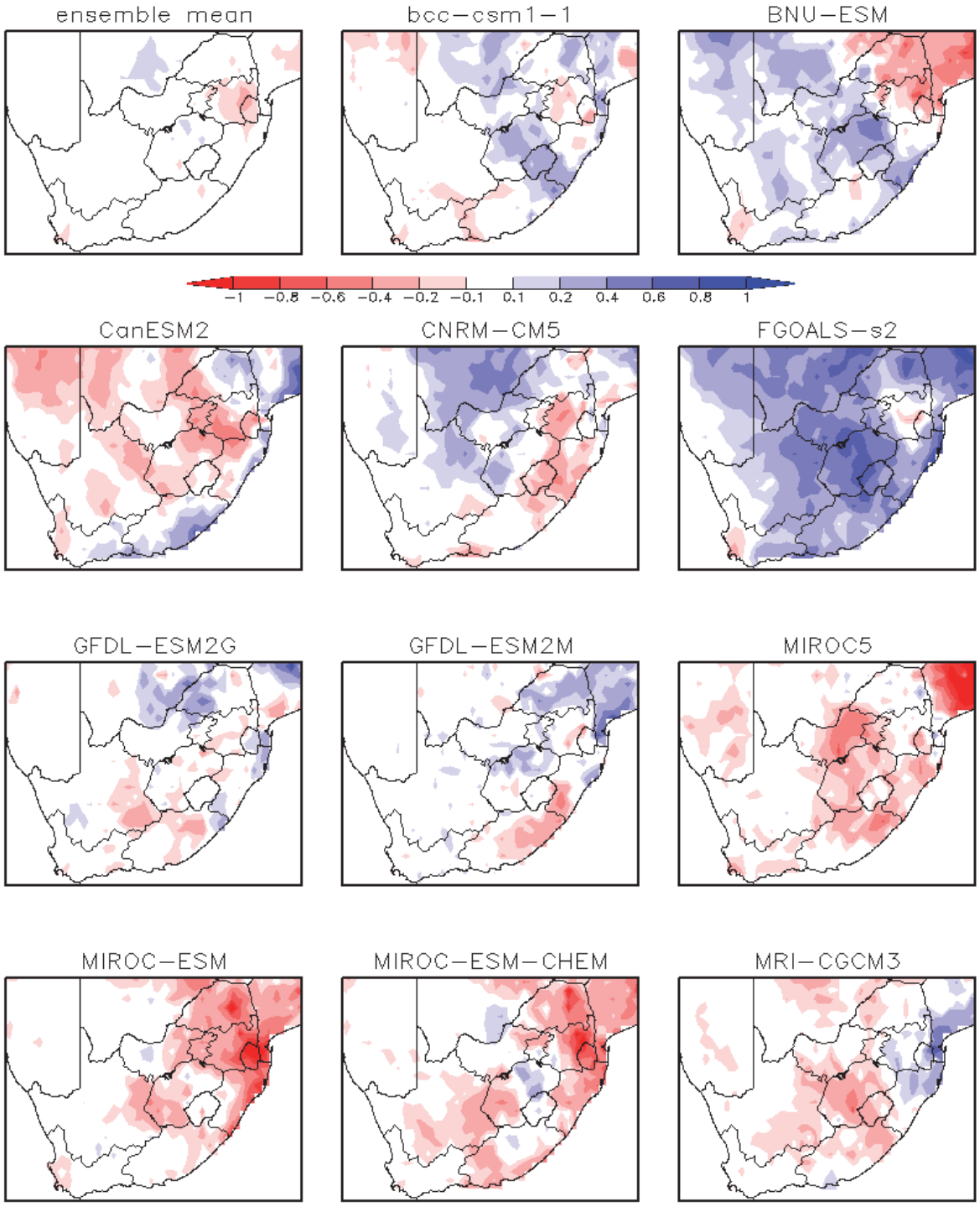

Figure 5.18 | *Future anomalies for spring (SON) daily mean precipitation (mm/day) for the mid-21st century (2041-2070 – 1976-2005) under the RCP8.5 emission scenario for 11 statistically downscaled CMIP5 GCMs. Top left panel is the ensemble mean anomaly while all other plots are for individual models.*

The SOMD method is also used to statistically downscale station records. Figures 5.19 and 5.20 illustrate the results for two locations, namely Warmbad Towoomba in the Limpopo

Provide and Cape Town Weather Office in the Western Cape. The top panel displays the projected change in monthly average maximum temperature, while the bottom panel shows projected change in monthly total precipitation by the mid-20th century (2040-2060). The monthly anomaly for each model is shown as a black line graph and a guide to the inter-model spread is provided by the bars which show the range between the 10th and 90th percentile. The observed climatology (grey bars) is also included in the precipitation plots to indicate the relative importance of these projected changes against the observed monthly precipitation totals.

A number of messages are illustrated by these figures. Firstly it shows that for temperature, the models all agree on the sign of warming at both locations, but that the exact magnitude of warming differs between models and between months for each model. The largest warming is projected to occur during spring at Warmbad while Cape Town is projected to experience more moderate and consistent warming through the year. These two stations clearly show the uncertainty in projected change in precipitation. Most months have a disagreement in the sign of change and the general message changes between drying and wetting from one month to the next. If model agreement is used as a measure of confidence, then there is a slight suggestion that the rainy season in Warmbad will end earlier and intensity during the core of the season (negative anomalies during April and May and positive anomalies during January). For the Cape Town Weather Office, the only month during the core rainy season which shows a confident message is May which has a negative anomaly into the future.

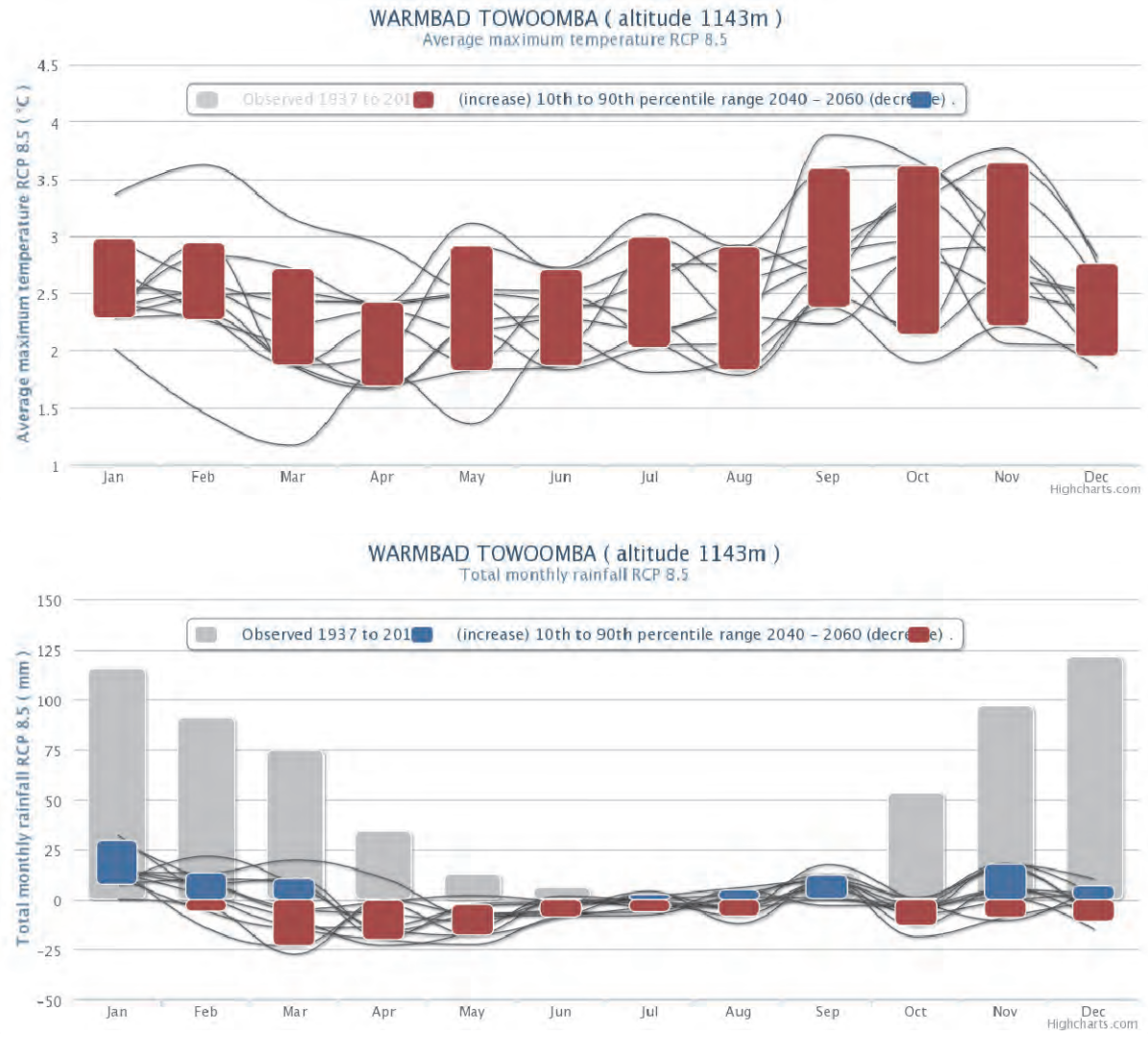

Figure 5.19 | *Statistical downscaled average maximum temperature (top) and monthly total precipitation (bottom) results for Warmbad Towoomba station using 11 GCM under the RCP8.5 emission scenario for the period 2040-2060 minus 1980-2000. The future anomaly for each GCM is represented by a black line, while the ensemble 10th and 90th percentile is shown in red or blue depending on which statistic is being investigated. The observed climatology is presented as grey bars for the precipitation statistics.*

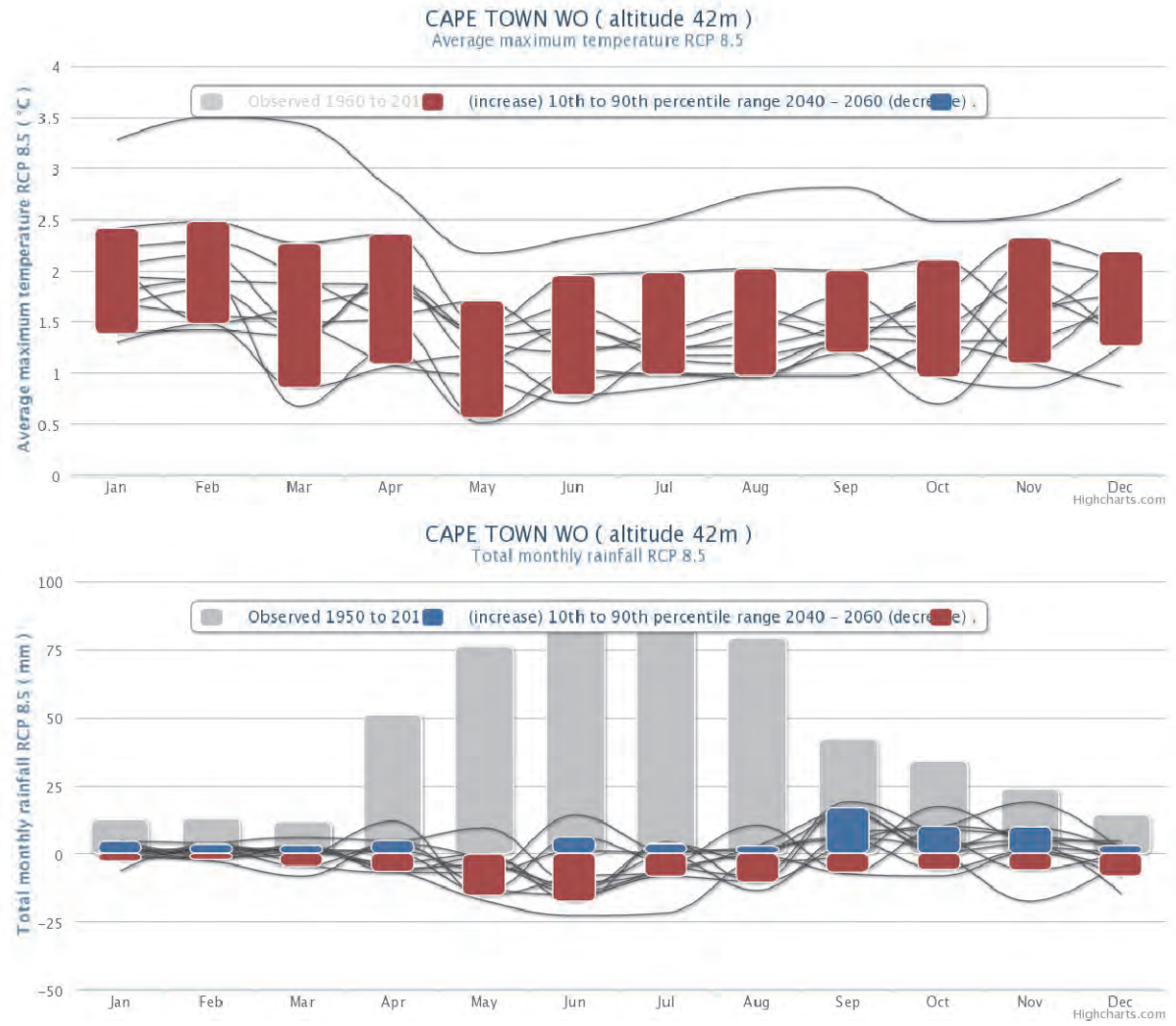

Figure 5.20 | *Statistical downscaled average maximum temperature (top) and monthly total precipitation (bottom) results for Cape Town Weather Office station using 11 GCM under the RCP8.5 emission scenario for the period 2040-2060 minus 1980-2000. The future anomaly for each GCM is represented by a black line, while the ensemble 10th and 90th percentile is shown in red or blue depending on which statistic is being investigated. The observed climatology is presented as grey bars for the precipitation statistics.*

5.7. CONCLUSION

Regional messages of climate change are needed by users of climate information. Global Climate Models are too coarse to provide this information and therefore downscaling methods are needed to provide the climate change information at scale needed to make decisions. Downscaling can be separated into two main classes; dynamical downscaling using Regional Climate Models and statistical/empirical downscaling which represent a range of different techniques. Both classes of downscaling have their own strengths and weaknesses and in this chapter we present results from both.

A clear message of warming over South Africa is seen in the raw GCM output as well as both downscaling methods (results from the dynamical downscaling were not presented in this version of the report). Warming is projected to be most intense over the drier parts of the interior, while less intense along the coast. Disagreement in the exact spatial distribution and magnitude of warming is evident between GCMs and between different downscaling products.

Projected changes in precipitation into the future are less confident than for temperature. GCMs disagree on the sign of change over the region with some projecting strong wetting while others projecting strong drying. The range projected by the two downscaling methods is narrower than that of the driving GCMs. However, there is still strong disagreement in the sign of change and placement of areas of wetting or drying. The ensemble mean change also disagrees between the two downscaling methods which widens the spread of projected changes.

This chapter highlights the dangers of using a single GCM or a GCM downscaled by a single downscaling method. The alternative – using multiple downscaling methods driven by a range of GCMs and emission scenarios – is far more complicated and time consuming. The messages coming out of each data source can also be contradictory – as in this case – but this disagreement is still a valid message and needs to be communicated to the users of climate information. The next step is to explore ways of better distilling relevant and robust messages from the different sources and interpreting them in the light of historic trends and variability and understanding the large-scale dynamics and processes responsible for these changes.

CHAPTER 6

FRAMEWORK FOR INTEGRATING LINES OF EVIDENCE

6.1. Objectives

The preceding chapters opened up the exploratory lines for assessing historical change, process change in GCMs and associated issues of uncertainty, and downscaling. These are the foundations of the framework to integrate the multiple lines of evidence towards scale-relevant messages on climate change. The following discussion draws heavily on Hewitson et al. (2014) and related unpublished reports from complementary activities that explore the development of the integrative framework as outlined in Figure 1.1 in Chapter 1.

In any climate data source there is both implied and real information, and the final robustness of any message is subject to the interpretation of the scientists and users. Context is highly relevant, and a product can be robust at larger scales but questionable at small scales. In addition, in any quasi-deterministic system uncertainty in the range of outcomes is inherent, and thus one may identify three criteria against which climate data should be assessed—is it: plausible, defensible, and actionable (PDA)?

- Plausible. The results are consistent with the known dynamics of the physical system.
- Defensible. There is a physical basis that can explain the results. For example, a regional climate projection may show a decrease in rainfall, and there is evidence of a decrease in frontal intensity.
- Actionable. Defined as evidence strong enough to guide real-world decisions in the context of an accepted level of risk. Risk is necessarily subjective and context dependent, however, this does not absolve the scientist of responsibility to at least consider whether the data are robust within their own personal risk framework.

There are no definitive answers to the PDA criteria, and the actionable criterion is naturally scale dependent and contingent on a user-defined acceptable risk. To robustly address this requires substantial interaction between the climate community and the user community; the scientist needs to be fully cognizant of the user context so that they may mutually assess the degree of "actionable" information. While some sectors of society, such as the insurance industry, are proficient at making decisions with uncertain information, the delivery of downscaled data is most often not communicated with articulated limits, and there is a need to communicate how a data product fits the landscape of information for climate change, and the possible/probable contradictions that may exist with other products.

6.2. What climate data ideally seeks to achieve

The information required by users is highly dependent on the application, the relevant scales in time and space, and the user's risk exposure. Figure 1 encapsulates this. For a given spatial scale the y-axis represents some measure of information, and the x-axis is the range of relevant time scales. The curves are speculative representations of the actual and required levels of information, and the theoretical limit. The nature of the information changes across the time scales from a prediction of absolute values at short lead times, to a projection of some probable mean system state or derived statistics at long lead times. For example, at weather forecasting lead times the target is the state of the atmosphere at a particular location (e.g. daily temperature) while on longer "climate" prediction lead times the target is the distribution of states (e.g. means, variances).

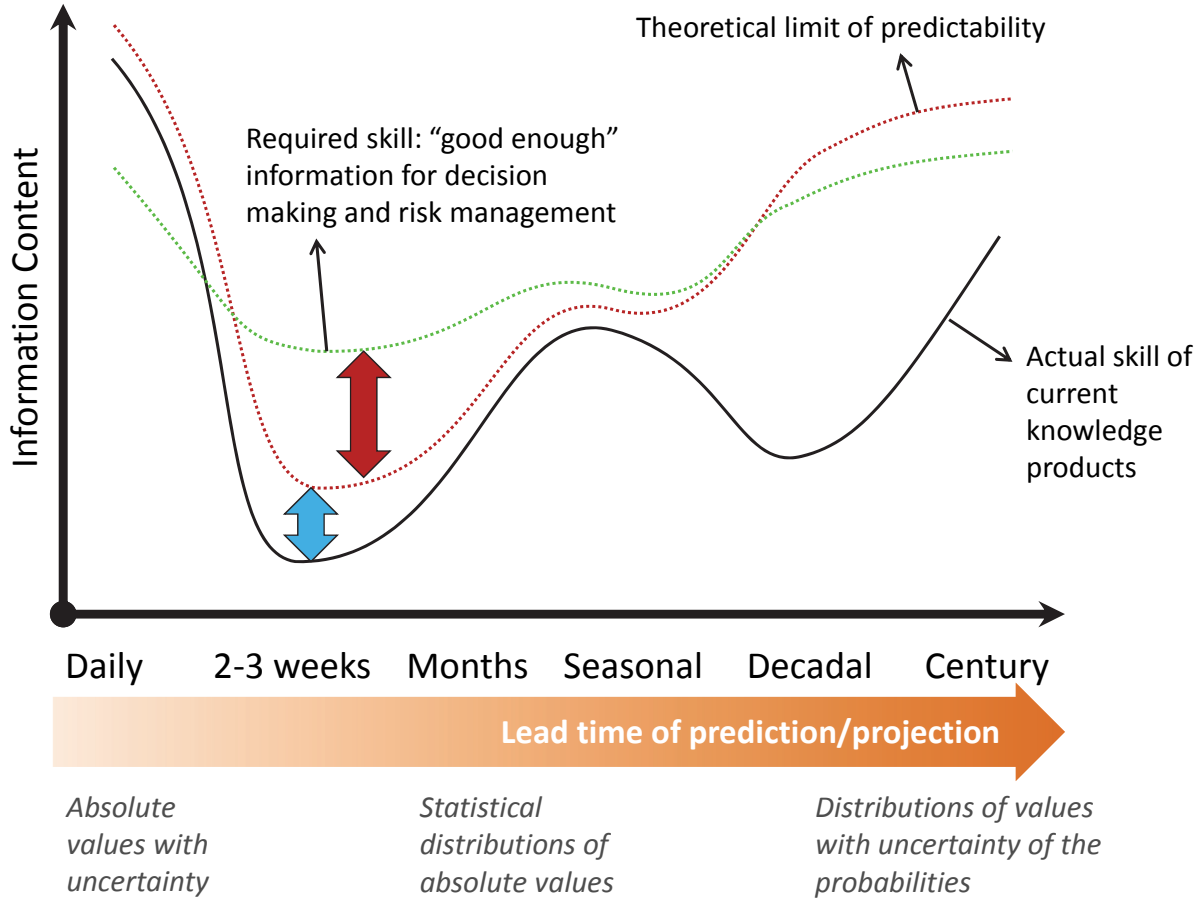

Figure 6.1 | *Idealized representation of conceptual information issues in relation to using climate information for a given scale, variable, metric, and application. The curves are hypothetical, and in practice each line is a zone of gradation, but is represented here as a simple line for clarity (after Landman et al., 2010).*

At any time scale there is a level of information content useful for decision making. For example, faced with the need to plan for a wet tomorrow, is the weather forecast "good

enough" to predict rain or no rain? Or, at the 3 month lead time, what risk does one take by selecting a crop planting date based on the seasonal forecast. In other words, what information is "good enough" to manage the risk? By contrast is the actual skill of a forecast/projection good enough? The current skill of short term weather forecasts may be "good enough". However, on the 2-3 week lead time the skill is low, there is variable skill on seasonal time scales, uncertain skill on intra-decadal scales, and possibly good skill at multi-decadal scales for the statistics at some measure of spatial and temporal aggregation.

The objective is to move the "actual skill" curve toward the curve of "good enough" information where the risk inherent in a decision becomes acceptable. However, a third curve introduces a critical issue; that of the limit to predictability. In any quasi-deterministic system there is a limit to the predictive skill (in terms of knowledge and/or tools and methods). If this limit is less than the required skill, then there is a fundamental constraint to developing actionable climate information.

A point on uncertainty bears mentioning here. Uncertainty on the shorter lead times can be quantified in probabilistic terms, whereas uncertainty on the longer lead times is an issue of uncertainty about the probabilities. For example, we are less certain about the absolute global mean temperature 100 years from now, than we are about the global mean temperature 20 years from now. However, we have more confidence that the global mean temperature in 100 years, as opposed to 20 years, will be warmer than at present. If our decisions are sensitive to knowledge regarding *changes* to climate rather than absolute values of the climate state (such as the annual mean temperature) then we have more actionable information on the longer prediction lead times.

6.3. Frameworks for using regional downscaling information

In any application, whether decisions on resource management, policy development, or climate change adaptation actions, the climate information sits within a broader context of multiple co-dependent non-climate stressors. For example, growth in urban water demand, changing land cover, evolving political governance, the economy, or even international trade. Depending on the time scale climate information on regional change may be of greater or lesser importance. Recognizing the relative role of the climate information as early on as possible is important for the effective allocation of resources.

This project does not explore the role of the non-climate factors, other than to demonstrate how the climate information may be a) distilled to key messages, and b) integrated with the sector and/or place-based context of any application.

6.3.1. *Physical climate information*

There is a strong temptation to adopt a single source of information and thus limiting the spread of possibilities the user has to consider. This may be due to pragmatic issues such as limited accessibility to information, or less tangible reasons such as a preference for a favourite model, or the non-trivial challenge of understanding and distilling clear messages from a diverse and contradictory evidence base.

From a physical science perspective it is clear that no one source can provide the definitive message. GCMs provide skill on synoptic circulation and larger scale processes that are informative of regional change, but are weak at representing local scale surface climate. Moreover, GCMs produce area averages and are fundamentally not the same as observations. Likewise the historical record provides information about local trends, but extrapolation of these trends is problematic. Thus, drawing on multiple sources is imperative for achieving robust understanding of local change and even then there is no guarantee that actionable information will be achieved.

The fourfold approach as advocated by the Intergovernmental Panel on Climate Change (IPCC) 4th Assessment report (AR4) (Christensen et al., 2007) was outlined in figure 1.1 in Chapter 1. This considers the Atmosphere-Ocean Global Climate Models (AOGCMs); downscaling of AOGCMs; physical understanding of the circulation changes; and recent historical climate change.

The foundations of this assessment framework are:

- A historical record that is uncertain: The spatial and temporal paucity of observations has led to multiple data products that agree on the essentials of historical change, but deviate amongst each other at local scales. For example, the TRMM satellite offers global observations of rainfall, but contains regional biases compared to other observational sources (e.g. Gopalan et al., 2010).
- System dynamics and process understanding: The global modes of variability, teleconnections, and synoptic scale dynamics directly inform our understanding of how local and regional climates are established and may change.
- AOGCM data: Simulations with the coupled AOGCMs give a view of the large-scale changes. The local scale skill is poor, particularly with regards to the surface diagnostic variables (such as the temporal and spatial distribution of precipitation). However, at aggregate scales of time and space, the models do provide a coherent, large-scale picture of change, albeit with uncertainty in absolute magnitudes.
- Downscaled data: This source promises a region-specific high resolution and scale relevant data product conditioned by the AOGCM simulations, and is often the source for driving impacts modeling and adaptation decision making. In practice there remains great disparity between the results from different methods and approaches (e.g. Wilby et al., 2000).

None of these sources are without error, but collectively they represent a means for developing defensible information and regional integrated messages. These may be storylines of change based on the qualitative assessment of multiple lines of evidence, or numerical data for use with impact models. Interfacing this with the concerns of the user community adds the context and relevance, and feeds back to inform continuing research.

6.3.2. *Integration in a context of non-climate stressors*

While there are many variants of decision support tools that incorporate climate information, as tools they are usually limited in terms of transferability and scalability. There is a need for a structure in which the climate information can be practically layered onto a sector and/or location with all the non-climate factors and drivers, and examine the intersection with the messages from the climate data.

The approach presented here was formulated to be transferrable and scalable, and by leveraging co-funded opportunities was tested in a workshop with African cities on climate change. The approach consists of first examining the non-climatic system in terms of the elements that make up the system, and the principle drivers and stressors on the system.

The following outlines the concept approach, while in Chapter 7 a worked example is presented. The approach is based on the idea of progressive layering of information to find the intersection of individual elements of robust information, and so to lead to a conclusion that is defensible and informative to the user.

We start by ignoring the climate information. This seems counter-intuitive, yet it is important to first identify the points of vulnerability in a system, and then consider whether and how these points of system vulnerability are sensitive to climate factors.

The underlying concept is that of thresholds: impact from system stress is where the system is pushed beyond the threshold of viability for normal dynamic response. Thresholds may be sharp, or progressive. For example, an urban water supply has a sharp threshold if drought leads to an interruption of supply, with consequent massive impact. A progressive threshold would be one where concentration of a contaminant in a water supply increases with the increase in temperature and reduction of base flow, resulting in incremental degradation and reduction of eco-system services until failure is experienced as a final threshold of viability is crossed.

Against this idea we first explore the system vulnerabilities. Figure 6.2 presents an idealized example for a peri-urban place-based system study. In this matrix the key cells of sensitivity by the system elements (y axis) to changes in the drivers / stressors (x axis) are readily identified in terms of low, medium, and high sensitivity. This quickly gives an overview of where the critical vulnerabilities may occur in a system. Figure 6.3 gives a more specific example from the workshop for the city of Maputo.

Concept example from cklimate impact workshop in cities, Dar es Salaam, Feb 2013
Hypothetical matrix of sensitivity to stressors

Stressors / Drivers Place based (or sector) element	City maintenance capacity	Finances and taxes	Energy supply	Inter-basin water transfers
Road network	H	H	M	L
Peri-urban garden agriculture	L	M	M	M
Storm water system	M	H	L	L
Public health services	M	H	M	L

Figure 6.2 | *Idealized and hypothetical matrix of a place-based approach to identify sensitivities and vulnerabilities to changes in drivers and stressors.*

With this initial assessment of a systems vulnerabilities, independent of the climate factors, one is now in a position to begin layering additional climate information. To do this we develop two additional matrices. First, we examine the climate information on past variability and trend. This is done in terms of the climate attributes of relevance (the x axis) and the time scale (y axis) of the climate variability. The focus here is to identify where we have clear understood signals of change, that is, were the signal of change is apparent or discernible from the noise of natural variability. In particular, not only where a signal is apparent, but where the signal of change is defensible and robust from the multiple lines of evidence and in terms of physical understanding. These are the analyses of historical trends in observed surface climate and the atmospheric circulation processes that inform our physical understanding of the historical change, within the envelope of uncertainty from our incomplete observational systems. Figure 6.3 shows how this is constructed, and highlights that we have incomplete knowledge and understanding of variable certainty about the integrated messages derived from the multiple lines of evidence.

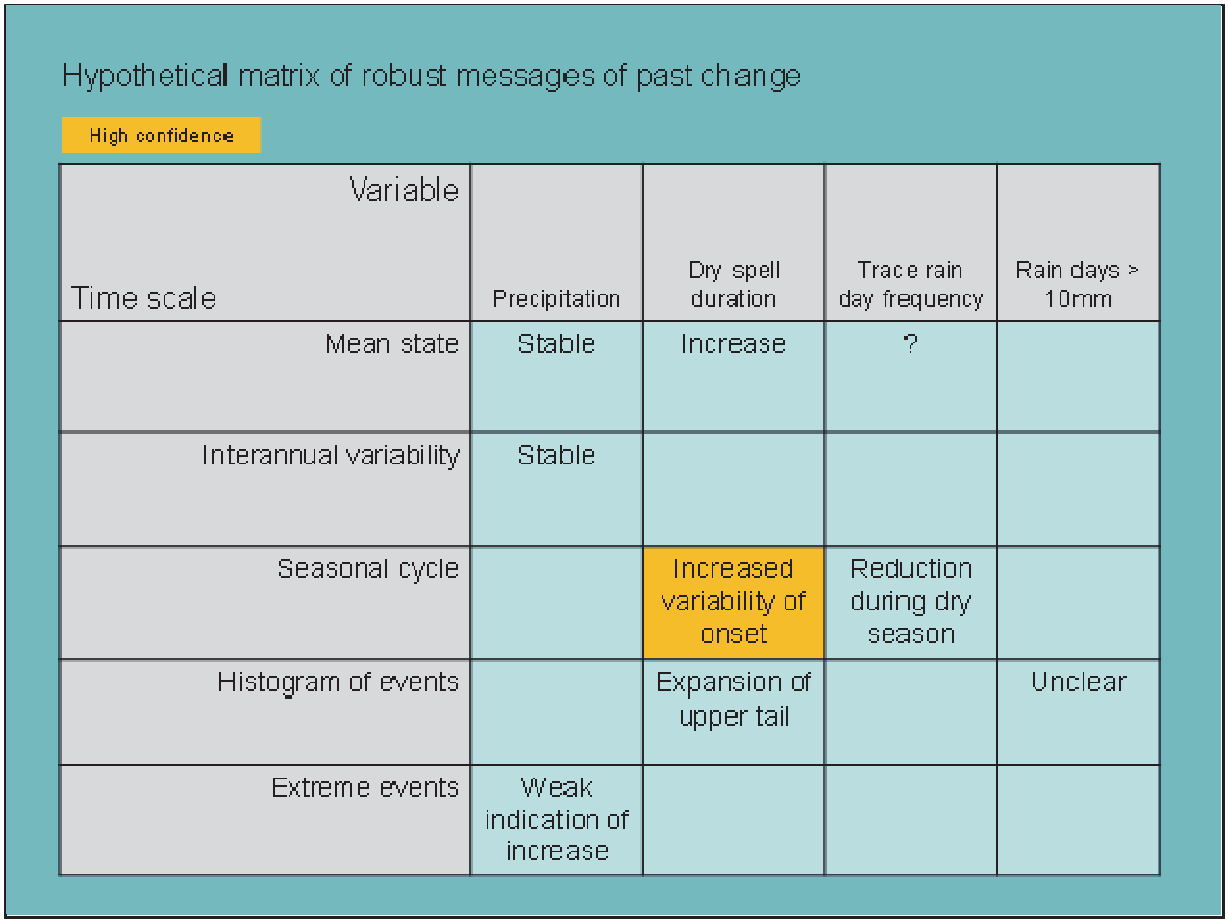

Figure 6.3 | *Idealized and hypothetical example of a matrix for identifying robust understanding of past climate change.*

At this point we have an emerging picture of the system vulnerabilities alongside what we can say with reasonable robustness about the past changes in the climate system. The next step is the logical layering of the future climate projections. Some key decisions need to be made at this point, informed by the context of the user. These include in particular how far in the future one is concerned with, and the range of emissions scenarios one wishes to consider.

With respect to how far in the future one looks, if one is planning for the near term, that is looking forward 1-2 decades from the present, the climate projections will be indicative of the direction of change, but the absolute magnitudes of change are likely to be small relative to recent natural variability. Nonetheless, decisions made now will establish a trajectory of adaptation and development, and thus the long term change should still be considered. The choice of emission scenarios is a risk decision; it is unlikely, under present circumstances, that the world will follow a low emissions scenario for at least the next decade, and if business as usual prevails, then a high emissions scenario is probably. This is particularly relevant as it establishes a time frame for when a threshold will be reached … low emission scenarios will reach a relevant threshold later in the future than a high emissions scenario.

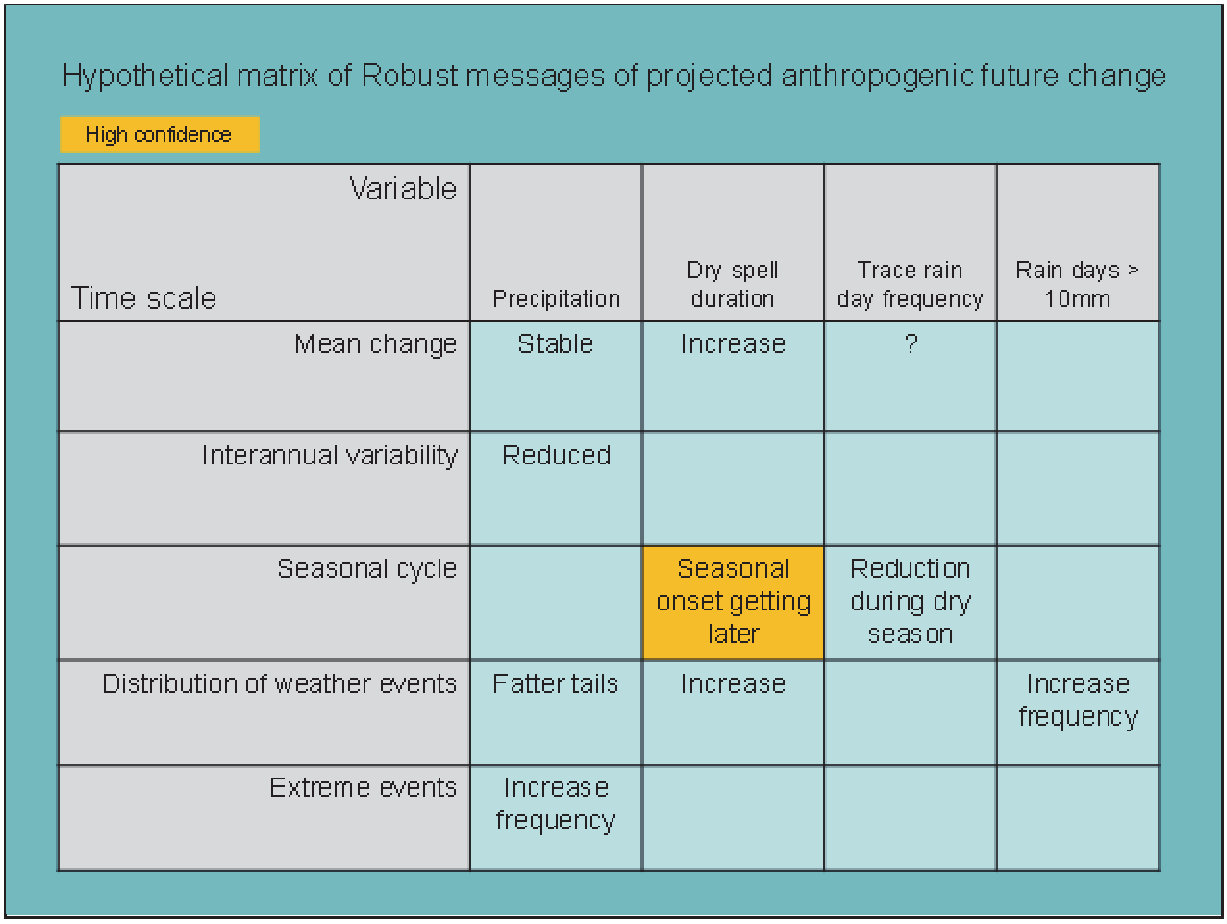

Figure 6.4 | *Idealized example of a matrix for identifying robust understanding of projected future climate change.*

Within the choices thus made, a similar matrix may be constructed for the future change messages, based again on an examination and interpretation of the multiple lines of evidence, in this case now focusing on the projected GCM, circulation and downscaled data. Figure 6.4 illustrates an example.

In the final stage, we now assess the matrices alongside each other to look for the intersection of sensitivities in the sector / place with the identified strong messages of change (Figure 6.5). This approach allows for quick identification of how critical points of vulnerability that are sensitive to climate forcing relate to the defensible climate change understanding. Figure 6.6 gives an example of the one attempt to synthesize these into a common matrix.

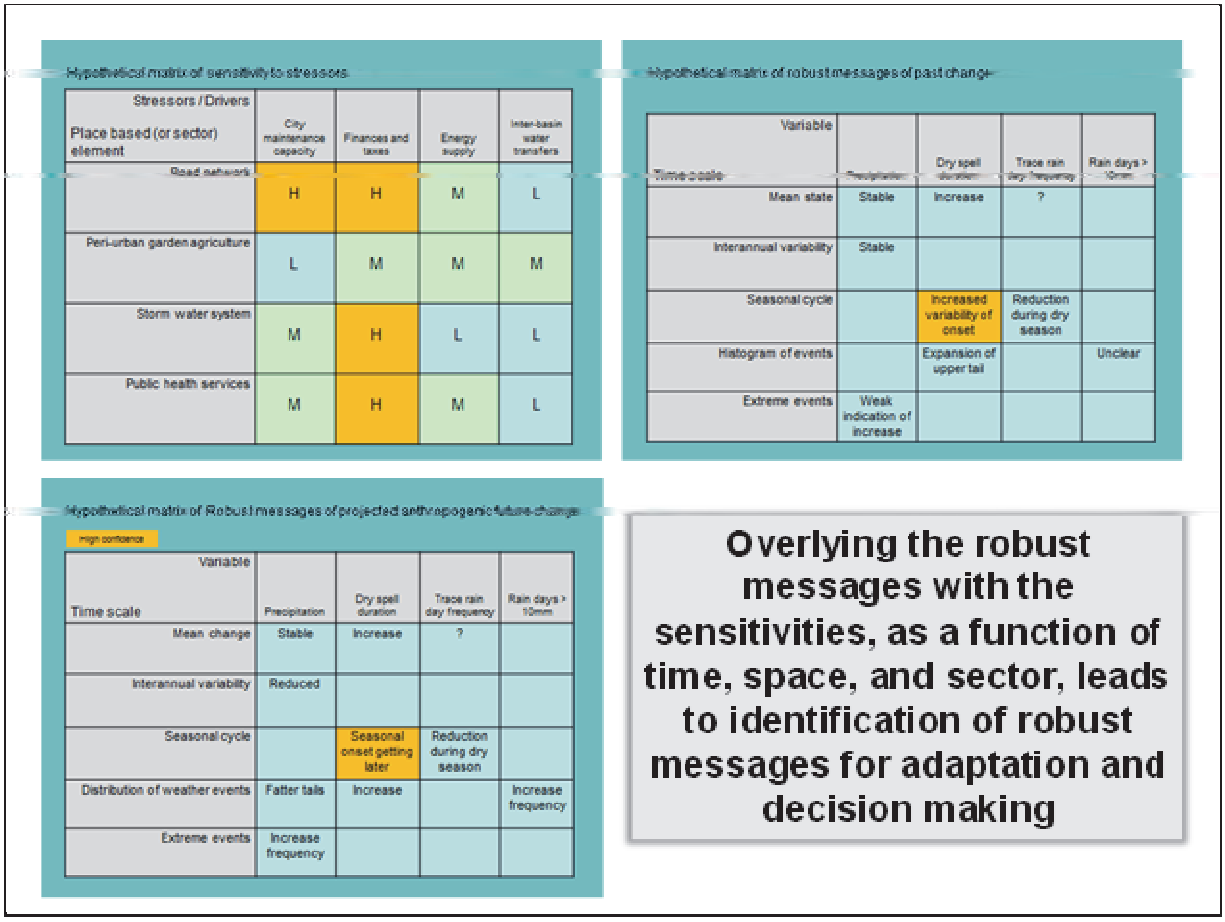

Figure 6.5 | *Considering the sensitivities in terms of the disaggregated climate information to examine the overlay of strong messages with the system vulnerabilities.*

Non-Climate Stressors → / **Elements** ↓	Population Growth		Water and Soil Pollution		Poor Road Building		Increase in food prices		Poor urban planning		Malaria and Cholera	
Economic Activities and Livelihoods												
Agriculture (Specifically Maize)	H	M	H	H+	M	H	H	H+	H	H+	H	H+
Fishing	H	/	H	H+	/	/	H	H+	/	/	H	H+
Informal Trading	H	/	L	M	H	H+	H	H+	H	H+	H	H+
Infrastructure												
Roads and Railways	M	/	/	/	H	H+	/	/	H	H+	/	/
Drainage/ Sewage and dumping sites	H	/	H	H+	H	H+	/	/	H	H+	/	/
Coastal Protection Line	H	/	/	/	H	H+	/	/	H	H+	/	/
Services												
Water Supply	H	/	H	H+	L	M	/	/	H	H+	L	M
Transport	H	/	L	L	H	H+	H	H+	H	H+	L	M

Figure 6.6 | *Example matrix from the City of Maputo. Note: Each cell within the matrix is divided in half. The left half corresponds to the impact of the non-climate stressor on the element (Low, Medium or High), and the right half corresponds to the change in impact when bringing in the climate stressor.*

6.4. Summary

The underlying principles to integrating climate information in a user's context may be summarized as follows:

a) Articulate the points of vulnerability independent of the climate forcings
b) Evaluate and interpret the robust messages of past changes to the extent that the data will support it, and express these in terms of relevant attributes of the climate variables (such as rainfall onset, extremes, and variability)
c) Assess the projected changes in the climate system where the multiple lines of evidence concur and are defensible in the understanding of the physical system dynamics.
d) Relate the defensible and robust climate messages against the assessed system vulnerabilities.

In some respects the process is relatively intuitive. However, articulating vulnerabilities in terms of thresholds is difficult, and often not attempted. Further, the propensity of users to treat data as information means the distillation of the multiple lines of evidence is commonly not undertaken, which leads to subsequent confusion when climate data introduces contradictions.

CHAPTER 7

EXAMPLES OF INTEGRATING LINES OF EVIDENCE

7.1. Background

This chapter provides an overview of key activities where the framework, as presented in Chapter 6, has been evolved and refined. This is not intended to be a definitive or prescriptive representation of the framework, but rather indicative of the uniqueness of each context that requires an adaptive response for implementation in specific contexts.

In recent years there has been a strong drive, both within developed and developing countries, to enhance the uptake of climate science and climate information by a wide range of decision makers/users. This objective has been made more complex by the move towards provision of ensemble projections of change for the users to work with. To date there is no standard methodology for incorporating these types of projections. There is nonetheless a growing discourse in the conference arena[11], with emergent issues on praxis and ethics.

The key overarching message is that under current paradigms the decision making space is contorted by the supply-chain mentality of climate information. In this way of considering the problem there is a prevailing tendency for adaptation questions to be formed in response to climate data outputs, rather than climate data queries originating from genuine decision making needs set in the context of specific time- and location-dependent vulnerabilities.

Many decision makers operate in a highly complex decision space and are often times unaware of the role of climate in these contexts. Furthermore, decisions are seldom made in isolation and usually have to consider multiple sectors, disciplines, or locations that are interlinked and interdependent. Identifying climate stressors, amongst a myriad of other important non-climate stressors, in these complex decision environments is non-trivial and certainly cannot be done through a simple questioning or survey process. A multi-sectoral, multi-disciplinary approach is therefore essential for engaging with real world decision making contexts.

To overcome this impasse, the framework concepts as outlined in Chapter 6 has been explored by CSAG and its partners to develop a process that moves beyond the classic supply driven approach, and instead complement this with a bottom up approach. The approach (as detailed in Chapter 6) has been successfully applied, and offers some significant advantages in enhancing the uptake of climate information into decision making.

[11] For example, see http://www.climate-services.org/iccs/iccs-3/home and http://www.climate-services.org/

7.2. A stressor-driven approach in the Berg River Municipality

Leveraging the additional support from, and collaboration with the Western Cape Government, this activity was a proof of concept for a multi-evidence stressor-driven approach in the Berg River municipality, and was implemented in a three-stage workshop process[12].

7.2.1. *Investigating vulnerabilities and historical climate*

The assumption that underpinned the premise of the first workshop is that climate change is an additive factor to many non-climate stressors and which can amplify existing vulnerabilities. Therefore, the first step of the workshop process was to identify the leading non-climate stressors impacting the community, and then the key climate attributes of importance. This starting point also had the advantage of pulling in many of the communities climate change "sceptics" because the issue of climate change was not discussed at the first workshop.

Many people are resistant to talking about climate change but do not realize that the impacts of climate change are not necessarily distinct from how the climate is already impacting their community. Starting from this approach allowed for an investigation into the historical climate and the associated sensitivities of the community to it.

The first workshop took place on the 18 October 2012 in Piketberg. It was reasonably well attended by around 20 people making up a group of municipal officials, councilors, and external stakeholders.

The first presentation introduced the basic concepts of climate change and climate adaptation, as well as outlining the proposed process associated with the Municipal Support Programme, for which this workshop process was a part. This was followed by a short presentation on vulnerability and a participatory exercise whereby the participants were asked to identify and prioritize key stressors being experienced in the area. It was not specified whether these stressors should be climatic or non-climatic so the participants had free reign to identify priorities for the area. The participants broke into four groups that identified a number of key stressors which were then grouped into nine overarching topics. Participants then voted on which of these nine they regarded as the most significant, resulting in six key stressors being identified. The priority stressors identified were as follows:

- Poor infrastructure and limited services
- High dependency on grants
- Degraded environment due to development
- Poor water quality (river)

[12] This experience has also been further made available as an e-learning course from the CSAG website at: http://www.csag.uct.ac.za/elearning/

- Limited employment opportunities
- Migration and seasonal work (leading to HIV and competition for jobs)

Figure 7.1 | *A group discussion around current stressors*

Figure 7.2 | *Example of identified stressors from the Berg River Municipality*

Following the development of the key stressors in the area, a presentation on the observed climate and trends was shown to the group. At this stage, the group was given the information that there is a trend of increasing temperatures across the region. The trend in precipitation is more complex and has a seasonal and topographical component. There doesn't appear to be a distinct trend in total monthly rainfall, however, there appears to be a decreasing trend across the Berg River municipality with respect to wet days. The analysis of heavy rainfall events was not sufficient to make inferences here; however, previous work

suggested that there may be an increase in heavy rainfall events. This would compensate for the decrease in wet days in the region. The participants were left to consider how/if the information they had just heard may have influenced the identification of the stressors from the previous exercise.

7.2.2. *Investigating climate impact on current activities*

The second workshop was held in Piketberg on the 22nd November 2012, and focused primarily on the link between current vulnerability and climate impacts.

Having already identified non-climate stressors of importance to the community, the workshop participants were asked to undertake an exercise called the Local Climate Impacts Profile (developed by the UK Climate Impacts Programme[13]). This exercise was designed to highlight climate stressors for the region. During the exercise the participants were asked to fill out a table identifying past weather events that have impacted the community together with their associated impact and consequences. This exercise highlighted particular climate variables that required further investigation.

Once stressors and historical climate trends had been identified, the next step was to identify economic livelihood activities within the community that might be impacted by these stressors. The identification of these activities enabled the stressors to be cross-referenced with the livelihood activities in order to pull out where the high impact areas are currently. Livelihood activities included elements such as infrastructure, agriculture, service delivery, etc. (see table 7.1)

Using a simple High, Medium, Low ranking system the stressors were cross-referenced against the livelihood activities in the area. In the example below, the climate stressors were used as the primary stressors but participants were asked to bear in mind the non-climate stressors and take into account the influence that these might have on the ranking. This approach allowed for quick identification of where current critical sensitivities occur.

[13] http://www.ukcip.org.uk/wizard/current-climate-vulnerability/lclip/

Table 7.1 | *Example of a stressor vs livelihood matrix from the Berg River Municipality*

Community stressors that may exacerbate climate stress

- Poor infrastructure and limited services
- High dependency on grants
- Degraded environment due to development
- Poor water quality (river)
- Limited employment opportunities
- Migration and seasonal work (leading to HIV and competition for jobs)

	Climate stressors			
Key sectors / activities	**High temp**	**Flood**	**Erratic rainfall**	**Heavy winds**
Infrastructure – Roads	L	M	L	L
Infrastructure – Structures / buildings	M	L	L	M
Infrastructure – Low income housing	M	H	L	M
Infrastructure – Storm water	L	H	H	M
Service delivery – Water	M	M	L	L
Service delivery – Electricity	M	M	L	M
Natural Resources – veld / soil / land	H	M	M	L
Natural Resources – water quality / quantity	M	M	M	L
Residents' health	L	M	L	M
Seasonal work (employment)	M	M	L	L
Agric – wheat	M	L	H	M
Agric – potato	M	M	M	M
Agric – table grapes & wine grapes	M	L	M	L
Agric – fruit (bo-berge)	M	L	L	M
Fishing	M	L	L	H
Tourism	M	M	M	M
Manufacture & trade	M	L	L	L

7.2.3. *Examining the impact of future projections of change and adaptation options*

The third workshop was held in Piketberg on the 30th January 2013 and was well attended, with the new Municipal Manager also attending.

Following on from the current vulnerability analysis conducted in the previous workshop, the group were shown future projections of change for the region and the uncertainties associated with these projections.

The projections show agreement that the temperatures of the region may increase in the future, however, the precipitation projections are less clear. The only clear signal coming out of the projections of precipitation is that it is likely to decrease in the SON (spring) period. However, this is at odds with the station level downscaling which suggests an increase in rainfall in the SON period. For this reason it is difficult to say anything about changes in rainfall, except that general signals of climate change indicate a more erratic type of rainfall. Wind is a very difficult variable to project so nothing can be said about the changes in wind speeds for this area.

Using these projections and their associated limitations, the current vulnerability table was presented again but this time a direction of change was presented next to the rankings where a projection of change can be robustly forecast (see table 7.2). The group discussed whether this changed any of the rankings, i.e. whether any of the medium risks became high risks or vice versa. This discussion allowed for the identification of potential future high priority risks that required investigation for adaptation.

Table 7.2 | *Including future projections in stressors vs livelihoods matrix*

	CLIMATE RISKS																			
	High Temp				Flood				Erratic rainfall				Heavy winds							
STRESSORS				CC				CC				CC				CC				CC
Infrastructure Roads	H	M	L	+ = -	H	M	L	+ = -	H	M	L	+ = -	H	M	L	+ = -	H	M	L	+ = -
LIVELIHOODS																				
Infrastructure Structures / buildings	H	M	L	+ = -	H	M	L	+ = -	H	M	L	+ = -	H	M	L	+ = -	H	M	L	+ = -
LIVELIHOODS																				
Infrastructure Housing Low income	H	M	L	+ = -	H	M	L	+ = -	H	M	L	+ = -	H	M	L	+ = -	H	M	L	+ = -
LIVELIHOODS																				
Infrastructure Storm water	H	M	L	+ = -	H	M	L	+ = -	H	M	L	+ = -	H	M	L	+ = -	H	M	L	+ = -
LIVELIHOODS																				
Service delivery - Water	H	M	L	+ = -	H	M	L	+ = -	H	M	L	+ = -	H	M	L	+ = -	H	M	L	+ = -
LIVELIHOODS																				
Service delivery - Electricity	H	M	L	+ = -	H	M	L	+ = -	H	M	L	+ = -	H	M	L	+ = -	H	M	L	+ = -
LIVELIHOODS																				
Natural Resources - veld / soil / land	H	M	L	+ = -	H	M	L	+ = -	H	M	L	+ = -	H	M	L	+ = -	H	M	L	+ = -
LIVELIHOODS																				
Natural Resources - water quality / quantity	H	M	L	+ = -	H	M	L	+ = -	H	itive	L	+ = -	H	M	L	+ = -	H	M	L	+ = -
Negative water quality - flood, also retention capacity re																				
LIVELIHOODS																				
Social capital (health)	H	M	L	+ = -	H	M	L	+ = -	H	M	L	+ = -	H	M	L	+ = -	H	M	L	+ = -
LIVELIHOODS																				
Employment (seasonal work)	H	M	L	+ = -	H	M	L	+ = -	H	M	L	+ = -	H	M	L	+ = -	H	M	L	+ = -
Agric - wheat	H	M	L	+ = -	H	M	L	+ = -	H	M	L	+ = -	H	M	L	+ = -	H	M	L	+ = -
Agric - potato	H	M	L	+ = -	H	M	L	+ = -	H	M	L	+ = -	H	M	L	+ = -	H	M	L	+ = -
Agric - table grapes & wine. Grapes love flooding - (eg Olifants river). Erratic rainfal - can have hail damage - large bursts of hail, die druiwe is vrekgeslaan. There are times	H	M	L	+ = -	H	M	L	+ = -	H	M	L	+ = -	H	M	L	+ = -	H	M	L	+ = -
Agric - fruit (bo-berge). Temp - it is important when you get the high temps, as to how high the impact is. E.g. blossoms. Erratic rainfall - low impacts because farmers irrigate.	H	M	L	+ = -	H	M	L	+ = -	H	M	L	+ = -	H	M	L	+ = -	H	M	L	+ = -
Fishing	H	M	L	+ = -	H	M	L	+ = -	H	M	L	+ = -	H	M	L	+ = -	H	M	L	+ = -
Heavy winds - boats cant go out. Fog impacts on boats going																				
Tourism	H	M	L	+ = -	H	M	L	+ = -	H	M	L	+ = -	H	M	L	+ = -	H	M	L	+ = -
Flooding - links to greater regional picture, if access																				
Manufacture & trade	H	M	L	+ = -	H	M	L	+ = -	H	M	L	+ = -	H	M	L	+ = -	H	M	L	+ = -

To guide the discussion on adaptation options, the participants agreed that they would restrict the identification of adaptation interventions to the activity areas identified through the

matrix exercise as currently being at high risk. The projections did not indicate that any of these high risk areas may become lower risk in the future so this seemed a sensible way forward as a starting point given time constraints. It was decided that, although the fishing industry was identified as a high priority risk, this would not be addressed as there was no representation from this sector present. So the following high risk areas were focused on:

- Low income housing
- Storm water infrastructure
- Natural resources – veld/soil/land
- Agriculture – wheat

Before breaking into groups, the following key discussion points emerged around the climate adaptation process, climate vulnerability, the current status quo of related projects, and problem areas and barriers to implementation.

- A priority that needs to be addressed is how to get increased political buy-in to the climate adaptation process. It was stressed that municipal members and councilors need to be provided with the Climate Adaptation Plan, in order to facilitate adequate political will and support to ensure that the identified adaptation interventions can be taken forward effectively. This can be done in the form of a public participation process.

- The timeline for the implementation of identified adaptation interventions will depend on the availability of funding, and if there is no available funding how long it will take to source funding Successful implementation is also dependent on the coordination of environmental forums/structures.

The workshop participants then divided into two groups to focus on two identified priority areas. One group focused on mitigating the risk relating to the 'natural' environment, and the other on mitigating the risk relating to the 'built environment'. Adaptation interventions were discussed and have been taken forward in municipal planning activities. These adaptation measures are not detailed here.

7.3. African Cities case study

This second example is drawn from an ancillary activity; a collaboration between CSAG and START[14] and funded by CDKN[15]. The workshop focused on applying the developed framework for the peri-urban areas of 5 major Africa cities. This was not a workshop under the auspices of this WRC project, but directly leveraged the activities of the WRC project as a major framing for the workshop. A full report is available on request, and we reproduce here the summary of the workshop.

[14] http://www.start.org
[15] http://cdkn.org/

7.3.1. *CSAG/START workshop summary*

A workshop was held in Dar es Salaam on 13-15 February 2013 to implement a guidance framework (exemplar) for using climate model data to support adaptation planning in Africa. The main purpose of this workshop was to pilot the methodology (developed under the auspices of WRC project K5/2061) with interdisciplinary teams from five African cities (Addis Ababa, Kampala, Dar es Salaam, Maputo and Lusaka). The participants for this event were technical experts in the areas of meteorology/climatology, agriculture, water resource management, disaster risk management and land-use planning, and city managers and local government. The climate-application focus of the workshop was on peri-urban areas of these five cities, which typify the intensive land-use change pressures from urban encroachment that African cities are facing. These pressures have implications for, among others, food production, water resources and flood risk management for cities.

The learning process for integrating climate data into decision making took place through the development of a matrix that encompassed interlocking non-climatic and climatic stressors that act on important exposure units in peri-urban areas. The matrix development occurred through a step-wise process that involved identifying critical exposure units related to livelihoods, infrastructure and services that occur in peri-urban areas, identifying non-climate stressors that act on these exposure units and then identifying where climate stressors have an important influence on the exposure units. This step-wise process allowed the city teams to identifying critical vulnerabilities in livelihoods, infrastructure and services of their peri-urban environments that then provided a targeted, contextual basis for identifying climate sensitivities to which they could integrate climate information. Additionally, the focus on a place-based situation, rather than a sectoral one, promoted discovery of critical linkages between energy, transport health, food, etc. that shape vulnerability and resilience.

The three days of discussions provided an excellent opportunity for co-exploration (among and between teams and between workshop organizers and teams) of applying climate data to decision making, which served to advance the development of an exemplar based methodology that when fully developed will be widely applicable to other settings and groups.

This workshop represented an important step in addressing a key objective of CORDEX-Africa in fostering inter-disciplinary investigations and engaging users of climate information in transforming climate data into useful, usable information. The organizers wish to thank CDKN for their support.

7.4. Conclusions and Outcomes

It is apparent from the experiences that the conceptual approach of layered matrices, as outlined in Chapter 6, presents a powerful co-exploration paradigm that productively departs from the linear supply chain mentality. Of particular note is how the climate scientists

learned from, and were greatly sensitized by the sector participants, and vice versa; this mutual exchange of understanding was a significant factor to finding defensible and rational messages for action.

The activities clearly indicate that it is possible to identify robust points of intersection between the multiple and disparate data sources – arguably the leading threat to maladaptation in the decision maker's sphere of activities. Equally, while this is demonstrable a responsible way forward in the interface of science and society, this process has also highlighted a leading challenge; how to scale this activity beyond the human capacity of co-exploration activities?

While workshops and face-to-face engagements are undeniable productive (when appropriately structured), the limitations due to constrained human capacity necessitate exploring a virtual process to facilitate wide adoption and application. Some of this is already in process and the understanding from this project has:

- Strongly informed the curriculum of a wide range of extension activities[16]
- Guided the development of the CSAG winter school[17]
- Been included in the development of online e-learning[18]
- Informed the engagement in a number of international activities, including among others, the ICCS3[19] and guidance documents in preparation for the WCRP WGRC[20] and the IPCC TGICA[21]

Finally, it is important to note that climate change is research in progress, and operationalization of the science is a tension that will necessarily exist for some time to come. Consequently, evolution of the paradigm will remain and the work of this report should be viewed as a foundation to be built on, and continually developed into the future as our understanding evolves. Nonetheless, the point to which we have now developed is a robust platform that allows (some) responsible action decisions to be developed, and gives clarity on the challenges remaining and WRC project K5/2249 "Limits to skill" now picks up on some of these issues.

[16] http://www.csag.uct.ac.za/category/projects/consulting/capacity-building/
[17] http://www.csag.uct.ac.za/winterschool/
[18] http://www.csag.uct.ac.za/elearning/
[19] http://www.climate-services.org/iccs/iccs-3/home
[20] http://www.wcrp-climate.org/index.php/key-deleverables/regional-climat6
[21] http://www.ipcc.ch/activities/activities.shtml#tabs-4

REFERENCES

ACHUTARAO K and SPERBER K (2006) ENSO simulations in coupled ocean-atmosphere models: are the current models better? *Clim. Dyn*. **27**, 1-16

ALORY G, WIJFFELS S and MEYERS G (2007) Observed trends in the Indian Ocean over 1960-1999 and associated mechanisms, *Geophys. Res. Lett.*, **34**, L02606

AN S-I and JIN F-F (2004), Nonlinearity and Asymmetry of ENSO, *J. Clim*, **17**, 2399-2412

ANNAN JD and HARGREAVES JC (2010) Reliability of the CMIP3 ensemble. *Geophys. Res. Lett.*, **37(2)**, n/a-n/a. doi:10.1029/2009GL041994

BEHERA SK and YAMAGATA T (2001) Subtropical SST dipole events in the southern Indian Ocean, *Geophys. Res. Lett*., **28**, 327-330

BEHERA SK, LUO J-J, MASSON S, DELECLUSE P, GUALDI S, NAVARRA A and YAMAGATA T (2005) Paramount impact of the Indian Ocean dipole on the East African short rains: A CGCM study. *J. Clim.*, **18**, 4514-4530

BELLENGER H., GUILYARDI E, LELOUP J, LENGAIGNE M and VIALARD J (2013) ENSO representation in climate models: from CMIP3 to CMIP5. *Clim. Dyn*., doi:10.1007/s00382-013-1783-z

BOULARD D, POHL B, CRÉTAT J, VIGAUD N and PHAM-XUAN T (2012) Downscaling large-scale climate variability using a regional climate model: the case of ENSO over Southern Africa. *Clim. Dyn.*, published online. doi:10.1007/s00382-012-1400-6

CAI W, COWAN T and SULLIVAN A (2009) Recent unprecedented skewness towards positive Indian Ocean Dipole occurrences and its impact on Australian rainfall. *Geophys. Res. Lett*. **36**, L11705.

CAI W, ZHENG X-T, WELLER E, COLLINS M, COWAN T, LENGAIGNE M, YU W and YAMAGATA T (2013) Projected response to the Indian Ocean Dipole to greenhouse warming, *Nature Geoscience*, **6**, 999-1007.

CHRISTENSEN JH, HEWITSON B, BUSUIOC BA, CHEN A, GAO X, HELD I, JONES R, KOLI RK, KWON WT, LAPRISE R, UEDA VMR, MEARNS L, MENÉNDEZ CG, RÄISÄNEN J, RINKE A, SARR A and WHETTON P (2007) Regionalclimateprojections. Climate Change 2007: The Physical Science Basis. Contribution of Working Group I to the Fourth Assessment Report of the Intergovernmental Panel on Climate Change, S. Solomon, D. Qin, M. Manning, Z. Chen, M. Marquis, K.B. Averyt, M. Tignorand H.L. Miller, Eds., Cambridge University Press, Cambridge, 847-940.

COLLINS, M, AN S-I, CAI W, GANACHAUD A, GUILYARDI E, JIN F-F, JOCHUM M, LENGAIGNE M, POWER S, TIMMERMANN A, VECCHI G and WITTENBERG A (2010) The impact of global warming on the tropical Pacific Ocean and El Niño. *Nat. Geosci.*, **3(6)**, 391-397. doi: 10.1038/NGEO868

COLLINS M, KNUTTI R, ARBLASTER J, DUFRESNE J-L, FICHEFET T, FRIEDLINGSTEIN P, … M., W. (2013). Long-term Climate Change: Projections, Commitments and Irreversibility. In T. F. Stocker, D. Qin, G.-K. Plattner, M. S. Tignor, K. Allen, J. Boschung, … P. M. Midgley (Eds.), *Climate Change 2013: The Physical Science Basis. Contribution of Working Group I to the Fifth Assessment Report of the Intergovernmental Panel on Climate Change*. Cambridge University Press, Cambridge, United Kingdom and New York, NY, USA.

COOK KH (2000) The South Indian Convergence Zone and Interannual Rainfall Variability over Southern Africa. *J. Clim.*, **13**, 3789-3804

COOK KH (2001) A Southern Hemisphere Wave Response to ENSO with Implications for Southern Africa Precipitation. *J. Atmos. Sci*., **58**, 2146-2162

DARON JD and STAINFORTH DA (2013) On predicting climate under climate change. *Environmental Research Letters*, **8(3)**, 034021. doi:10.1088/1748-9326/8/3/034021

FARMER G (1988) Seasonal forecasting of the Kenya Coast short rains 1901-84. *Int. J. Climatol.*, **8**, 489-497

FAUCHEREAU N., B. POHL B, REASON CJC, ROUAULT M and RICHARD Y (2009) Recurrent daily OLR patterns in the Southern Africa/Southwest Indian Ocean region, implications for South African rainfall and teleconnections. *Clim. Dyn.*, **32**, 575-591

FEDOROV AV and PHILANDER SG (2000) Is El Niño changing? *Science,* **288**, 1997-2002.

GIORGI K, JONES C and ASRAR G (2009) Addressing climate information needs at the regional level: The CORDEX framework. *WMO Bull*., **58**, 175-183.

GLECKLER PJ, TAYLOR KE and DOUTRIAUX C (2008) Performance metrics for climate models, *J. Geophs. Res.*, (Atmosphere), **113**, doi:10.1029/2007JD008972

GONG D and WANG S (1999) Definition of Antarctic Oscillation Index, *Geophys. Res. Lett*., **26**, 459-462.

GOPALAN K, WANG NY, HERRARO R and LIU C (2010) Status of the TRMM 2A12 Land Precipitation Algorithm. *Journal of Atmospheric & Oceanic Technology*, ***27,*** 8.

GRAINGER S, FREDERIKSEN CS and ZHENG X (2008) A method for evaluating the modes of variability in general circulation models. *ANZIAM J,* **50**, C399-C412

GRAINGER S, FREDERIKSON CS and ZHENG X (2013) Modes of interannual variability of Southern Hemisphere atmospheric circulation in CMIP3 models: assessment and projections. *Clim. Dym*., doi: 10.1007/s00382-012-1659-7

GUILYARDI E, GUALDI S, SLINGO J, NAVARRA A, DELECLUSE P, COLE J, MADEC G, ROBERTS M, LATIF M and TERRAY L (2004) Representing El Niño in coupled ocean-atmosphere GCMs: the dominant role of the atmospheric component, *J. Clim.*, **17**, 4623-4629

GUILYARDI E, WITTENBERG A, FEDOROV A, COLLINS M, WANG CZ, CAPOTONDI A, VAN OLDENBORGH GJ and STOCKDALE T (2009A) Understanding El Niño in ocean-atmosphere general circulation models: progress and challenges, *Bull. Am. Met. Soc.*, **90**, 325-340.

GUILYARDI E, BRACONNOT P, JIN F-F, KIM ST, KOLASINSKI M, LI T and MUSAT I (2009b) Atmosphere feedbacks during ENSO in a coupled CGM with a modified atmospheric convection scheme, *J. Clim.*, **22**, 5698-5718.

HARRISON MSJ (1984) A generalized classification of South African rain-bearing synoptic systems. *International J. Climat.*, **4**, 547-560.

HART NCG, REASON CJC and FAUCHEREAU N (2012) Cloud bands over southern Africa: seasonality, contribution to rainfall variability and modulation by the MJO, *Clim. Dyn*., DOI 10.1007/s00382-012-1589-4

HASTENRATH S, NICKLIS A and GREISCHAR L (1993) Atmospheric-hydrospheric mechanisms of climate anomalies in the western equatorial Indian Ocean. *J. Geophys. Res.*, **98**, 20219-20235

HAWKINS E and SUTTON R (2009) The Potential to Narrow Uncertainty in Regional Climate Predictions. *Bull. Am. Meteorol. Soc*., ***90*(8)**, 1095-1107. doi:10.1175/2009BAMS2607.1

HEWITSON BC and CRANE RG (1996) Climate downscaling: techniques and application. *Clim Res* **7**, 85-95

HEWITSON BC and CRANE RG (2002) Self-organizing maps: applications to synoptic climatology, *Clim. Res*., ***22***, 13-26

HEWITSON BC and CRANE RG (2006) Consensus between GCM climate change projections with empirical downscaling: Precipitation downscaling over South Africa. *Int J Climatol* **26**, 1315-1337

HEWITSON BC, DARON J, CRANE R, ZERMOGLIO M and JACK C (2014) Interrogating empirical-statistical downscaling. *Climate Change*, **122**, 539-554.

HUFFMAN GJ, ADLER RF, RUDOLF B and SCHNEIDER U (1995) Global precipitation estimates based on a technique for combining satellite-based estimates, rain gauge analysis, and NWP model precipitation information. *J. Clim.*, **8**, 1284-1295.

HUFFMAN GJ, ADLER RF, ARKIN P, CHANG A, FERRARO R, GRUBER A, JANOWIAK J, McNAB A, RUDOLF B and SCHNEIDER U (1997) The global precipitation climatology project (GPCP) combined precipitation dataset. *Bull. Am. Meteorol. Soc*., **78**, 5-20

HUTCHINSON P (1992) The Southern Oscillation and prediction of 'Der' season rainfall in Somalia. *J. Clim.*, **5**, 525-531

IHARA, C, KUSHNIR Y and CANE MA (2008) Warming trend of the Indian Ocean SST and Indian Ocean Dipole from 1880 to 2004, *J. Clim*., 21, 2035-2046

IPCC (2013) Climate Change 2013: The Physical Science Basis. Contribution of Working Group I to the Fifth Assessment Report of the Intergovernmental Panel on Climate Change [STOCKER TF, QIN D, PLATTNER G-K, TIGNOR M, ALLEN SK, BOSCHUNG J, NAUELS A, XIA Y. BEX V and MIDGLEY PM (eds.)]. Cambridge University Press, Cambridge, United Kingdom and New York, NY, USA, 1535 pp.

JIN F.-F, KIM ST and BEJARANO L (2006) A coupled-stability index for ENSO. *Geophys. Res. Lett*, 33, L23708, doi: 10.1029/2006/GL027221

JONES CG, GIORGI F and ASRAR G (2011) The Coordinated Regional Downscaling Experiment: CORDEX; An international downscaling link to CMIP5. CLIVAR Exchanges, International CLIVAR Project Office, No. 56, Southampton, United Kingdom, 34-40.

JURY MR (1992) A climatic dipole governing the interannual variability of convection over the SW Indian Ocean and SE Africa region. *Trends in Geophysical Research*, **1**, 165-172

KALOGNOMOU EA, LENNARD C, SHONGWE M, PINTO 9, FAVRE A, KENT M, … and BUCHNER M (2013) A diagnostic evaluation of precipitation in CORDEX Models over Southern Africa. *J. Clim.*, **26**, 9477-9506.

KANAMITSU M, EBISUZAKI W, WOOLLEN J, YANG S-K, JHNILO JJ, FIORINO M and POTTER GL (2002) NCEP-DOE AMIP-II reanalysis (R-2). *Bull. Am. Meteorol. Soc*., **83**, 1631-1643

KIDSON JW (1988) Interannual variations in the Southern Hemisphere circulation, *J. Clim*., **1**, 1177-1198.

KNUTTI R (2010) The end of model democracy? *Climatic Change*, ***102*****(3-4)**, 395-404. doi:10.1007/s10584-010-9800-2

KNUTTI R, ABRAMOWITZ G, COLLINS M, EYRING V, GLECKLER PJ, HEWITSON B and MEARNS L (2010) *Good practice guidance paper on assessing and combining multi model climate projections. Meeting Report of the Intergovernmental Panel on Climate Change Expert Meeting on Assessing and Combining Multi-Model Climate Projections.*

KOHONEN T (1995) *Self Organising Maps*, 2nd Edition, Springer-Verlag, Heidelberg

LANDMAN W, ENGELBRECHT F, LANDMAN S (2010) I get all the news I need on the weather report. Pretoria: Council for Scientific and Industrial Research. Retrieved from http://hdl.handle.net/10204/6959

LATIF M and KEENLYSIDE NS (2009) El Nino/southern oscillation response to global warming. *Proc. Natl. Acad. Sci.*, USA, **106**, 20578-20583

LIN J-L (2007) The Double-ITCZ Problem in IPCC AR4 Coupled GCMs: Ocean-Atmosphere Feedback Analysis, *J. Clim*., **20**, 4497-4525.

LINDESAY JA (1988) South African rainfall, the Southern Oscillation and a southern hemisphere semi-annual cycle. *Journal of Climatology*, **8**, 17-30

LORENZ EN (1970) Climatic Change as a Mathematical Problem. *Journal of Applied Meteorology*, ***9*(3)**, 325-329. doi:10.1175/1520-0450(1970)009<0325:CCAAMP>2.0.CO;2

MACKELLER N, NEW M and JACK C (2014) Observed and modelled trends in rainfall and temperature for South Africa: 1960-2010, *submitted to South Africa Journal of Science*.

MASLIN M and AUSTIN P (2012) Uncertainty: Climate models at their limit? *Nature*, **486**, 183-184.

MASSON D and KNUTTI R (2011) Climate model genealogy. *Geophys. Res. Lett.*, ***38*(8)**, n/a–n/a. doi:10.1029/2011GL046864

MCPHADEN MJ, ZEBIAK SE and GLANTZ MH (2006) ENSO as an integrating concept in earth science. *Science*, **314**, 1739-1745

MECHOSO CR, ROBERTSON AW, BARTH N, DAVEY MK, DELECLUSE P, GENT PR, INESON S, KIRTMAN B, LATIF M, LE TREUT H, NAGAI T, NEELIN JD, PHILANDER SGH, POLCHER J, SCHOPF PS, STOCKDALE T, SUAREZ MJ, TERRAY L, THUAL and TRIBBIA JJ **(**1995) The seasonal cycle over tropical Pacific in coupled ocean-atmosphere general circulation models. *Mon. Wea. Rev*., **123**, 2825-2838

MEEHL GA and TENG H (2007) Multi-model changes in El Niño teleconnections over North America in a future warmer climate. *Clim. Dyn*., **29**,779-790, doi: 10.1007/s00382-007-0268-3.

MEEHL GA, BOAR G, COVEY C, LATIF M and STOUFFER R (2000) The Coupled Model Intercomparison Project (CMIP). *Bulletin of the American Meteorology Society*, **81**, 313-318.

MEYERS G, MCINTOSH P, PIGOT L and POOK M (2007) The years of El Niño, La Niña, and interactions with the tropical Indian Ocean. *J. Clim.*, **20**, 2872-2880

MOSS R, EDMONDS J, HIBBARD K, MANNING M, ROSE S, VAN VUUREN DP, CARTER TR, EMORI S, KAINUMA M, KRAM T, MEEHL GA, MITCHELL JFB, NAKICENOVIC N, RIAHI K, SMITH SJ, STOUFFER RJ, THOMSON AM, WEYANT JP and WILBANKS TJ (2010) A new approach to scenario development for the IPCC Fifth Assessment Report. *Nature*, ***463***, doi:10.1038/nature08823.

NIKULIN G JONES C, GIORGI F, ASRAR G, BUCHNER M, CEREZO-MOTA and SUSHAMA L (2012) Precipitation Climatology in an Ensemble of CORDEX-Africa Regional Climate Simulations. *J. Clim.*, **25**, 6057-6078.

PANITZ HJ, DOSIO A, BUCHNER M, LUTHI D and KEULER K (2013) COSMO-CLM (CCLM) climate simulations over Africa domain: analysis of the ERA-Interim driven simulations at 0.44 and 0.22 resolution. *Clim. Dyn*. DOI 10.1007/s00382-013-1834-5

PHILIPPON N, ROUAULT M, RICHARD Y and FAVRE A (2011) The influence of ENSO on winter rainfall in South Africa. *Int. J. Climatol.*, doi: 10.1002/joc.3403

PIERCE DW, BARNETT TP, SANTER BD and GLECKLER PJ (2009) Selecting global climate models for regional climate change studies. Proceedings of the National Academy of Sciences of the United States of America, 106(21), 8441-6. doi:10.1073/pnas.0900094106

RAYNER NA, PARKER DE, HORTON EB, FOLLAND CK, ALEXANDER LV, ROWELL DP, KENT EC and KAPLAN A (2003) Global analyses of sea surface temperature, sea ice, and night marine air temperature since the late nineteenth century. *J. Geophys. Res. (Atmos)*, **108** (D14), 4407, doi: 10.1029/2002JD002670

REASON CJC. And MULENGA HM (1999) Relationship between South African rainfall and SST anomalies in the southwest Indian Ocean. *Int. J. Climatol.*, **19**, 1652-1673.

REASON CJC (2001) Subtropical Indian Ocean SST dipole events and southern African rainfall. *Geophys. Res. Lett*., **28**, 2225-2227

REASON CJC (2002) Sensitivity of the Southern African circulation to dipole Sea-Surface Temperature patterns in the South Indian Ocean. *Int. J. Climatol.*, **22**, 377-393

REASON CJC and ROUAULT M (2005) Links between the Antarctic Oscillation and winter rainfall over western South Africa, Geophy. Res. Lett., 32, L07750, doi: 10.1029/2005GL022419

REASON CJC, ALLAN RJ, LINDESAY JA and ANSELL TJ (2000) ENSO and climatic signals across the Indian Ocean Basin in the global context: part I, interannual composite patterns. *Int. J. Climatol.*, **20**, 1285-1327

REYNOLDS RW, RAYNER NA, SMITH TM, STOKES DC and WANG W (2002) An improved in situ and satellite SST analysis for climate. *J. Clim.*, **15**, 1609-1625

RIAL JA, PIELKE Sr RA, BENISTON M, CLAUSSEN M, CANADELL J, COX P, … and SALAS JD (2004) Nonlinearities, Feedbacks and Critical Thresholds within the Earth's Climate System. *Climatic Change*, ***65*(1/2)**, 11-38. doi:10.1023/B:CLIM.0000037493.89489.3f

ROBERTS MJ, CLAYTON A, DEMORY M-E, DONNERS J, VIDALE PL, NORTON N, SHAFFREY L, STEVENS DP, STEVENS I, WOOD RA and SLINGO J (2009) Impact of resolution on the tropical Pacific circulation in a matrix of coupled models. *J. Clim*, **22**, 2541-2556.

ROCHA A and SIMMONDS I (1997) Interannual variability of south-eastern African summer rainfall. Part 1: Relationships with air-sea interaction processes. *Int. J. Climatol.*, **17**, 235-265

ROCKEL BA, WILL, A and HENSE A (2008) The regional climate model COSMO-CLM (CCLM). *Meteor. Z.* **17**, 347-248.

ROPELEWSKI CF and HALPERT MS (1987) Global and regional precipitation patterns associated with El Niño/southern oscillation. *Mon. Wea. Rev.*, **115**, 1606-1626.

ROUAULT M, FLORENCHIE P, FAUCHEREAU N and REASON CJC (2003) South east tropical Atlantic warm events and southern African rainfall. *Geophys. Res. Lett.*, **30**, 8009-8013

SAJI NH, and YAMAGATA T (2003) Structure of SST and surface wind variability during Indian Ocean Dipole mode events: COADS observations, *J. Clim.*, **16**, 2735-2751

SAJI NH, GOSWAMI BN, VINAYACHANDRAN PN and YAMAGATA T (1999) A dipole in the tropical Indian Ocean, *Nature*, **401**, 360-363

SAMUELSSON PS JONES CG, WILLEN U, ULLIERSTIG A, GOLLVIK S, HANSSON U, … and WYSER K (2011) The Rossby Centre regional climate model RCA3: Model description and performance. *Tellus*, **63A**, 4-23.

SINGLETON AT and REASON CJC (2006) Numerical Simulations of a Severe Rainfall event over the Eastern Cape coast of South Africa: Sensitivity to sea surface temperature and topography. *Tellus A*, **58**, 355-367.

SINGLETON AT and REASON CJC (2007) A numerical model study of an intense cut-off low pressure system over South Africa. *Mon. Wea. Rev.*, **135**, 1128-1150.

SMITH RL, TEBALDI C, NYCHKA D and MEARNS LO (2009) Bayesian Modeling of Uncertainty in Ensembles of Climate Models. *Journal of the American Statistical Association*, ***104*(485)**, 97-116. doi:10.1198/jasa.2009.0007

STAINFORTH DA, ALLEN MR, TREDGER ER and SMITH LA (2007) Confidence, uncertainty and decision-support relevance in climate predictions. *Philosophical Transactions. Series A, Mathematical, Physical, and Engineering Sciences*, ***365*(1857)**, 2145-61. doi:10.1098/rsta.2007.2074

STEVENSON SL (2012) Significant changes to ENSO strength and impacts in the twenty-first century: Results from CMIP5. *Geophys. Res. Lett*., **39**, doi:10.1029.2012GL052759

SAREWITZ D (2011) Does climate change knowledge really matter? *WIRES Climate Change*, **2**, 475-481

TAYLOR KE, STOUFFER RJ and MEEHL GA (2012) Overview of CMIP5 and the experiment design. *Bull. Am. Meteor. Soc.*, **93**, 485-498

TEBALDI C and KNUTTI R (2007) The use of the multi-model ensemble in probabilistic climate projections. *Philosophical Transactions. Series A, Mathematical, Physical, and Engineering Sciences*, ***365*(1857)**, 2053-75. doi:10.1098/rsta.2007.2076

THOMPSON DWJ and WALLACE JM (2000) Annular modes in the extratropical circulation. part I: Month-to-month variability, *J. Clim*., **13**, 1000-1016.

TRENBERTH KE (1997) The definition of El Niño. *Bull. Am. Meteor. Soc.,* **78**, 2771-2777.

TRENBERT, KE, BRANSTATOR GW, KAROLY D, KUMAR A, LAU N-C and ROPELEWSK C (1998) Progress during TOGA in understanding and modelling global teleconnections associated with tropical sea surface temperatures, *J.Geophys. Res*., **103**, 14,291-14,324

VAN OLDENBORGH GJ, PHILIP SY and COLLINS M (2005) El Niño in a changing climate: a multi-model study. *Ocean Sci.,* **1**, 81-95

VIGAUD N, RICHARD Y, ROUAULT M, and FAUCHEREAU N (2009) Moisture transport between the South Atlantic Ocean and Southern Africa: relationships with summer rainfall and associated dynamics. *Clim. Dyn.,* **32**, 113-123

WANG C and PICAUT J (2004) Understanding ENSO physics: a review. *Geophys. Monogr*. AGU, **147**, 21-48

WASHINGTON R and PRESTON A (2006) Extreme wet years over Southern Africa: role of Indian Ocean Sea Surface Temperatures. *J. Geophys. Res.,* **111**, doi: 10.1029/2005JD00672415

WEARE BC (2012) El Niño teleconnections in CMIP5 models. *Clim Dyn*. DOI 10.1007/s00382-012-1537-3.

WEBSTER PJ, MAGAÑA V, PALMER TN, SHUKLA J, TOMAS RA, YANAI M, and YASUNARA T (1998) Monsoons: processes, predictability and the prospects for prediction, *J. Geophys. Res.*, **103**, 14451-14510

WELLER E and CAI W (2013) Realism of the Indian Ocean Dipole in CMIP5 models: the implication for climate projections. *J. Climate*, **26**, 6649-6659.

WILBY RL and WIGLEY TM (1997) Downscaling general circulation models output: a review of methods and limitations. *Progress in Physical Geography*, **21.4**, 530-548.

WILBY RL, HAY LE, GUTOWSKI WJ ARRITT RW, TAKLE ES, PAN Z, LEAVESLEY GH and CLARK MP (2000) Hydrological responses to dynamically and statistically downscaled climate model output. *Geophys. Res. Lett.*, **27**, 1199-1202. doi:10.1029/1999GL006078

WILBY RL, WIGLEY TM, CONWAY D, JONES PD, HEWITSON BC, MAIN J and WILKS DS (1998) Statistical downscaling of general circulation model output: a comparison of methods. *Water Resour. Res.*, **34**, 2995-3008. doi:10.1029/98WR02577

YAMAGATA T, BEHERA SK, RAO SA, GUAN Z, ASHOK K and SAJI NH (2003) Comments on "Dipoles, Temperature Gradient, and Tropical Climate Anomalies", *Bull. Am. Meteorol. Soc*., **84**, 1418-1422

YU J-Y and KIM ST (2010) Identification of Central-Pacific and Eastern- Pacific types of ENSO in CMIP3 models. *Geophys. Res. Lett*., **37**, L15705

APPENDIX A

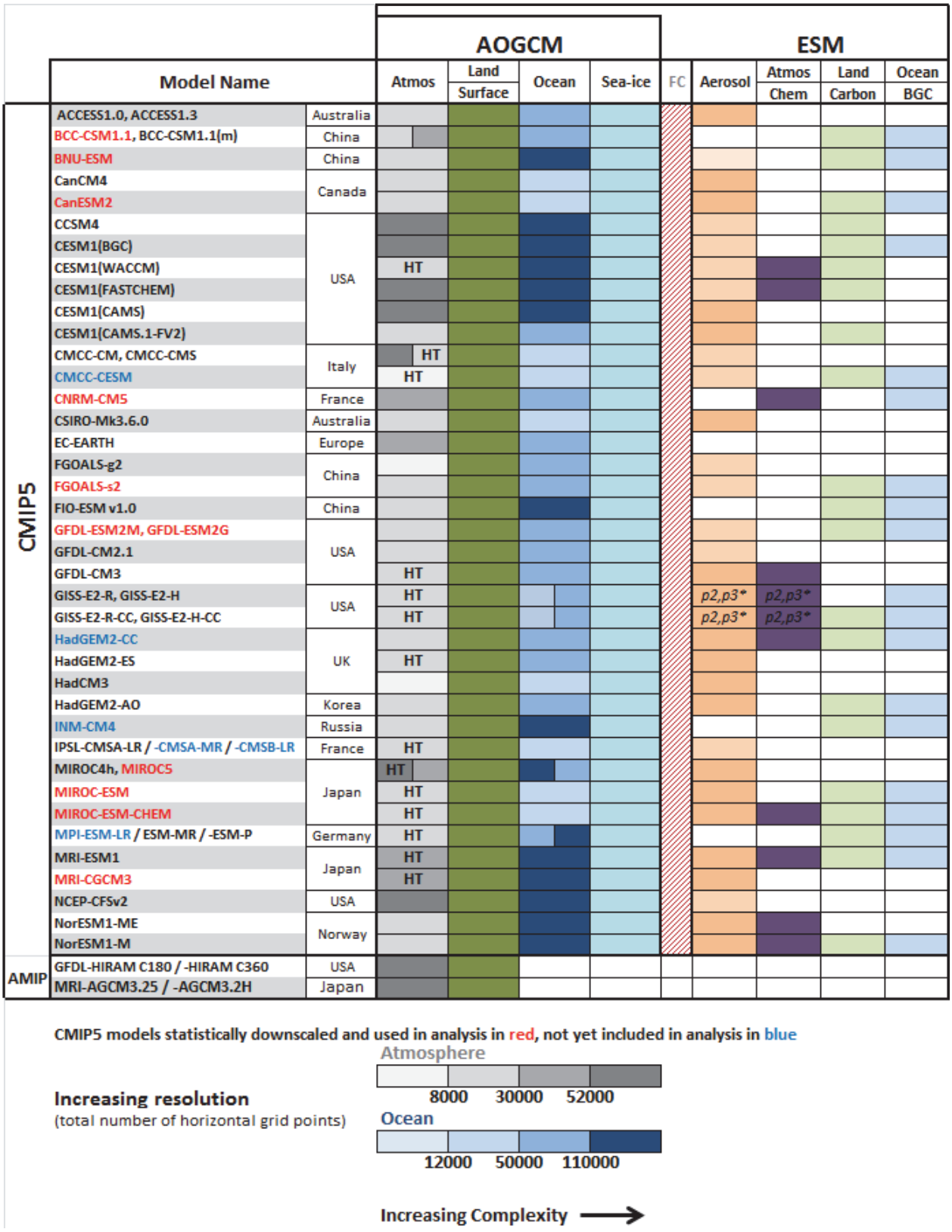
AOGCM
ESM
Model Name
Atmos
Land Surface
Ocean
Sea-ice
FC
Aerosol
Atmos Chem
Land Carbon
Ocean BGC
CMIP5
AMIP
ACCESS1.0, ACCESS1.3 Australia
BCC-CSM1.1, BCC-CSM1.1(m) China
BNU-ESM China
CanCM4 Canada
CanESM2
CCSM4 USA
CESM1(BGC)
CESM1(WACCM) HT
CESM1(FASTCHEM)
CESM1(CAMS)
CESM1(CAMS.1-FV2)
CMCC-CM, CMCC-CMS Italy HT
CMCC-CESM HT
CNRM-CM5 France
CSIRO-Mk3.6.0 Australia
EC-EARTH Europe
FGOALS-g2 China
FGOALS-s2
FIO-ESM v1.0 China
GFDL-ESM2M, GFDL-ESM2G USA
GFDL-CM2.1
GFDL-CM3 HT
GISS-E2-R, GISS-E2-H USA HT p2,p3* p2,p3*
GISS-E2-R-CC, GISS-E2-H-CC HT p2,p3* p2,p3*
HadGEM2-CC UK
HadGEM2-ES HT
HadCM3
HadGEM2-AO Korea
INM-CM4 Russia
IPSL-CMSA-LR / -CMSA-MR / -CMSB-LR France HT
MIROC4h, MIROC5 Japan HT
MIROC-ESM HT
MIROC-ESM-CHEM HT
MPI-ESM-LR / ESM-MR / -ESM-P Germany HT
MRI-ESM1 Japan HT
MRI-CGCM3 HT
NCEP-CFSv2 USA
NorESM1-ME Norway
NorESM1-M
GFDL-HIRAM C180 / -HIRAM C360 USA
MRI-AGCM3.25 / -AGCM3.2H Japan
CMIP5 models statistically downscaled and used in analysis in red, not yet included in analysis in blue
Increasing resolution
(total number of horizontal grid points)
Atmosphere
8000 30000 52000
Ocean
12000 50000 110000
Increasing Complexity

Table A3.1 (opposite page) | Main features of the Atmosphere-Ocean General Circulation Models (AOGCMs) and Earth System Models (ESMs) participating in the Coupled Model Intercomparison Project Phase 5 (CMIP5). Adapted from *Table 9* in IPCC (2013). Information also includes components and resolution of the atmosphere and the ocean models. The models used in this report are highlighted in red text. *HT* stands for High-Top atmosphere, which has a fully resolved stratosphere with a model top above the stratopause. *AMIP* stands for models with atmosphere and land surface only, using observed sea surface temperature and sea ice extent. A component is coloured when it includes at least a physically based prognostic equation and at least a two-way coupling with another component, allowing climate feedbacks. For *aerosols*, lighter shading means 'semi-interactive' and darker shading means 'fully interactive'. The resolution of the land surface usually follows that of the atmosphere, and the resolution of the sea ice follows that of the ocean.

APPENDIX B

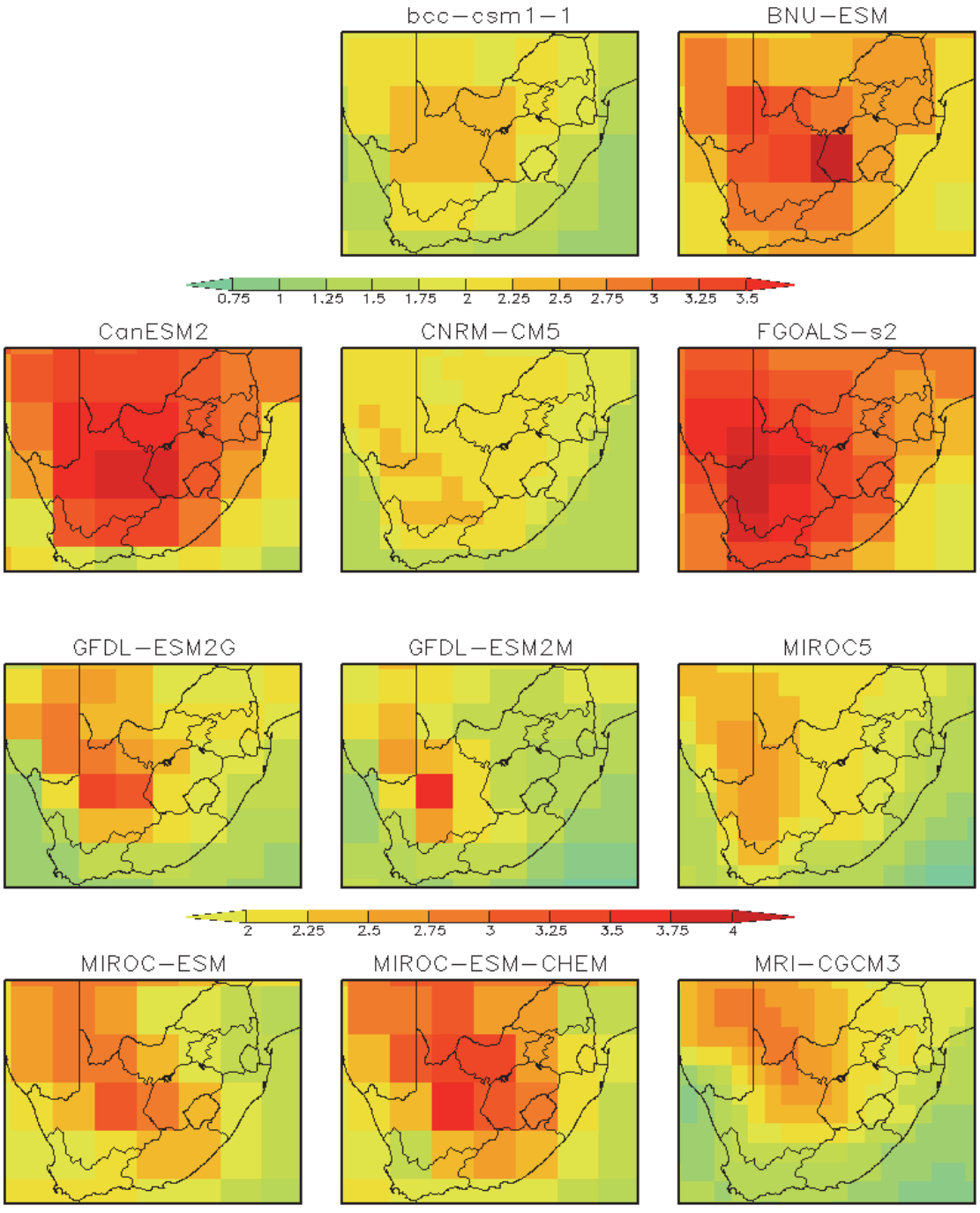

Figure B5.1 | *Future anomalies for summer (DJF) daily minimum temperature (°C) for the mid-21st century (2041-2070 – 1976-2005) under the RCP8.5 emission scenario for 11 raw CMIP5 GCMs.*

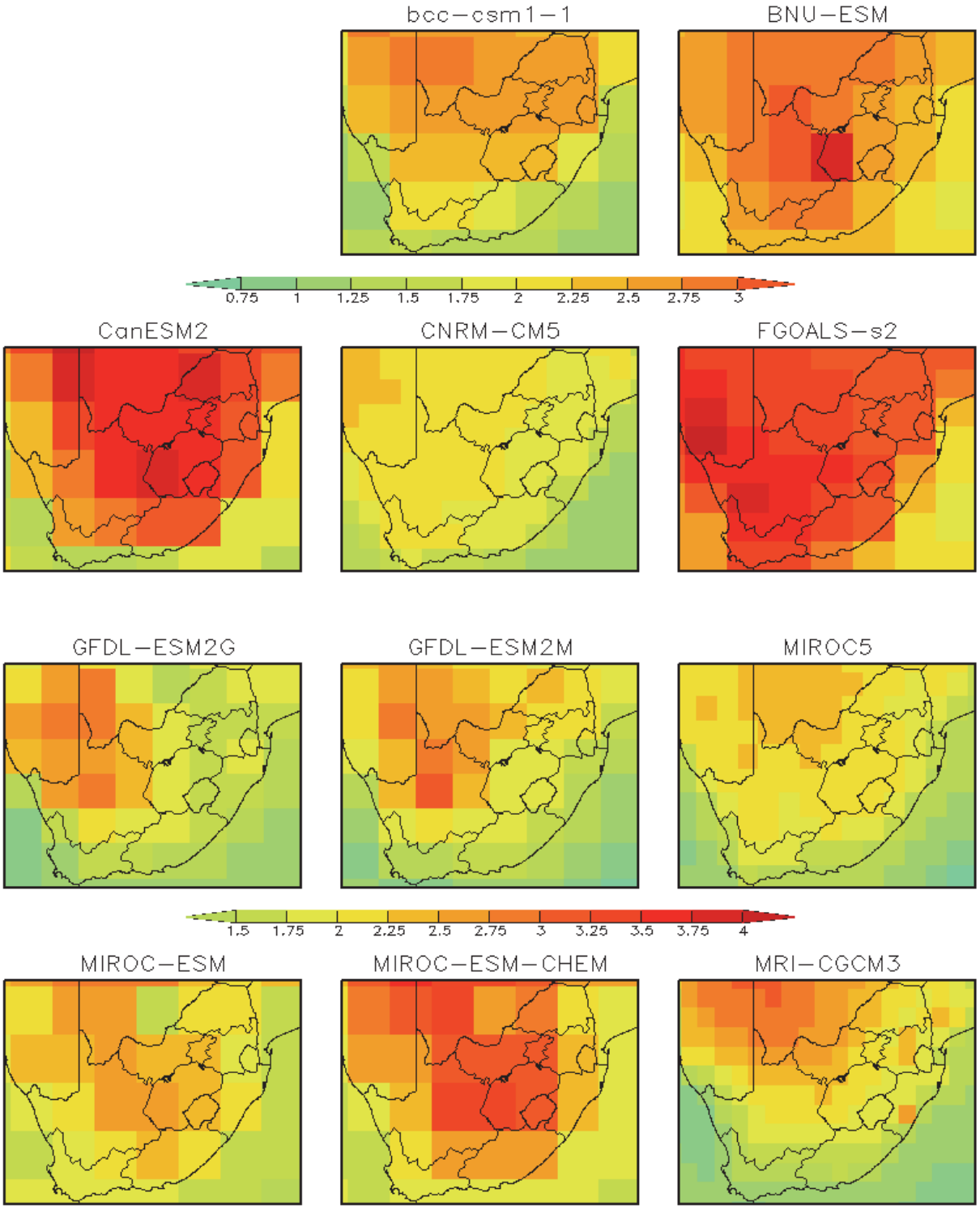

Figure B5.2 | *Future anomalies for autumn (MAM) daily minimum temperature (°C) for the mid-21st century (2041-2070 – 1976-2005) under the RCP8.5 emission scenario for 11 raw CMIP5 GCMs.*

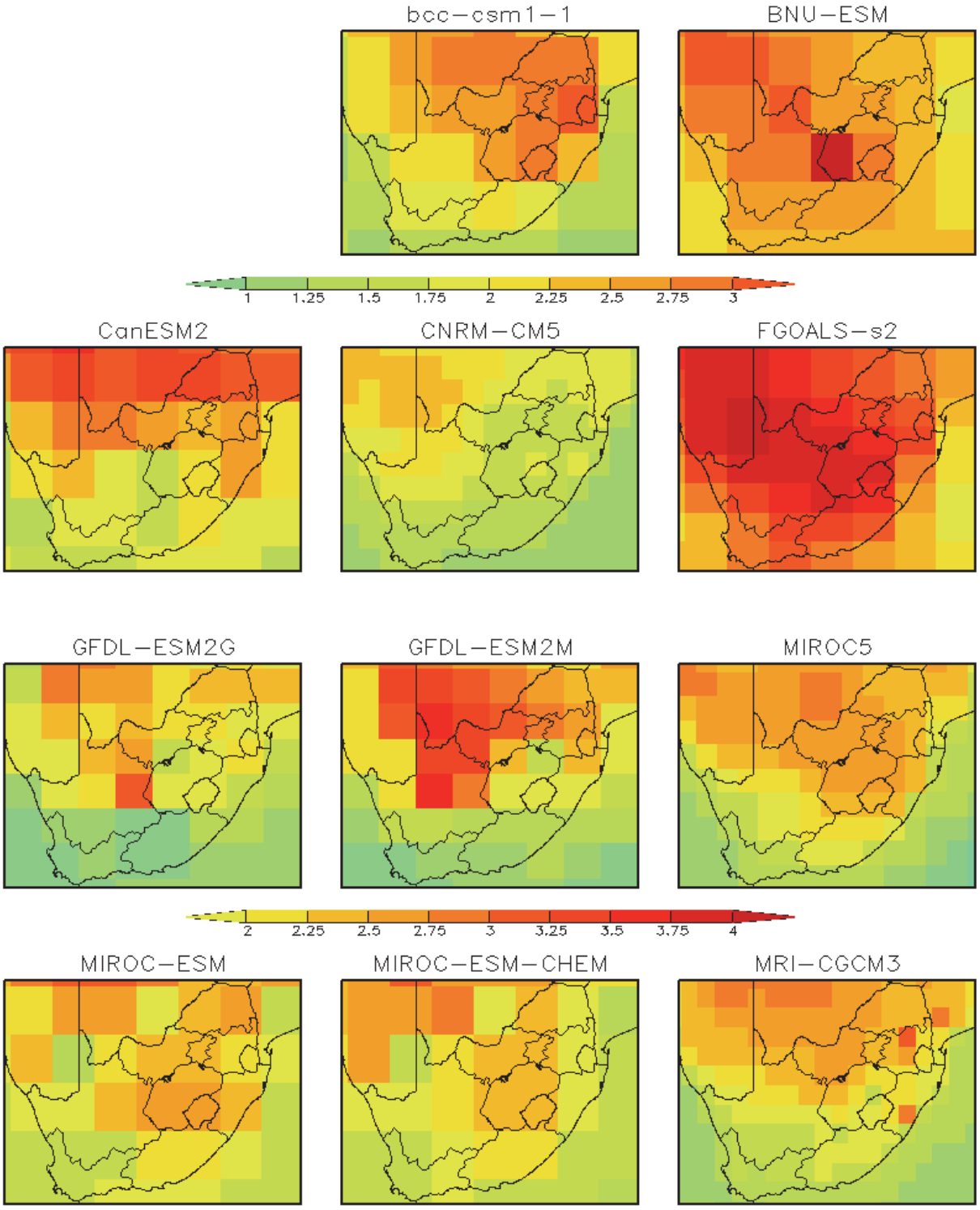

Figure B5.3 | *Future anomalies for winter (JJA) daily minimum temperature (°C) for the mid-21st century (2041-2070 – 1976-2005) under the RCP8.5 emission scenario for 11 raw CMIP5 GCMs.*

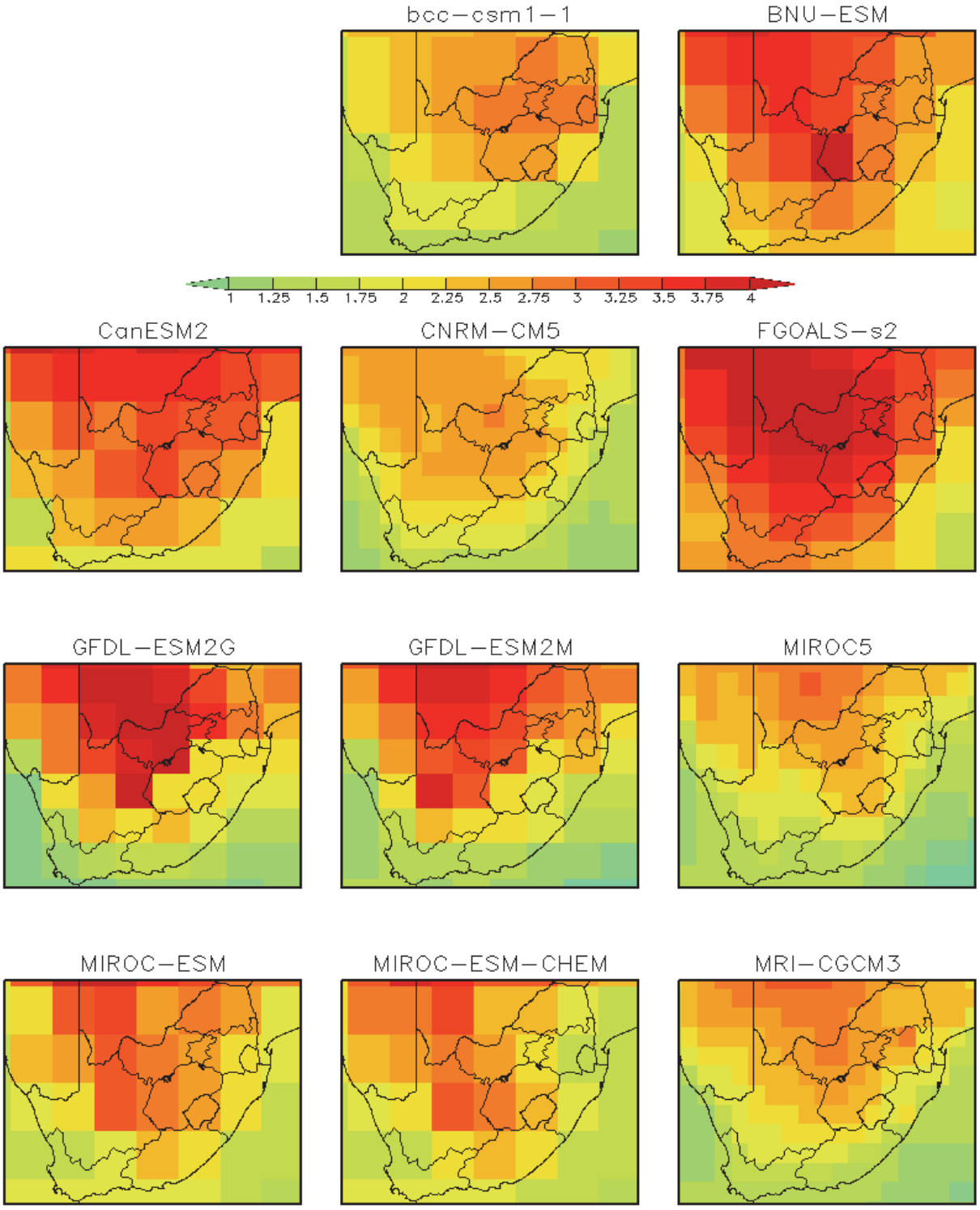

Figure B5.4 | *Future anomalies for spring (SON) daily minimum temperature (°C) for the mid-21st century (2041-2070 – 1976-2005) under the RCP8.5 emission scenario for 11 raw CMIP5 GCMs.*

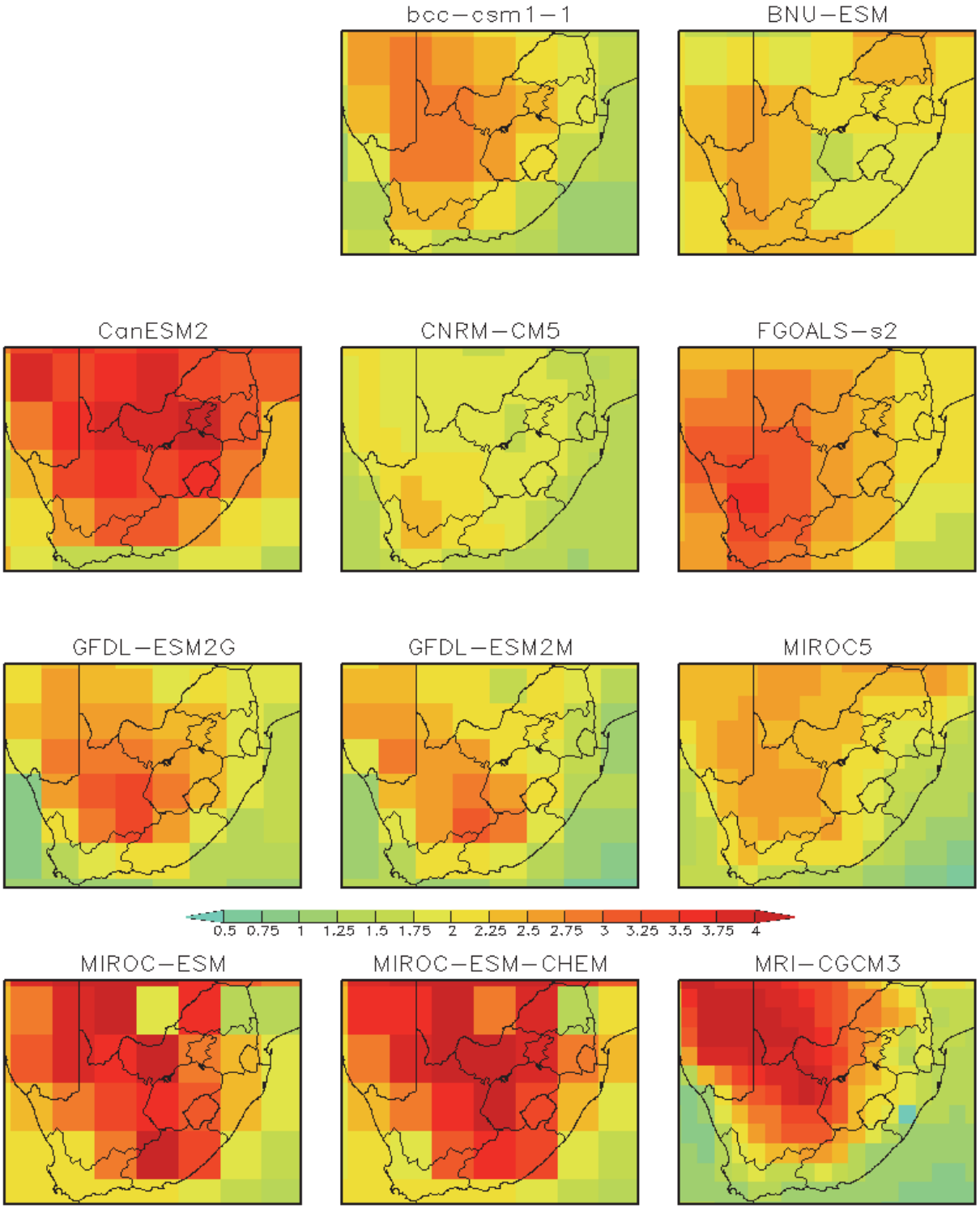

Figure B5.5 | *Future anomalies for summer (DJF) daily maximum temperature (°C) for the mid-21st century (2041-2070 – 1976-2005) under the RCP8.5 emission scenario for 11 raw CMIP5 GCMs.*

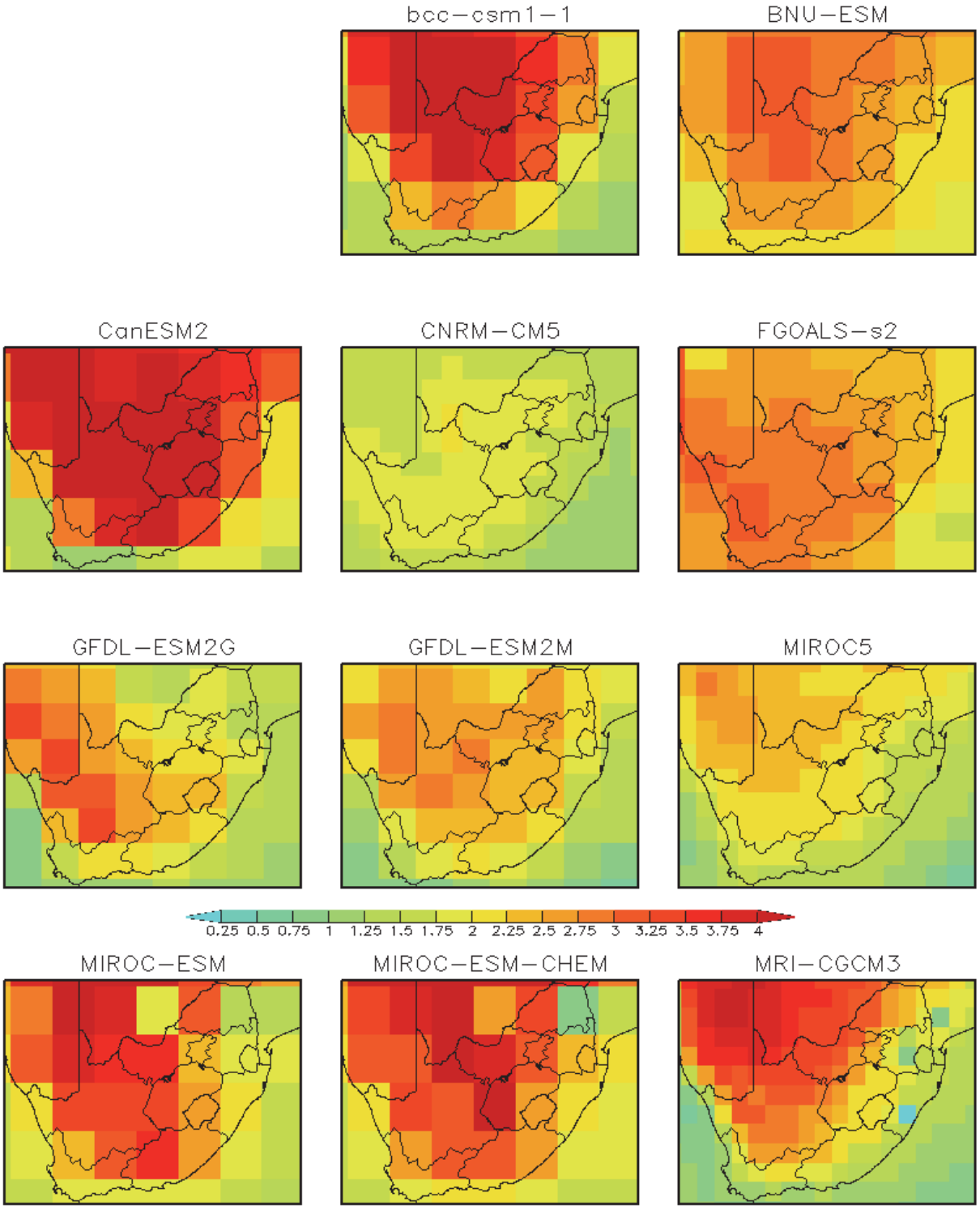

Figure B5.6 | *Future anomalies for autumn (MAM) daily maximum temperature (°C) for the mid-21st century (2041-2070 – 1976-2005) under the RCP8.5 emission scenario for 11 raw CMIP5 GCMs.*

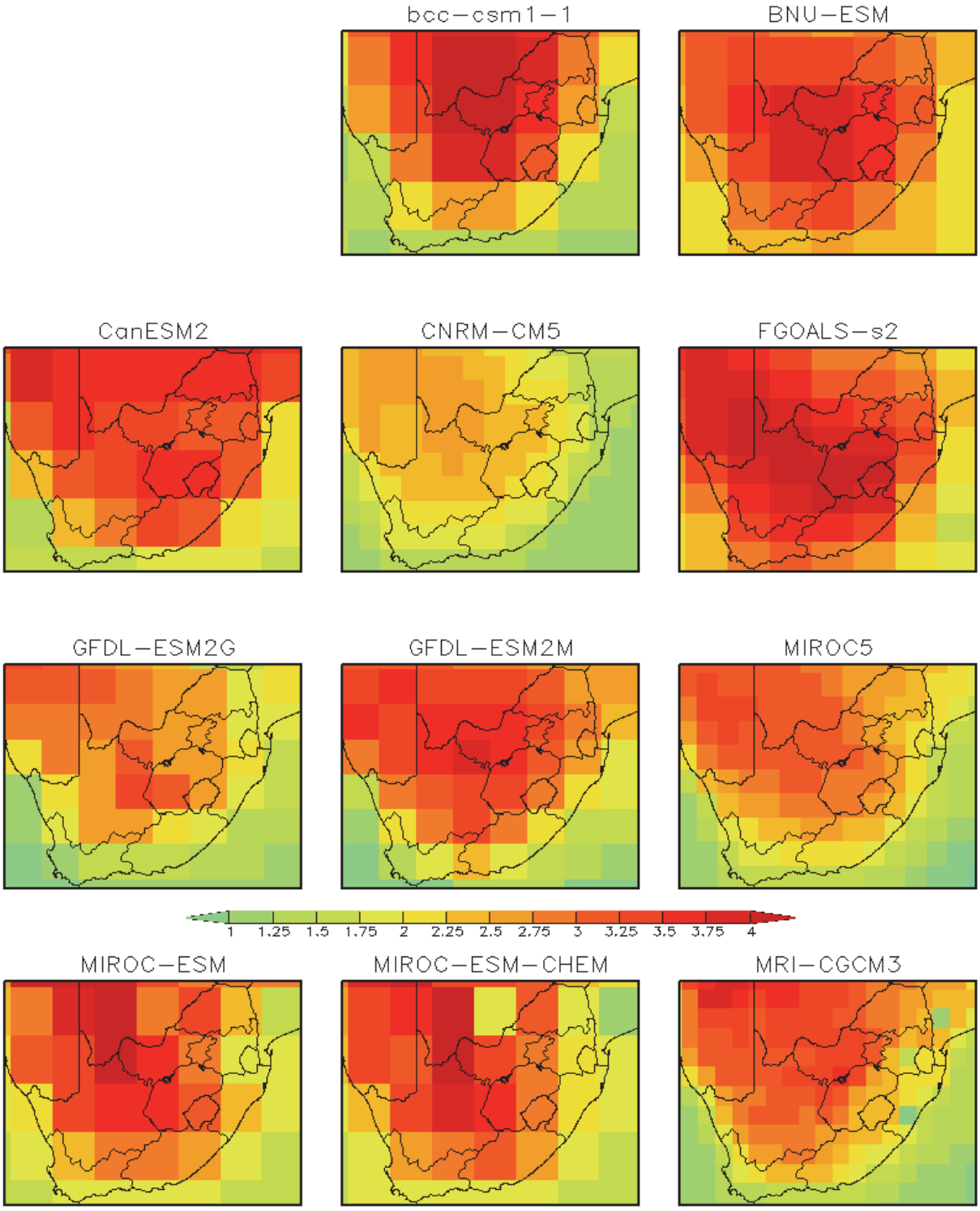

Figure B5.7 | *Future anomalies for winter (JJA) daily maximum temperature (°C) for the mid-21st century (2041-2070 – 1976-2005) under the RCP8.5 emission scenario for 11 raw CMIP5 GCMs.*

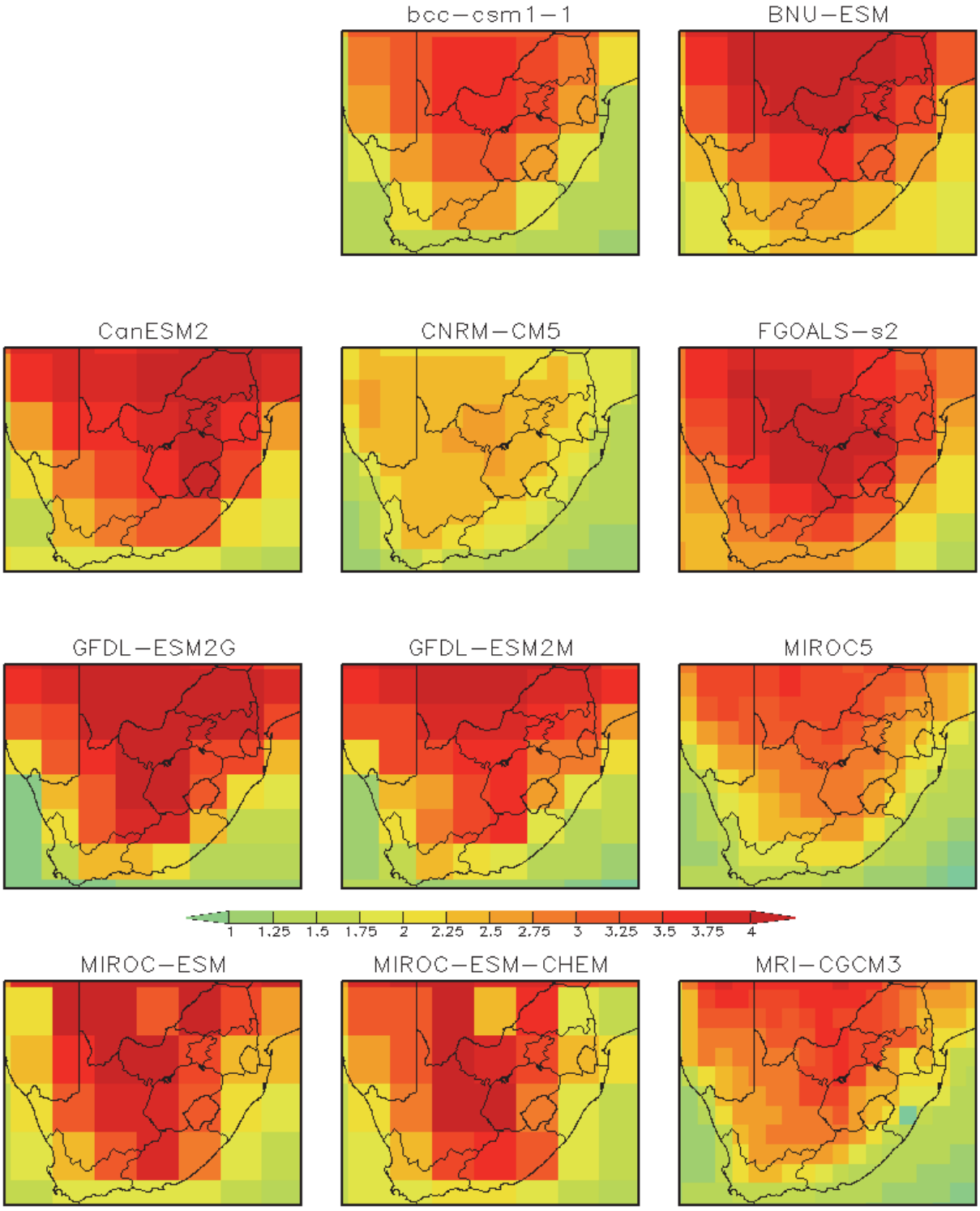

Figure B5.8 | *Future anomalies for spring (SON) daily maximum temperature (°C) for the mid-21st century (2041-2070 – 1976-2005) under the RCP8.5 emission scenario for 11 raw CMIP5 GCMs.*

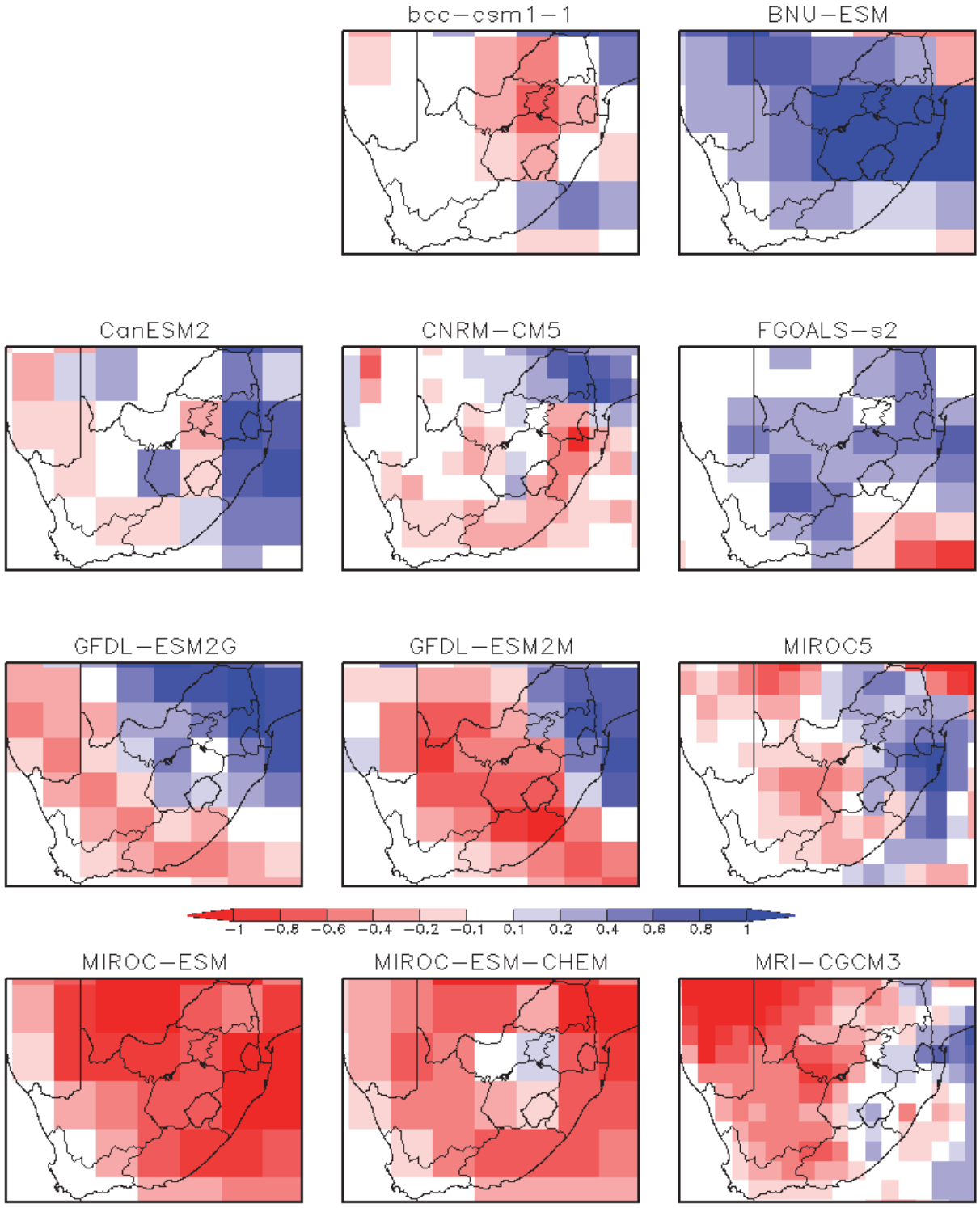

Figure B5.9 | *Future anomalies for summer (DJF) daily mean precipitation (mm/day) for the mid-21st century (2041-2070 – 1976-2005) under the RCP8.5 emission scenario for 11 raw CMIP5 GCMs.*

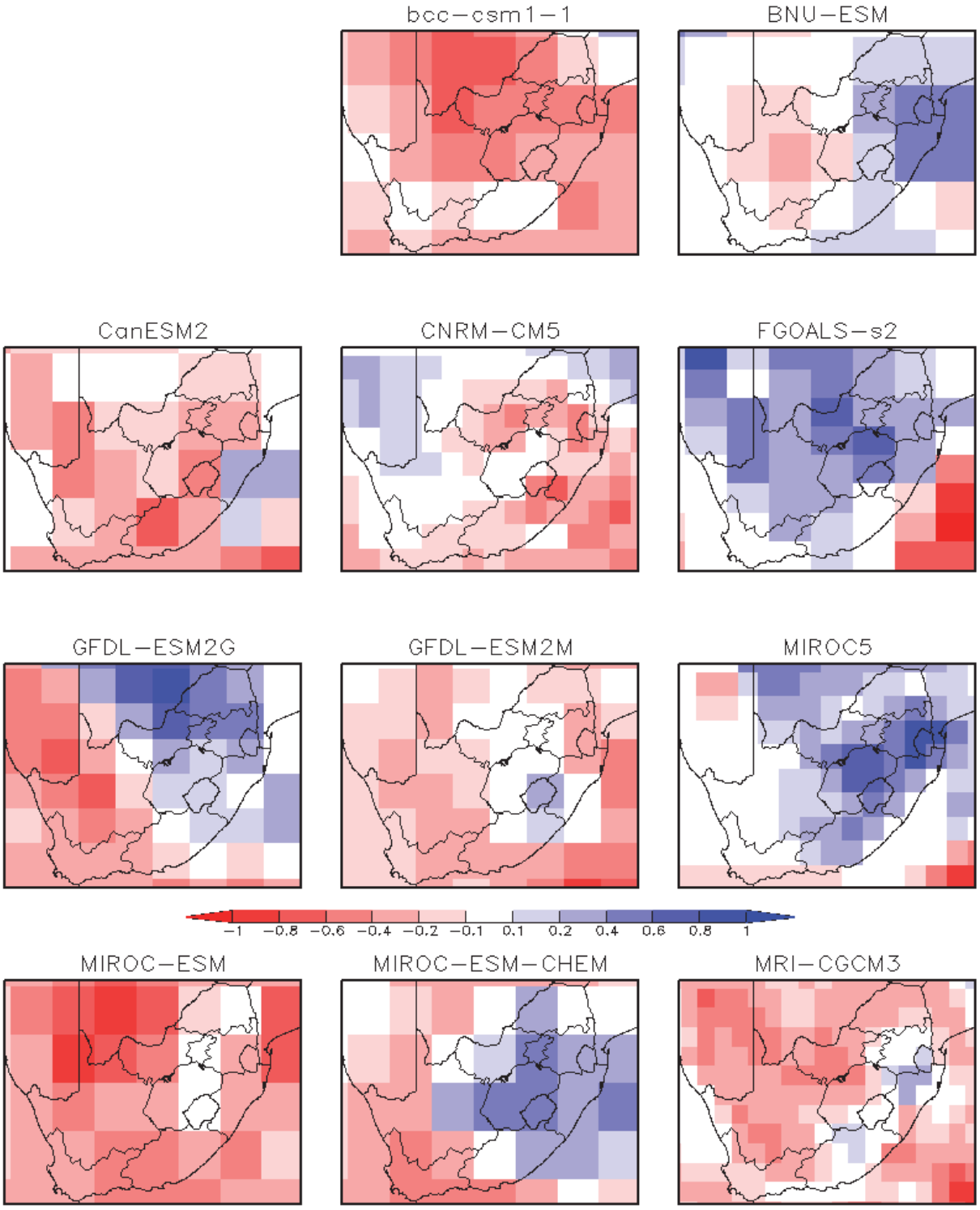

Figure B5.10 | *Future anomalies for autumn (MAM)) daily mean precipitation (mm/day) for the mid-21st century (2041-2070 – 1976-2005) under the RCP8.5 emission scenario for 11 raw CMIP5 GCMs.*

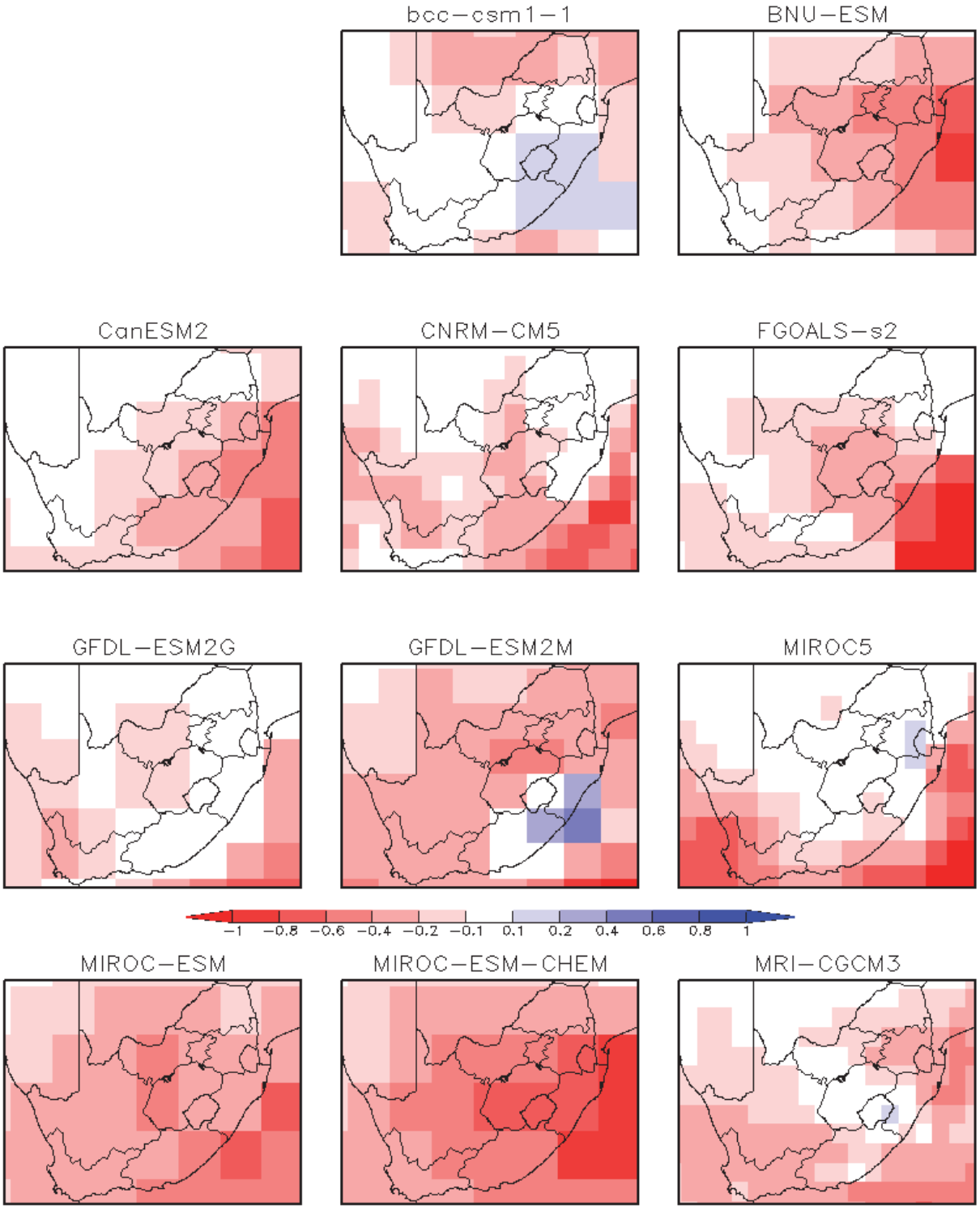

Figure B5.11 | *Future anomalies for winter (JJA) daily mean precipitation (mm/day) for the mid-21st century (2041-2070 – 1976-2005) under the RCP8.5 emission scenario for 11 raw CMIP5 GCMs.*

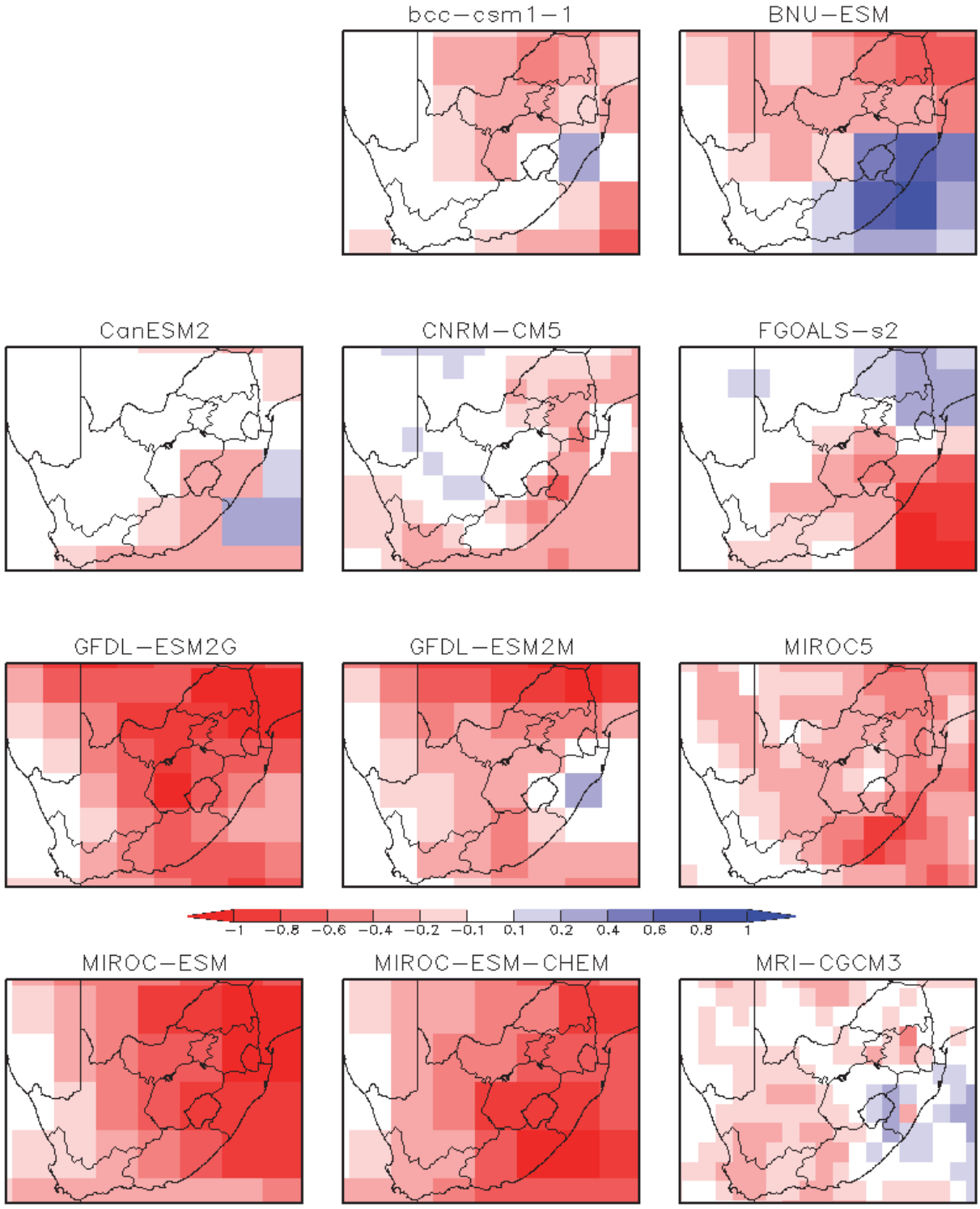

***Figure B5.12** | Future anomalies for spring (SON) daily mean precipitation (mm/day) for the mid-21st century (2041-2070 – 1976-2005) under the RCP8.5 emission scenario for 11 raw CMIP5 GCMs.*

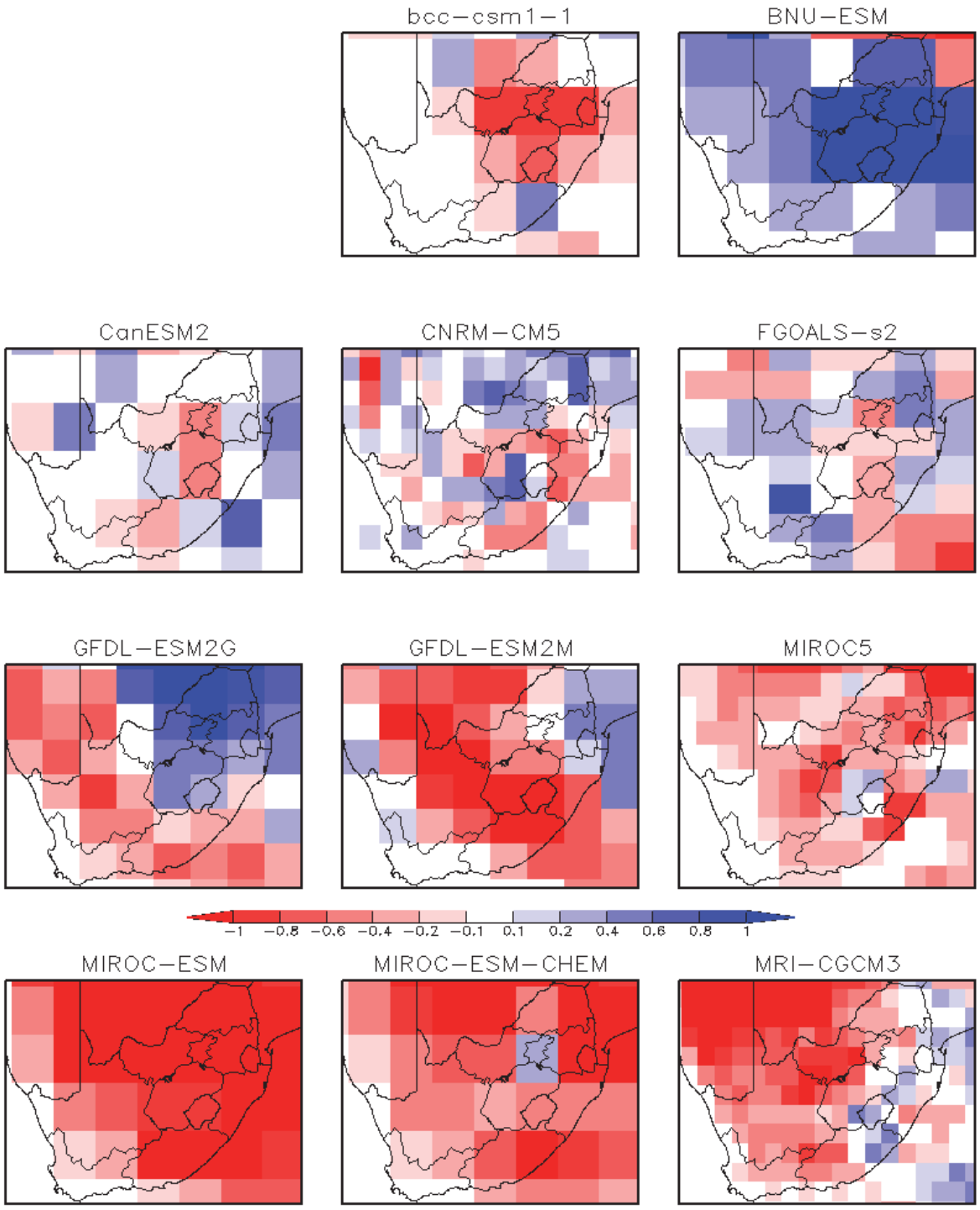

Figure B5.13 | *Future anomalies for summer (DJF) days with precipitation above 10 mm (days) for the mid-21st century (2041-2070 – 1976-2005) under the RCP8.5 emission scenario for 11 raw CMIP5 GCMs.*

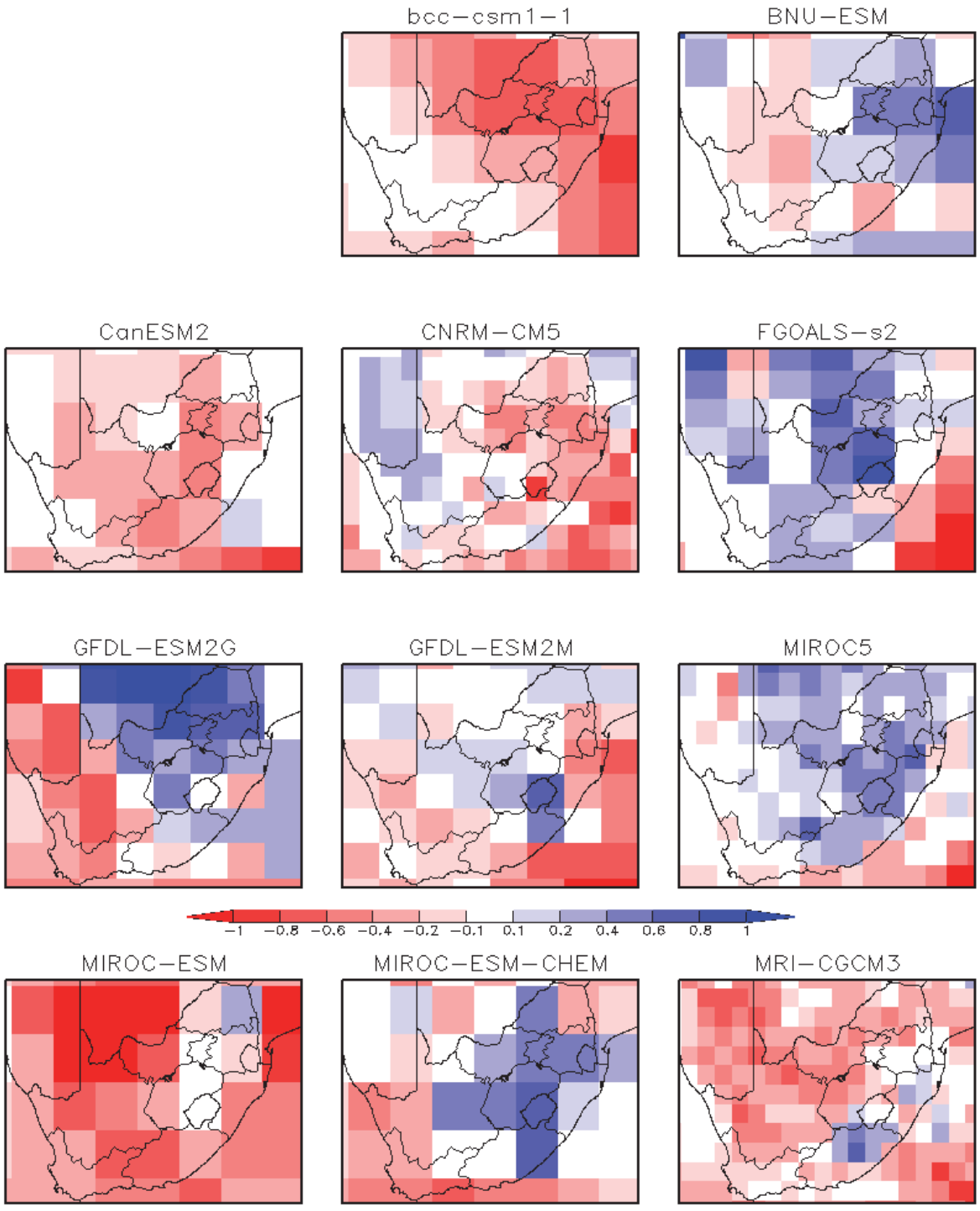

Figure B5.14 | *Future anomalies for autumn (MAM) days with precipitation above 10 mm (days) for the mid-21st century (2041-2070 – 1976-2005) under the RCP8.5 emission scenario for 11 raw CMIP5 GCMs.*

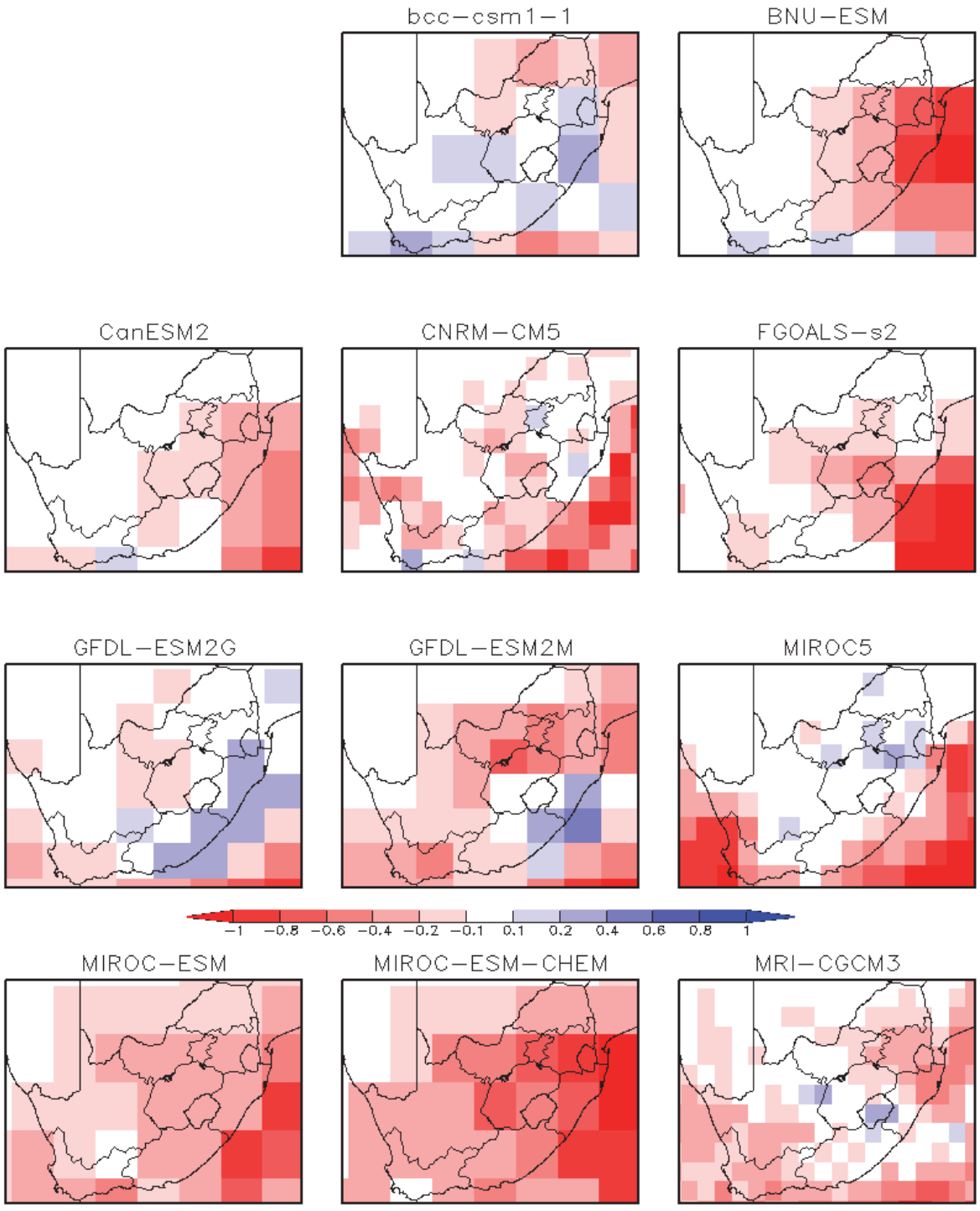

Figure B5.15 | *Future anomalies for winter (JJA) days with precipitation above 10 mm (days) for the mid-21st century (2041-2070 – 1976-2005) under the RCP8.5 emission scenario for 11 raw CMIP5 GCMs.*

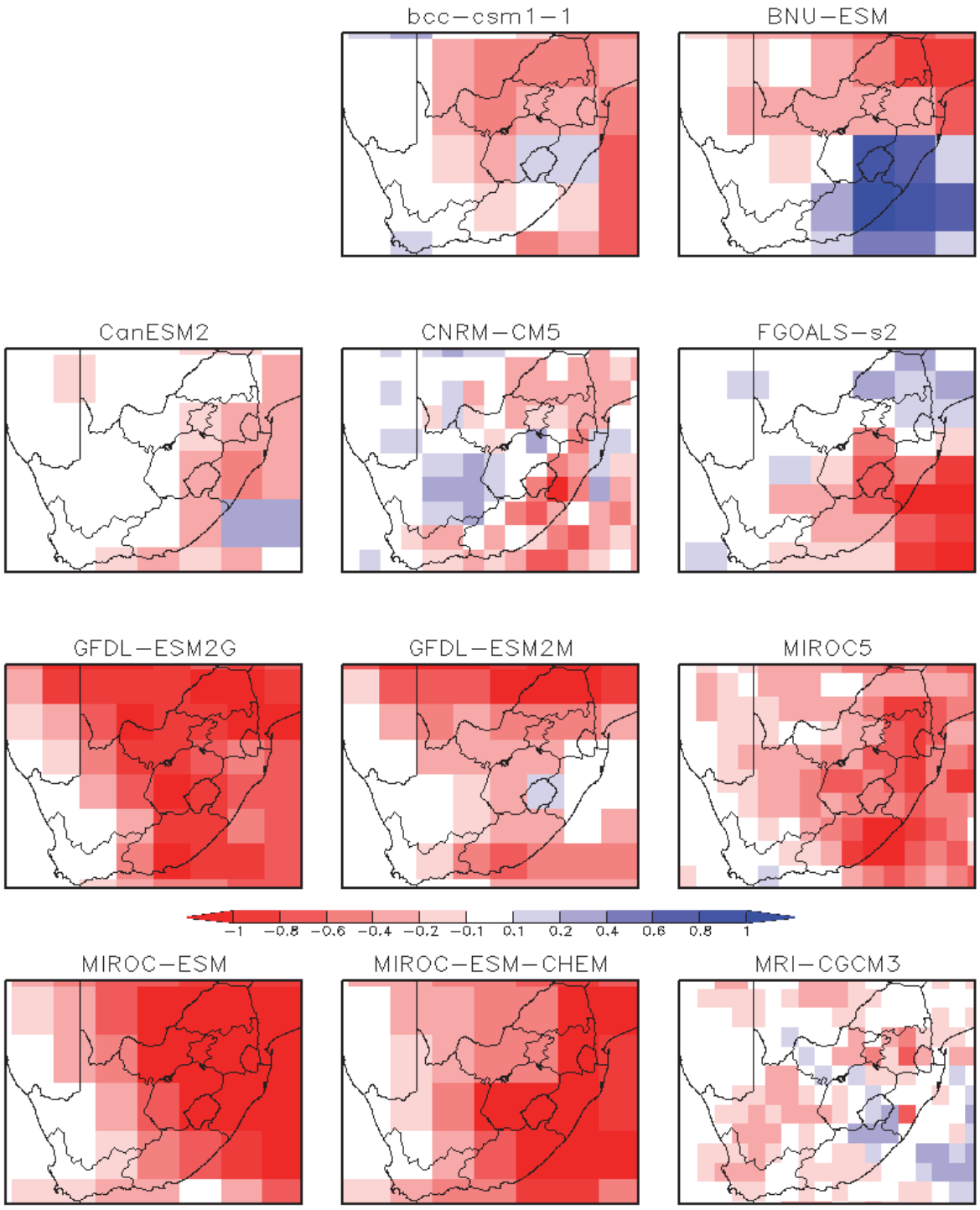

Figure B5.16 | *Future anomalies for spring (SON) days with precipitation above 10 mm (days) for the mid-21st century (2041-2070 – 1976-2005) under the RCP8.5 emission scenario for 11 raw CMIP5 GCMs.*

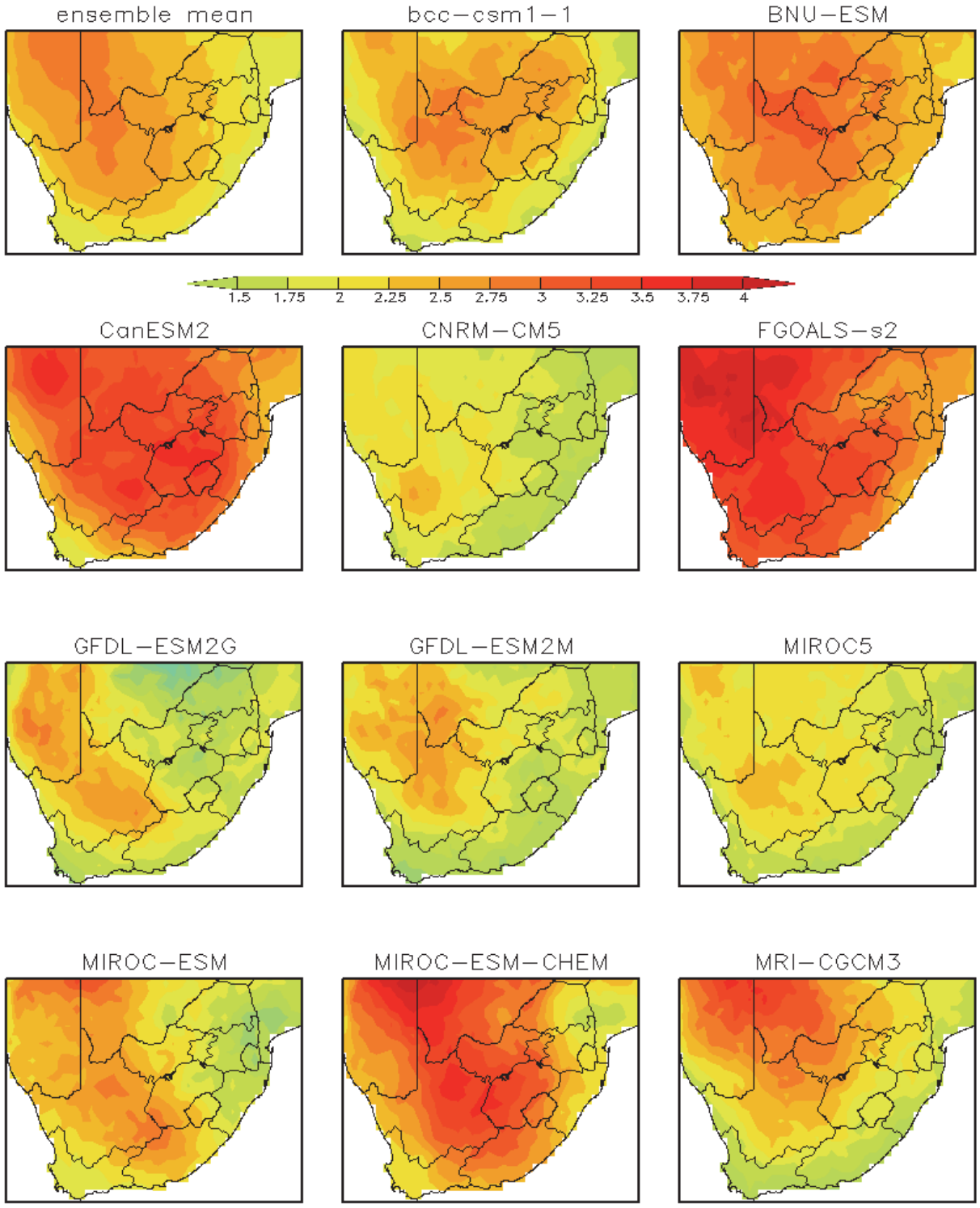

Figure B5.17 | *Future anomalies for summer(DJF) daily minimum temperature (°C) for the mid-21st century (2041-2070 – 1976-2005) under the RCP8.5 emission scenario for 11 statistically downscaled CMIP5 GCMs. Top left panel is the ensemble mean anomaly while all other plots are for individual models.*

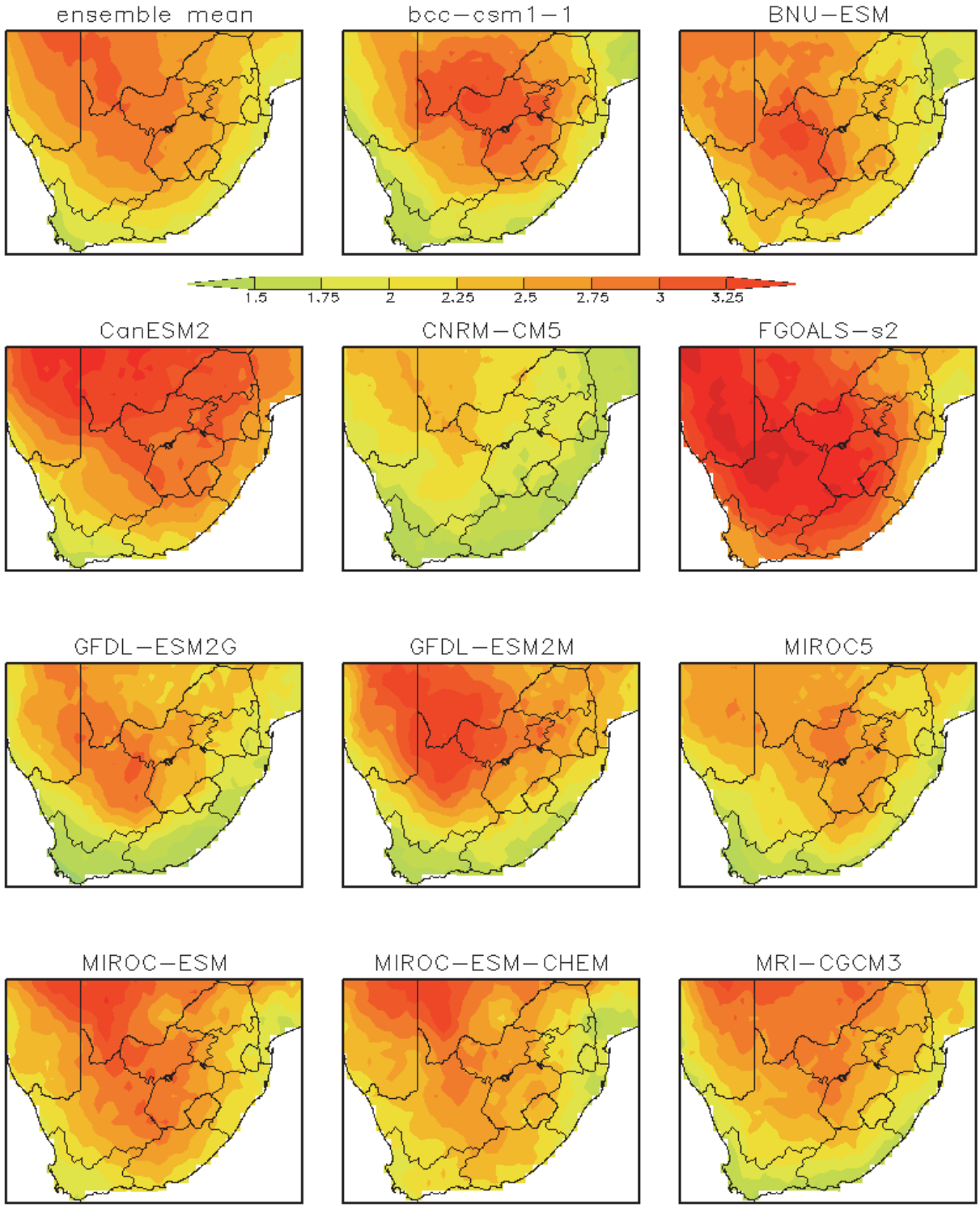

Figure B5.18 | *Future anomalies for autumn (MAM)) daily minimum temperature (°C) for the mid-21st century (2041-2070 – 1976-2005) under the RCP8.5 emission scenario for 11 statistically downscaled CMIP5 GCMs. Top left panel is the ensemble mean anomaly while all other plots are for individual models.*

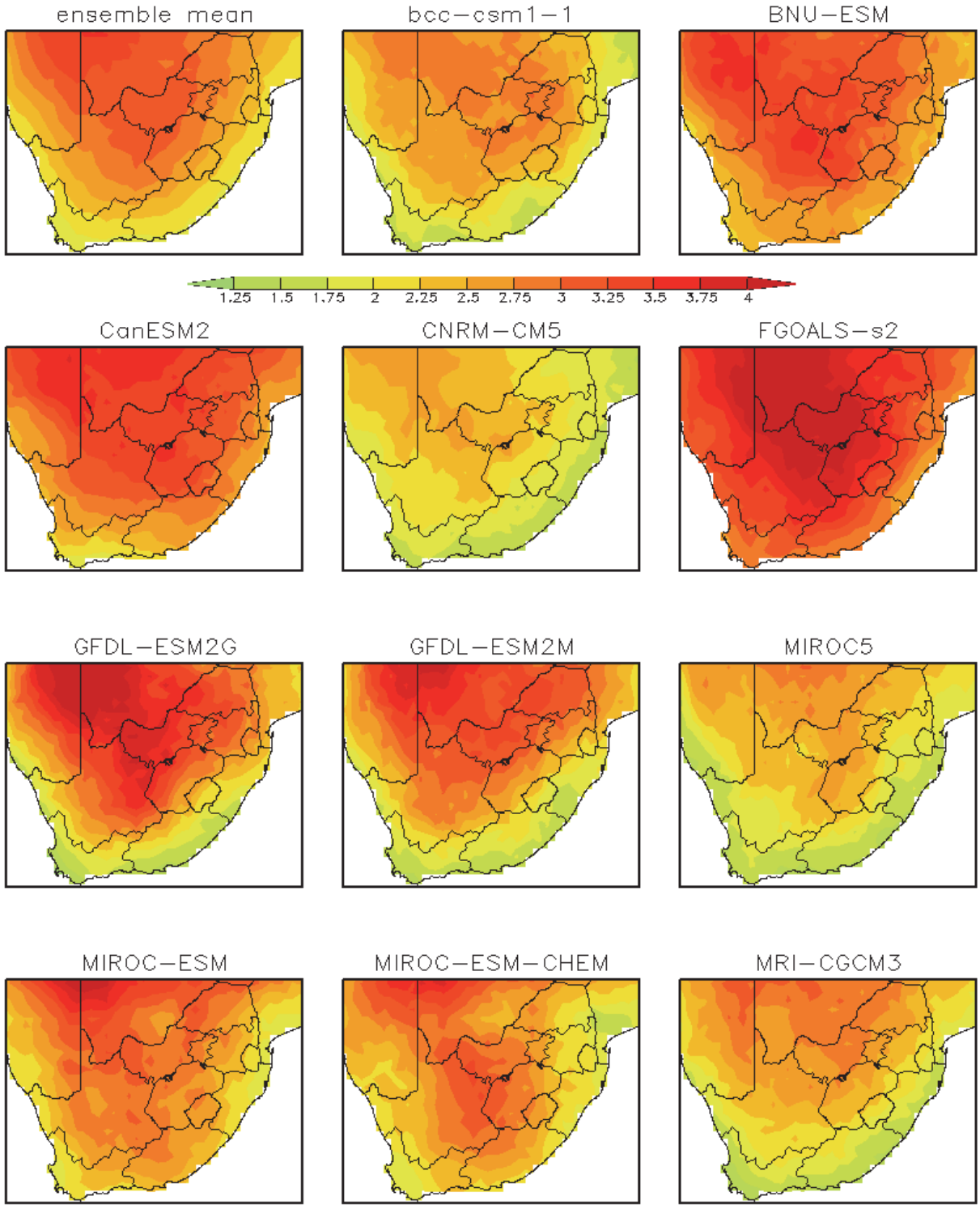

Figure B5.19 | *Future anomalies for winter (JJA) daily minimum temperature (°C) for the mid-21st century (2041-2070 – 1976-2005) under the RCP8.5 emission scenario for 11 statistically downscaled CMIP5 GCMs. Top left panel is the ensemble mean anomaly while all other plots are for individual models*

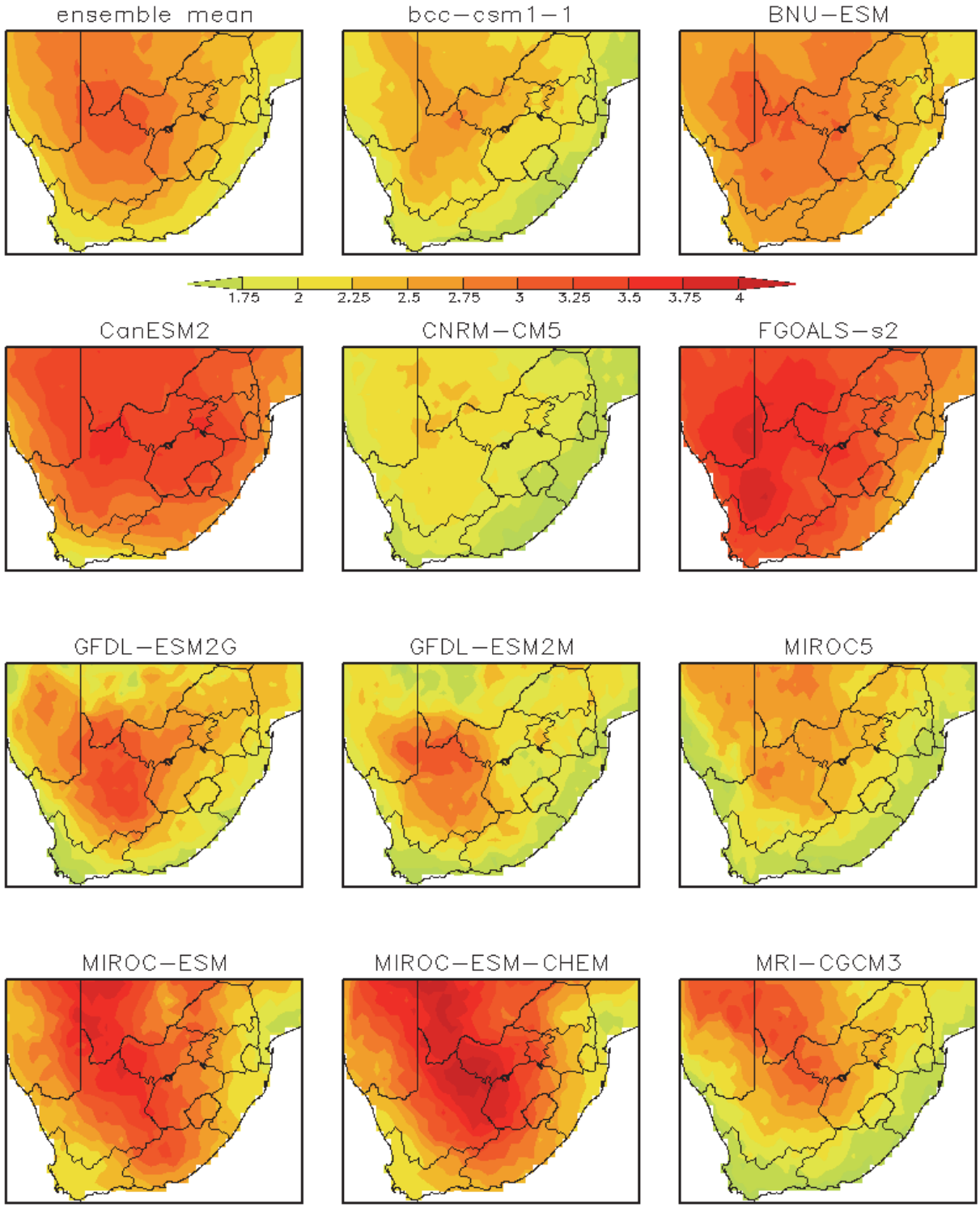

Figure B5.20 | *Future anomalies for spring (SON) daily minimum temperature (°C) for the mid-21st century (2041-2070 – 1976-2005) under the RCP8.5 emission scenario for 11 statistically downscaled CMIP5 GCMs. Top left panel is the ensemble mean anomaly while all other plots are for individual models*

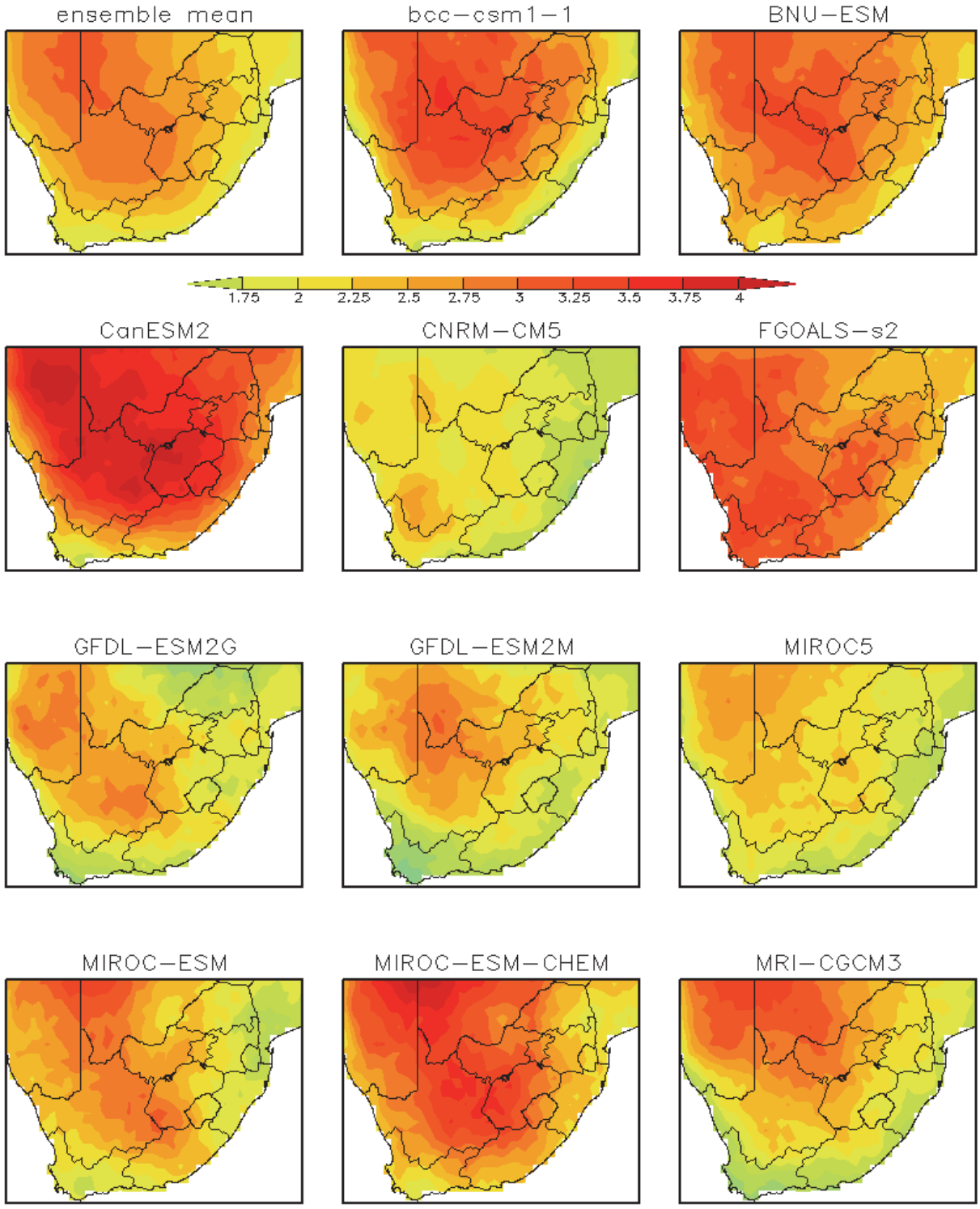

Figure B5.21 | *Future anomalies for summer(DJF) daily maximum temperature(°C) for the mid-21st century (2041-2070 – 1976-2005) under the RCP8.5 emission scenario for 11 statistically downscaled CMIP5 GCMs. Top left panel is the ensemble mean anomaly while all other plots are for individual models.*

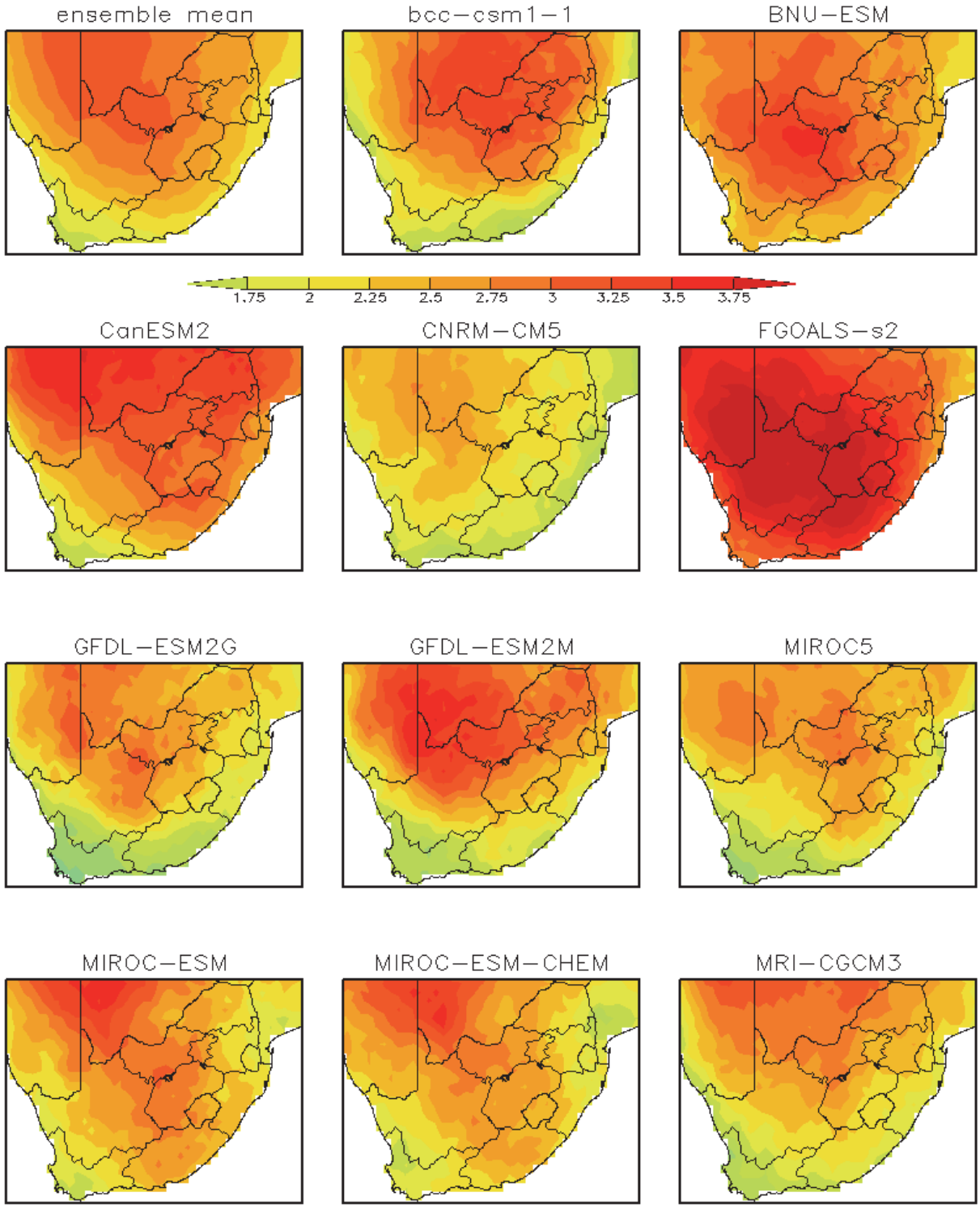

Figure B5.22 | *Future anomalies for autumn (MAM) daily maximum temperature(°C) for the mid-21st century (2041-2070 – 1976-2005) under the RCP8.5 emission scenario for 11 statistically downscaled CMIP5 GCMs. Top left panel is the ensemble mean anomaly while all other plots are for individual models.*

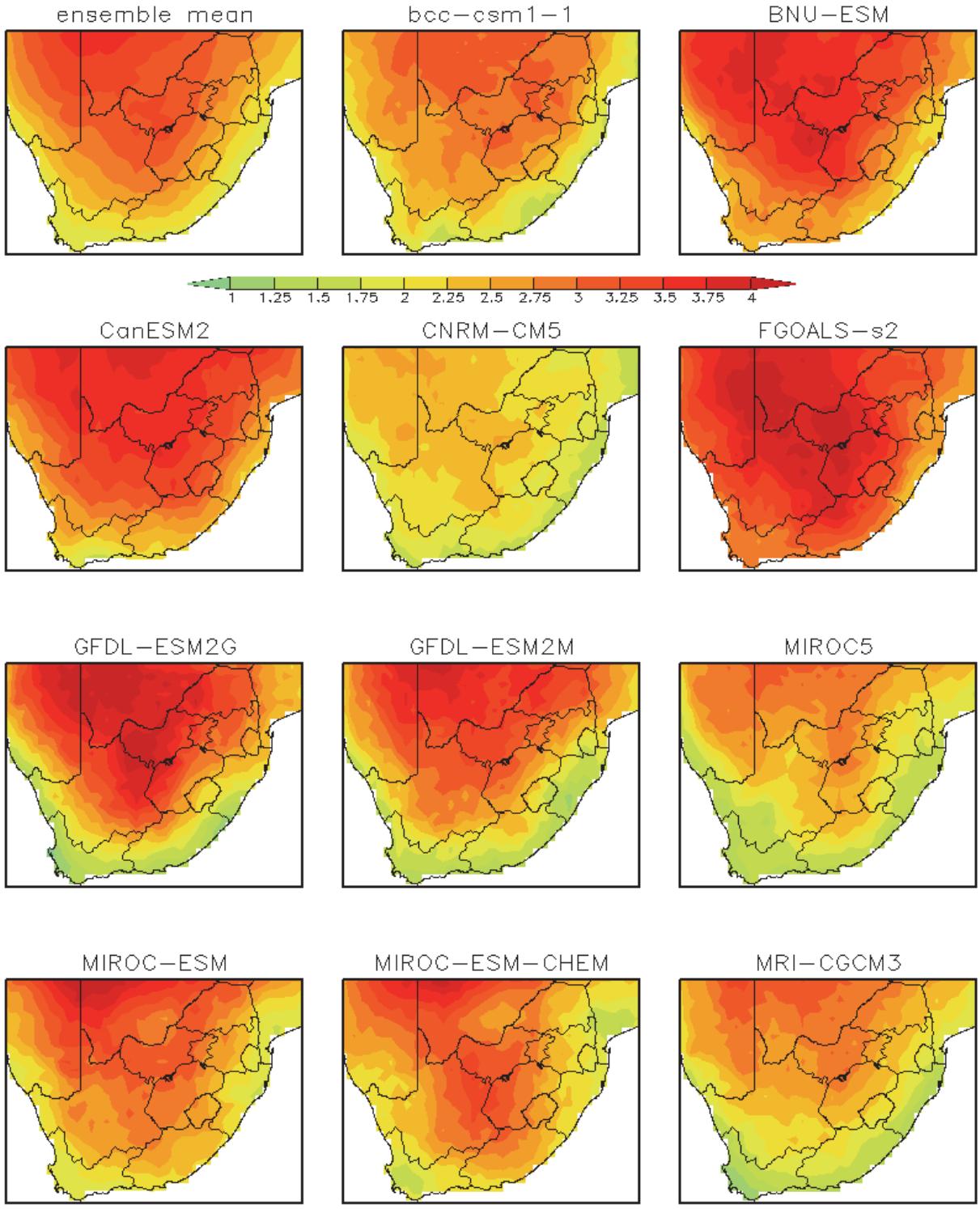

Figure B5.23 | *Future anomalies for winter (JJA) daily maximum temperature(°C) for the mid-21st century (2041-2070 – 1976-2005) under the RCP8.5 emission scenario for 11 statistically downscaled CMIP5 GCMs. Top left panel is the ensemble mean anomaly while all other plots are for individual models.*

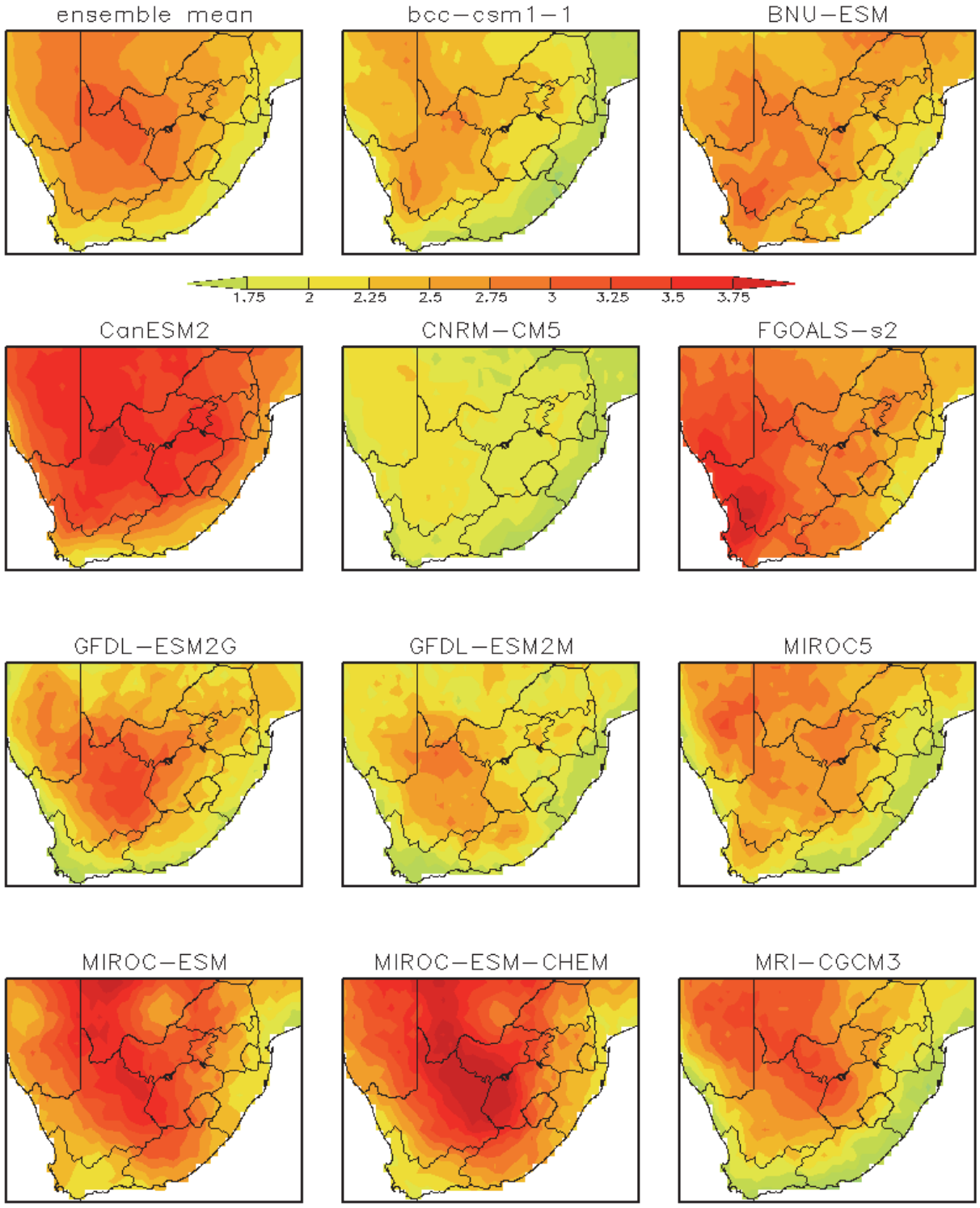

Figure B5.24 | *Future anomalies for spring (SON)) daily maximum temperature(°C) for the mid-21st century (2041-2070 – 1976-2005) under the RCP8.5 emission scenario for 11 statistically downscaled CMIP5 GCMs. Top left panel is the ensemble mean anomaly while all other plots are for individual models.*

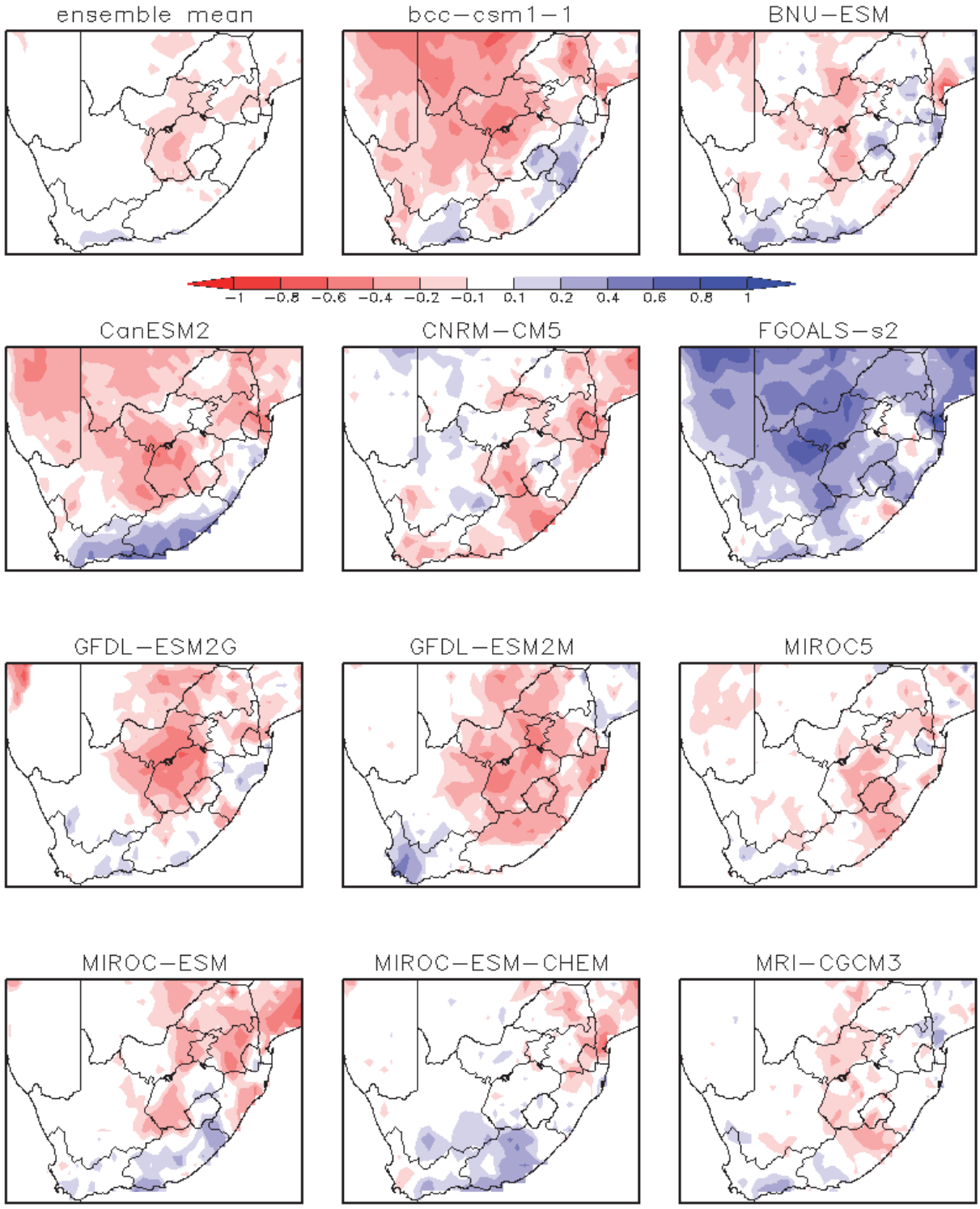

Figure B5.25 | *Future anomalies for summer(DJF) daily mean precipitation (mm/day) for the mid-21st century (2041-2070 – 1976-2005) under the RCP8.5 emission scenario for 11 statistically downscaled CMIP5 GCMs. Top left panel is the ensemble mean anomaly while all other plots are for individual models.*

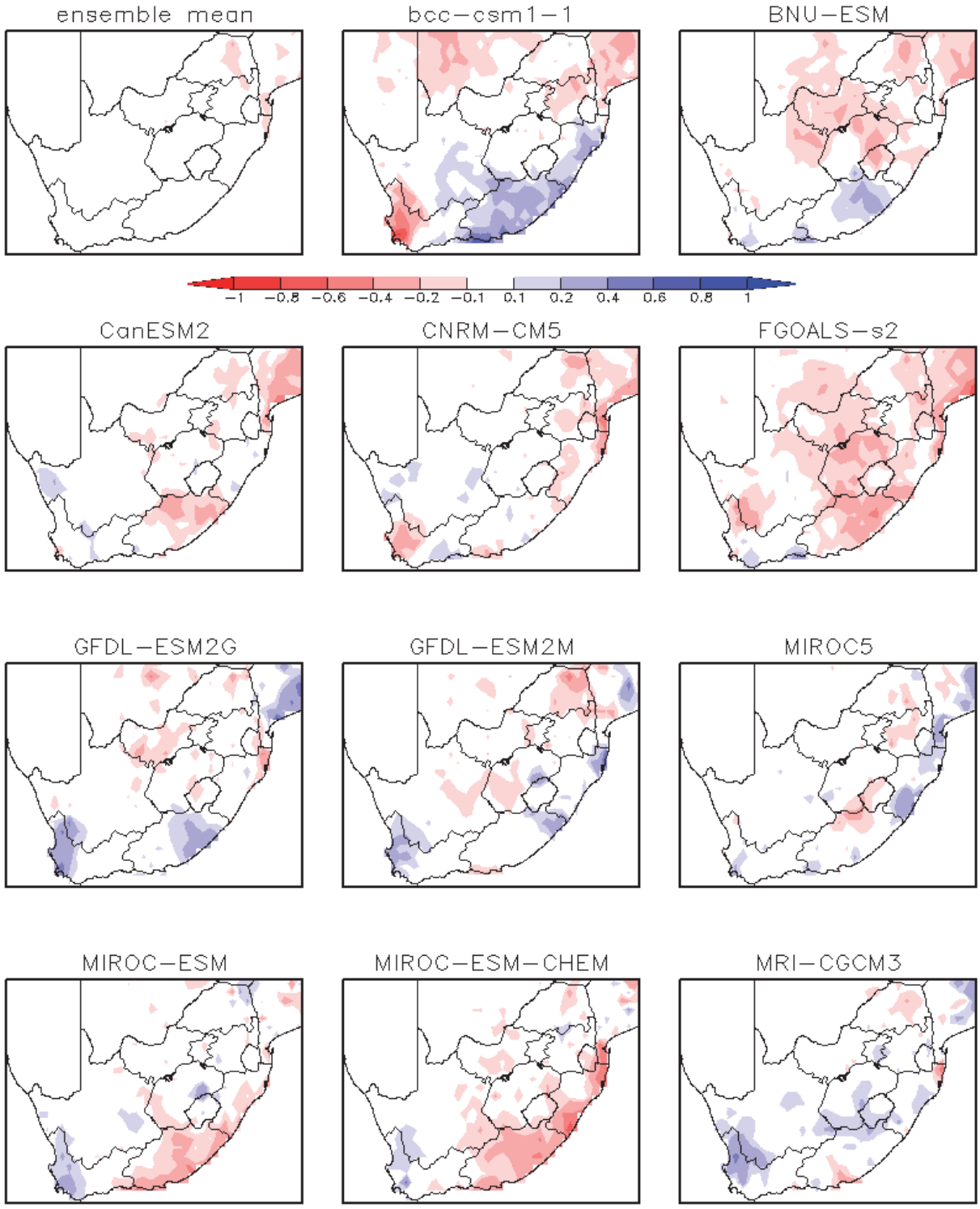

Figure B5.26 | *Future anomalies for autumn(MAM) daily mean precipitation (mm/day) for the mid-21st century (2041-2070 – 1976-2005) under the RCP8.5 emission scenario for 11 statistically downscaled CMIP5 GCMs. Top left panel is the ensemble mean anomaly while all other plots are for individual models.*

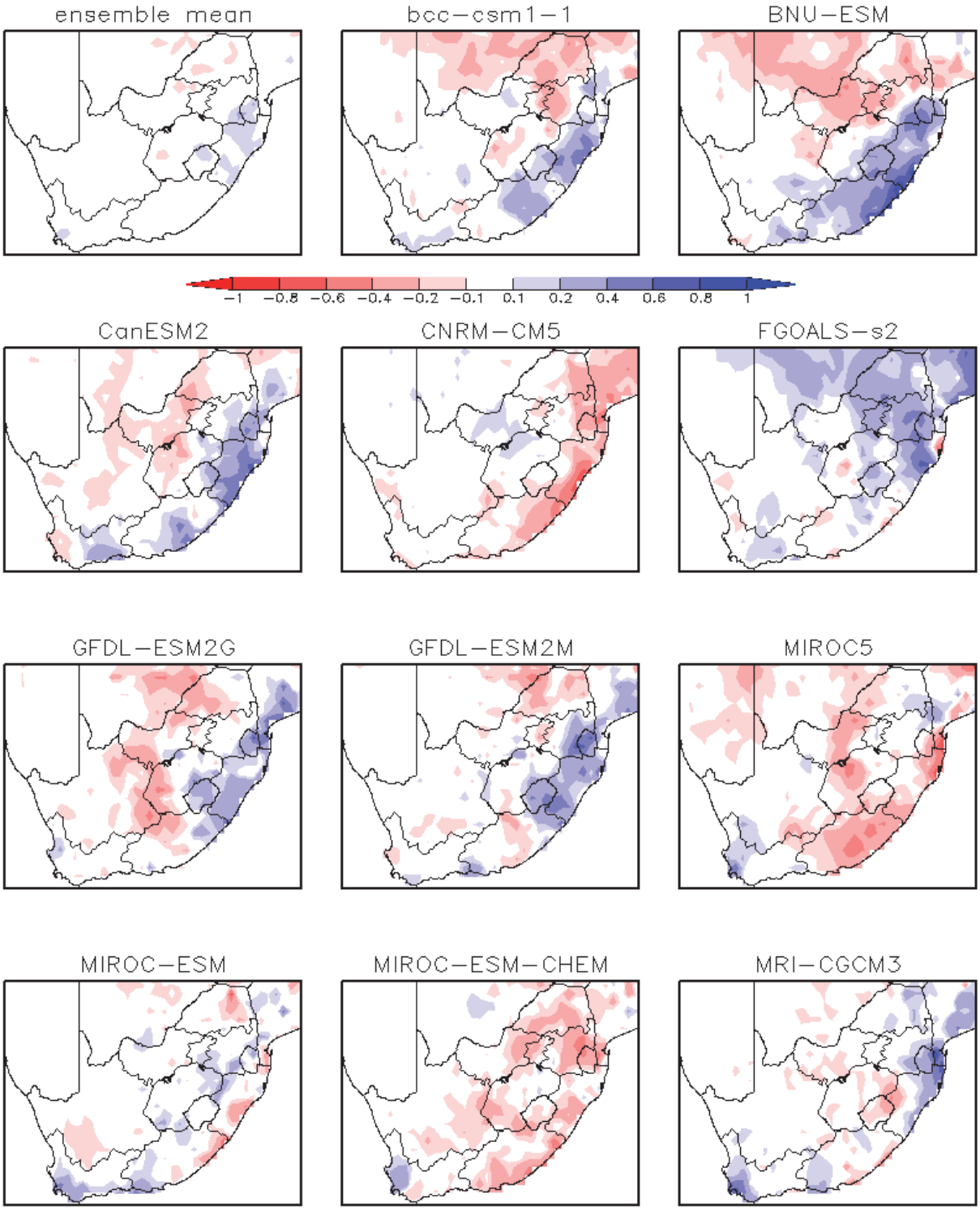

Figure B5.27 | *Future anomalies for winter(JJA) daily mean precipitation (mm/day) for the mid-21st century (2041-2070 – 1976-2005) under the RCP8.5 emission scenario for 11 statistically downscaled CMIP5 GCMs. Top left panel is the ensemble mean anomaly while all other plots are for individual models.*

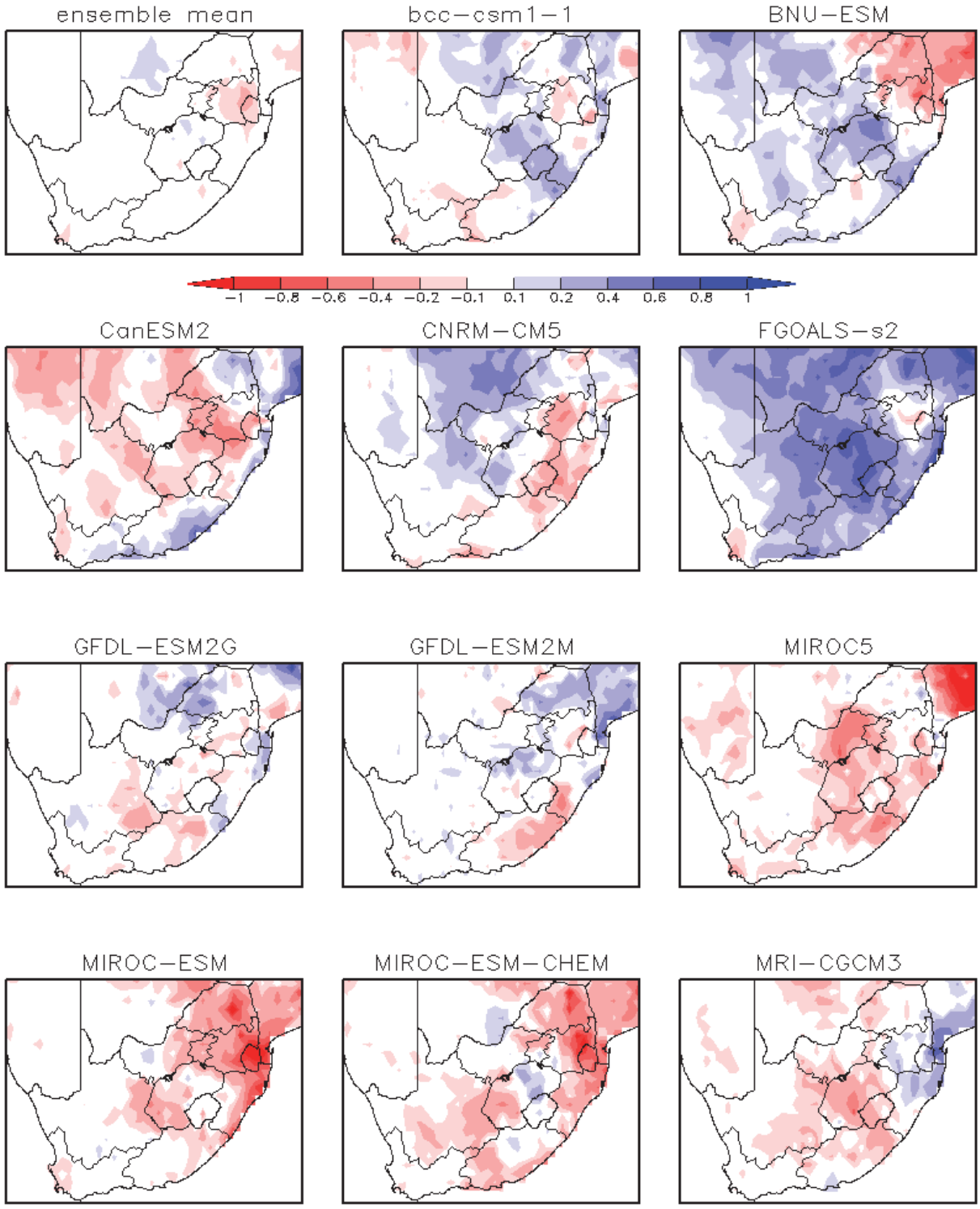

Figure B5.28 | *Future anomalies for spring(SON) daily mean precipitation (mm/day) for the mid-21st century (2041-2070 – 1976-2005) under the RCP8.5 emission scenario for 11 statistically downscaled CMIP5 GCMs. Top left panel is the ensemble mean anomaly while all other plots are for individual models.*

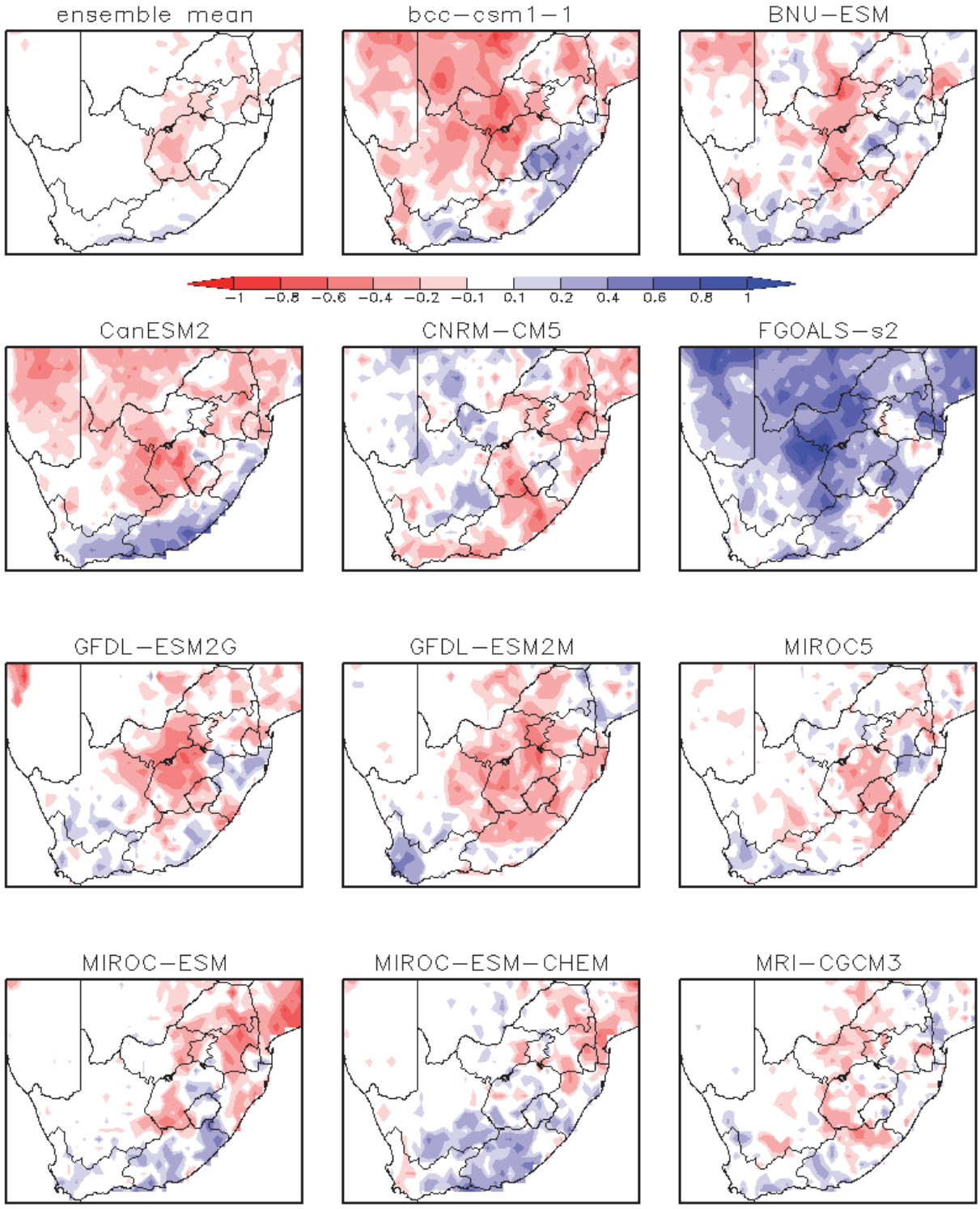

Figure B5.29 | *Future anomalies for summer(DJF) days with precipitation over 10 mm (days) for the mid-21st century (2041-2070 – 1976-2005) under the RCP8.5 emission scenario for 11 statistically downscaled CMIP5 GCMs. Top left panel is the ensemble mean anomaly while all other plots are for individual models.*

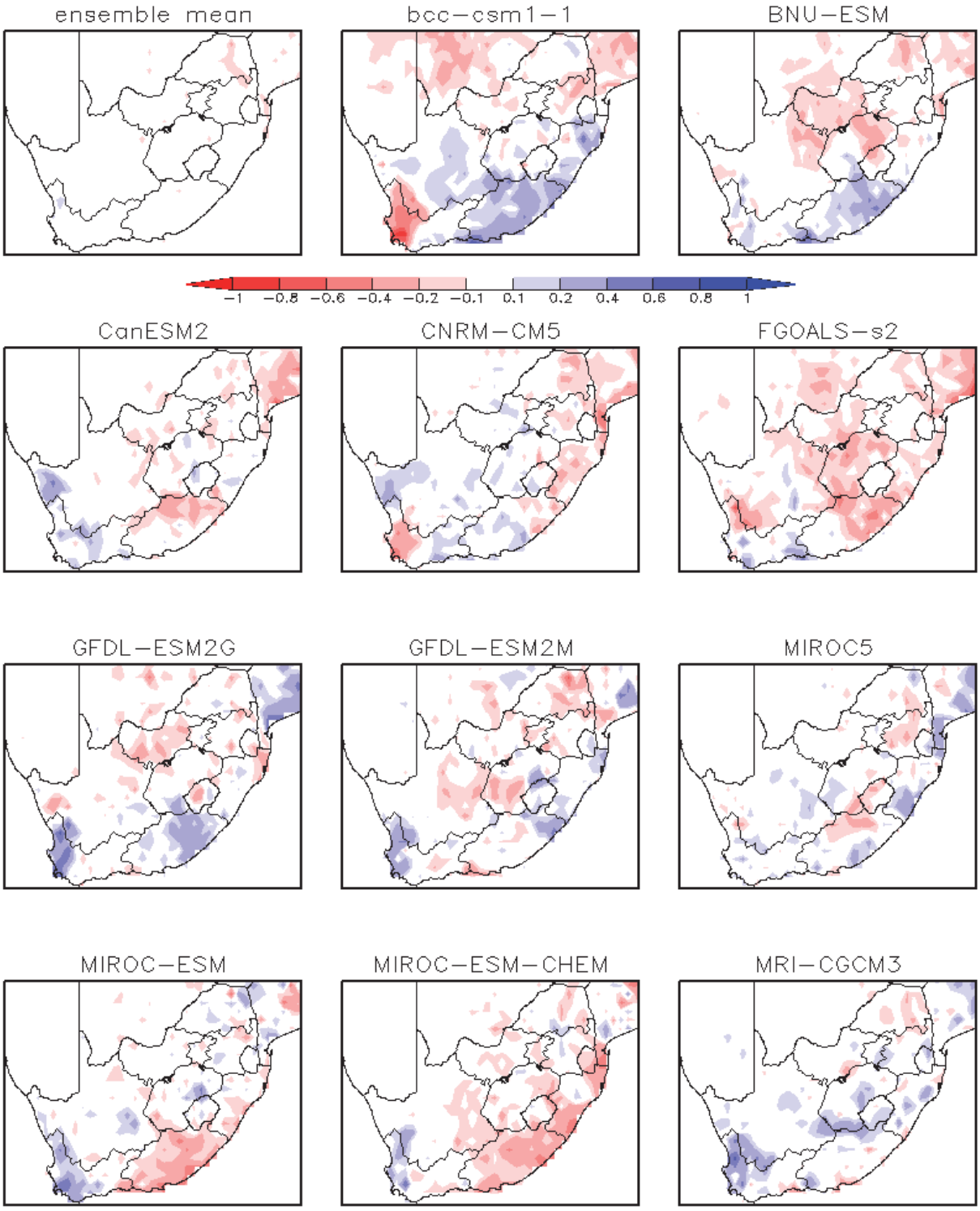

Figure B5.30 | *Future anomalies for autumn(MAM) days with precipitation over 10 mm (days) for the mid-21st century (2041-2070 – 1976-2005) under the RCP8.5 emission scenario for 11 statistically downscaled CMIP5 GCMs. Top left panel is the ensemble mean anomaly while all other plots are for individual models.*

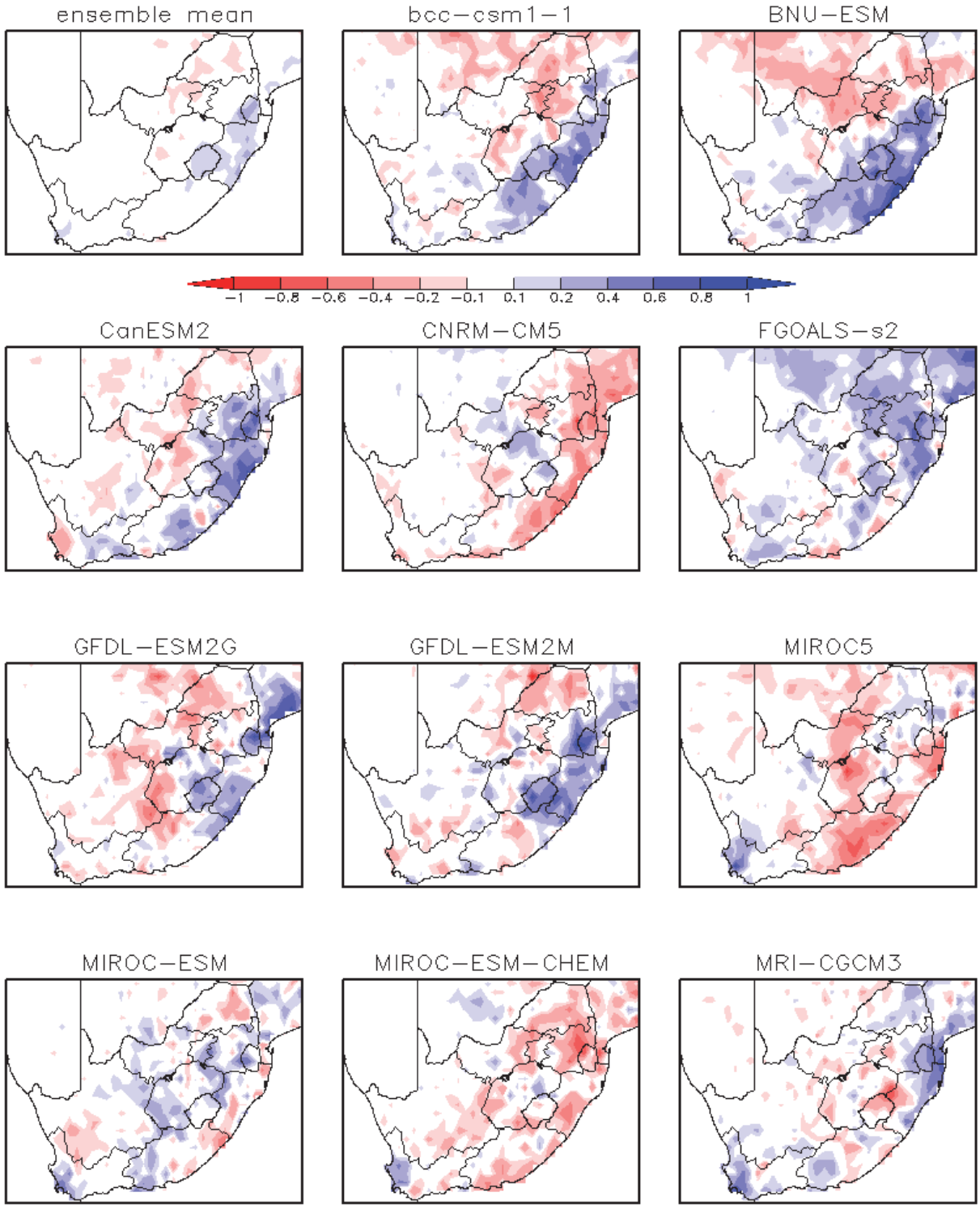

Figure B5.31 | *Future anomalies for winter(JJA) days with precipitation over 10 mm (days) for the mid-21st century (2041-2070 – 1976-2005) under the RCP8.5 emission scenario for 11 statistically downscaled CMIP5 GCMs. Top left panel is the ensemble mean anomaly while all other plots are for individual models.*

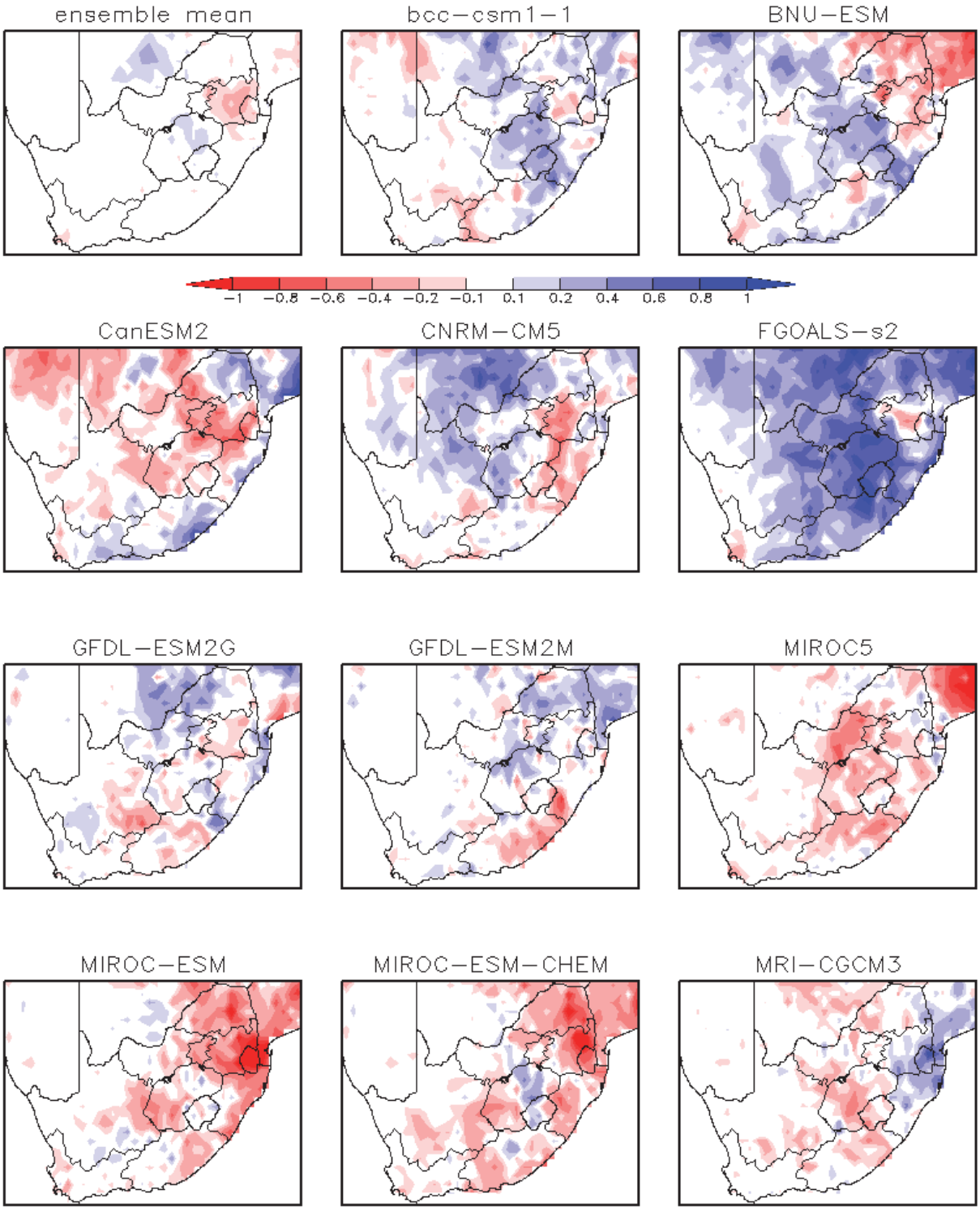

Figure B5.32 | *Future anomalies for spring(SON) days with precipitation over 10 mm (days) for the mid-21st century (2041-2070 – 1976-2005) under the RCP8.5 emission scenario for 11 statistically downscaled CMIP5 GCMs. Top left panel is the ensemble mean anomaly while all other plots are for individual models.*

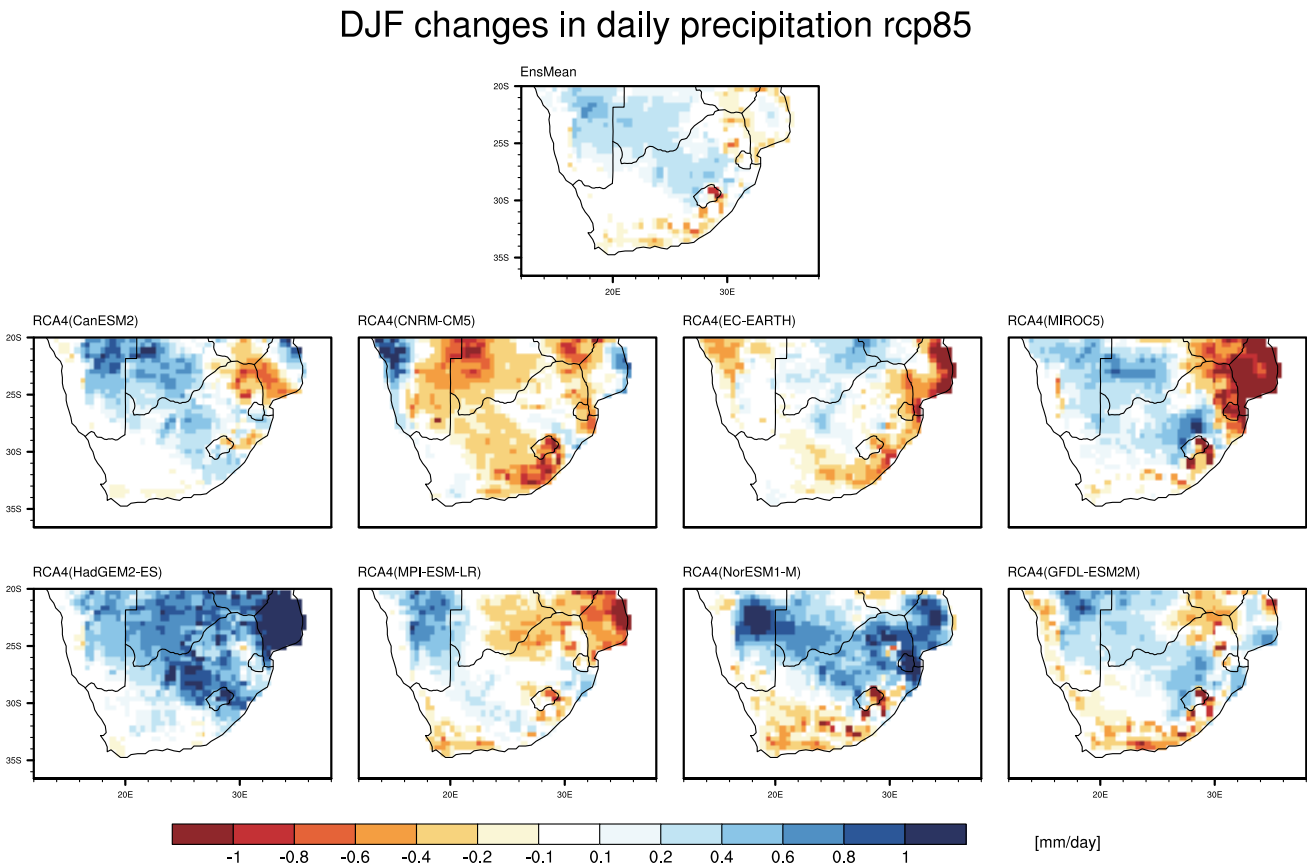

Figure B5.33 | *Future anomalies for summer (DJF) daily precipitation (mm/day) for the mid-21st Century (2041-2070 – 1976-2005) under the RCP8.5 emission scenario for 8 CMIP5 GCMs dynamically downscaled using the SHMI-RCA4 RCM. Top panel is the ensemble mean anomaly while all other plots are for individual models.*

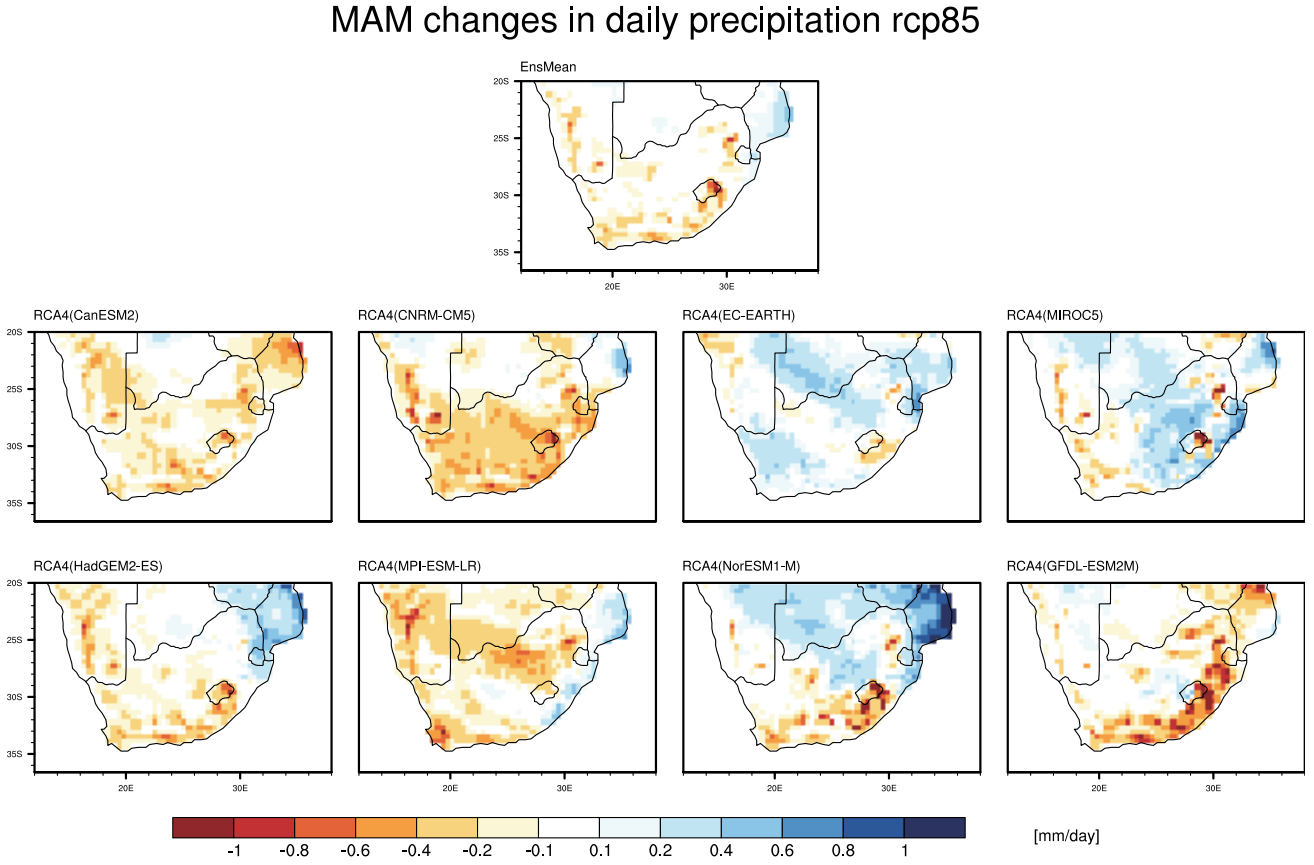

Figure B5.34 | *Future anomalies for autumn (MAM) daily precipitation (mm/day) for the mid-21st Century (2041-2070 – 1976-2005) under the RCP8.5 emission scenario for 8 CMIP5 GCMs dynamically downscaled using the SHMI-RCA4 RCM. Top panel is the ensemble mean anomaly while all other plots are for individual models.*

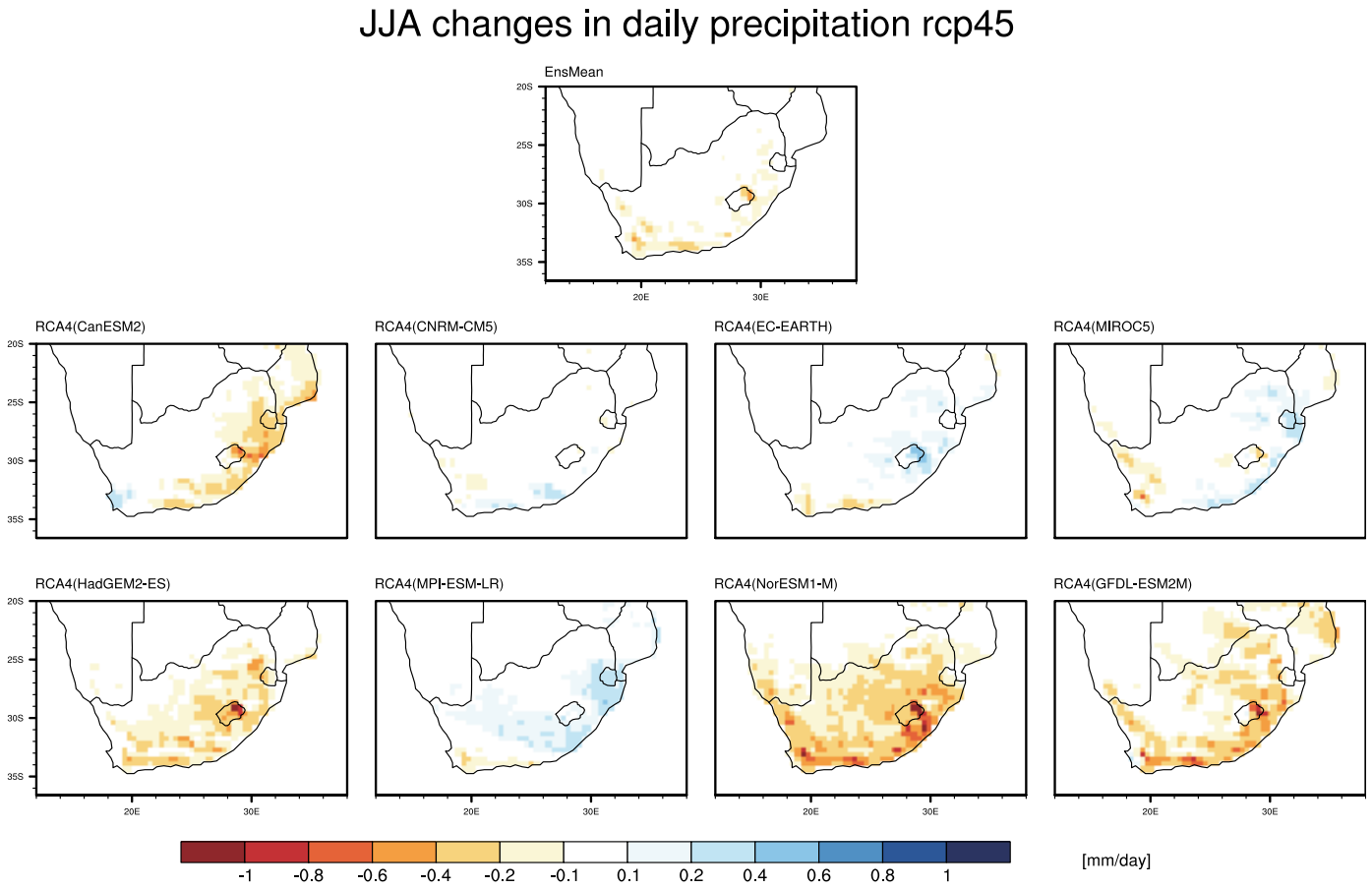

Figure B5.35 | *Future anomalies for winter (JJA) daily precipitation (mm/day) for the mid-21st Century (2041-2070 – 1976-2005) under the RCP8.5 emission scenario for 8 CMIP5 GCMs dynamically downscaled using the SHMI-RCA4 RCM. Top panel is the ensemble mean anomaly while all other plots are for individual models.*

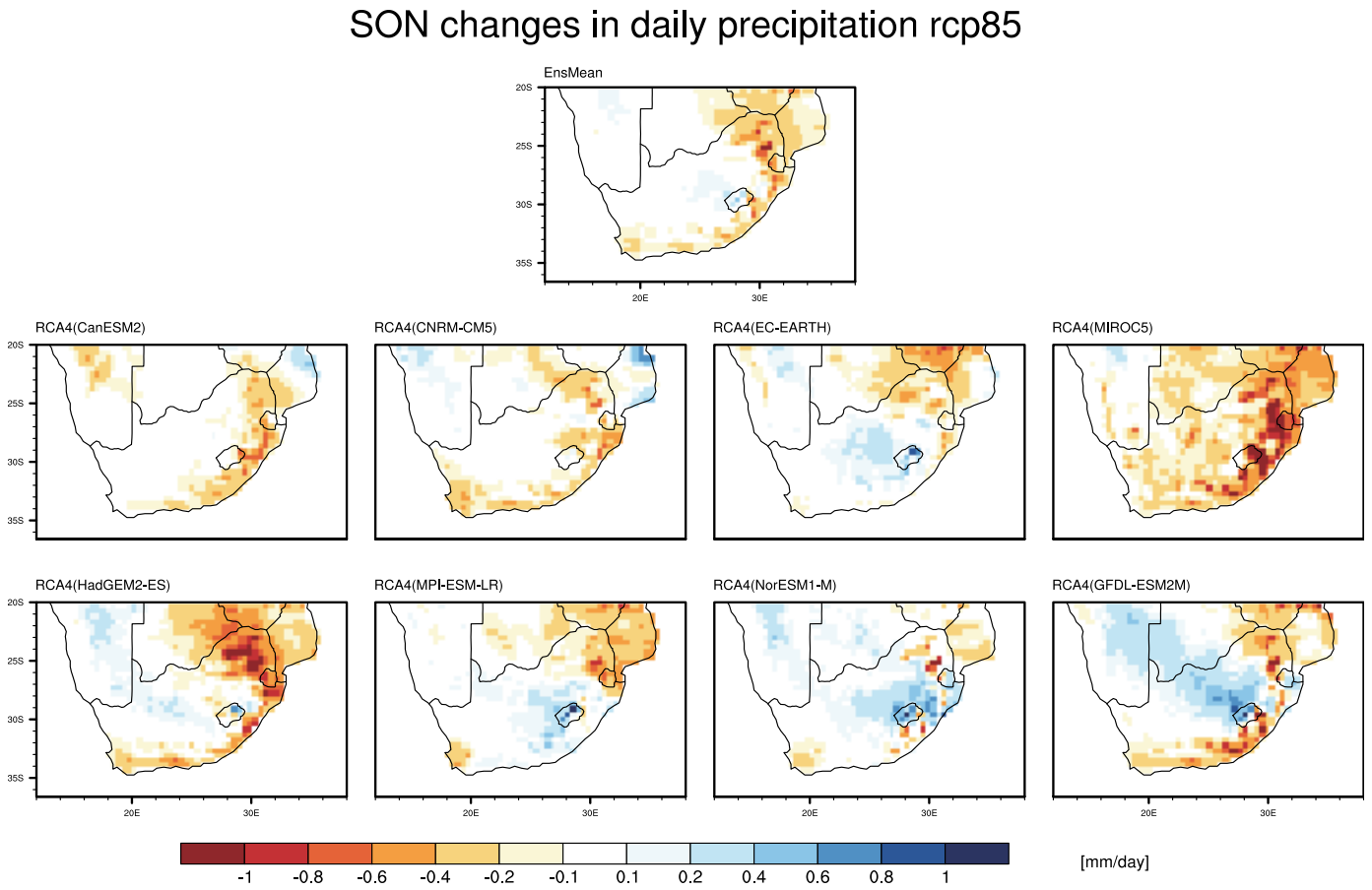

Figure B5.36 | *Future anomalies for spring (SON) daily precipitation (mm/day) for the mid-21st Century (2041-2070 – 1976-2005) under the RCP8.5 emission scenario for 8 CMIP5 GCMs dynamically downscaled using the SHMI-RCA4 RCM. Top panel is the ensemble mean anomaly while all other plots are for individual models.*

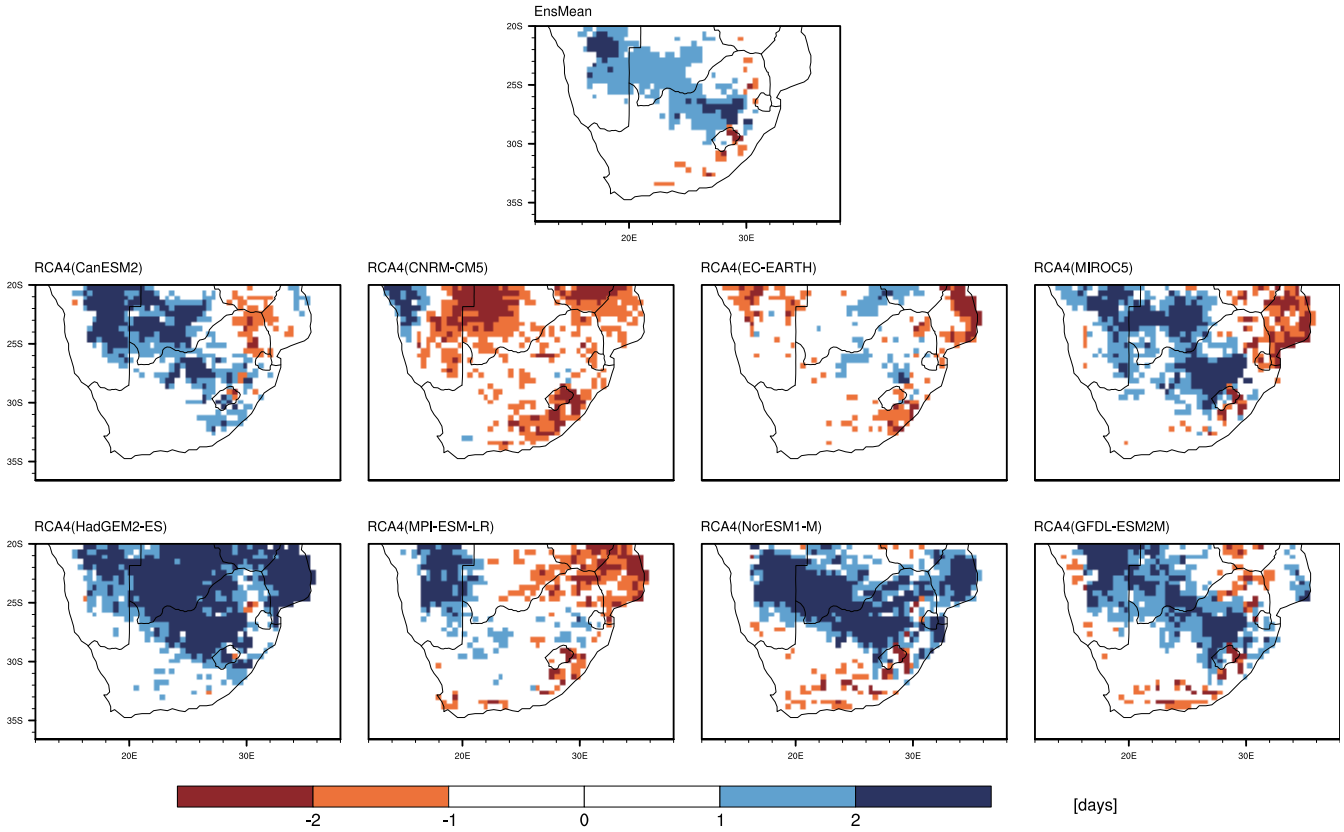

Figure B5.37 | *Future anomalies for summer (DJF) days with precipitation above 10 mm (days) for the mid-21st Century (2041-2070 – 1976-2005) under the RCP8.5 emission scenario for 8 CMIP5 GCMs dynamically downscaled using the SHMI-RCA4 RCM. Top panel is the ensemble mean anomaly while all other plots are for individual models.*

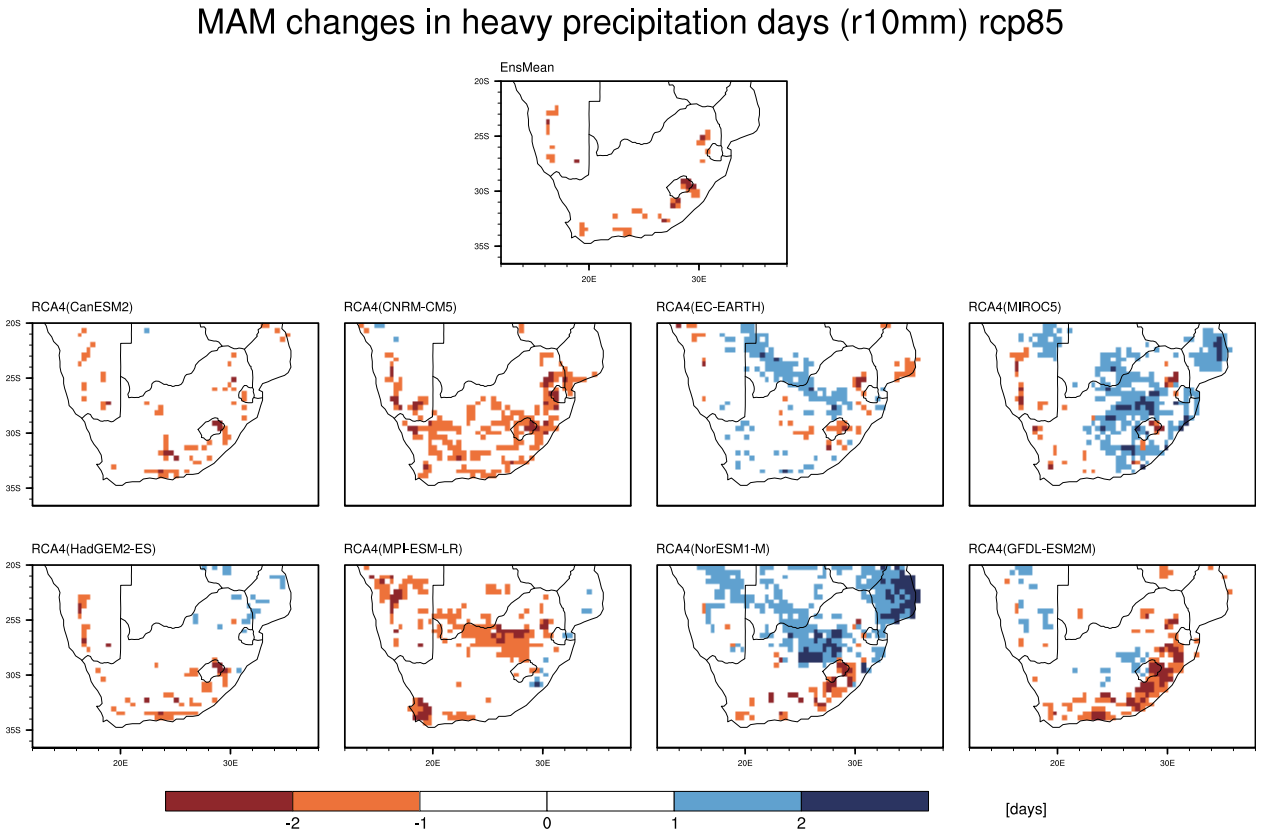

Figure B5.38 | *Future anomalies for autumn (MAM) days with precipitation above 10 mm (days) for the mid-21st Century (2041-2070 – 1976-2005) under the RCP8.5 emission scenario for 8 CMIP5 GCMs dynamically downscaled using the SHMI-RCA4 RCM. Top panel is the ensemble mean anomaly while all other plots are for individual models.*

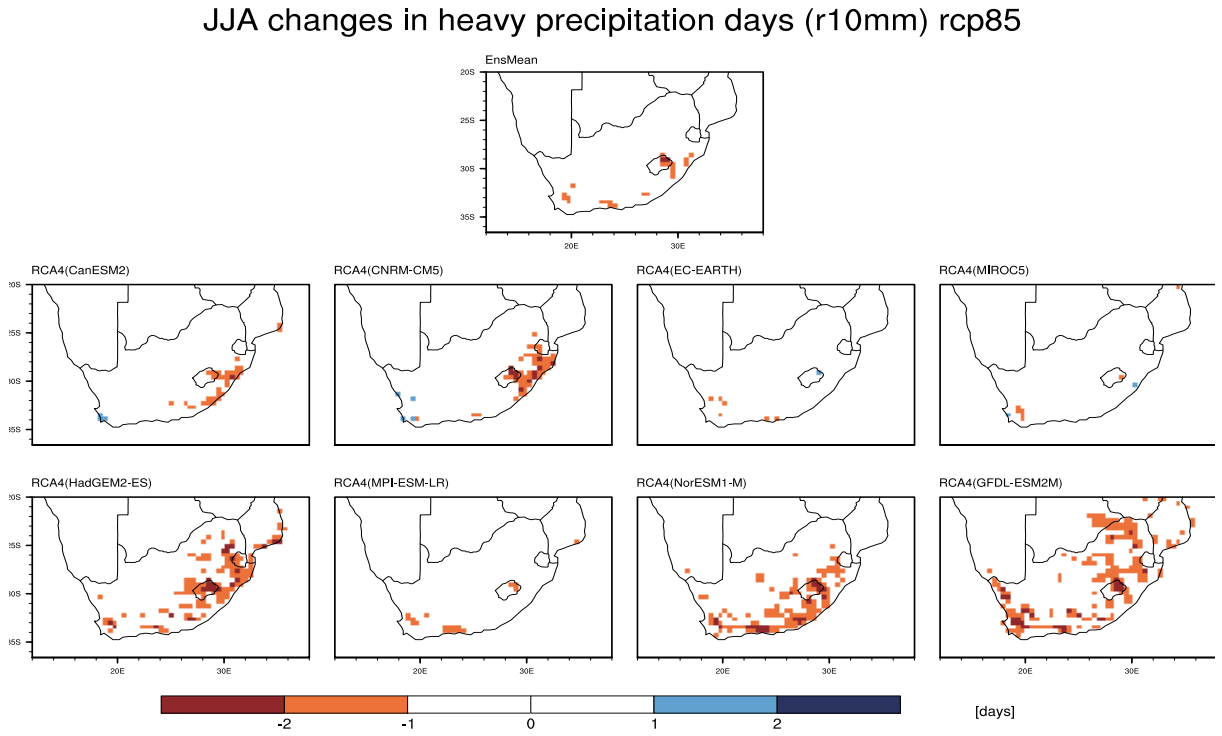

Figure B5.39 | *Future anomalies for winter (JJA) days with precipitation above 10 mm (days) for the mid-21st Century (2041-2070 – 1976-2005) under the RCP8.5 emission scenario for 8 CMIP5 GCMs dynamically downscaled using the SHMI-RCA4 RCM. Top panel is the ensemble mean anomaly while all other plots are for individual models.*

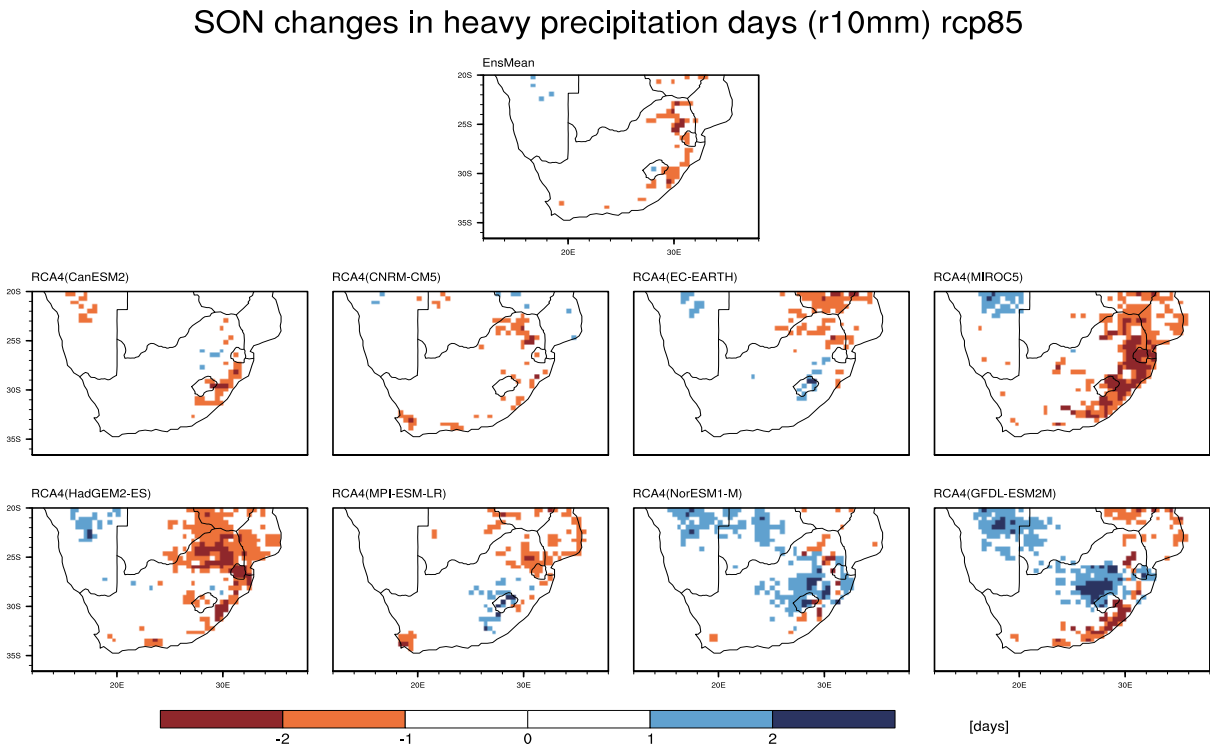

Figure B5.40 | *Future anomalies for spring (SON) days with precipitation above 10 mm (days) for the mid-21st Century (2041-2070 – 1976-2005) under the RCP8.5 emission scenario for 8 CMIP5 GCMs dynamically downscaled using the SHMI-RCA4 RCM. Top panel is the ensemble mean anomaly while all other plots are for individual models.*